UNCLASSIFIED

AD NUMBER
AD514939
CLASSIFICATION CHANGES
TO: unclassified
FROM: secret
LIMITATION CHANGES
TO: Approved for public release, distribution unlimited
FROM: Distribution: Further dissemination only as directed by Chief, Office of Naval Research, 875 North Randolph St., Attn: Code 414. Arlington, VA 22203-1995, 29 MAY 1970, or higher DoD authority.
AUTHORITY
DARPA ltr, 19 Aug 1996; DARPA ltr, 19 Aug 1996

THIS PAGE IS UNCLASSIFIED

AD- 514939

SECURITY REMARKING REQUIREMENTS

DOD 5200.1-R, DEC 78

REVIEW ON 29 MAY 90

SECURITY MARKING

The classified or limited status of this report applies to each page, unless otherwise marked.
Separate page printouts MUST be marked accordingly.

THIS DOCUMENT CONTAINS INFORMATION AFFECTING THE NATIONAL DEFENSE OF THE UNITED STATES WITHIN THE MEANING OF THE ESPIONAGE LAWS, TITLE 18, U.S.C., SECTIONS 793 AND 794. THE TRANSMISSION OR THE REVELATION OF ITS CONTENTS IN ANY MANNER TO AN UNAUTHORIZED PERSON IS PROHIBITED BY LAW.

NOTICE: When government or other drawings, specifications or other data are used for any purpose other than in connection with a definitely related government procurement operation, the U.S. Government thereby incurs no responsibility, nor any obligation whatsoever; and the fact that the Government may have formulated, furnished, or in any way supplied the said drawings, specifications, or other data is not to be regarded by implication or otherwise as in any manner licensing the holder or any other person or corporation, or conveying any rights or permission to manufacture, use or sell any patented invention that may in any way be related thereto.

SECRET

NOFORN

DDC

Proceedings of the

MAY BELL TECHNICAL WORKSHOP OF 18-22 MAY 1970 (U)

Held at RAYTHEON COMPANY SPENCER LABORATORY
BURLINGTON, MASSACHUSETTS

FILE COPY

AD 514939L

CONTROLLED ITEM
No. S70P4733

NOFORN

SECRET

11200

In addition to security requirements which apply to this document and must be met, it may be further distributed by the holder only with specific prior approval of the Office of Naval Research; Attention: Code 418.

No [redacted] of [redacted] copies
This document consists of 254 pages
Printed 29 May [redacted]70

(11)

12 235p.

Proceedings of the

MAY BELL TECHNICAL WORKSHOP OF 18-22 MAY 1970, [redacted]

Held at RAYTHEON COMPANY SPENCER LABORATORY, BURLINGTON, MASSACHUSETTS [U].

Prepared for
OFFICE OF NAVAL RESEARCH
CONTRACT NOO14-69-C-0466
UNDER ARPA ORDER 1459

115

N00014-69-C-0466,
ARPA Order-1459

Prepared by:
RAYTHEON COMPANY
OHD ADVANCED DEVELOPMENT DEPARTMENT
BURLINGTON, MASSACHUSETTS

In addition [illegible]

C/A 2/attn Code 418

This material contains information affecting the national defense of the United States within the meaning of the espionage laws, Title 18, U.S.C., Sections 793 and 794, the transmission or revelation of which in any manner to an unauthorized person is prohibited by law.

GROUP 1
EXCLUDED FROM AUTOMATIC DOWNGRADING AND DECLASSIFICATION.

SPECIAL HANDLING REQUIRED.
NOT RELEASABLE TO FOREIGN NATIONALS.

The information contained in this document will not be disclosed to foreign nationals or other representatives except Canada and the U.K.

416374

112nd

THIS PAGE INTENTIONALLY LEFT BLANK

CONTENTS (U)

PROJECT MAY BELL WORKSHOP PARTICIPANTS (U)

Advanced Research Projects Agency

Alvin Van Every

Army Missile Command

Samuel Uptain

Naval Research Laboratory

Jack Ahearn
James Headrick
James Hudall
Richard Sheil
Paul Stine
Dennis Trizna
Dr. Lew Wetzel

Office of Naval Research

Stan Curley
Jack Kane
Dr. William Kielhorn
Frank Mullen
Thomas Quinn

Applied Physics Laboratory (JHU)

Dr. Frank Bader
Dr. James Follin, Jr.
Richard Hunt
Mace Miyasaki
Dr. Edwin Shotland
Albert Stone

Battelle Memorial Institute

Dr. Donald Barrick

Environmental Science Services Administration

Douglas Crombie
Dr. Randolph Ott
Dr. William Utlaut

Scripps

Daniel Brown

Stanford Research Institute

Dr. George Oetzel
Dr. Allen Peterson

Astrophysics Research Corporation

Howard Grizzle
Dr. Hans von Roos

ITT Electro-Physics Laboratories, Inc.

Dr. Roy Basler
Dr. John Kelso
Wesley Mollard
Thomas Scott
William Whelan

Raytheon Spencer Laboratory

Dr. Henry Alexander
Henry Baker
Richard Close
Robert Desmond
Leonard Edwards
Jerald Grimes
Harry Hoogasian
Frank Roberts
Bruce Whitehead

Sylvania Electronic Systems West

Robert Krulee
Kenneth Snow
John White, Jr.

PROJECT MAY BELL WORKSHOP COMMITTEES (U)

Executive
A. Van Every, Chairman
D. Barrick
R. Basler
L. Edwards
J. Follin

Path Loss
H. Hoogasian, Chairman
S. Curley
R. Ott
T. Quinn
T. Scott
E. Shotland
K. Snow
R. Trizna
L. Wetzel

Clutter
J. Grimes, Chairman
J. Ahearn
H. Alexander
D. Crombie
J. Headrick
E. Shotland
L. Wetzel

Sea State
H. Baker, Co-chairman
B. Whitehead, Co-chairman
F. Bader
W. Kielhorn
M. Miyasaki
R. Sheil

PROJECT MAY BELL WORKSHOP DISTRIBUTION LIST (U)

Copies 2, 3, 4
Director
Advanced Research Projects Agency
The Pentagon
Washington, D.C. 20301
Attn: Mr. Alvin Van Every, STO

Copy 5
Headquarters
U.S. Army Missile Command
Redstone Arsenal
Huntsville, Alabama 35809
Attn: Mr. Samuel T. Uptain, AMSMI-RNS

Copy 6
U.S. Department of Commerce
Environmental Science Services Administration
Boulder, Colorado 80302
Attn: Mr. Doug D. Crombie

Copy 7
U.S. Department of Commerce
Environmental Science Services Administration
Boulder, Colorado 80302
Attn: Dr. Randolph Ott

Copy 8
U.S. Department of Commerce
Environmental Science Services Administration
Boulder, Colorado 80302
Attn: Dr. William F. Utlaut

Copy 9
Director
Naval Research Laboratory
Washington, D.C. 20390
Attn: Mr. Jim Headrick, Code 5323

Copy 10
Director
Naval Research Laboratory
Washington, D.C. 20390
Attn: Dr. Lew Wetzel, Code 5400

Copies 11, 12
Chief
Office of Naval Research
Washington, D.C. 20360
Attn: Mr. Jack Kane, Code 418

Copy 13
Mr. Charles S. Lerch, Jr.
Institute for Defense Analyses
400 Army-Navy Drive
Arlington, Virginia 22202

Copy 14
Commander
Rome Air Development Center
Griffiss Air Force Base
Rome, New York 13442
Attn: Mr. R.A. Ackley, EMATS

Copy 15
Commander
Rome Air Development Center
Griffiss Air Force Base
Rome, New York 13442
Attn: Mr. Salvador DiGennaro, EMASO

Copy 16
Headquarters
Electronic Systems Division
Air Force Systems Command
L. G. Hanscom Field
Bedford, Massachusetts 01731
Attn: Lt Col. D.F. Connors, ESSLG

Copy 17
Headquarters
Foreign Technology Division
Air Force Systems Command
Wright-Patterson AFB, Ohio 45433
Attn: Mr. S.G. Zabetakis, TDDEP

Copy 18
Office of Naval Research
495 Summer Street
Boston, Massachusetts 02210
Attn: Mr. Stanley R. Curley

Copy 19
Headquarters
Electronic Systems Division
Air Force Systems Command
L.G. Hanscom Field
Bedford, Massachusetts 01731
Attn: Major Joe Dixon, ESSLG

Copy 20
Headquarters
National Security Agency
Fort George Meade, Maryland 20755
Attn: Mr. Jerry Fuller, Code N-2

Copies 21, 22
The Johns Hopkins University
Applied Physics Laboratory
8621 Georgia Avenue
Silver Spring, Maryland 20910
Attn: Dr. James W. Follin, Jr.

Copy 23
The John Hopkins University
Applied Physics Laboratory
8621 Georgia Avenue
Silver Spring, Maryland 20910
Attn: Dr. Edwin Shotland

Copy 24
Dr. Allen Peterson
Stanford Research Institute
Menlo Park, California 94025

Copy 25
Mr. James Barnum
Stanford Electronics Laboratories
Stanford University
Stanford, California 94305

Copy 26
Dr. O.G. Villard, Jr.
Stanford Electronics Laboratories
Stanford University
Stanford, California 94305

Copy 27
Dr. Walter H. Munk
University of California. San Diego Institute of
Geophysics and Planetary Physics
La Jolla Laboratories
La Jolla, California 92037

Copy 28
Dr. Henry Booker
University of California, San Diego
La Jolla, California 92037

Copy 29
Mr. Sam Hunt
The Mitre Corporation
Post Office Box 208
Bedford, Massachusetts 01730

Copy 30
Battelle Memorial Institute
Columbus Laboratories
505 King Avenue
Columbus, Ohio 43201
Attn: Dr. Donald E. Barrick

Copy 31
Mr. Robert Schulz
Stanford Research Institute
Menlo Park, California 94025

Copy 32
Mr. L.C. Edwards
Raytheon Company
Spencer Laboratory, Dept. 8822
Wayside Road
Burlington, Massachusetts 01803

Copy 33
Mr. Harry Hoogasian
Raytheon Company
Spencer Laboratory, Dept. 8822
Wayside Road
Burlington, Massachusetts 01803

Copy 34
Dr. Roy P. Basler
ITT Electro-Physics Laboratories, Inc.
3355 52nd Avenue
Hyattsville, Maryland 20781

Copy 35
Dr. John Kelso
ITT Electro-Physics Laboratories, Inc.
3355 52nd Avenue
Hyattsville, Maryland 20781

Copy 36
Mr. Ken Snow
Sylvania Electronic Systems
Western Operation
Post Office Box 205
Mountain View, California 94042

Copy 37
Dr. Hans vonRoos
Astrophysics Research Corporation
Tishman Airport Center
Suite 1130, 9841 Airport Boulevard
Los Angeles, California 90045

Copies 1, 38-60
Mr. Henry M. Baker
Raytheon Company
Spencer Laboratory, Dept. 8822
Wayside Road
Burlington, Massachusetts 01803

THIS PAGE INTENTIONALLY LEFT BLANK

INTRODUCTION (U)

THIS PAGE INTENTIONALLY LEFT BLANK

INTRODUCTION (U)

(S) A five-day meeting was held on 18-22 May 1970 at the Raytheon Company Spencer Laboratory, Burlington, Mass., under the sponsorship of the Advanced Research Projects Agency and the US Navy. Mr. A. Van Every of ARPA was chairman. The papers are published in four sections, divided into the following subject areas:

Section 1.	Executive Summary
Section 2.	Summary of Papers
	Program Objectives
	Theory and Measurements
	Fleet Air Defense
	Buoy Tactical Early Warning
Section 3.	Panel Reports
Section 4.	Task Abstracts

(C) These meetings are regularly held to allow contractors and government agencies active in surface wave radar research to exchange information and report their findings.

(U) A list of attendees is given at the end of Section 1.

(U) Copies of these Proceedings may be requested through the Office of Naval Research, Department of the Navy, Washington, D.C. 20360, Attn: Code 418.

THIS PAGE INTENTIONALLY LEFT BLANK

SECTION 1

EXECUTIVE SUMMARY (U)

EXECUTIVE SUMMARY (U)

I PROJECT MAY BELL OVERVIEW (U)

(S) Project MAY BELL is directed towards ocean surveillance and tactical early warning and is investigating the feasibility of detecting and tracking aircraft, missiles, ships and submarines at over-the-horizon distances using HF monostatic and bistatic radar.

(U) Concepts using the basic geometric configurations shown in Figure 1 are being explored.

(U) In support of these concepts various theoretical predictions, propagation measurements, cross-section studies and feasibility detection demonstrations have been made.

(S) The program emphasis during the past eighteen months has been specifically directed towards determining the attenuation and clutter propagation aspects that apply to the concepts that use the surface wave; and investigating the basic feasibility of detecting and tracking aircraft using Mode III, Fleet Air Defense (FAD), and Mode IV (a) and (b), Buoy Tactical Early Warning (B-TEW).

(U) The various efforts and their relation and importance to the basic geometric configurations are shown in Figure 2.

II SUMMARY OF RESULTS (U)

A. Theory and Measurements (U)

1. Path Loss (U)

(C) Measurements of received signal strength were made over a 300-km path extending from Carter Cay in the Bahamas to the receiving site at Cape Kennedy, Florida. Detailed measurements extended from January through March, 1970.

(C) The mean signal strength measurements agree well with predicted[1] received signal strengths in absolute level. The spread of points about the mean conforms to loss predictions versus sea state at 5 and and 10 MHz. Insufficient data were available at 15 and 20 MHz to permit comparisons. Day-to-day correlation of measured signal level with sea state was not reliable because only crude hindcast date was available on sea state. System drifts are concluded to be less than 2 dB. Effects of ducting on measured signal strengths are unknown. Possible spectral broadening of the direct signal by the moving sea during high sea states appeared on some records.

MODE I
SKY WAVE - SKY WAVE

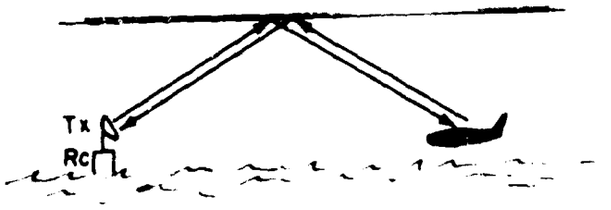

MODE II
SURFACE WAVE - SURFACE WAVE

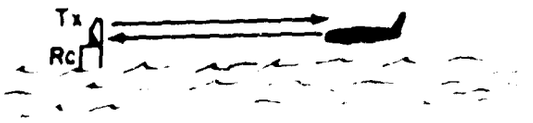

MODE III
SKY WAVE - SURFACE WAVE
FAD

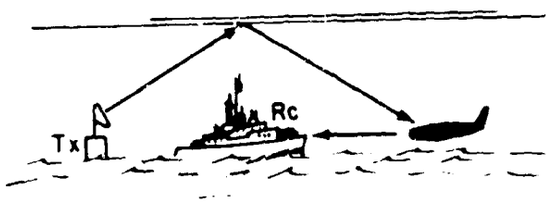

MODE IV-A
DIRECT OR SURFACE WAVE -
SURFACE WAVE
BTEW-1

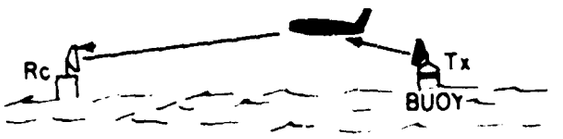

MODE IV-B
DIRECT OR SURFACE WAVE -
SKY WAVE
BTEW-2

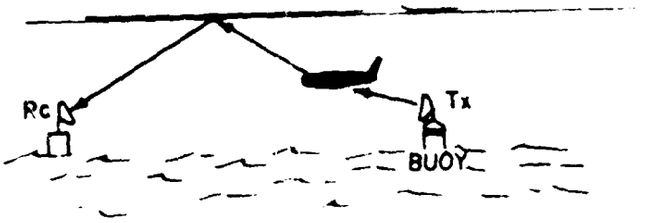

(S) Figure 1. Basic Geometric Configurations (U)

(S)

TASK	ORGANIZATION	OBJECTIVE
A. Theory & Measurements		
1. Attenuation & Clutter Calculations	BMI	Determine surface wave attenuation and clutter as a function of sea state, frequency, and range
2. Clutter measurements	ESSA	Obtain simultaneous multifrequency backscatter sea clutter measurements
3. Attenuation & Clutter Measurements	Raytheon/ APL	Obtain bistatic clutter and path loss measurements as a function of distance and frequency
4. Attenuation Over Irregular Inhomogenous Terrain	ESSA	Calculate the extra path loss for surface waves over irregular inhomogenous terrain
5. Cross Section Studies	SRI	Compile and evaluate known cross-section information on SLBM
6. Ship Model Measurements	SU	Calculation and model measurements of two typical ship's cross-section as a function of aspect, and frequency and polarization
7. Ship Cross Section	NRL	Measurement of the actual ship cross-section with the MADRE radar
8. Wake Study	ESSA	Theoretical investigation of the HF radar cross-sections of ship and submarine wakes as a function of frequency and aspect angle
B. Fleet Air Defense		
1. Feasibility Demonstration Test	ITT/NRL/APL	Initial feasibility demonstration of fleet air defense concept using skywave illumination with a distant transmitter and bistatic reception with close in receiver
2. Ship Detection	NRL	Investigation of detecting ships on a Doppler basis using the MADRE radar.
3. Ship Detection	SU	Investigating the detection of ships on a power basis using FM/CW high resolution technique.

(S) Figure 2. Participating Organizations, Tasks and Objectives (U)

(S)

TASK	ORGANIZATION	OBJECTIVES
C. Buoy Tactical Early Warning (BTEW)		
1. BTEW Feasibility Demonstration No.1	Raytheon/APL	Investigating the feasibility of detecting and tracking aircraft at short ranges using a buoy-based transmitter and land-based receiver using surface wave mode
2. BTEW Feasibility Demonstration No.2	Sylvania	Investigating the feasibility of detecting and tracking at long range using a buoy-based transmitter and a land-based receiver using skywave
D. Planning and Coordination	APL	Technical assistance to ARPA in the overall planning, and coordination of program

(S) Figure 2. Participating Organizations, Tasks and Objectives (cont) (U)

2. Sea Clutter (U)

(C) Sea-scattered energy was observed at 5 and 10 MHz, with transmissions both from a buoy moored 120 km from the shore and from Carter Cay. The observations were made both with CW signals and phase-coded signals, the latter with effective pulse lengths of 25 and 200 μs.

(C) The transmissions from the buoy proved considerably more important because the scatter area near the buoy is deep ocean water, rather than land or shoals, as in the case of the Carter Cay transmissions. The signal spectrum showed that the sea scatter was confined to two bands, or "pedestals", tenths of a hertz wide and located symmetrically within ½ hertz of the carrier; these observations agree with theory and predictions relating the Doppler shifts to the velocities of the Bragg resonant ocean waves responsible for scatter. The observed intensity for the sea clutter signal corresponds to an average scattering cross-section per unit area, σ^o, of between -24 and -30 dB, this agrees with a predicted upper limit of -23 dB.

B. Fleet Air Defense and Ship Detection (U)

1. Fleet Air Defense (FAD) (U)

(S) Detection of low-flying threats to surface vessels at a range sufficient to give useful warning time and tracking information is a problem which must be solved if the surface navy is to survive. Because of the advantage of denying the enemy the opportunity of using simple direction finding techniques to locate fleet units, it is desirable that the solution not require radiation from the fleet.

(S) The feasibility of using a hybrid (sky-wave/surface wave) system to solve this problem has been demonstrated during FY 70 as part of the MAY BELL Program. In this concept, the target is illuminated by sky-waves from transmitters (either shipborne or land-based) located over-the-horizon at ranges of perhaps 1000-2000 km. Surface waves which propagate from the target to a receiving system aboard a ship permit detections to be made even when the target is below the line of sight radar horizon.

(S) An experiment was performed at Cape Kennedy, Florida, where a shore-based receiving station was used to simulate the shipboard environment. A Navy P3V) aircraft served as a target by flying off-shore in a series of controlled flight plans, and illumination was provided by the MADRE and CHAPEL BELL transmitters located respectively in Maryland and Virginia. For most of these flights the target altitude was 200 feet, and detections were made at ranges as great as 100 km. It was shown to be possible to track the target in both range and azimuth with accuracies of about 5 nmi and one degree (depending on SNR). These results were obtained using a receiving/processing system which was assembled using existing equipment, and this equipment was in many ways not well matched to the experimental requirements, therefore, these results should not be taken as representing the capabilities or the limitations of a properly designed system.

(S) The dynamic range requirements imposed by the necessity of receiving small target echoes in the presence of the incident sky-wave and of clutter were found to be well within the capability of existing technology. Cross-polarized, bistatic target cross sections were also found to be of sufficient magnitude (up to 100 m^2 for the P3V) to permit detection. Clutter was found to be composed primarily of the resonant spectral lines which are generally well understood in terms of existing theory.

2. Ship Detection (U)

(S) The following is a summary of the various HF propagation techniques considered for ship detection.

(S) Monostatic Groundwave Radar has demonstrated a capability for the detection of surface vessels. On the ocean (away from land), it is predicted that very modest systems (two element antennas and a few hundred watts average power) can provide detections beyond 50 nmi. The limits of location accuracy, particularly in azimuth, have not been studied.

(S) Monostatic Skywave Radar has demonstrated a capability for detecting ships at one hop refraction ranges out to more than 1000 nmi. This has been done with coarse spatial resolution (60 nmi by 12-degree cell) and fine Doppler (0.1 Hz and smaller) resolution. If higher spectral resolution is employed, it is predicted that good ocean traffic surveys can be made on a daily basis. Optimum balance between the several forms of resolution has not been studied.

(S) Hybrid tests using skywave illumination to the target and groundwave propagation from target to receiver have been conducted. Examination of reference targets on the surface and of returns from the sea permit some predictions. It appears that a hybrid bistatic system can (in addition to its primary function of detecting A/C, SSM, and ASM) provide a surface vessel detection capability. That is, a "quiet" fleet unit equipped with the bistatic system could have many of the sensing abilities ordinarily provided by conventional active radar plus additional capabilities.

(S) It is recommended that the propagation of monostatic skywave radar illumination of the area around a fleet unit be further tested. In particular, determinations of the possibilities of ship unit observation of any attacking missiles or missile boat detections should be made. These tests should study contributions gained from the various forms of high resolution techniques and the requirements for real-time ionosphere assessment for optimum illumination.

(S) The bistatic hybrid surface wave concept should be tested in the ship-mounted environment; such tests could be concurrent with the monostatic tests. The potential of slow target detection should be confirmed and thoroughly described.

C. Buoy Tactical Early Warning (BTEW) (S)

1. BTEW-1 (U)

(S) The BTEW-1 concept involves detection of low flying aircraft at OTH distances by illuminating the target with a transmitter located on an off-shore buoy and reception of the target echo signal at a shore based receiver site via a ground wave propagation mode. Feasibility tests were conducted off the Florida coast using a transmitter located on Carter Cay (just north of Grand Bahama Island) and a receiving station at Cape Kennedy. The path length was 300 km and the target was a Navy P3V Aircraft.

(S) The feasibility tests were successful and demonstrated that standard radar calculation techniques, with application of Barricks' loss model could be used with reasonable confidence, to describe the coverage afforded by the BTEW-1 concept. The tests, then, established and validated a model for calculating coverage.

(S) Several variations of the original concept were examined, using the model, in a first attempt to assess potential capabilities in application to the defense of the CONUS, of special strategic areas, and of the fleet. The results of these analyses indicate that surveillance can be maintained out to ranges of 300 to 400 km from a shore station with systems of practical dimensions. For example, the east coast of the U.S. from Nova Scotia to the Straits of Florida, could be covered by about 10 shore stations and a fence of 30 buoys.

(S) Although the primary objective of the Florida tests was to detect low flying aircraft there was also the opportunity to observe the launch of a Poseidon missile from sea. Excellent detection results were obtained. No analysis has been attempted to describe the early warning potential of this kind of system against SLBM's; however, it seems apparent that significant coverage of this threat can be achieved with a very small number of terminals.

(C) The program has reached the point where basic feasibility has been demonstrated. Some refinement to the understanding of fundamental limitations is required but more emphasis now should be placed upon the definition of performance and interface requirements, of detailed concept definition, and upon examination of some of the more obvious engineering problems.

2. BTEW-2 (U)

(S) The BTEW-2 concept involves target detection at long OTH ranges by illuminating the target with a buoy mounted transmitter and reception of the target signal at a remote receiver site via sky-wave. Tests of this concept were successful but indicated that coverage would be very limited for any presently practical level of buoy transmitter power.

III RECOMMENDATIONS (U)

A. Additional Measurements (U)

(C) The committee recommends that additional measurements be undertaken over a 5 to 6 month period. The primary purpose of such measurements would be to obtain needed information about daily path loss fluctuations with sea state and atmospheric refractivity. Data presently available are insufficient to study these effects or establish trends and conclusions. In addition, the water along the previous path is not typical of the deep ocean. An ideal path, for example, would be the 300 - 400 km over-water stretch from Cape Cod to Northern Maine. Daily signal strength measurements should be made on 5, 10, 15, and 20 MHz and with phase-coded signals so as to eliminate sky-wave contamination.

B. Reduction of Existing Data (U)

(C) As much as possible of the existing path loss measurements on 5, 15, and 20 MHz should be processed by Raytheon. Means, variances, and confidence levels of the path loss data should then be computed. NRL personnel should complete the reduction of aerial profilometer wave-height data taken on several days during the radio measurements. These should provide some positive basis for comparison and correlation with sea state. Where possible, brief analyses should be undertaken to permit rough estimates of the effects of atmospheric ducting on the received signal.

C. Fleet Air Defense (FAD) (U)

(S) Now that the feasibility of the hybrid (sky-wave/surface wave) system concept for Fleet Air Defense has been demonstrated beyond any reasonable doubt, it is recommended that during the coming year (FY ~1) the following efforts should be carried out as the next step toward the goal of developing an operational system:

- Provide a receiving/processing system which is mobile and suitable for installation aboard a ship such as a destroyer, which can eventually be integrated into a fully automated system.
- Investigate the shipboard antenna problem, select elements best suited to the FAD requirements, and provide an antenna system for shipboard use.
- Test the performance of this receiving/processing and antenna system in a land-based experiment using available illuminators (MADRE and CHAPEL BELL).
- Repeat these tests in a shipboard experiment.

(S)
- Pursue Fleet Air Defense System studies to further define the performance requirements, the interaction with other systems, and the operational utility.
- Make model measurements of the cross sections of representative aircraft and missile targets for various frequencies, polarizations, and bistatic geometries.

D. Buoy Tactical Early Warning (BTEW)

(S) It is recommended that systems analysis be continued with emphasis in the following areas:

- To provide a more complete description of coverage capabilities for various deployment concepts.
- To establish the mission and provide a definition of performance and interface requirements.
- To perform a preliminary cost trade-off analysis of the various deployment concepts.
- To investigate the antenna gain and land-sea interface problems.
- To recommend techniques for target location and tracking.
- To assess the magnitude of the dynamic range problem and to recommend solutions.
- To obtain bistatic cross-section information on representative aircraft and missile targets.

REFERENCE

1. D.E. Barrick, "Theory of Ground-Wave Propagation Across a Rough Sea at Dekameter Wavelengths (U), "Research Report, Battelle Memorial Institute, Columbus, Ohio, January 1970, UNCLASSIFIED

SECTION 2

SUMMARY OF PAPERS (U)

PROGRAM OBJECTIVES (U)

THIS PAGE INTENTIONALLY LEFT BLANK

DETAILED PROGRAM OBJECTIVES AND KEY ISSUES (U)

Dr. J. W. Follin, Jr.

The Johns Hopkins University
Applied Physics Laboratory
8621 Georgia Avenue
Silver Spring, Md. 20910

I INTRODUCTION (U)

(S) The MAY BELL program is aimed at obtaining solutions to the sea surveillance problem both for tactical early warning of missiles and aircraft attacking the continental United States and for fleet air defense; that is, over-the-horizon surveillance of attacking missiles, aircraft and ships. (See Figures 1 and 2.) A large number of system configurations can be used to solve parts of these problems. At this workshop we wish to determine the best combinations of systems to do the job and to estimate the effectiveness of these combinations.

(S) For tactical early warning it is possible to use land-based monostatic skywave or surface wave radars or a ship-based surface wave radar. Various bistatic systems involve buoys providing line-of-sight or surface wave target illumination with either surface wave, or skywave, transmission to a land-based receiver. One interesting possibility would be transmission in the opposite direction since much higher power can be achieved, leading to a 40 dB improvement in system performance. In some geometries it appears that a buoy-to-buoy bistatic system would be effective. Finally, the use of an aircraft to generate a synthetic receiving aperture in conjunction with a skywave illuminator may provide the surveillance desired.

(S) For the fleet air defense system, choices are limited if it is desired to maintain radar silence aboard ship. A monostatic land-based skywave radar can monitor the ocean around the fleet and transmit the information through appropriate communication links. Bistatic systems include the skywave target illumination and surface wave propagation to the ship, buoy line-of-sight or surface wave target illumination, and surface wave propagation to ship, and airborne synthetic aperture as above.

(S)

TACTICAL EARLY WARNING

TARGETS

SLBM
SLCM
A/C

SYSTEMS

MONOSTATIC
SURFACE WAVE RADAR
SKYWAVE RADAR

BISTATIC
BUOY LOS TARGET SURFACE WAVE TO LAND OR REVERSE
BUOY LOS TARGET SKYWAVE TO LAND OR REVERSE
BUOY-BUOY
SKYWAVE ILLUMINATE – A/C SYNTHETIC APERTURE RECEIVE

FLEET AIR DEFENSE

TARGETS

SLCM
A/C
SHIPS

SYSTEMS

MONOSTATIC

LAND-BASED SKYWAVE RADAR

BISTATIC
LAND-BASED SKYWAVE ILLUMINATE SURFACE WAVE TO SHIP
BUOY LOS ILLUMINATE – SURFACE WAVE TO SHIP
SKYWAVE ILLUMINATE – A/C SYNTHETIC APERTURE RECEIVE

(S) Figure 1. MAY BELL Program Objectives, Sea Surveillance (C)

(S)

SECRET

SURFACE WAVES

- CLUTTER
- PROPAGATION
- CROSS SECTIONS

SKYWAVES

- COHERENCE OF PROPAGATION IN NEARBY PATHS
  - FADING
  - DOPPLER SHIFT
  - FARADAY ROTATION
  - MULTIPATH

SHIPS

- ANTENNAS
- RFI (LOCAL)

BUOYS

- ANTENNA
- POWER
- SECURITY

SYSTEMS

- ECM
- NUCLEAR ENVIRONMENT
- GIVE-AWAY OF INFORMATION TO ENEMY

SECRET

(S) Figure 2. Key Problems (U)

(S) Before the effectiveness of these systems can be determined, the following key technical problems that must be answered: for surface waves, the effects of sea state on clutter and propagation; for sky-waves, the coherence of the ionosphere on nearby paths. For ships one problem is effective antenna aperture and beam steering in the presence of resonant superstructure, and second, the problem of RFI from intermodulation products from other transmitters aboard ship. For buoy platforms, the problems are adequate antennas, power and security and to some extent survivability of the buoy. Key system problems, in addition to accuracy, coverage, and effectiveness, are ECM, a nuclear environment, and finally possible give-away of information to the enemy as a result of our transmissions.

(U) These key problems are the basis of the questions prepared for the discussion groups and it is hoped that most of them can be answered at this workshop.

II REQUIREMENTS FOR EARLY WARNING (U)

(S) The usefulness of an OTH early warning system depends on the probability of detection, the probability of false detections, and the accuracy of location and identification. These parameters are interrelated and depend on the amount of additional warning time achieved.

(S) For Fleet Air Defense (see "Fleet Air Defense Requirements (U)" by Paul T. Stine, SECRET and "Fleet Air Defense Requirements for Early Warning (U)" by Richard J. Hunt, CONFIDENTIAL), a minimum of five minutes (until the threat comes over-the-horizon is required to get the ship to general quarters, and fifteen minutes if fighters have to be scrambled. The required accuracy is ±5° since the target must be designated within the 15 - 20° acquisition sector scan of the fire control radars. It is especially important to note that attempts to defeat a cruise missile by ECM or chaff are much more effective before a missile locks on a ship.

(S) For buoy tactical early warning aircraft detections should allow interceptors to be scrambled for intercept outside ASM range. Typically this requires ranges of 200 - 300 nmi and an accuracy of 5 nmi.

THEORY AND MEASUREMENTS (U)

THIS PAGE INTENTIONALLY LEFT BLANK

THEORY OF ATTENUATION AND CLUTTER (U)

Donald E. Barrick

Battelle Memorial Institute
505 King Avenue
Columbus, Ohio 43201

1 INTRODUCTION (U)

(U) Over the past year and a half, work has been underway on the problem of the interaction of an HF radio wave with the rough sea. Two main phenomena were of concern in the study: 1) attenuation suffered by a ground wave propagating across the ocean under varying sea state conditions; and 2) the scatter (or clutter) returned to the receiver from the ocean and its relationship to sea state. Both phenomena could conceivably be limiting factors in radar performance, and a knowledge of their magnitude is of importance in the design and development of such a system.

(U) On the question of increased attenuation versus sea state, no measurements made before the MAY BELL Program were complete enough to either confirm or deny any dependence on sea state. Nor was any theoretical prediction available as to the expected magnitude of such an effect. With regard to clutter or sea scatter, measurements have been available for nearly 15 years which have satisfactorily explained the nature and mechanism of the interaction. From observed Doppler shifts it was surmised that ocean waves scatter according to the Bragg mechanism, in the same manner as a simple diffraction grating. Measurements of the magnitude of the sea scatter echo and its relationship to sea state at HF have been considerably less complete; only recently have more thorough measurements along these lines been undertaken by Crombie of ESSA, Headrick and others at NRL, and Barnum of Stanford, as well as the work on data reduction presently underway at Raytheon. These efforts, all reported under the MAY BELL Program, should provide valuable data on observed sea clutter strength. As to the theory, it was only in recent years that Wetzel and Barrick related the strength of the received signal spectrum directly to the ocean waveheight spectrum evaluated at the Bragg spatial wavenumbers. This enables a quantitative connection between echo strength and sea state which should complement the measured data.

II SUMMARY OF ATTENUATION PREDICTIONS (U)

(U) The problem of attenuation of a surface wave propagation above a rough sea has been attacked in the following manner. First, an effective surface impedance is derived which accounts for the roughness as well as the finite conductivity of sea water. Then this effective surface impedance is used in an ESSA computer program to predict the basic transmission loss between two points over the sea versus sea state.*

(U) The calculation of the effective surface impedance of the sea at HF is facilitated because 1, the ocean wave height is small compared to wavelength, 2, the surface slopes are small, and 3, the sea water is highly conducting at HF. Consequently, the boundary perturbation approach of Rice was used along with the Leontovich boundary condition for the surface. The results show that the effective impedance (accounting for roughness) consists of two terms, one which is merely the impedance of sea water alone and the other which contains the effect of roughness. The latter involves an integral over the ocean wave height spectrum. In evaluating the latter numerically, the Phillips wind-wave spectrum for the ocean surface was selected as a "typical" model. The presence of swell is neglected in this model, as well as any actual directionality. One thus obtains results for the effective impedance which are functions of wind speed.

(U) When these effective impedances are employed in the ESSA groundwave program, numbers for basic transmission loss are obtained. To show clearly the effect of sea state, loss difference (in decibels) between a perfectly smooth sea and various conditions of roughness were plotted. Figure 1 shows such an example for 10 MHz, versus range and wind speed. The conductivity of ocean water was taken as 4 mho/m and a 4/3 earth refractivity factor was used in the program. Transmitter and receiver are assumed located on the surface in Figure 1. In Figure 2, the actual basic transmission losses (rather than the differences) are shown from a surface-based source to an elevated receiver. The first number is the loss for a perfectly smooth sea and the second is for sea state 5 (i.e., 25-knot wind).

(U) The results show that sea state effects become more pronounced at greater ranges. For example, at 10 MHz and 100 nmi range, the signal variation due to sea state is of the order of 8 dB for one-way propagation.

*A report showing the details and results of this work is available as "Theory of Ground Wave Propagation across a Rough Sea at Dekameter Wavelengths" by D. E. Barrick, Battelle Memorial Institute, January 1970.

III SUMMARY OF CLUTTER CALCULATIONS (U)

(U) The analysis of scatter from the rough ocean surface is approached with the same technique as used for the attenuation calculations – namely, the Rice perturbation analysis along with the Leontovich boundary condition.* The results of this study show that the incremental received power spectral density and absolute power scattered from the patch of sea, ds, can be expressed in the usual radar range equation form as

$$dP_R(\omega) = \frac{4P_T G_T G_R \lambda^2}{(4\pi)^3 R_T^2 R_R^2} F_T^2 F_R^2 \sigma(\omega)\, ds \quad , \quad dP_R = \frac{4P_T G_T G_R \lambda^2}{(4\pi)^3 R_T^2 R_R^2} F_T^2 F_R^2 \sigma^o\, ds$$

Transmitted power is P_T, antenna gains are G_T, G_R, distances from transmitter to the patch ds and from the patch ds to receiver are R_T, R_R, and wavelength is λ. The quantities F_T and F_R are the Norton attenuation functions from target patch to the transmitter and receiver, respectively. (They approach unity for short ranges.) They can be expressed in terms of the basic transmission loss, L_T (in dB), for example, as

$$F_T = \frac{2\pi R_T}{\lambda} \cdot 10^{L_T/20}$$

(U) The sea scatter cross section σ^o and related spectral density for vertical polarization obtained from the analysis are

$$\sigma(\omega) = \pi k_o^4 (1 - \cos\varphi)^2 W[k_o(\cos\varphi - 1), k_o \sin\varphi, \omega - \omega_o] \quad ,$$

$$\sigma^o = \pi k_o^4 (1 - \cos\varphi)^2 W[k_o(\cos\varphi - 1), k_o \sin\varphi]$$

where $k_o = 2\pi/\lambda$ $f_o = \omega_o/2\pi$ is the carrier frequency, φ is the bistatic angle from the forward scatter direction, $W(p, q, \omega)$ is the spatial-temporal waveheight spectrum for the sea and $W(p, q)$ is the spatial waveheight spectrum only. The normalization between power and power spectral density is

$$\sigma^o = \tfrac{1}{2} \int_{-\infty}^{\infty} \sigma(\omega)\, d\omega \quad .$$

(U) As seen in the above equations for $\sigma(\omega)$ and σ^o, the spatial wavenumbers appearing in the waveheight spectra for p and q are precisely those required for Bragg scatter. This confirms the interpretation deduced from measurements.

*A report giving derivations of sea scatter and the signal spectrum is in preparation. Most of the derivations are also found in a paper "The Interaction of HF/VHF Radio Waves with the Sea Surface and Its Implications", by D.E. Barrick, presented at AGARD "Electromagnetics of the Sea" Meeting, June 1970.

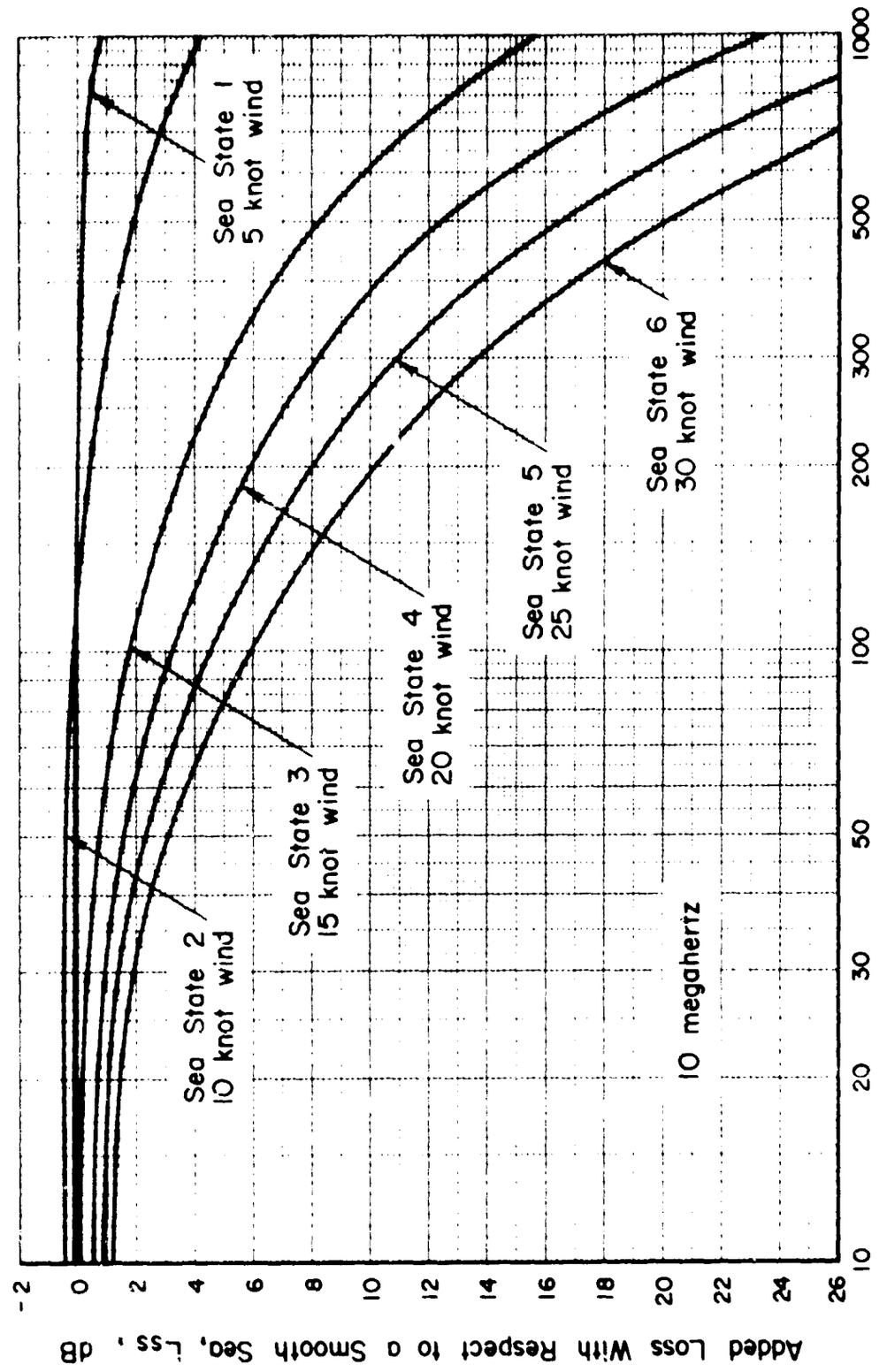

(U) Figure 1. Added Transmission Loss Due to Sea State at 10 MHz. Antennas are Located Just Above Surface. Phillips Isotropic Ocean-Wave Spectrum. (U)

UNCLASSIFIED

UNCLASSIFIED

(U)

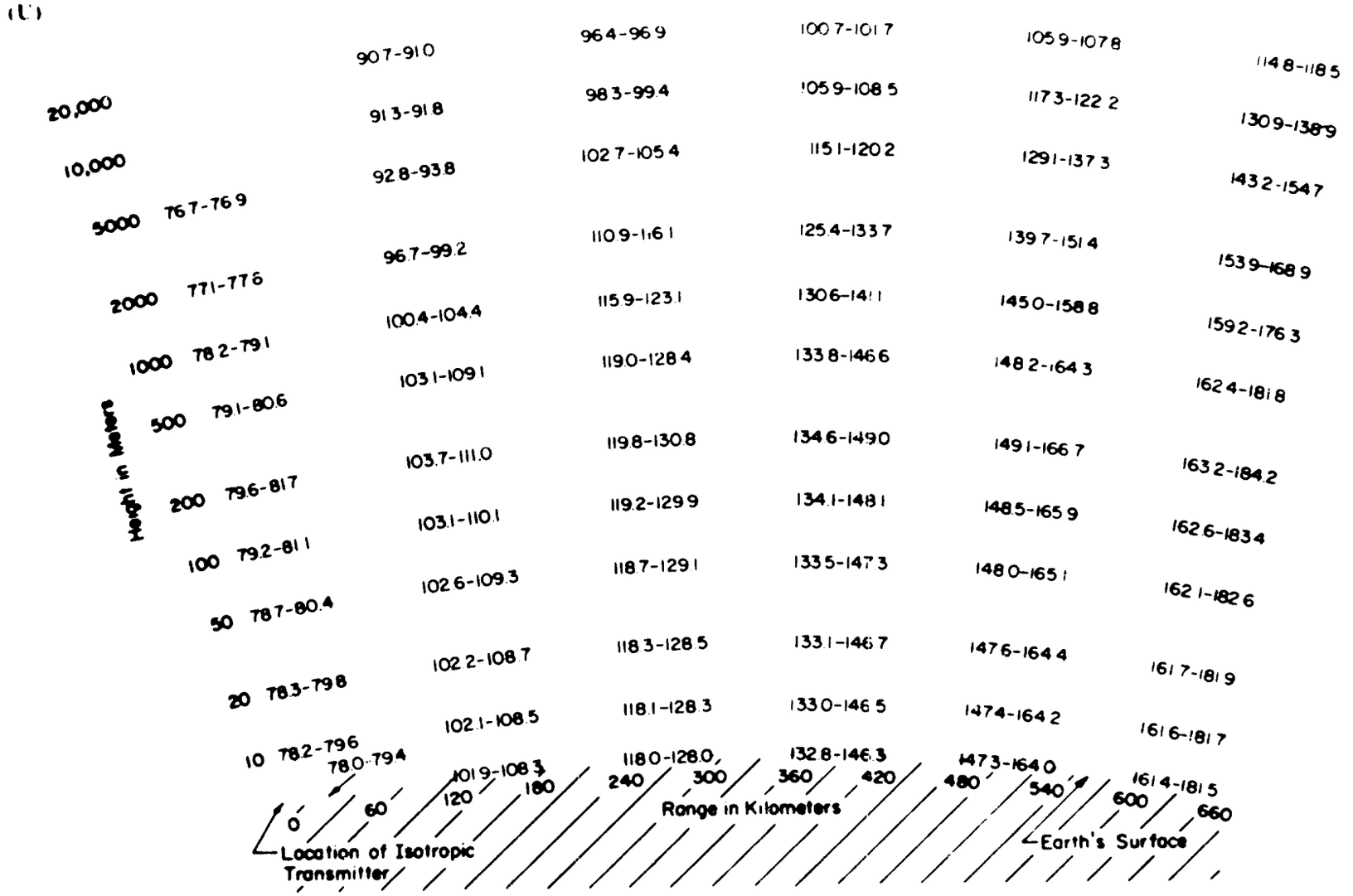

(U) Figure 2. Basic Transmission Loss to Points at Various Heights and Ranges above the Ocean at 10 MHz. First Number is for Perfectly Smooth Sea, Second is for Sea State 5 (25 knot wind). Phillips Ocean-Wave Spectrum. (U)

(U)

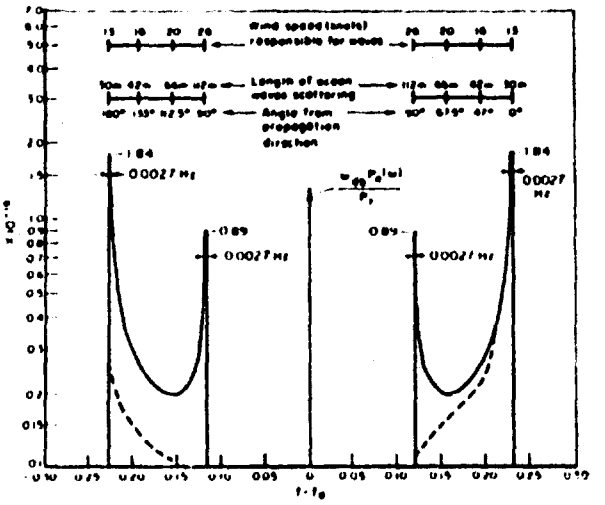

(U) Figure 3. Received Clutter Signal Spectrum at 5 MHz for Bistatic Radar with 100-km Baseline, Effective Pulse Length 12.5 μs, and for Time Delay One Pulse Length Behind Direct Pulse. Phillips Isotropic, Fully Aroused Ocean-Wave Spectrum is Assumed (Solid Line). Dashed Line Represents Likely Measurements from Nonisotropic Sea. (U)

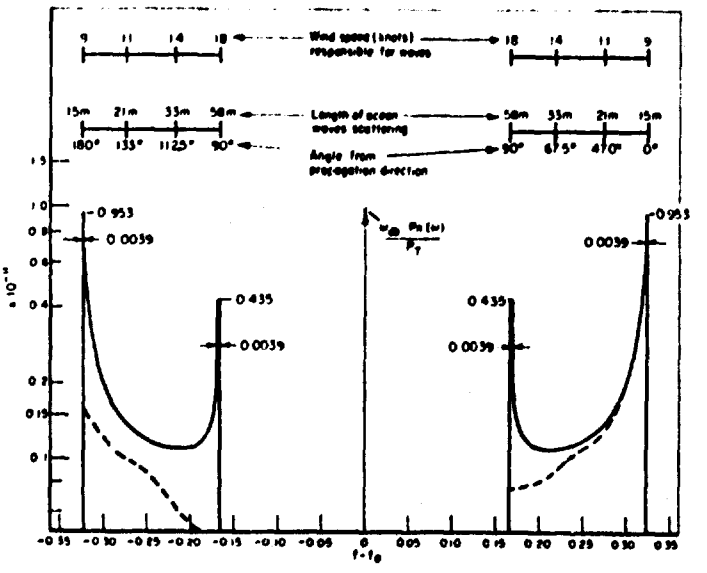

(U) Figure 4. Received Clutter Signal Spectrum at 10 MHz for Bistatic Radar with 100 km Baseline, Effective Pulse Length 12.5 μs, and for Time Delay One Pulse Length Behind Direct Pulse. Phillips Isotropic, Fully Aroused Ocean-Wave Spectrum is Assumed (Solid Line). Dashed Line Represents Likely Measurements for Nonisotropic Sea. (U)

(U) To estimate the level and shape of sea clutter signals, the Phillips isotropic wind-wave spectrum is again employed; σ^o, obtained in this manner for bistatic scatter, is -23 dB. This value is more likely an upper limit because the sea in practice is neither isotropic nor fully developed, as implied in the model.

(U) The Phillips isotropic wind-wave model is again used to calculate the clutter spectrum for a bistatic surface-surface radar. The sea is assumed fully developed. The antennas are quarter-wave vertical monopoles, located over sea water, separated by 100 km. The signal permits an effective time (or range) resolution of 12.5 μsec. The elliptical range cell selected corresponds to one pulse length after receipt of the direct signal. Figures 3 and 4 show the expected spectra at 5 and 10 MHz, normalized to the incident power. The frequency, $f_{db} = \omega_{db}/2\pi$ is the cutoff on the outer sides of the clutter pedestals, i.e., 0.228 and 0.322 Hz respectively. The height observed for the "ears" depends upon the processor resolutions; the less the resolution, the shorter the ears.

(U) The interpretation of these bistatic clutter spectra is again in conformance with the Bragg scatter mechanism. The higher frequencies in the pedestals come from the ends of the elliptical resolution cell near the backscatter directions. The lower frequencies in the pedestals come from the sides of the ellipse, nearer the forward scatter region. For larger ellipses corresponding to longer delays, the pedestals collapse to an impulse function centered on f_{db}, the backscatter Doppler.

(U) The total clutter power received in this range cell is about 23 dB below the direct signal. Again, observed clutter signals are likely to be lower because the sea is rarely fully developed and isotropic for these radar frequencies. Therefore, a difference between clutter and direct signal of 30 dB would be expected to be typical.

THIS PAGE INTENTIONALLY LEFT BLANK

BOMEX SEA SCATTER OBSERVATIONS (U)

D. D. Crombie

Institute for Telecommunication Sciences
ESSA Research Labs, Boulder, Colorado 80302

I INTRODUCTION

(U) Observations were made during the BOMEX project of the coherent backscatter of HF ground waves from the sea, along the east coast of Barbados Island. The data were taken using a multifrequency coherent HF radar system operating in the range of 1.7 to 12.37 MHz. Successive pulse pairs were transmitted in each of eight preselected frequencies in the above range. The demodulated signals were sampled at four ranges (22.5 - 100 km), passed through an A/D converter, and recorded digitally (10 bits) with an incremental tape recorder.

(U) Short vertical broadband monopoles were used for transmission and reception. Two of these were spaced 100 ft. apart and switched alternately to the receiver between each pair of transmitter pulses on the same frequency. Thus, 64 separate sets of data were recorded.

(U) The basic repetition rate of the transmitter was 60 pulses/second and the pulse length was 40 μs. Thus, each set of data (one antenna, one range and one frequency) was sampled 3¾ times per second.

(U) The radiated power and receiver/antenna sensitivity were determined using a field strength meter, and a small target transmitter located several hundred feet from the antennas. Calibrations were made at each operating frequency. Radiated powers ranged from 26 watts at 1.7 MHz to about 1 kW at the higher frequencies.

(U) The transmitting and receiving antennas were situated about 150 ft. from the edge of a cliff which was about 30 ft. above, and 200 ft. away from the water's edge.

II DATA ANALYSIS (U)

(U) Thirty-minute samples of data were taken and subjected to fast Fourier transformation in the computer at Boulder. The program was written to identify the spectral densities and the bandwidths at the -3, -10 and -20 dB levels as well as the frequencies of the spectral peaks. From these data the RMS signal level at each peak could be obtained. Knowing the receiver sensitivity and the radiated power, the scattering cross section, σ, of the sea could be calculated from the following formula,

$$\sigma = \frac{d^4 \ E^2_r}{2.25 \times 10^4 \ P} \bullet m^2$$

where

d = distance of the scatterer in km,
E_r = received field strength in μV/m, and
P = radiated power in kW

(U) This definition of σ, which is particularly appropriate to ground wave radar, results in values which are smaller by a factor of three than free space formula. The factor three arises because it is assumed that the scatterer behaves as a short vertical monopole contributing a factor of 1.5 that re-radiates into the hemisphere above the sea contributing a factor of 2. The effects of ground wave attenuation are not included in this formula.

III OBSERVED SCATTERING CROSS SECTIONS (U)

(U) Some of the values of σ observed at a range of 22.5 km, where ground wave attenuation can be ignored, are shown in Figure 1. The right-hand scale shows the value of relative scattering cross section σ° (i.e., cross section per unit illuminated area). The values shown are for approaching waves resulting from partially or fully developed seas at wind speeds of from 10 to 20 kts. The receding components have cross sections about 20 dB smaller. The values shown are averaged over the whole 180° sector illuminated by the transmitter.

IV SPECTRAL DENSITY OF THE SEA SURFACE (U)

(U) Knowing the scattering cross section and the bandwidth of the scattered signal, it is possible to determine the non-directional spectral density, S(f), of the sea surface for the wavelengths observed.

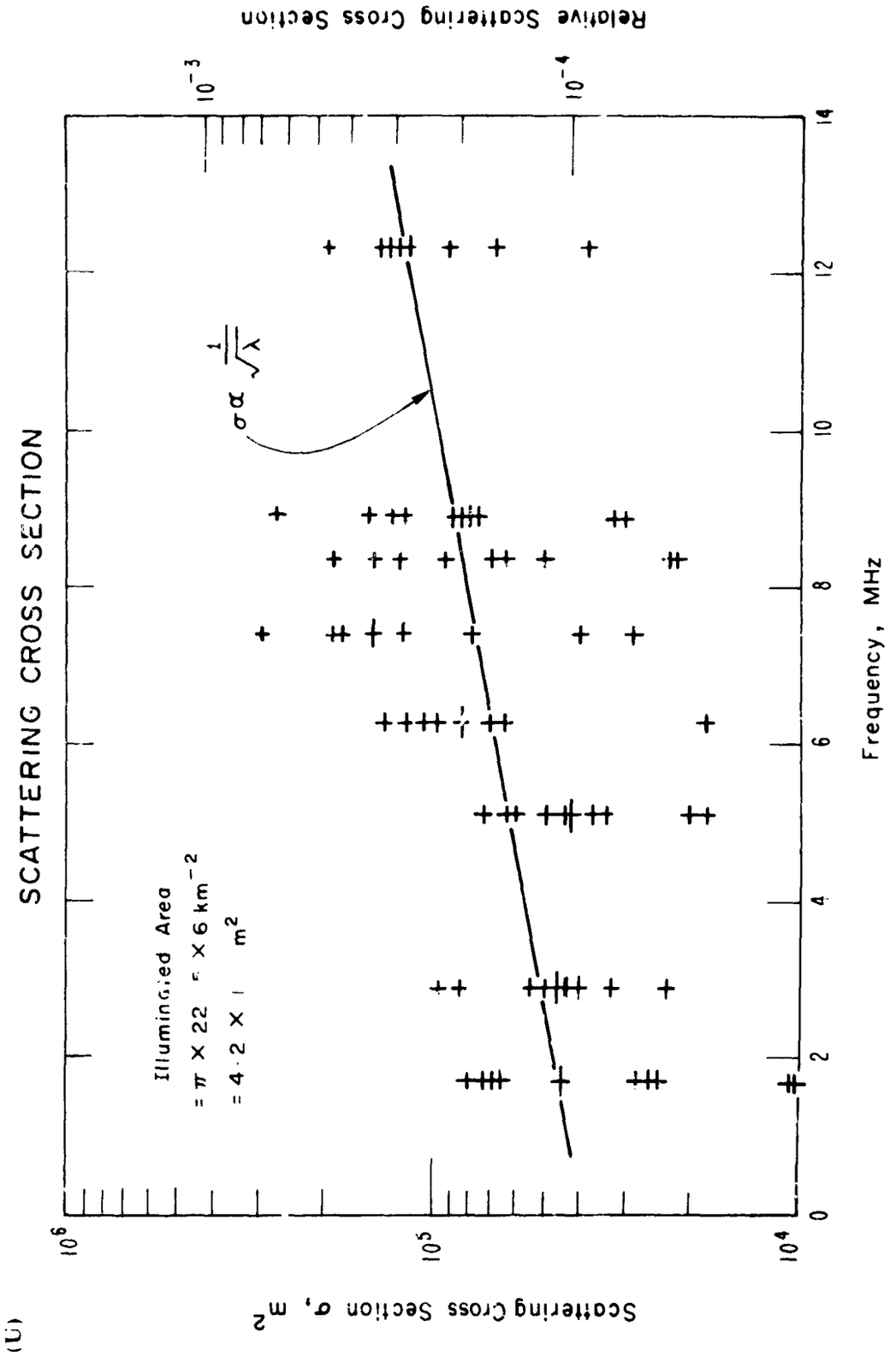

(U)

(U) Figure 1. Observed Scattering Cross-sections (U)

(U)
The required relationship is

$$S(f) = \frac{\sigma L^{2.5}}{\pi^2 d d_0 \sqrt{\frac{g}{2\pi}}} \quad m^2/sec$$

where σ is the scattering cross section in m^2 at a sea wavelength L meters or a wave frequency of F hertz, d is the range (m), d_0 the radial length (m) of the illuminated area, and g is the acceleration of gravity.

(U) Some examples of nondirectional frequency spectra obtained in this way are shown in Figure 2. The lower curve shows an observed spectrum for comparison with Moskowitz's 20-kt synoptic spectrum. The next curve shows the results for a wind believed to be lighter than for the lower curve. The two upper curves show spectra obtained at the same time as the NASA wave-measuring aircraft was flying over the area (in the downwind direction) where the radar data were obtained. Significant wave heights derived from the NASA data are also shown for comparison with those derived from the spectra shown. The agreement is good and although the wave heights are small, the comparison shows that wave heights and spectra can be obtained from backscatter data. However, to be useful under rougher conditions, the radar wavelengths need to be increased.

V BANDWIDTH OF THE BACKSCATTERED SIGNALS (U)

(U) Some representative bandwidths of backscattered signals are shown in Figure 3. The plotted values are the bandwidth 10 dB below the spectral peak. Plots of the spectra show a strong tendency towards a Gaussian shape rather than the sin x/x form expected from simple theory. The points in Figure 3 show that the Doppler bandwidth increases with frequency but that the rate of increase depends on sea state. The points for 11 July represent relatively rough conditions, while those for the 14 and 16 July represent rather quieter seas.

VI SHIP SCATTERING CROSS SECTION (U)

(S) During the BOMEX observations some data was obtained about the cross section of the USCGS ship Mt. Mitchell. The revised estimated cross section was ~ 400 m^2 using the definition of σ given in equation 1. The frequency used was 2.9 MHz. Observations at other frequencies were unsuccessful because of the high noise and interference levels present during the nighttime observations.

(U)

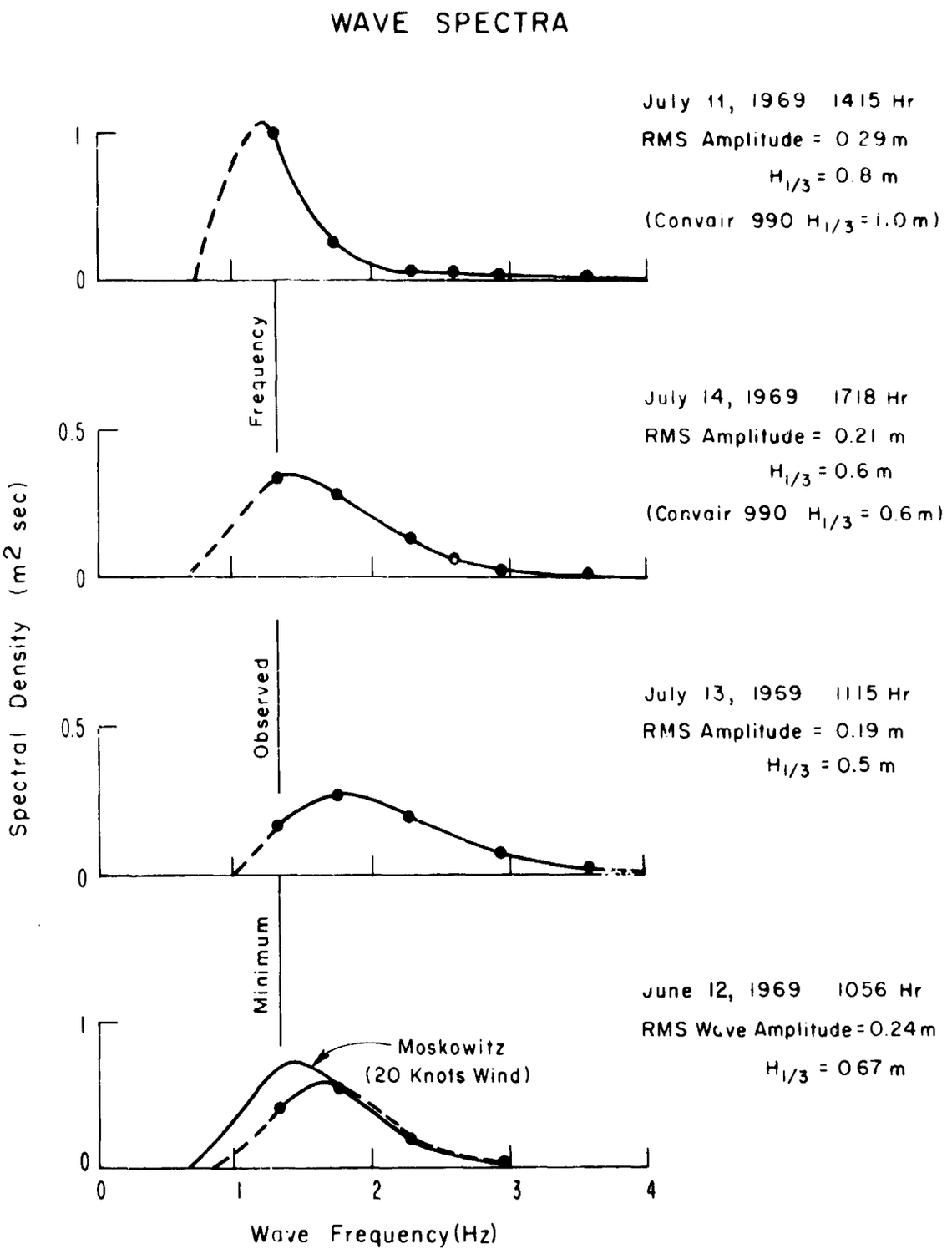

(U) Figure 2. Wave Spectra Deduced from Cross-sections (U)

(U)

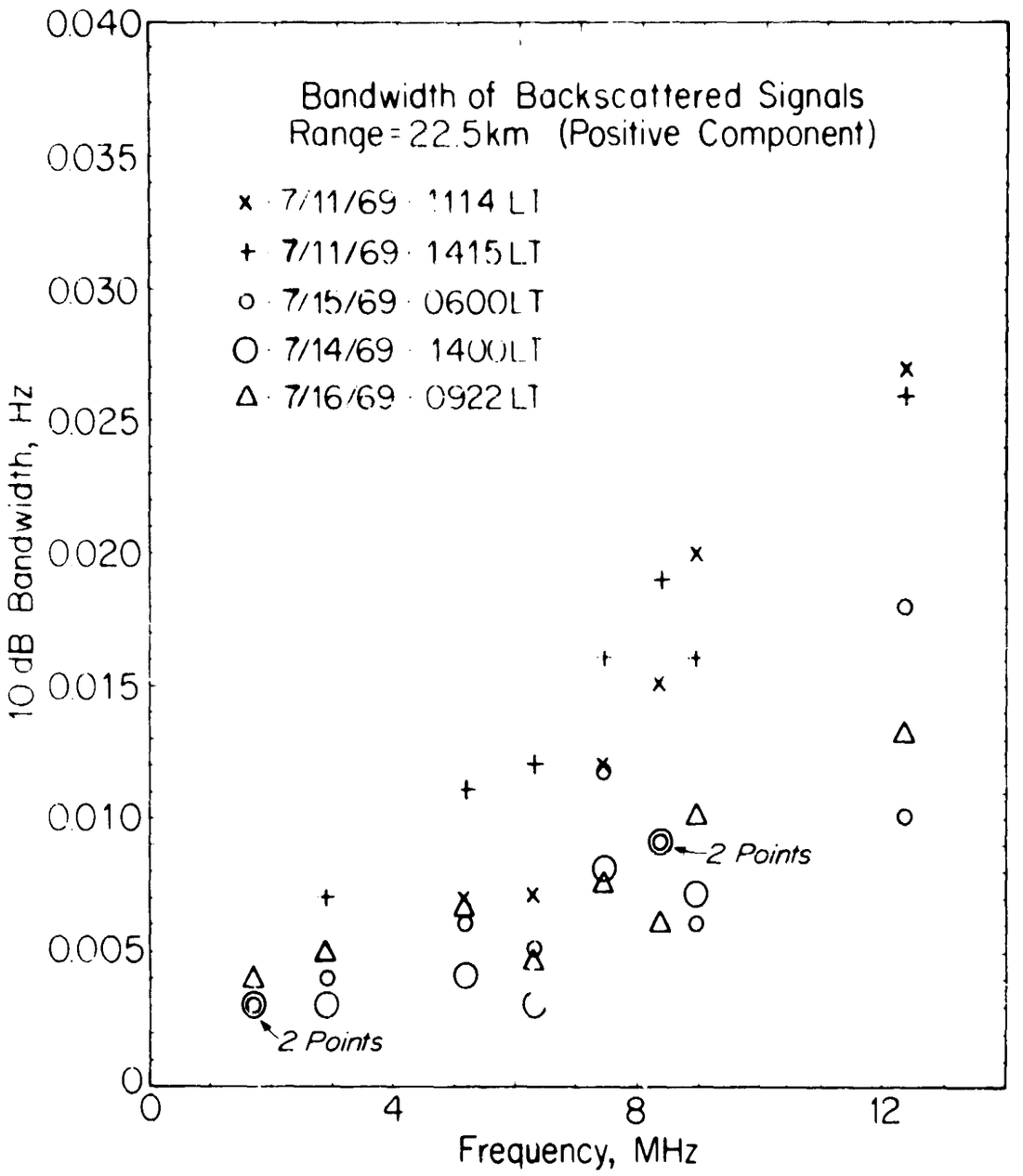

(U) Figure 3. Observed Bandwidths of Backscattered Signals (U)

(U) The Mt. Mitchell has an overall length of 231 feet, beam of 42 feet and a displacement of 1627 tons. The funnel top is approximately 40 feet above the water line, the top of the tallest mast is 70 feet above the water line. The masts are approximately 100 feet apart.

(S) When the cross section is increased by a factor of 3 to bring it in accordance with conventional free space definitions of σ the value becomes 1200 m^2. Theoretical estimates of the cross section of a dipole 140 feet long in free space, at 2.9 MHz gives ~1000 m^2. The agreement appears good, but the theoretical estimate is strongly dependent on the effective length of the mast.

VII CONCLUSIONS (U)

(S) The main conclusions from this work using a monostatic backscatter radar are the following.

- The average scattering cross section of the sea can be estimated if the non-directional spectrum of the sea is known.
- The intrinsic bandwidth of the back scattered signals is very small but increases with frequency and sea state.
- It appears that there is reasonable agreement between theoretical estimates of ship cross sections based on mast height, and a measurement (see Section VI).

THIS PAGE INTENTIONALLY LEFT BLANK

MEASUREMENTS OF PATH LOSS (U)

H. Hoogasian

Raytheon Company
Equipment Division
OHD Advanced Development Department
Spencer Laboratory
Burlington, Massachusetts

I OBJECTIVE (U)

(U) The primary interest of MAY BELL ground wave signal amplitude experiments was to measure path loss on several frequencies, to correlate the signal fluctuations with sea state, and to test the validity of the rough ocean scattering model developed by D. Barrick of BMI.

II APPROACH (U)

(U) Surface wave signal levels were measured on a propagation path between the transmitter site on Carter Cay in the Bahamas and the receiving site at Cape Kennedy. There were two transmitters on Carter, radiating about 1 kW over monopole antennas. During the first three months of 1970 operation was on four frequencies, near 5, 10, 15, and 20 MHz.

(U) Signals were received on the ITT 16-element array on all frequencies during the entire program and with reference monopole antennas on 5, 10 and 15 MHz over a shorter period. All transmitting and receiving antennas were in close proximity to the shoreline so that the propagation path was substantially over an open stretch of ocean for a distance of 300 km between path terminals. However, approximately 80 km of this distance lay inside a shoal line defining a region of low water with depths ranging from 1 to 5 fathoms.

(U) The index for sea state used in making comparisons was taken to be hindcast wave height (see Figure 1). The reference smooth sea datum was Norton's prediction for ocean water with conductivity of 5 mhos/m. In this analysis, computed signal levels were derived from Norton's formulation for a radiating elementary monopole. Estimates for the available power from a receiving monopole were then computed from the free space aperture, using the free space gain of 2 dB for the monopole.

III RESULTS (U)

(U) Path loss data on 5 MHz with monopole reception (see Figure 2) was available for 13 days in March. Signal level fluctuations over a range of 5 dB were measured. The lowest value of signal level was observed around the 9th of March where hindcast data showed a maximum wave height of 13 feet.

(U) On 10 MHz, loss data from the monopole system (see Figure 3) showed little convincing day-to-day correlation with hindcast data with the exception of the period 10 March - 15 March, during which rough seas were reported. During this time, the signal level dropped by approximately 10 dB below the estimate for a smooth sea. The overall spread in power measurements, 0 dB to 10 dB below reference, agrees closely with the Barrick predictions for a distribution of sea states ranging from 0 to 5.

(U) There were 11 days when the 15-MHz signal was received on the BSA. The BSA was calibrated against the 15-MHz monopole and BSA measurements were adjusted accordingly. Although the data base was more restricted, the 15-MHz data displayed trends similar to the 10-MHz data; little or no correlation with hindcast except for the March 10 - March 15 period, and a data spread ranging from 2 dB above to 10 dB below the smooth sea estimate. This compares to Barrick's estimate of about +1 to - 14 dB for sea states 0 to 5.

(U) The data base for 20 MHz (see Figure 4) was 6 days. Data was collected on the BSA but a reference monopole was not available for calibration. Consequently, the BSA gain was assumed to include the full 12-dB theoretical array factor. On this basis, the values of received power display a range to 15 dB below the smooth sea estimate. There was insufficient data to search for low signal values in the March 10 - March 15 period.

(U) A comparison was made of hindcast data (see Figure 1) with wind speeds recorded over the same period at GBI and Cape Kennedy. Only a fair correlation was noted. In the hindcast data, the occurence of northerly winds appeared to coincide with the highest values of wave height. This would imply ocean waves travelling in a direction more or less transverse to the propagation path, where the effect on path loss is minimal, and consequently would be expected to produce a decorrelating effect between sea state and signal level on a point-to-point basis.

(U) Skywave contamination proved to be a serious problem on all frequencies. On analysis, a substantial portion (about 40 per cent) of the data was rejected on the basis of suspected biasing by skywave signals. The elimination was accomplished primarily by examining the peaks of the signal spectral density for stability over a relatively long period.

IV SIGNIFICANCE (U)

(U) It is concluded that the measurements showed little day-to-day correlation with hindcast data for the sea except for one high sea state period in March. Treated as a whole, however, the body of data did exhibit an unquestioned frequency behaviour substantially in conformity with the referenced predictions for the sea states encountered.

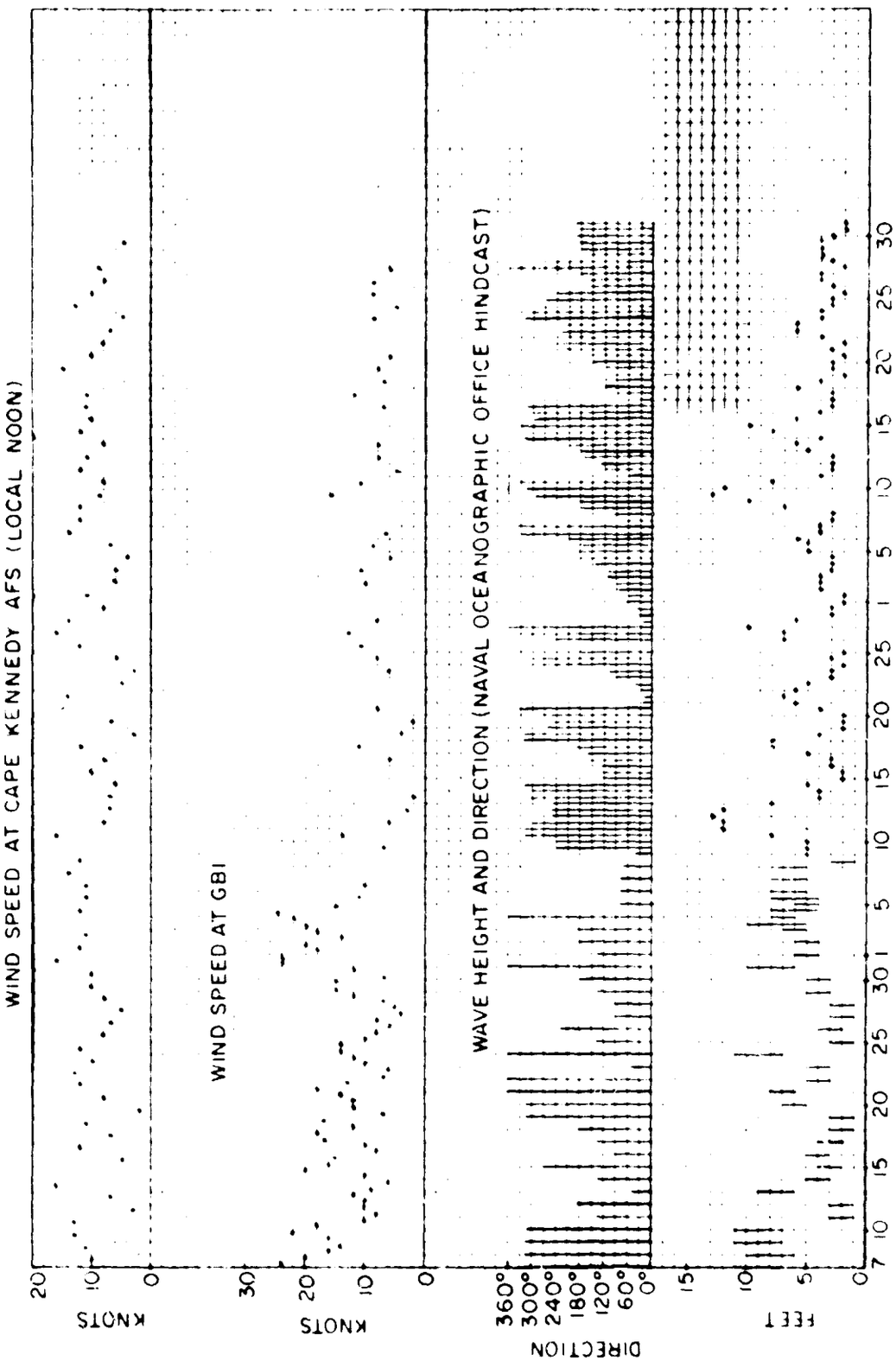

(U) Figure 1. Windspeed and Wave Height, January – March 1970 (U)

(U)

UNCLASSIFIED

UNCLASSIFIED

(U)

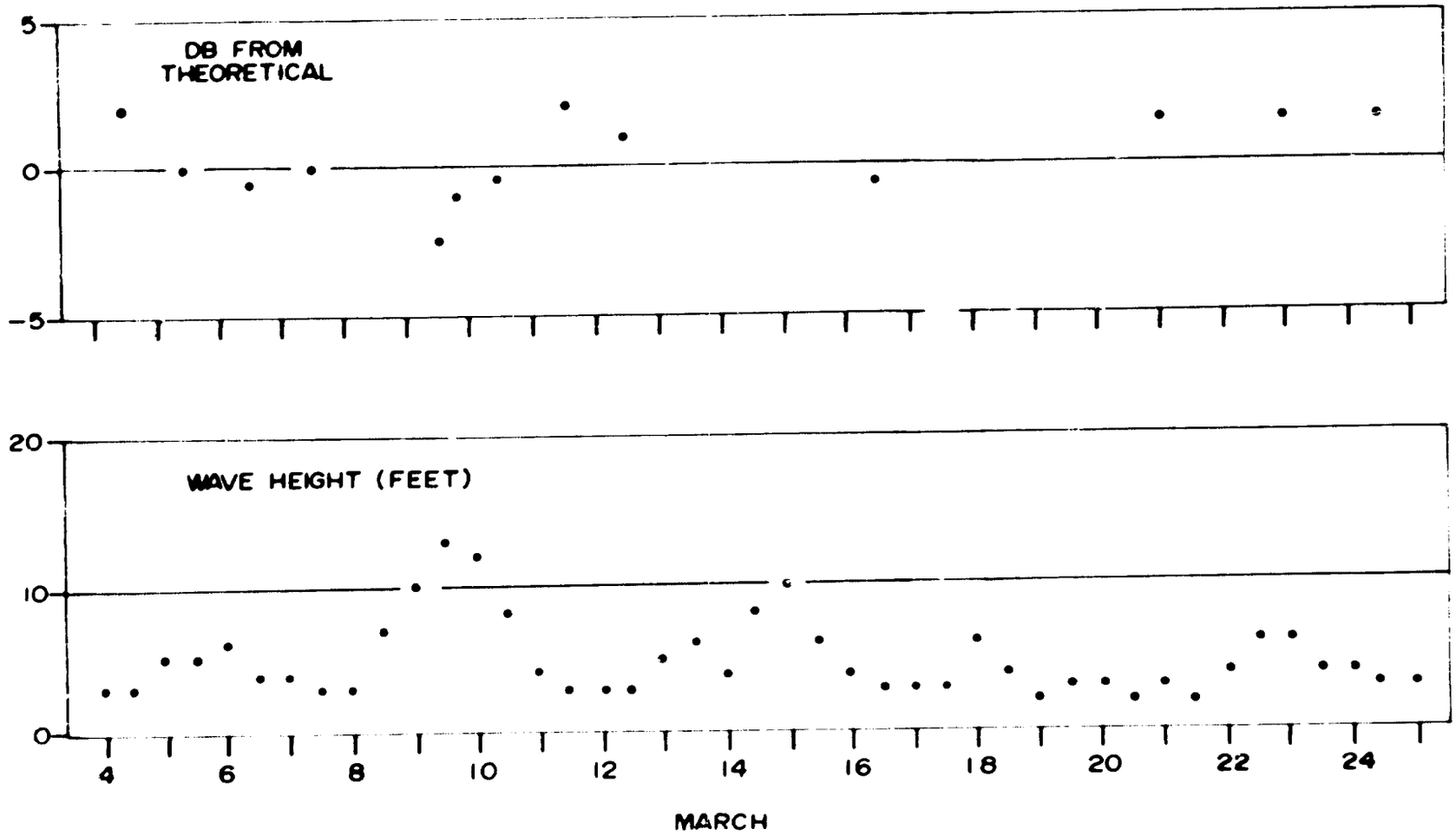

(U) Figure 2. Received Power 5 MHz Monopole vs Hindcast Wave Height (U)

(U)

UNCLASSIFIED

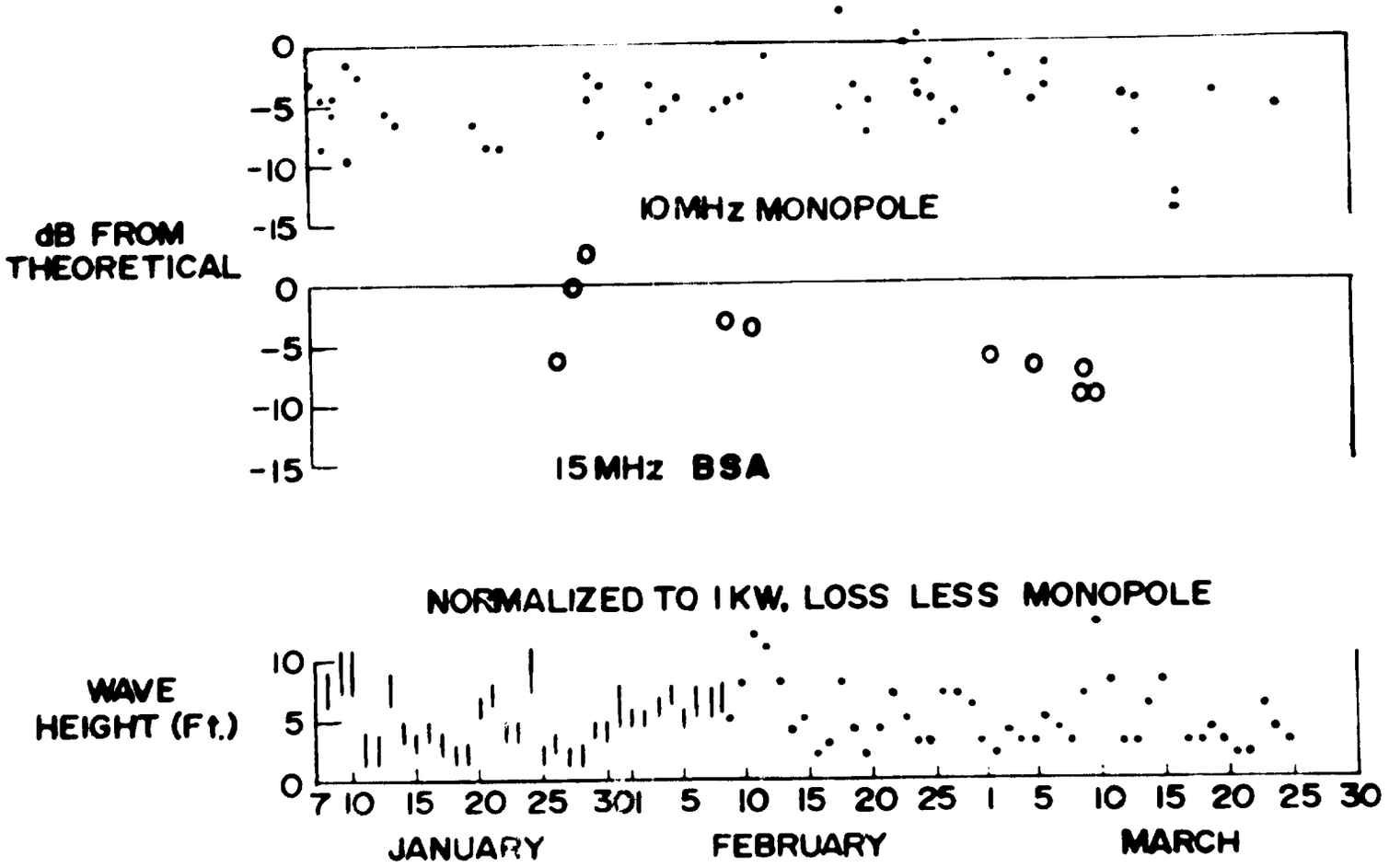

UNCLASSIFIED

(U) Figure 3. Received Power Measurements on 10 and 15 MHz, January – March 1970 (U)

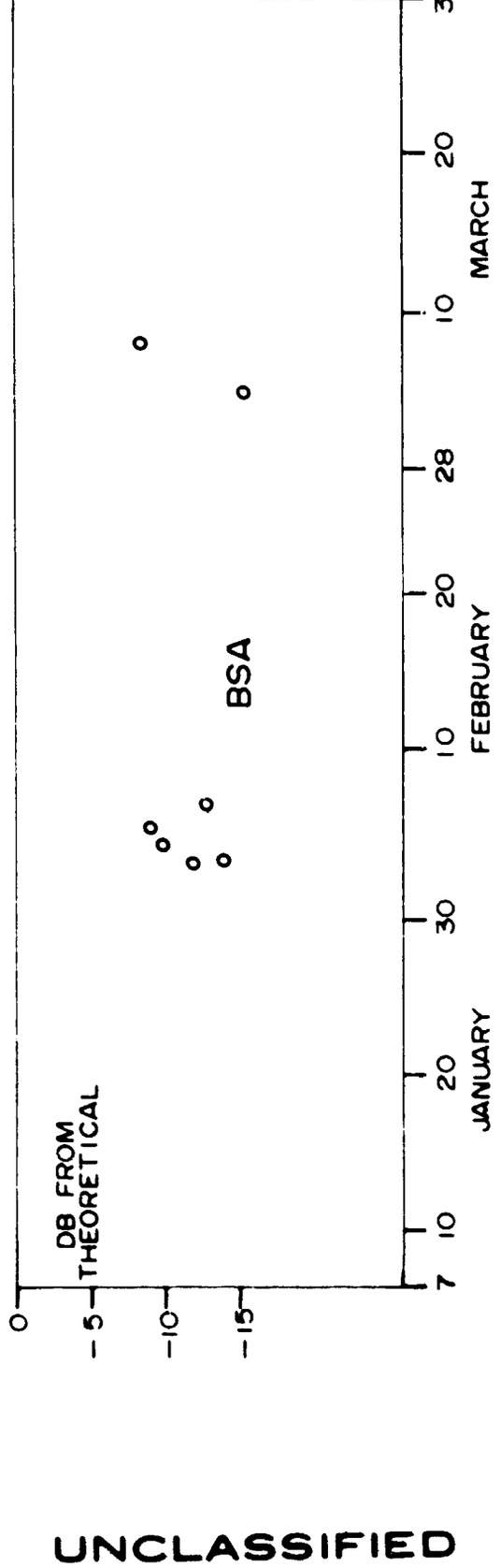

(U) Figure 4. Added Loss, 20 MHz (U)

(U)

THIS PAGE INTENTIONALLY LEFT BLANK

SEA CLUTTER PREDICTIONS AND MEASUREMENTS (U)

Jerald A. Grimes

Raytheon Company
Equipment Division
OHD Advanced Development Department
Spencer Laboratory
Burlington, Massachusetts

I INTRODUCTION (U)

(S) It has been expected that, in certain applications of a ground wave radar operating over ocean surfaces, clutter from sea waves would under some conditions be a limiting factor for detections. Consequently, an important part of the Raytheon MAY BELL experiments in Florida during the early months of 1970 was to attempt to determine the measured power spectrum of sea clutter under a range of geographical, system, and environmental parameters. These experiments constitute a direct test of predictions made by D. Barrick of BMI. Preliminary results are in good agreement with those predictions.

II PREDICTIONS (U)

(U) Barrick has predicted clutter peaks 23 to 40 dB below the direct signal at ± 0.25 Hz for a 5,800-MHz signal and at ± 0.315 Hz for a 9,259-MHz signal. In each case additional peaks at $\sqrt{2}$ times the original shift are predicted for sufficiently high sea states. Barrick further predicts a minimum clutter frequency equal to $\sqrt{\cos \theta}$ times the maximum (backscatter) shift, where θ is the half-scatter angle and the scattering ocean waves are in this case approaching or receding perpendicularly to the transmitter-receiver path. A further prediction is the absence of clutter if the maximum ocean wavelength is not equal to or greater than half the radio wavelength, i.e., low radio frequency and low sea state.

III DATA BASE (U)

(U) The primary data analyzed to date is summarized in relation to Navy Oceanographic Office hindcast wave height and direction in Figure 1. On 17 March the buoy was anchored offshore from the receiver site at Cape Kennedy. On 19 March the only other successful operation of the buoy high frequency was recorded from a 120-km range. No buoy transmissions were available during the two highest sea states of 9 and 15 March. The only significant change in sea state during buoy operation was in wave direction.

IV SYSTEM GEOMETRY (U)

(U) Figures 2 and 3 illustrate the buoy transmitter, receiver, and range gate locations along with an indication of the heights of the ellipsoidal range gate regions. Ocean wave, ground, and ionospheric scattering regions are identified in terms of these maps and related to observed returns from each range gate. Most important for clutter analysis is the relation of ocean wave direction in each range gate to physical requirements for scattering, together with the directivity pattern of the receiving antenna used; in this experiment either a narrow beam directed toward the transmitter or a nondirective monopole.

V WAVE INFORMATION (U)

(U) Direction and amplitude of ocean waves for periods in which buoy transmissions were recorded are summarized in Figure 4. Variability in either parameter is indicated on days when either direction, height, or both were changing significantly. These data are again those from the Navy Oceanographic Office hindcast. Direct determinations of sea state in the areas of interest have not been available. The uncertainties concerning true ocean wave behavior as opposed to best available estimates thereof must be kept in mind in interpreting observed clutter.

VI CLUTTER MEASUREMENTS (U)

(U) In general, sufficient data has been recorded and processed to investigate clutter variation with ocean wave direction, transmitted frequency, directivity of receiver antenna, and ocean wave amplitude. Variations in observed clutter with the specific geometry of individual range gates can also be investigated.

(U)

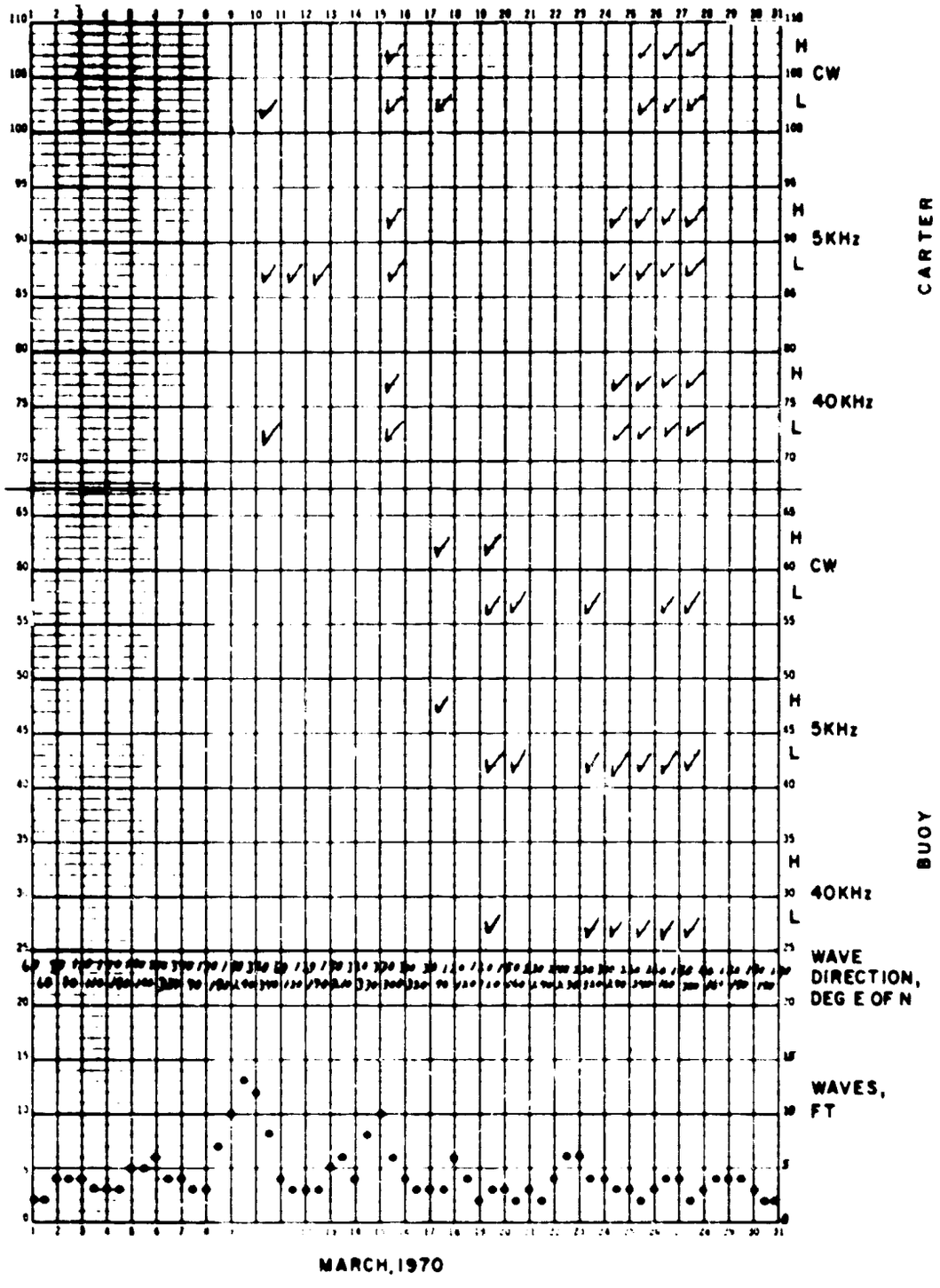

(U) Figure 1. APL Transmissions Recorded in March 1970 (U)

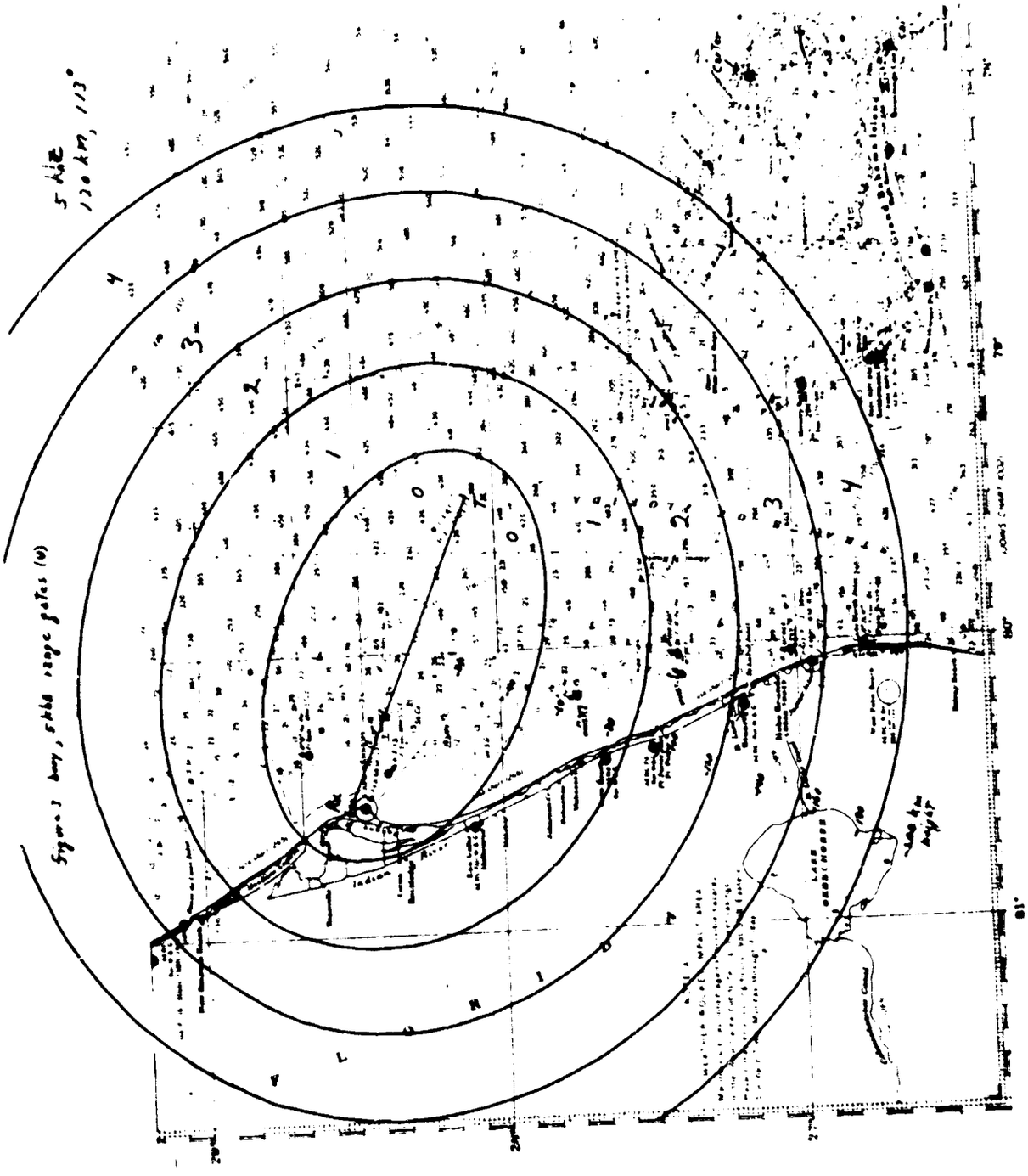

(U) Figure 2. Buoy 5-kHz Range Gates (U)

(U)

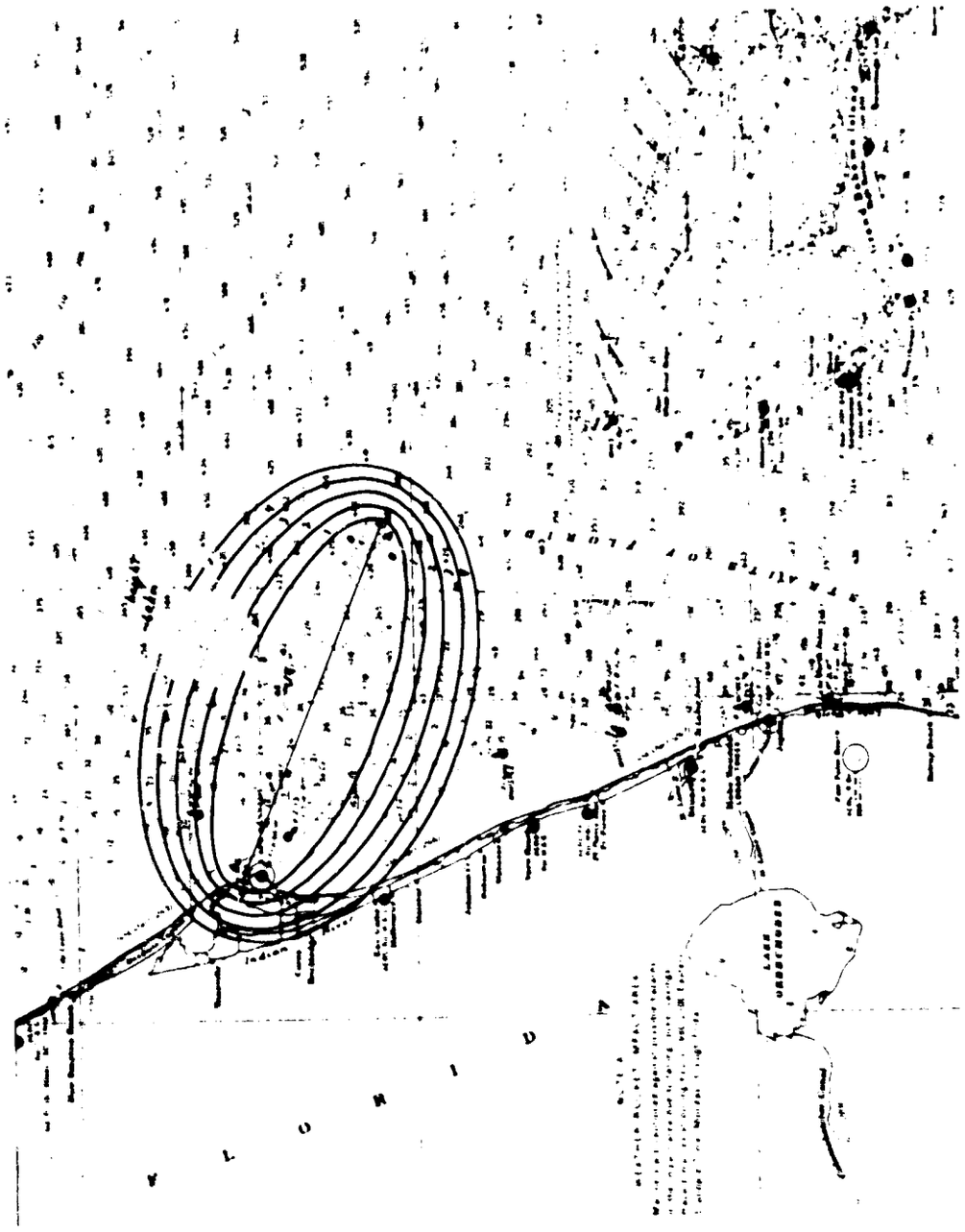

(U) Figure 3. Buoy 40-kHz Range Gates (U)

(U)

(U)

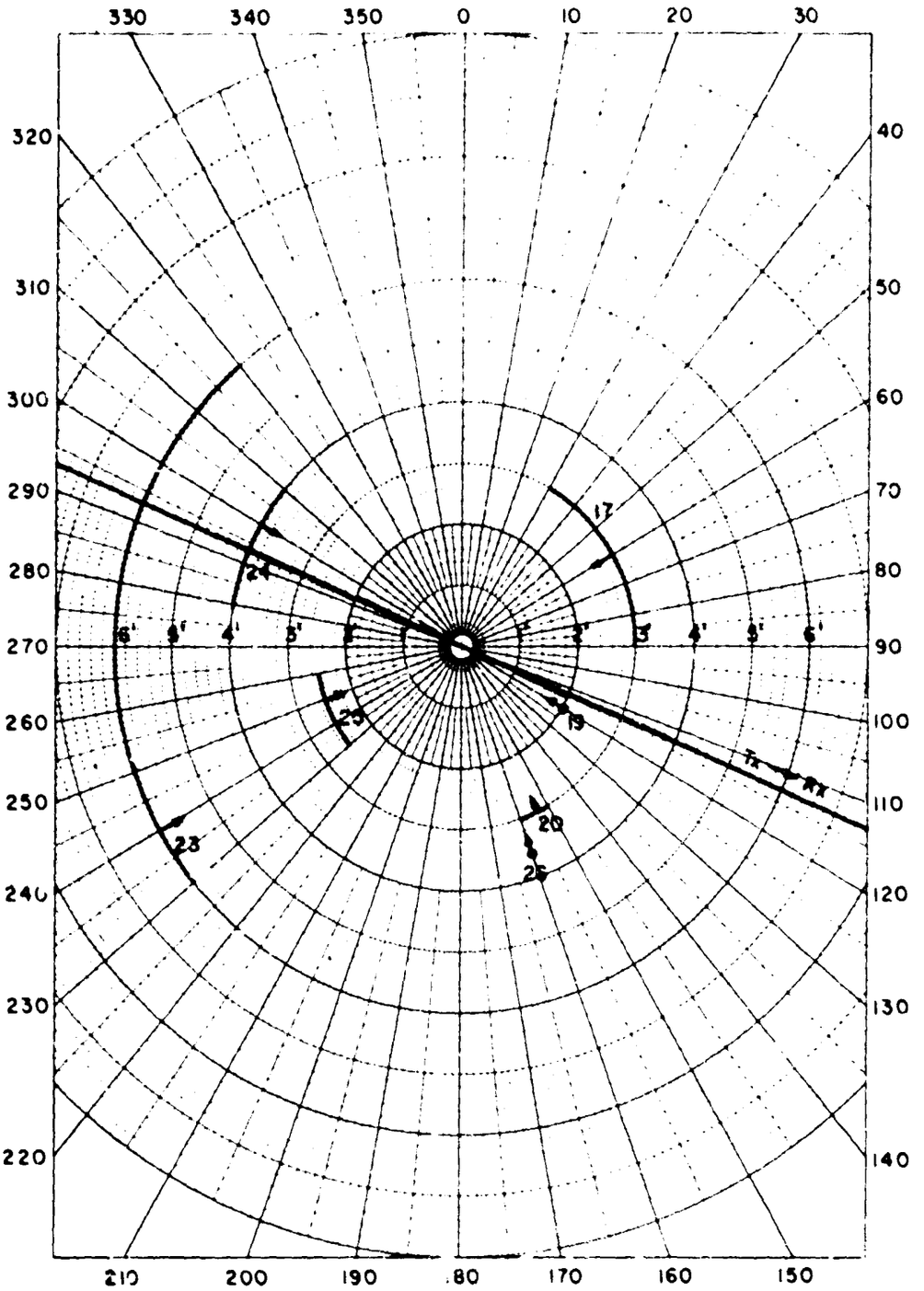

(U) Figure 4. Wave Heights and Directions, March Buoy Data Recorded (U)

(U) Figure 5 illustrates the variation of positive and negative clutter peaks with wave direction. Higher positive clutter is observed for waves approaching the transmitter and receiver, while higher negative clutter is seen for waves receding from the transmitter and receiver; since with the directive BSA and range gate one, the primary scatter region is beyond the transmitter. Figure 6 further illustrates that the detailed behavior of the negative clutter varies with individual range gate areas. Detailed geometrical study shows that the observed increase in amplitude of this negative clutter is expected.

(U) The general increase in clutter doppler with higher frequency signals is illustrated in Figure 7. This qualitatively substantiates predictions, and specific data will be sought in which the true maximum shift is believed to be observed at two different frequencies so that quantitative comparisons can be made with theory.

(U) Receiving antenna directivity is expected to differentiate between positive and negative clutter, or scatter, from regions of waves approaching or receding. Figure 8 illustrates that, in range gate zero (direct signal included), and range gates one and two as well, both positive and negative clutter is observed by both the directive and monopole antennas. The BSA sees much less positive clutter, which in this case came from far off the beam, than did the monopole, which does not favor any azimuthal angle of arrival. The greater positive clutter observed in this case via the monopole is further illustrated, along with the minimum and maximum clutter doppler, on a facsimile display, shown in Figure 9. Note that blackness is higher received power and carrier position is indicated as doppler zero.

(U) A considerably larger data base (three months, four frequencies) is available if we examine the Raytheon CW signals from Carter Cay. This is particularly valuable for investigating high sea state effects which did not occur with any significance during phase code operations. One preliminary sample was checked for this report, the highest reported sea state of 9 March, and for comparison the low sea state immediately following this on 12 March. The marked effect of this large change in ocean waves is indicated in Figure 10. The combined loss in signal power of several dB and the presence of clutter only about 25 dB down in the case of the high sea state is most evident. The possibility of higher order clutter peaks, further down but with higher doppler shifts, is also indicated in the 9 March power spectrum. In comparison with other data, it is expected that in this case observed energy to about ±1 Hz is most likely related to ocean wave effects. Analysis of this and other CW data will continue.

VII CONCLUSIONS

(U) Phase coded data clearly identifies clutter and, together with the good agreement of Dr. Barrick's predictions with a small sample of data, analyzed in terms of the best available measurements of environmental and system parameters, contributes guidelines to identifying clutter in a much larger set of CW data.

(U) Specific clutter levels and dopplers can be determined for the particular geometries and sea states experienced in this program. Completion of analysis of this data will result in statistics concerning the amplitude and frequency of all identifiable sea clutter in the phase code and CW data and comparison with available sea state data.

(U) Primary limitations to the completeness of this phase of the MAY BELL propagation experiment were the lack of better sea state information, phase code coverage of more varied sea states, and simultaneous high and low frequency signals from the buoy.

(U)

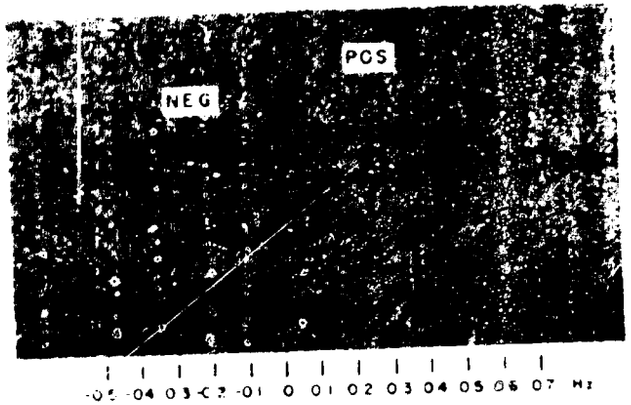

19 MARCH

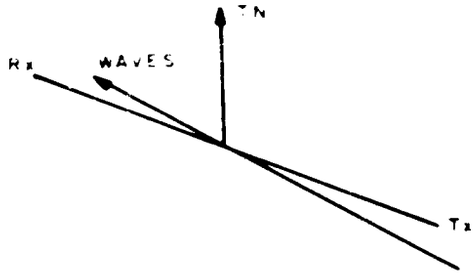

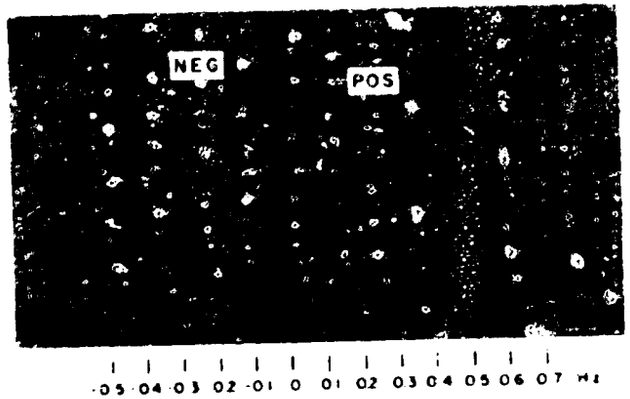

23 MARCH

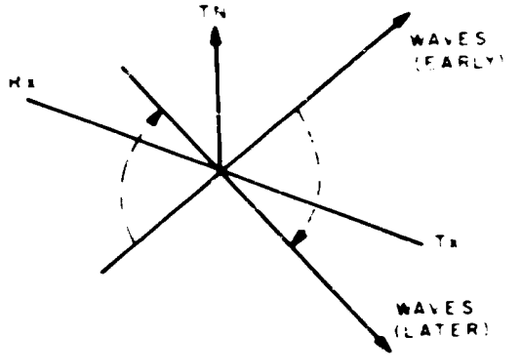

(U) Figure 5. Clutter Variation with Opposite Wave Directions, Buoy, low, 5-kHz, Range Gate 1, BSA (U)

UNCLASSIFIED

(U)

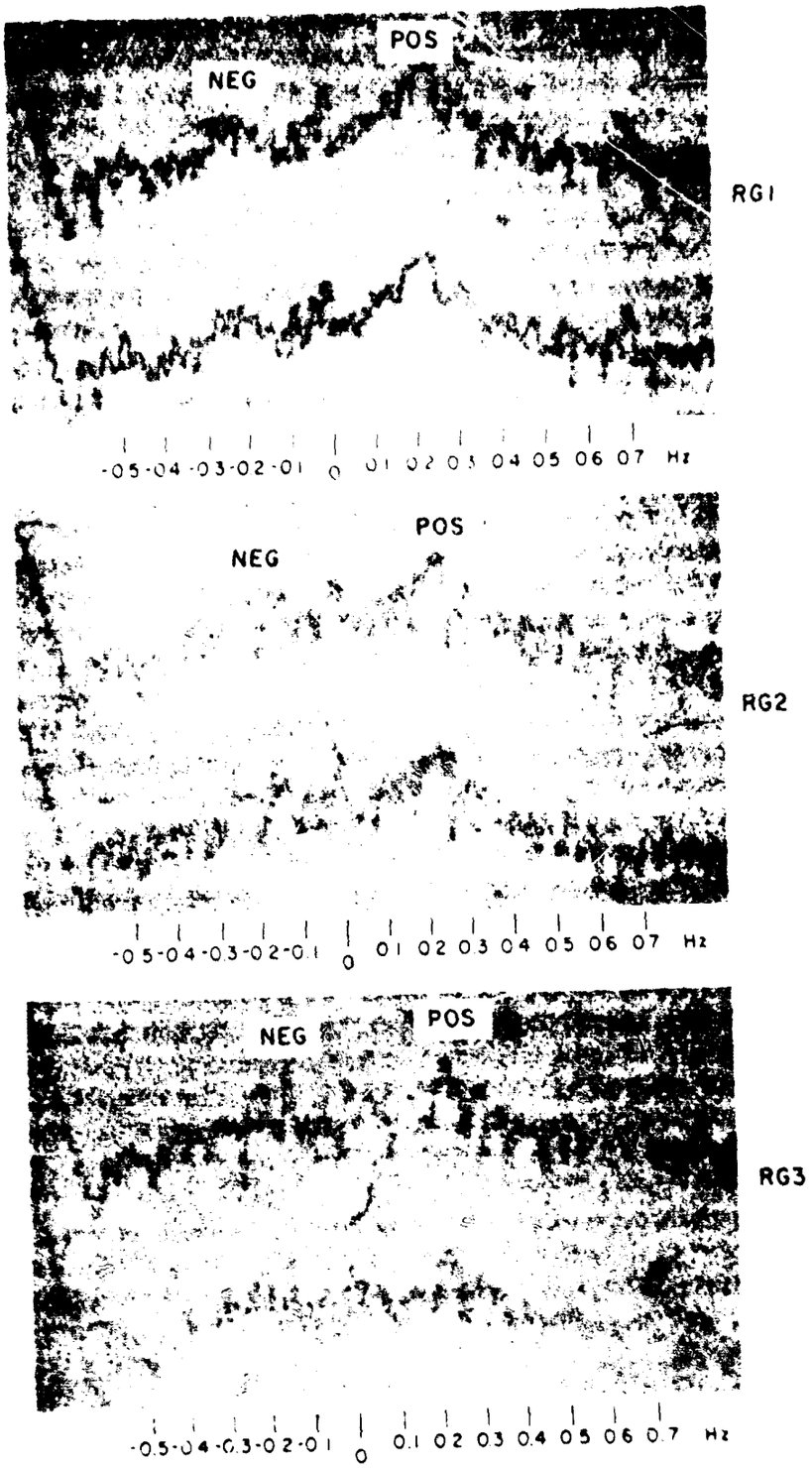

(U) Figure 6. Clutter Variation with Range Gate, Buoy, low, 40-kHz, Range Gates 1, 2, and 3, Monopole (U)

(U)

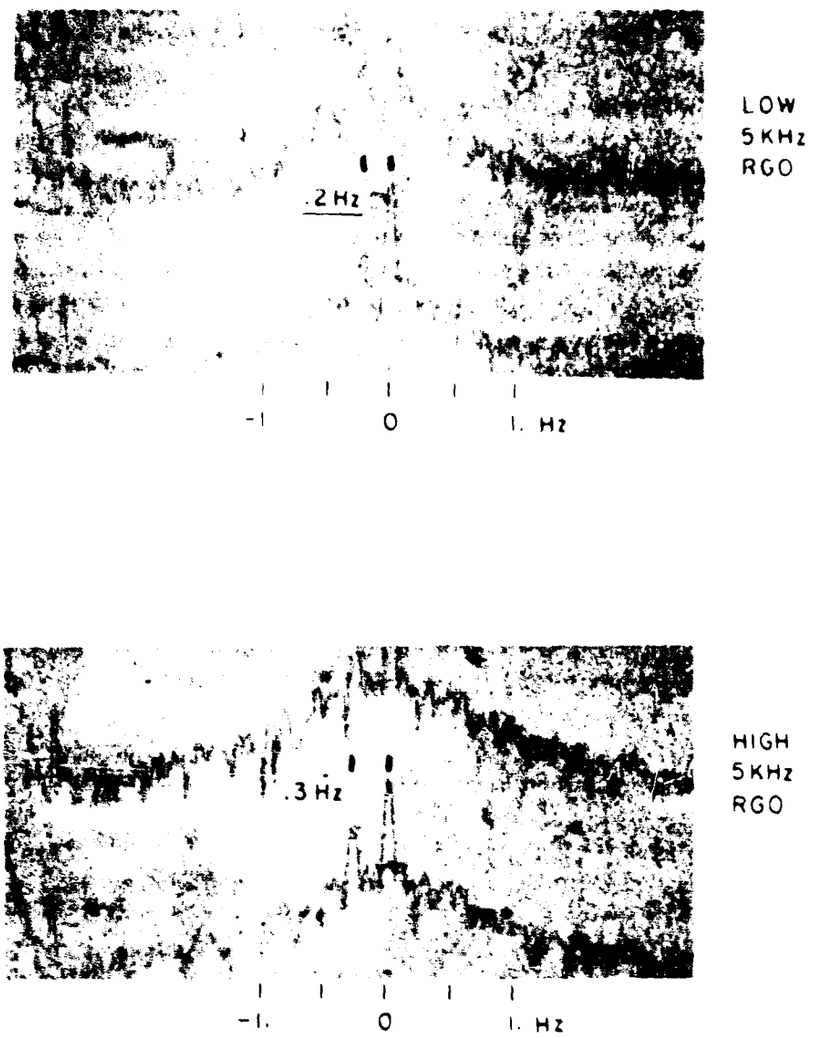

(U) Figure 7. Clutter Variation with Frequency of Transmission, Buoy, 5-kHz, Range Gate 0, BSA (U)

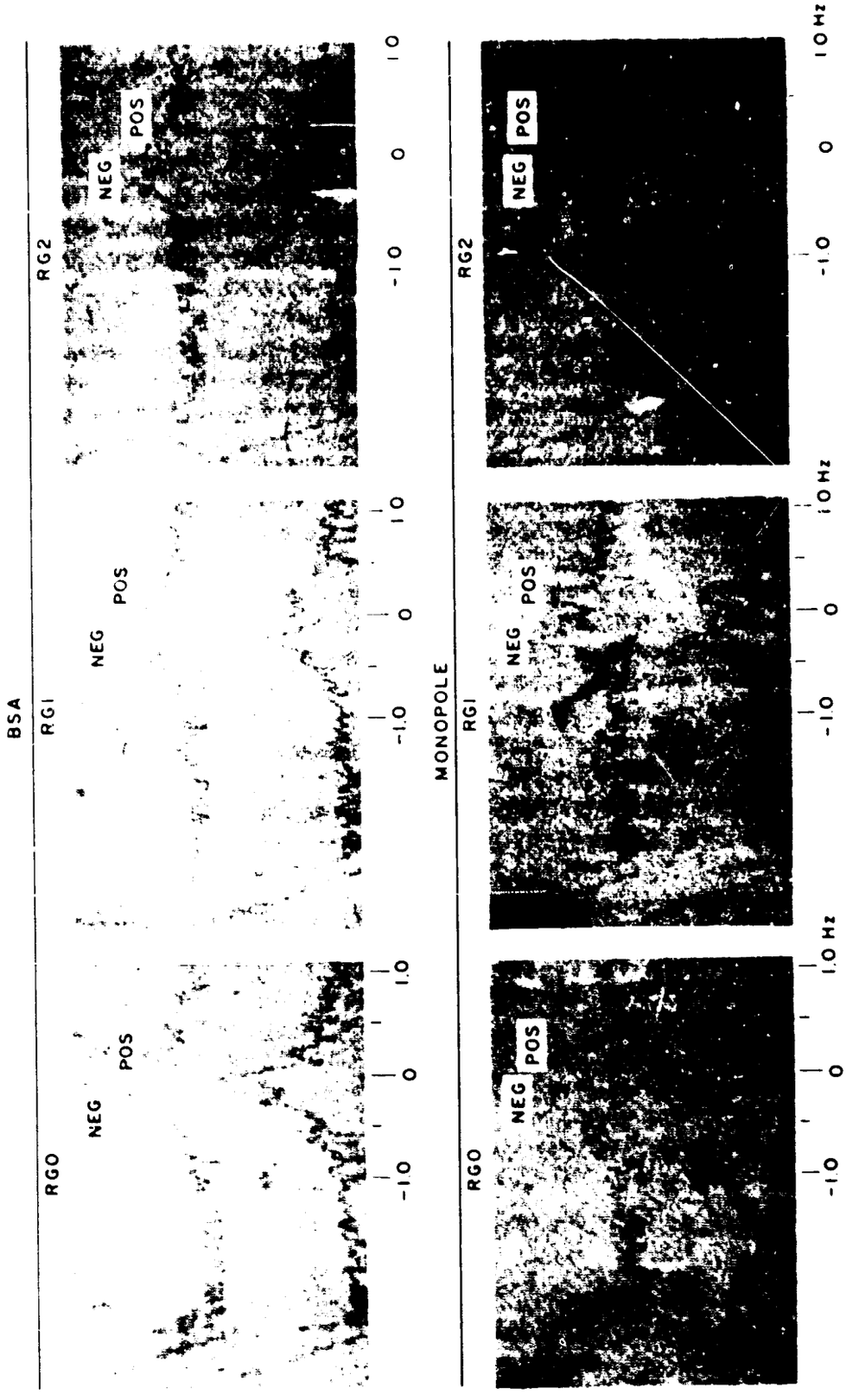

(U) Figure 8. Clutter Variation with Receiving Antenna, Buoy, low, 5 kHz, Range Gates 0, 1 and 2 (U)

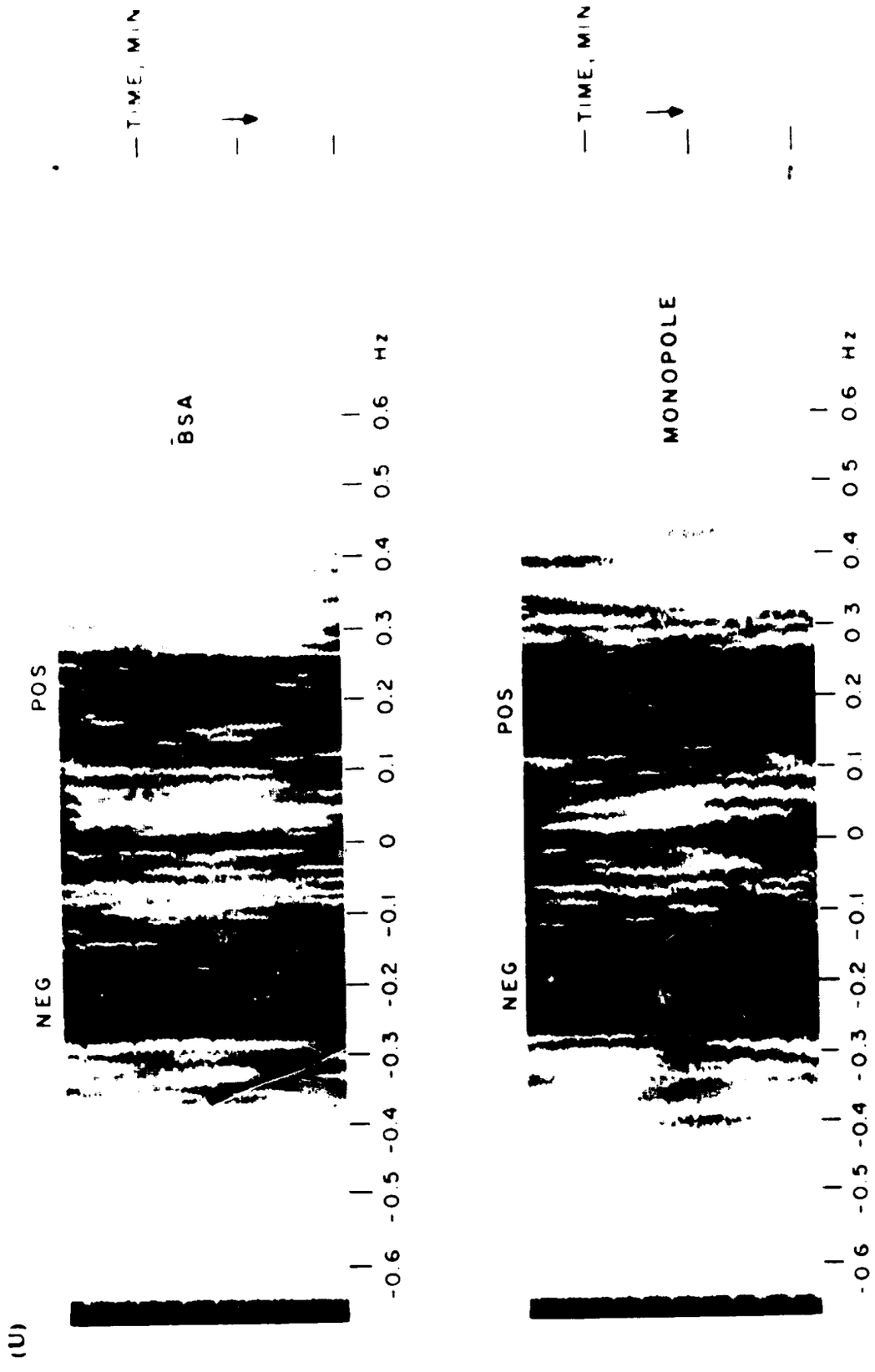

(U)

(U) Figure 9. Clutter Variation with Receiving Antenna, Buoy, low, 5-kHz, Range Gate 1, Facsimile Display (U)

UNCLASSIFIED

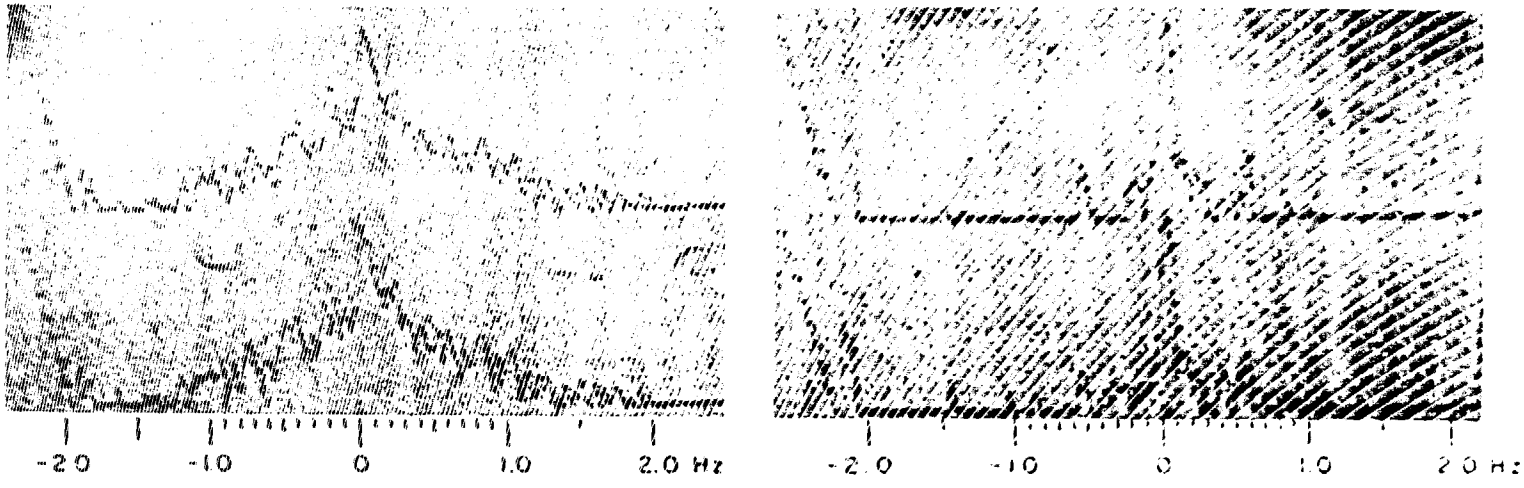

9 MARCH
13 FT WAVES FROM 290°
SEA STATE 6

12 MARCH
3 FT WAVES FROM 170°
SEA STATE 2

(U) Figure 10. Clutter Variation with Sea State, Raytheon 5-MHz CW, Carter, Monopole (U)

UNCLASSIFIED

THEORETICAL ATTENUATION FOR TERRAIN - SEA PATHS (U)

Dr. R. H. Ott

Institute for Telecommunication Sciences
ESSA Research Laboratories
Boulder, Colorado 80302

I INTRODUCTION (U)

(U) Recently[1] an integral equation for calculating the attenuation of radio waves propagating over irregular, inhomogeneous terrain was derived. In this paper, the integral equation is applied to four terrain profiles; a Gaussian-shaped ridge, a sea-land-sea path, a sea-land-sea path with an island and a sloping beach at high and low tide. For the case of the Gaussian-shaped ridge, the solution is compared with solutions obtained using classical methods such as diffraction theory.

II EXAMPLES (U)

A. A Gaussian-Shaped Ridge (U)

(U) The terrain profile is shown in Figure 1. The ridge is 1 km high at a distance of 5 km from the transmitting antenna. This example was chosen as a check on our formula's capability for treating terrain features having large slopes. The slopes for this example are near 45° for some points on the profile. The antenna is vertically polarized and the frequency is 1 MHz. The ground conductivity is 0.01 mho/m and the dielectric constant is 10. In Figure 1 the magnitude of the attenuation function normalized to twice the free space field is plotted versus distance in km from the antenna. The observation point (receiving antenna) is located on the profile shown in Figure 1. The three sets of data in Figure 1 correspond to three alternative methods for computing the attenuation function and two of these serve as a check on the accuracy of our formulation. The solid circles were computed using our new integral equation. The open circles were computed using the classical Hufford-Feinberg[2] integral equation. The crosses were computed using simple diffraction theory to compute the attenuation function for a

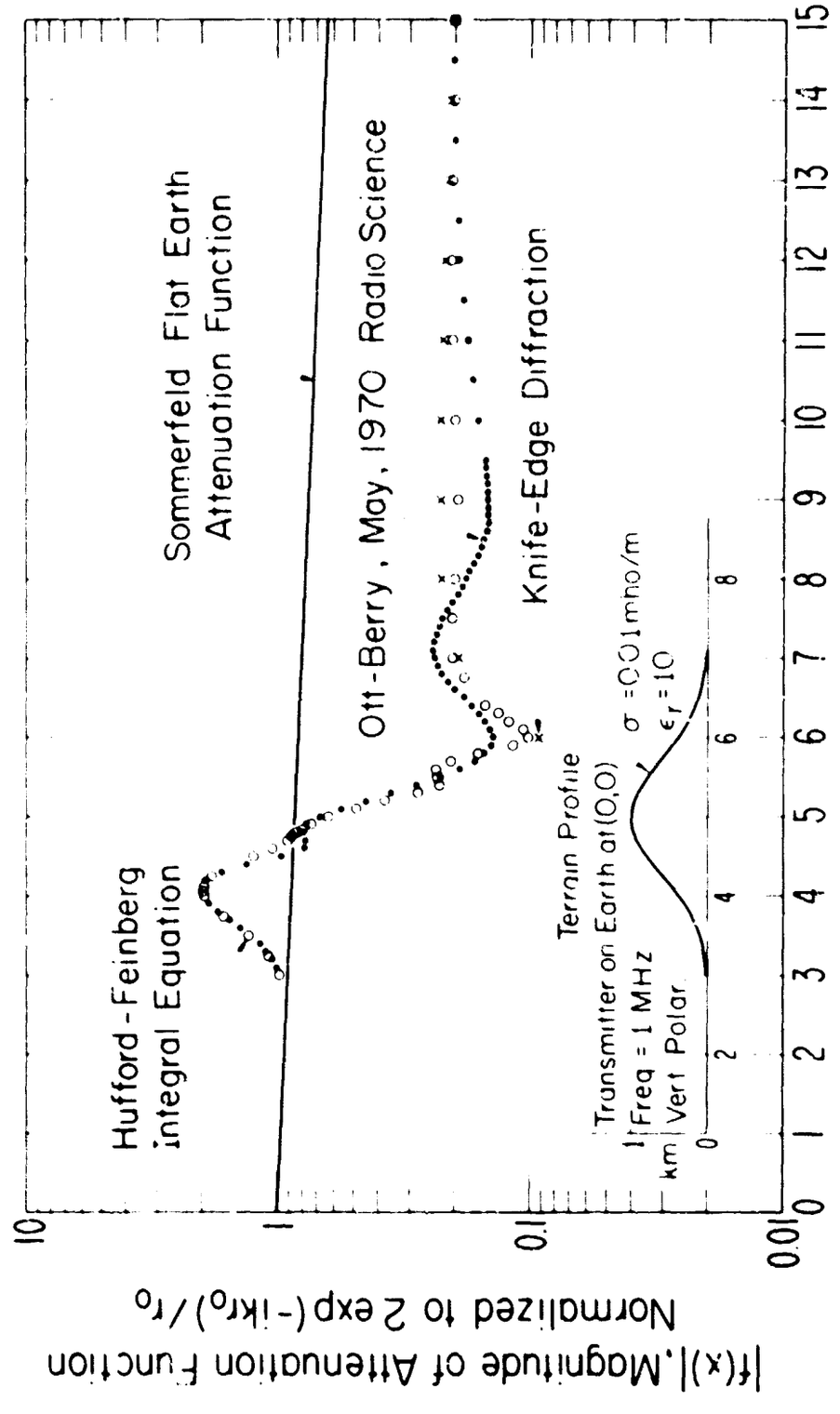

(U) Figure 1. Magnitude of the Attenuation Function vs Distance for a Gaussian-shaped Ridge. (U)

(U)

rounded knife-edge model for the ridge. The agreement between the open and solid circles over the entire range demonstrates the validity of our new formulation. The advantage of our formulation over the Hufford-Feinberg formulation is not brought out in this example since the frequency is sufficiently low so that accumulation of roundoff error characteristic of the Hufford-Feinberg formulation at frequencies above a few MHz does not occur. Both integral equation solutions agree well with the results based on diffraction theory on the shaded side of the hill. However, the diffraction results do not predict the large peak in the attenuation function on the lit side of the hill. This peak in the attenuation function can be explained by considering the constructive interference between a direct ray from the antenna to a point near the crest of the hill and a ray which travels along the surface before reaching the observation point near the crest. This peak has a magnitude approximately twice the free space field. The field drops sharply on the far side of the hill, then partially recovers as the ray diffracted at the crest is reinforced by the surface wave traveling down the slope.

B. A Sea-Land-Sea Path (U)

(U) The terrain profile is flat in this example and the ground constants change abruptly at the sea-land, land-sea interfaces. This example was selected as a check on the mixed path capabilities of our formulation. In Figure 2 the results for the magnitude of the attenuation function normalized to twice the free space field are plotted versus distance from the antenna in km. The antenna is vertically polarized and the frequency is 10 MHz. The solid circles represent the attenuation function computed numerically using our new formulation. The open circles in Figure 2 represent the attenuation function computed by Rosich (ITS 137)[9] using a perturbation approach. The data given by the crosses in Figure 2 represent the attenuation function computed using a method based upon the classical residue series. This latter method is exact for the three-section earth considered in this example. The agreement between the solid circles representing our new integral equation and the crosses appears to demonstrate the validity of the formulation in treating mixed path propagation problems. The abrupt changes in conductivity and dielectric constant used in this example do not represent a realistic sea-land interface. Our formulation is capable of treating a continuous variation of conductivity and dielectric constant.

C. A Sea-Land-Sea Path with an Island (U)

(U) This example is a combination of the terrain features of example A and the mixed path features of example B. The island is drawn to scale in Figure 3 and its elevation is 250m at the highest point. This elevation may be greater than the elevation of any point on islands of interest in the MAY BELL program; however, this elevation is much smaller than the elevation on some islands, for example Mt. Mauna Loa in Hawaii, which has an elevation of 4 km. The magnitude of the attenuation function normalized to twice the free-space field versus distance is plotted in Figure 3. The antenna is vertically polarized and the

(U)

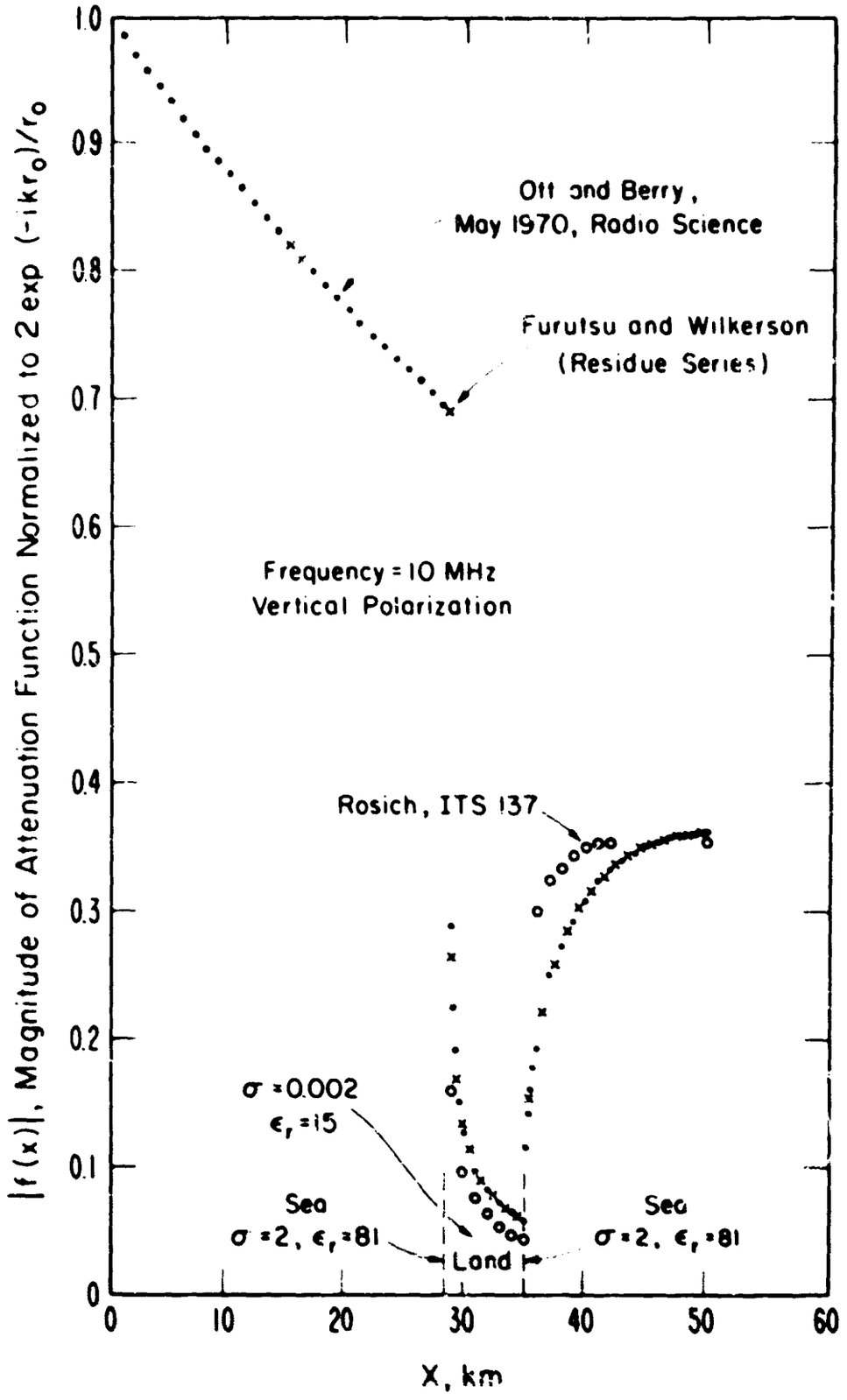

(U) Figure 2. Magnitude of the Attenuation Function vs Distance for a Sea-land-sea Path. (U)

(U)

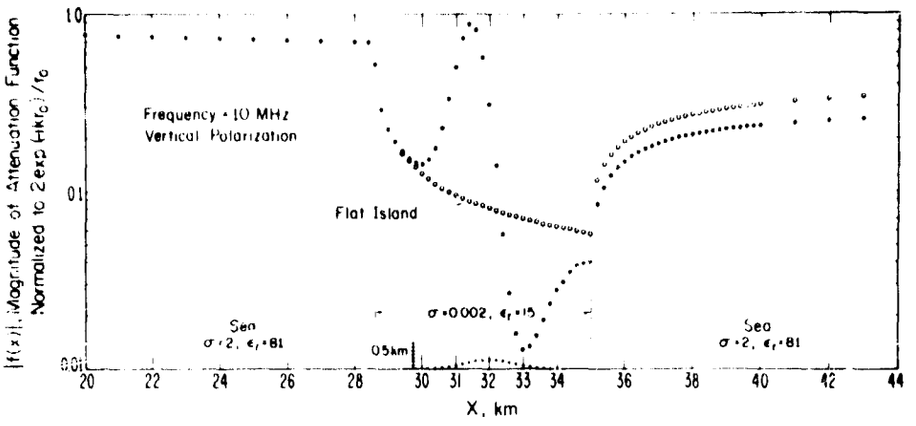

(U) Figure 3. Magnitude of the Attenuation Function vs Distance for a Sea-land-sea Path with an Island (U)

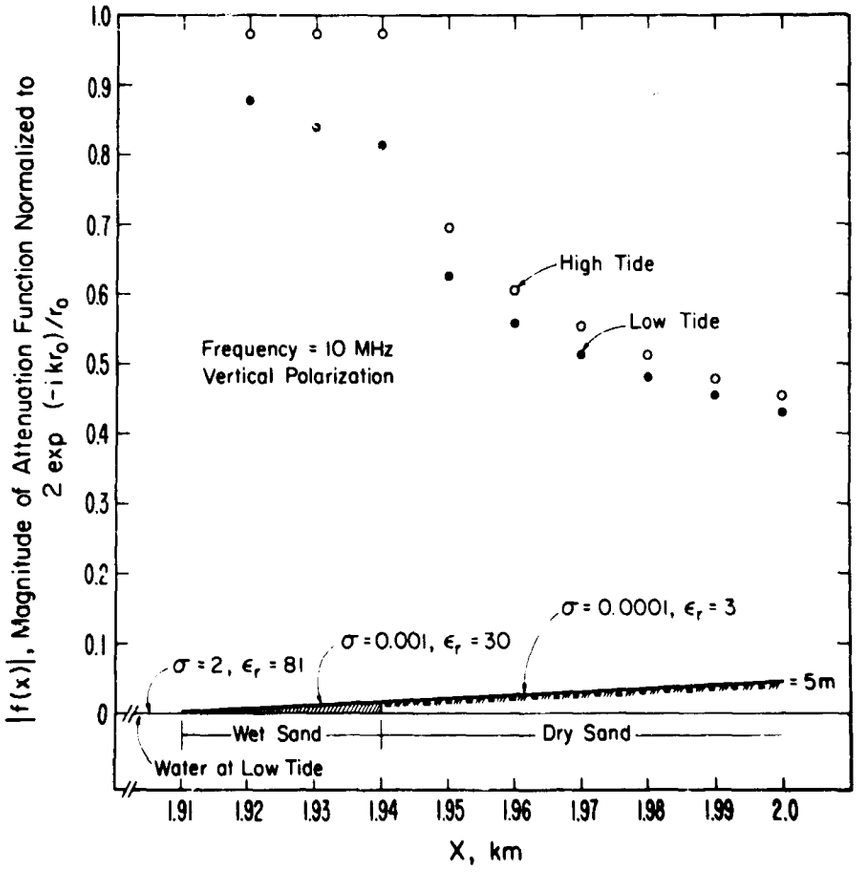

(U) Figure 4. Magnitude of the Attenuation Function vs Distance for a Sloping Beach at High and Low Tide. (U)

(U)

frequency is 10 MHz. For comparison, the magnitude of the attenuation function for a flat island is also shown in Figure 3. The most interesting feature of Figure 3 is that the terrain profile has a greater effect on the attenuation function than do changes in the ground constants. This may be an important consideration in the MAY BELL program since the field strength may be highly attenuated in the shadow of an island with moderate elevations.

D. A Sloping Beach at High and Low Tide (U)

(U) This example was brought to the author's attention by Barrick[4]. The terrain profile together with the assumed ground constants are shown in Figure 4. Figure 4 also shows the attenuation function normalized to twice the free space field plotted versus distance from the transmitting antenna in km. In cases of interest the transmitting antenna may be as far as 120 km from the beach[4]; however, for this numerical example the transmitting antenna was taken to be 2 km from the beach. This change in location for the transmitting antenna merely changes the ordinate scale in Figure 4, but not the general features of the attenuation function as the radio wave strikes the beach. The antenna is vertically polarized and the frequency is 10 MHz. The solid circles represent the attenuation at low tide while the open circles represent the attenuation at high tide. The difference in the attenuation function at high tide and low tide approaches zero for observation points high up the beach. This is partially caused by the focusing properties of the profile for observation points high up on the beach. The model used to study attenuation at high and low tides is an oversimplification of the true situation. For example, the water table under the dry sand may be less than one skin depth (approximately 16 meters for σ = 0.0001 mho/m and f = 10 MHz) below the surface. This would result in less contrast in σ and ϵ_r as the tide varied. There is the additional problem that the tide comes and goes every 12 hours which makes σ and ϵ_r functions of time. This in turn makes the attenuation of the radio wave a function of time. These further complications are however, completely within the scope of applicability of our formulation.

III REFERENCES (U)

1. R. H. Ott and L. A. Berry, "An Alternative Integral Equation for Propagation Over Irregular Terrain," Radio Science, May 1970, UNCLASSIFIED.

2. G. A. Hufford, "An Integral Equation Approach to the Problem of Wave Propagation Over an Irregular Terrain," Quart. Appl. Math., Vol. 9, No. 4, pp. 391-404, 1952, UNCLASSIFIED.

3. R. K. Rosich, "High-Frequency Ground-Wave Attenuation Over Inhomogeneous Path," ESSA Research Lab. Tech. Memo - ITS 137, August 1968, UNCLASSIFIED

4. D. E. Barrick, Private Communication, UNCLASSIFIED.

PRECEDING PAGE BLANK - NOT FILMED

SLBM RADAR CROSS SECTIONS AT HF (U)

G. N. Oetzel

Stanford Research Institute
Menlo Park, California

I INTRODUCTION (U)

(U) The submarine-launched ballistic missile (SLBM) is distinguished as a radar target chiefly by the fact that it is a much smaller and more difficult target than a large ICBM. It is physically smaller at launch, since both U.S. and Russian submarines will only accommodate missiles that are about 10 m long. Because of its smaller size there is less engine thrust, and the SLBM generally does not continue the engine burn as high in the ionosphere as the ICBM.

(S) The current Russian SLBM's, the SSN-4 and SSN-5 are very-short-range, liquid-fueled missiles. Both are single-stage missiles. The SSN-5, the larger of the two, has a maximum range of about 1300 km. Engine burnout occurs at about 70 km, when the missile velocity is only about 3.5 km/s.

(S) In the future, multi-stage Russian SLBM's with performance comparable with or exceeding that of the Polaris can be expected. The A3 Polaris has a maximum range close to 5000 km, and second-stage thrust termination occurs at about 170 km.

II LOW-ALTITUDE CHARACTERISTICS (U)

(S) When a missile is below 70 or 80 km, the burning engine does not increase the radar cross section very much, if at all. When radar illumination of the vehicle passes through the engine plume, attenuation may occur and reduce the radar cross section (RCS) to extremely small values. Because of this attenuation, a "blackout" of the missile echo is usually observed by backscatter radars located near the missile launch site.

(S) When the missile is viewed from aspects other than the rear, the RCS in the low-altitude regime is simply the skin cross section of the vehicle. Samples of the skin cross section, or static RCS, of the Polaris and SSN-5 are shown in Figures 1, 2, and 3. Figure 1 shows the maximum RCS of the Polaris

(S)
before staging, or below 30 km, as a function of frequency. In this calculation, the missile and incident field are assumed to be aligned so that the electric field vector and missile axis are parallel. Other orientations will reduce the RCS from the values shown.

(S) Figures 2 and 3 show similar calculations for the Polaris after staging, and for the SSN-5. Examination of these figures shows that the RCS is of the order of 10 m^2 or less at the frequencies below 10 MHz that are of most interest to MAY BELL. Because the SSN-5 is somewhat larger than the Polaris, its RCS at 10 MHz may be as large as 100 m^2, but no enhancement over this value should be expected at any altitude because of the low altitude of thrust termination.

III ENHANCEMENT IN THE IONOSPHERE (U)

(S) If the engine thrust continues above 80 km, the RCS increases with altitude due to shock ionization around the boundary of the exhaust plume. The increased RCS due to this mechanism continues up to an altitude of about 120 km, where the mechanism of RCS enhancement changes. In some cases, RCS values greater than 10^5 m^2 have been observed on Polaris launches in this altitude regime. However, it is not uncommon to find that the RCS never exceeds 10^4 m^2 on a particular launch.

(S) Figures 3 and 4 show the range of results obtained by ITT and AFCRL on the most favorable tests of the 1964 measurement series at AFETR. Of 18 Polaris launches observed, each organization chose to reduce data on just three launches for reasons of economy and because the data quality was poorer on the other launches.

(S) Observations of larger missiles, such as the Minuteman, show that the RCS generally rises as the missile continues to burn above 120 to 130 km in the daytime, but that the RCS falls dramatically above that altitude at night. The result is a considerable overall difference in detectability between day and night observations.

(S) Where the Polaris has been observed to burn above 130 km, the continued rise of RCS in the daytime has not been observed. The large RCS at about 140 km in the ITT data (Figure 3) is apparently associated with separation of the re-entry body. Making allowance for the separation peak, no high-altitude enhancement is seen in the data of Figures 3 and 4.

(S)

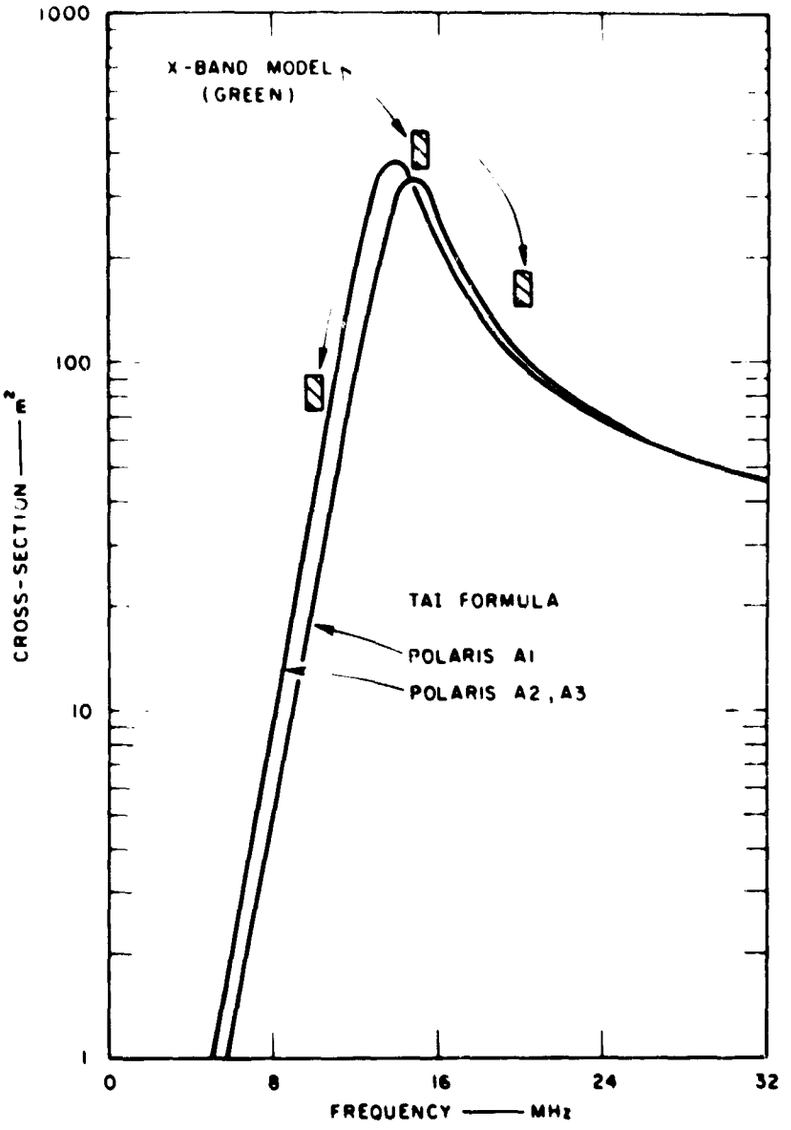

(S) Figure 1. Comparison of X-Band Model Measurements and Tai Formula Calculation for E-Plane Maximum RCS of Polaris (U)

(S)

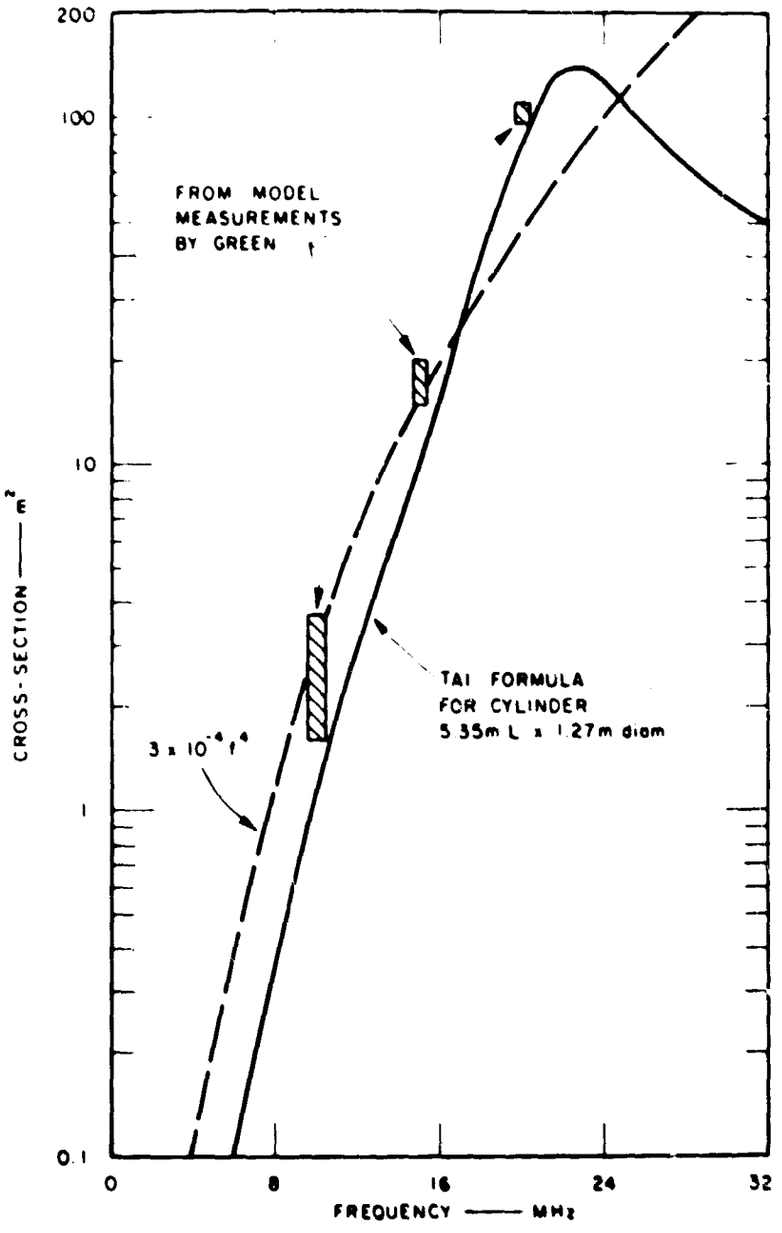

(S) Figure 2. E-Plane Maximum RCS for Polaris after First-Stage Separation (U)

(S)

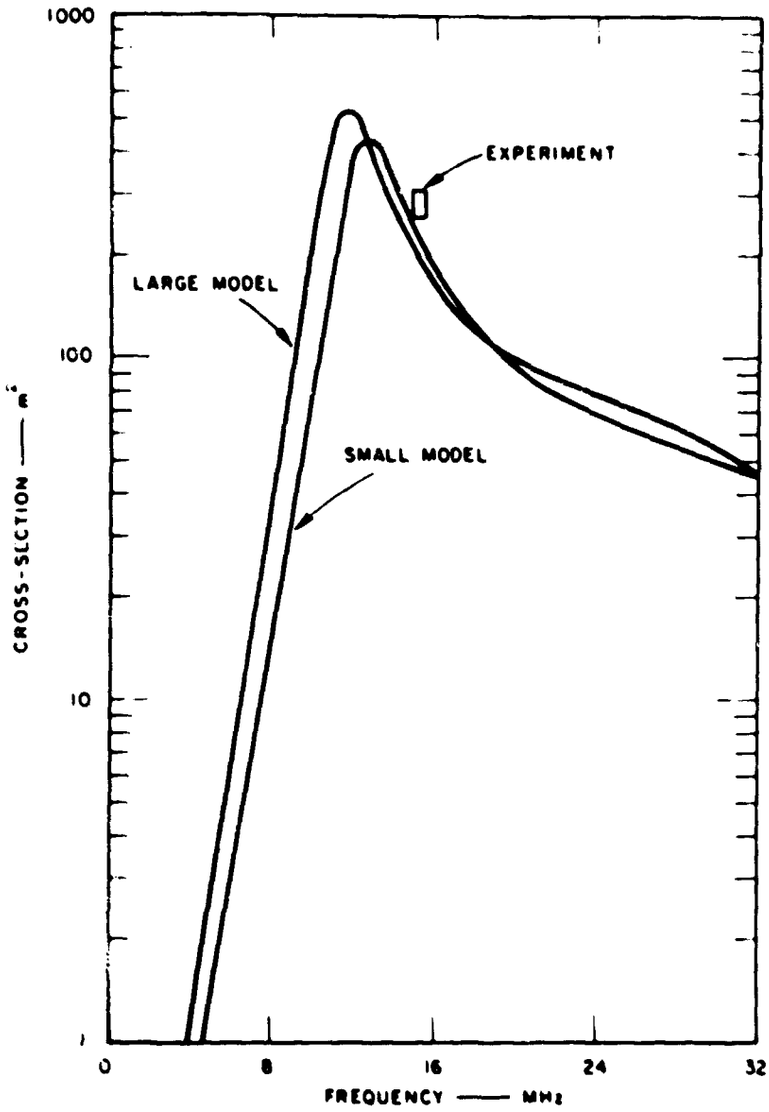

(S) Figure 3. E-Plane Maximum RCS Estimates for the Russian SSN-5 Missile (S)

(S) IV IMPLICATIONS FOR MAY BELL (U)

(S) The SLBM is an extremely demanding target for either an OTH system or a semi-OTH system with a low-power illuminating transmitter, such as is contemplated in the BTEW concept. While larger RCS values are obtained on occasion, it seems best to expect the RCS to be of the order of 50 m^2 in the first few km at launch, and 10^3 to 10^4 m^2 at 100 to 120 km. The enhanced RCS at high altitudes may last for a few seconds only, which provides an additional problem for detection.

(S) Observations prior to the present have generally been made at 12 MHz or above. It would be useful if tests of the MAY BELL equipment would also provide some observations in the 6- to 10-MHz range.

(S)

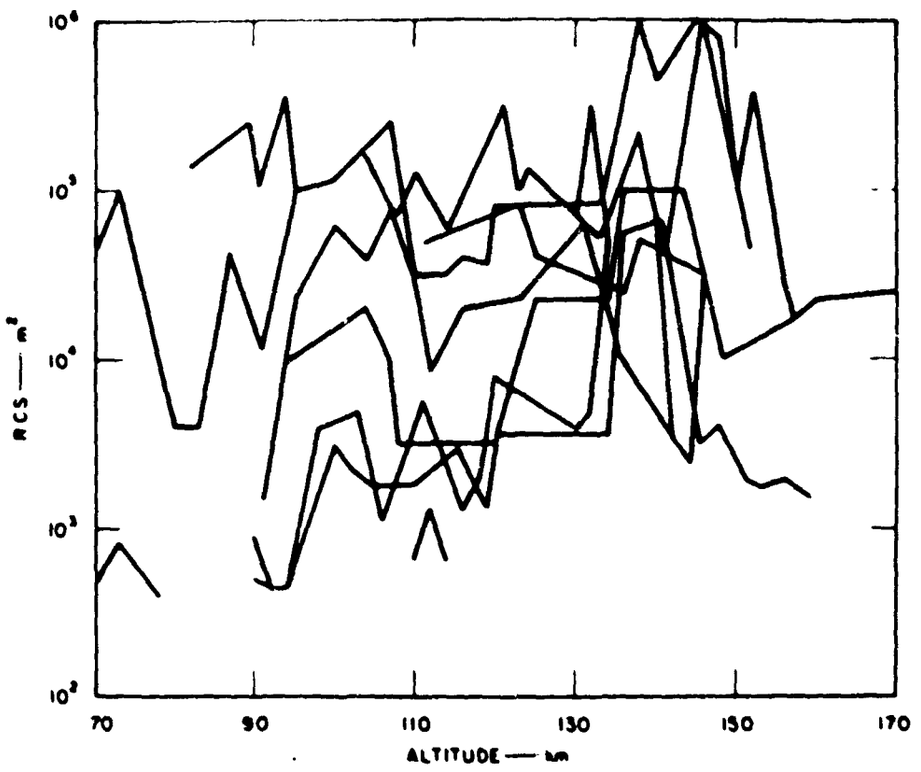

(S) Figure 4. Composite Plot of RCS as a Function of Altitude for the ITT Data from Tests 0324, 2903, and 2955 (U)

(S)

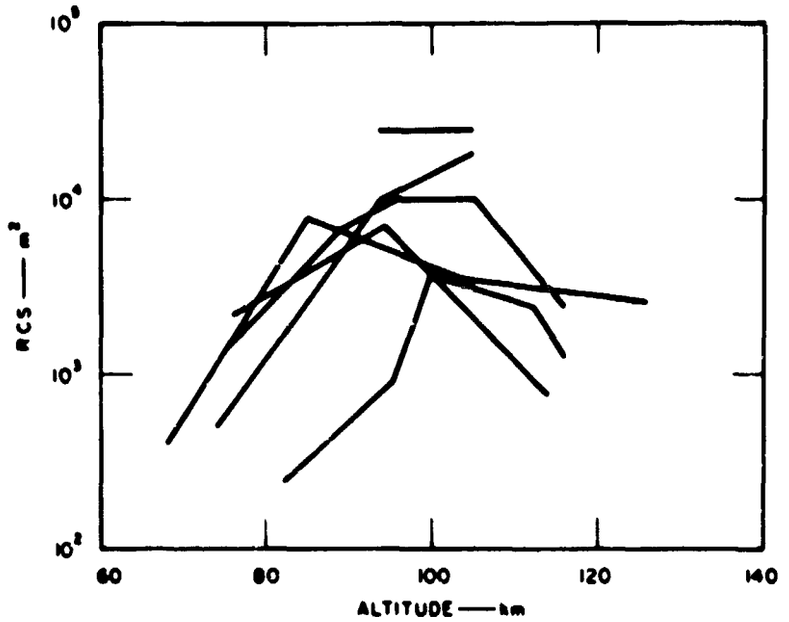

(S) Figure 5. Composite Plot of AFCRL Observations of Polaris Launches 0038, 2903, and 2955 from GBI (U)

PRECEDING PAGE BLANK - NOT FILMED

MEASURED SHIP CROSS SECTIONS (U)

J. M. Headrick

Naval Research Laboratory
Washington, D. C.

(S) Cross-section determinations have been made with the MADRE radar using ground-wave propagation. A quarter-wave monopole located on the Chesapeake Bay has been the gain standard used for antenna calibration. The water conductivity has been measured for each test and a path-loss determination made after the program of L. Berry of ESSA.

(S) Figure 1 shows a MAY BELL buoy that was fitted with a modulated (10-Hz) antenna by EPL-ITT. Figure 2 is an example of the characteristics of this type target. The left column contains, from top to bottom, the echo amplitude of one sideband versus time, the Dopplers (9.5 Hz and 10.5 Hz) versus time, and the amplitudes versus frequency. A one-half Hz offset from zero was used to obtain the above. In the column on the right a similar set of pictures (in different order) are shown but with a true zero frequency reduction. Notice that the two sidebands do interfere both constructively and destructively depending upon the time.

(S) Figure 3 shows the radar return from the final version of the buoy antenna target. The target appears at 7.5 and 8.5 Hz, the level reference at 10.5 Hz. The radar area determined for one sideband was 19 dB m^2. The relation used was

$$\sigma = \frac{P_r\ (4\pi)^3\ R^4\ F^2}{P_t\ G^2\ \lambda^2}$$

where F is the ground-wave loss factor per L. Berry of ESSA.

(U) Figure 4 gives normalized signal levels made using the above techniques on HMS Arethusa, a British frigate. The difference between the curve defined by these points and the plotted loss curve gives the radar area. The droop in the signal levels at the longer ranges due to shielding by Cove Point is seen in Figure 5.

(U) Figure 6 is a picture of the USS Thomas, and Figure 7 gives the radar area determination.

(U) Figure 8 is a picture of the USS Furer, and Figure 9 gives the radar area determination.

(U)

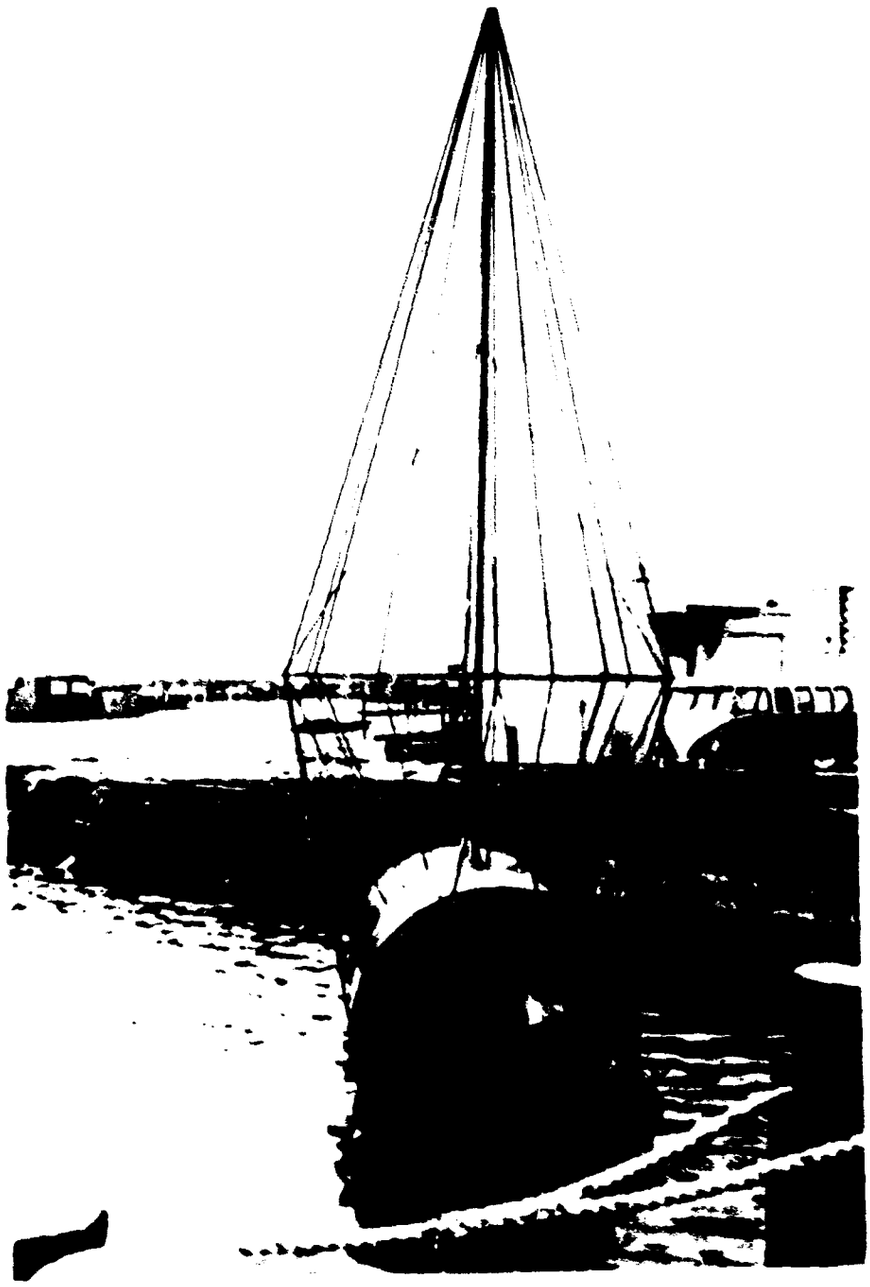

(U) Figure 1. Buoy with Target Antenna (U)

(S)

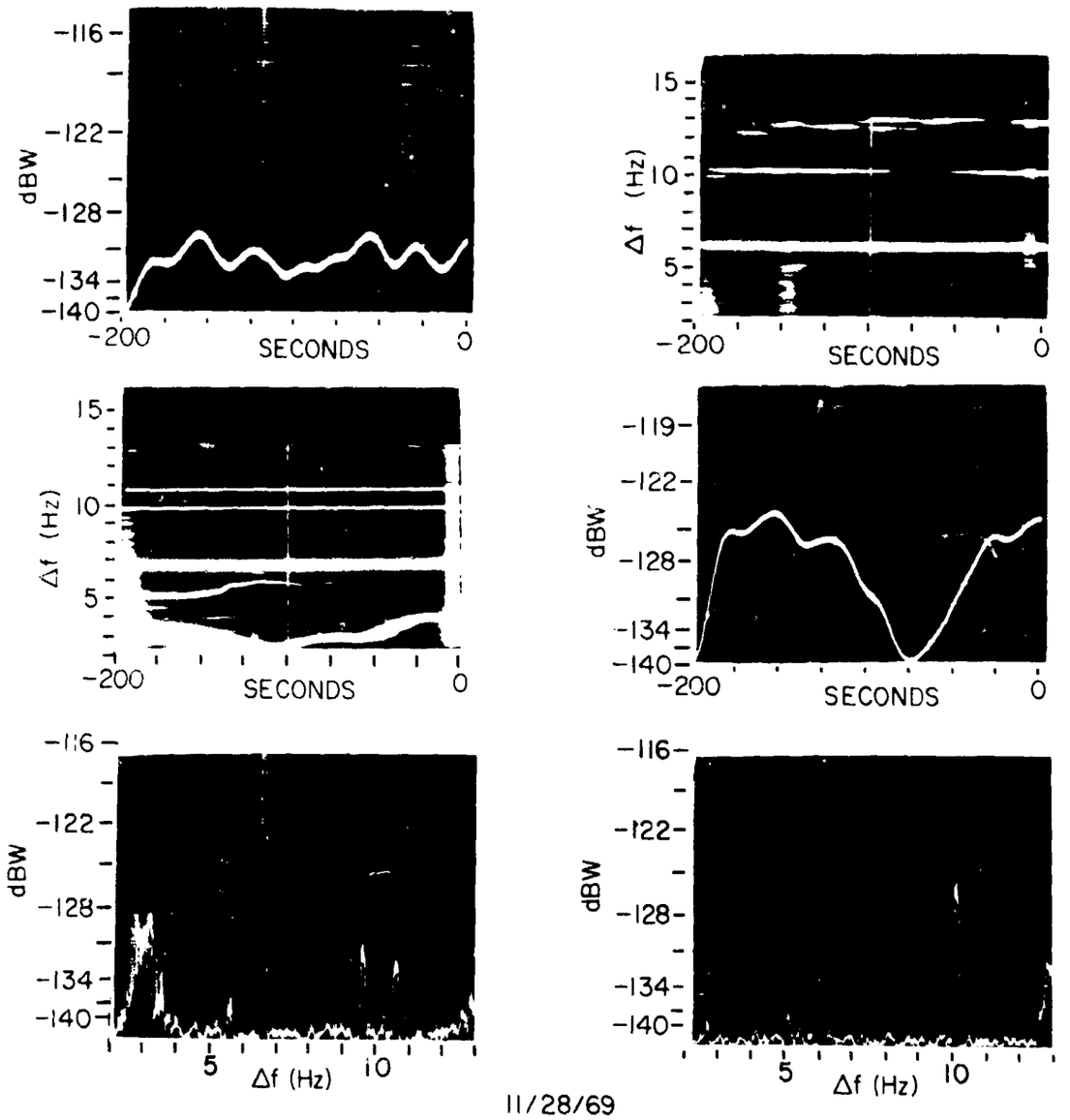

11/28/69

13.687 MHz, 60 dBW, 125 μs, 45 PRF, FTM, 8 kHz Sample rate, 0.15 Hz BW

(S) Figure 2. Buoy Echo (U)

(S)

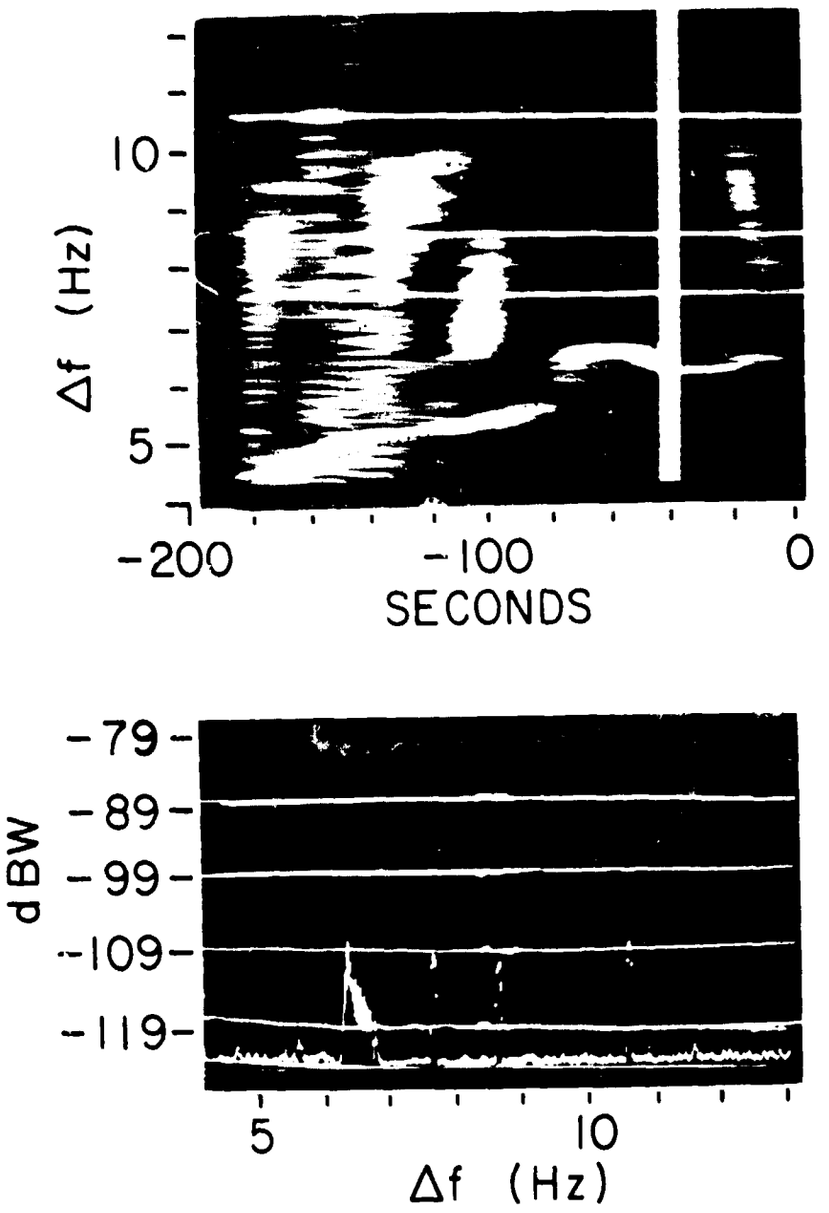

(S) Figure 3. TULIP 1912Z, 12/18/69, 10MHz, 60 dBW, 25 nmi (U)

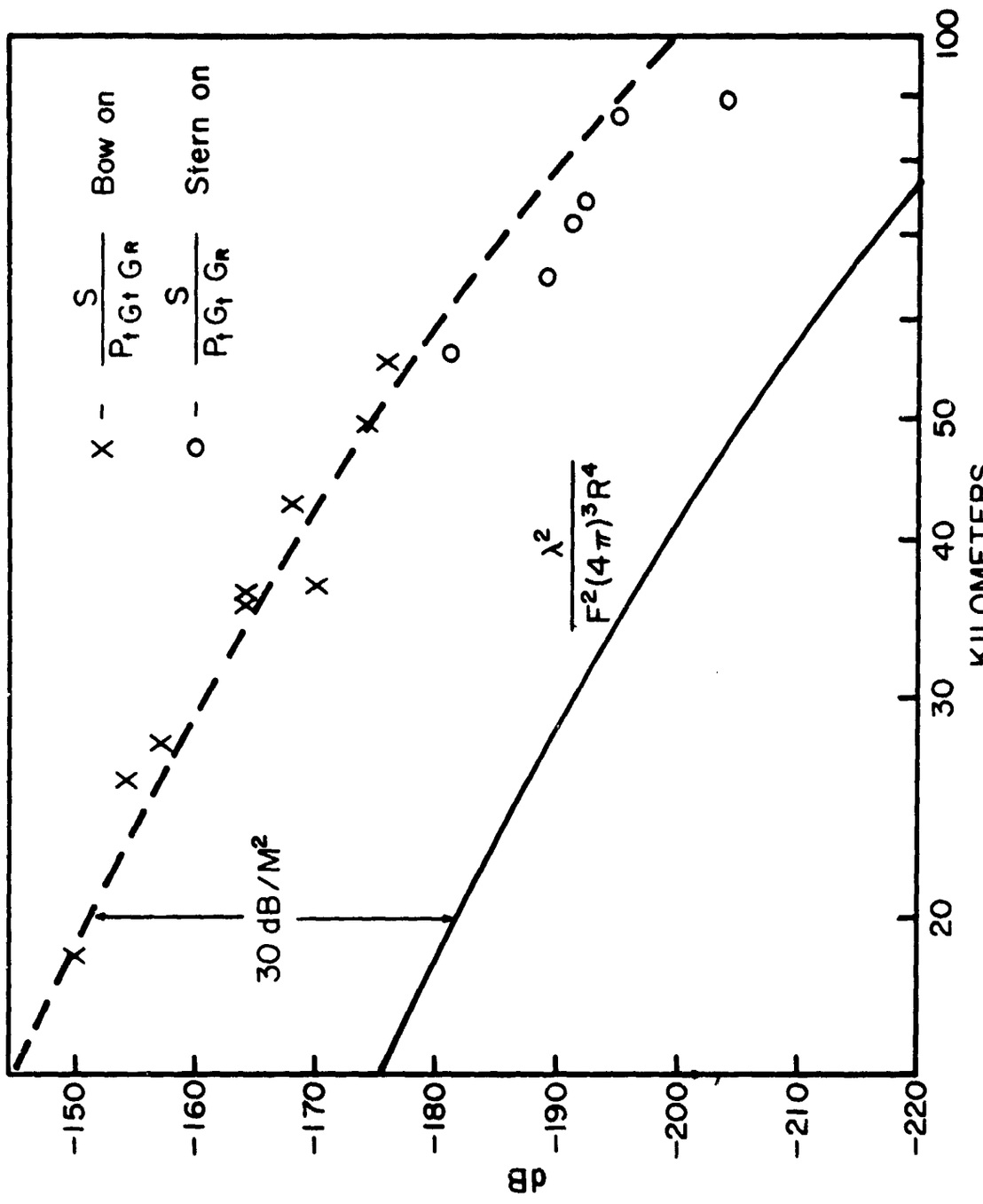

(S)

(S) Figure 4. Normalized Signal Levels from HMS Arethusa (U)

(U)

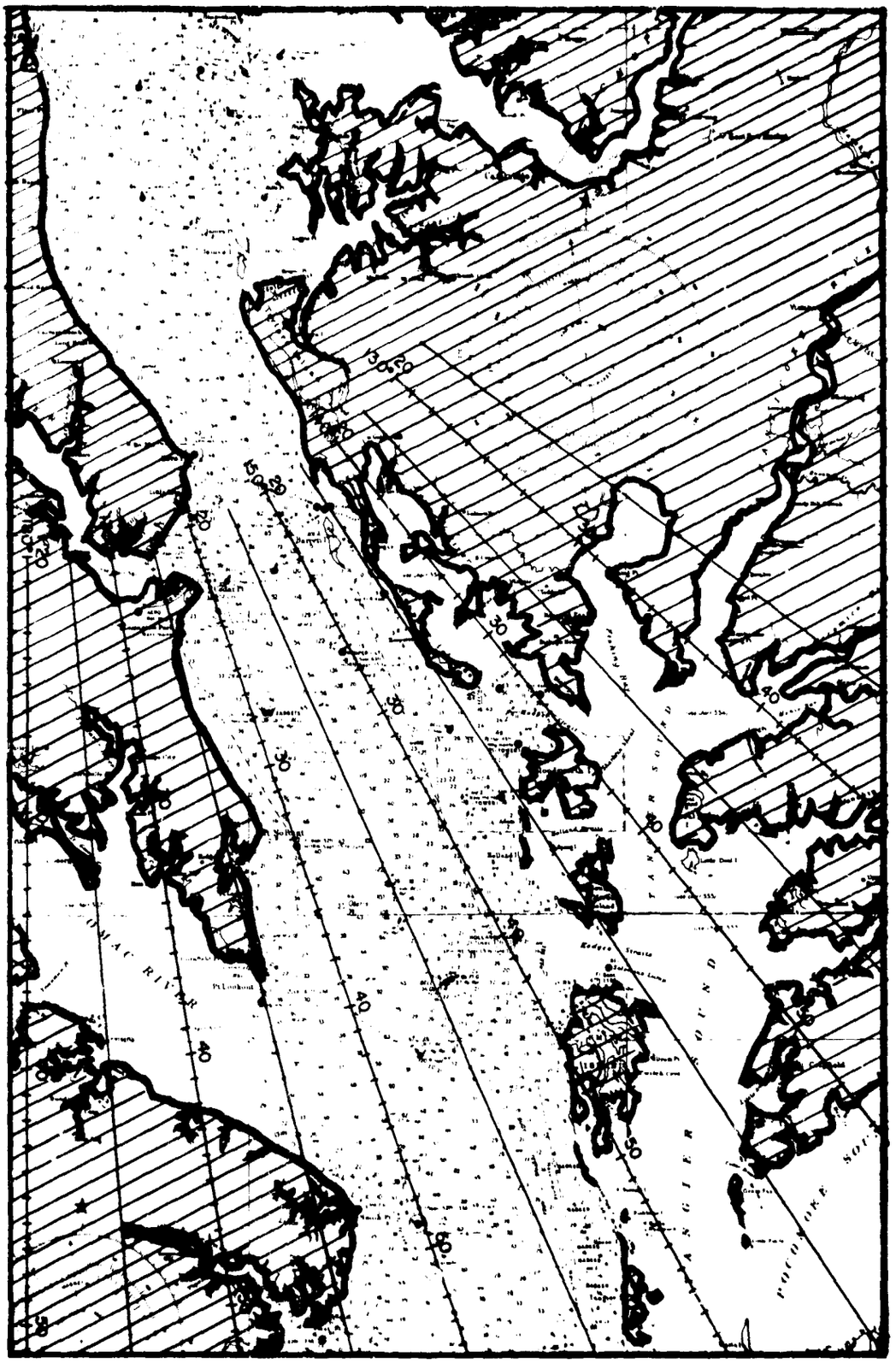

(U) Figure 5. Chesapeake Bay (U)

(U)

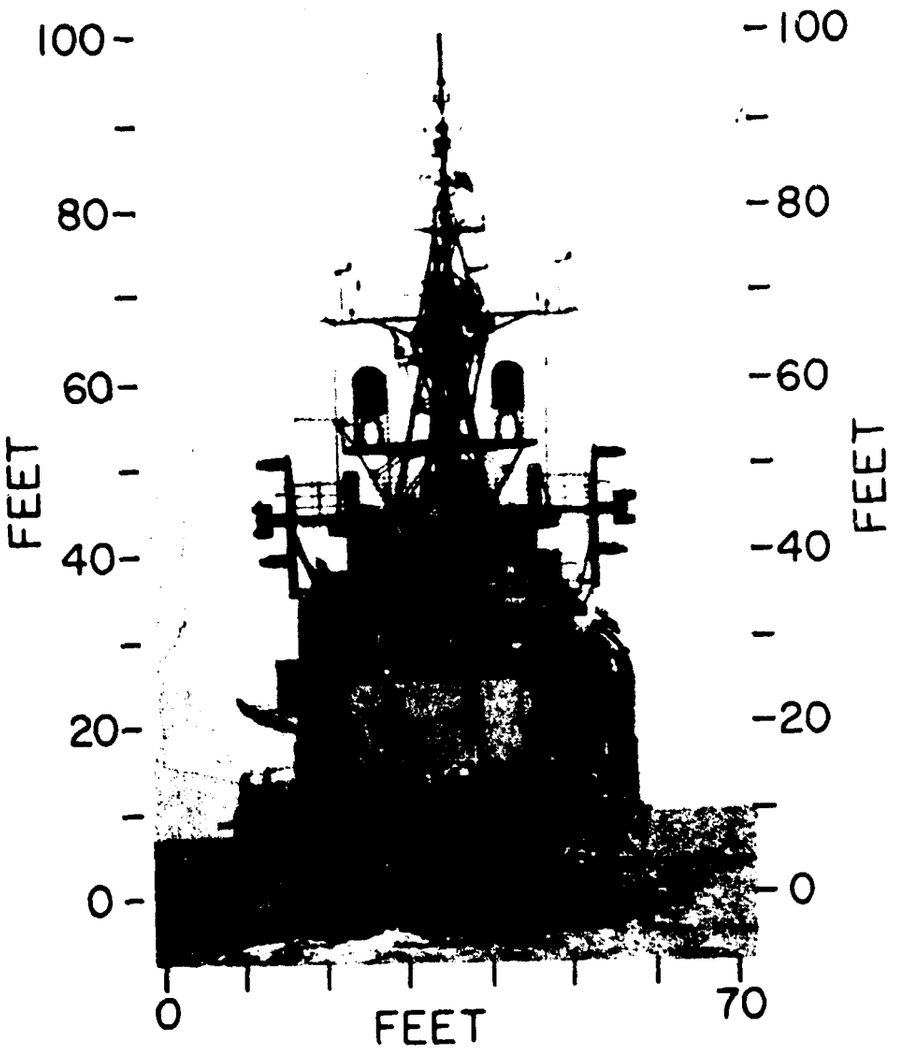

(U) Figure 6. USS Lloyd Thomas, DD-764 (U)

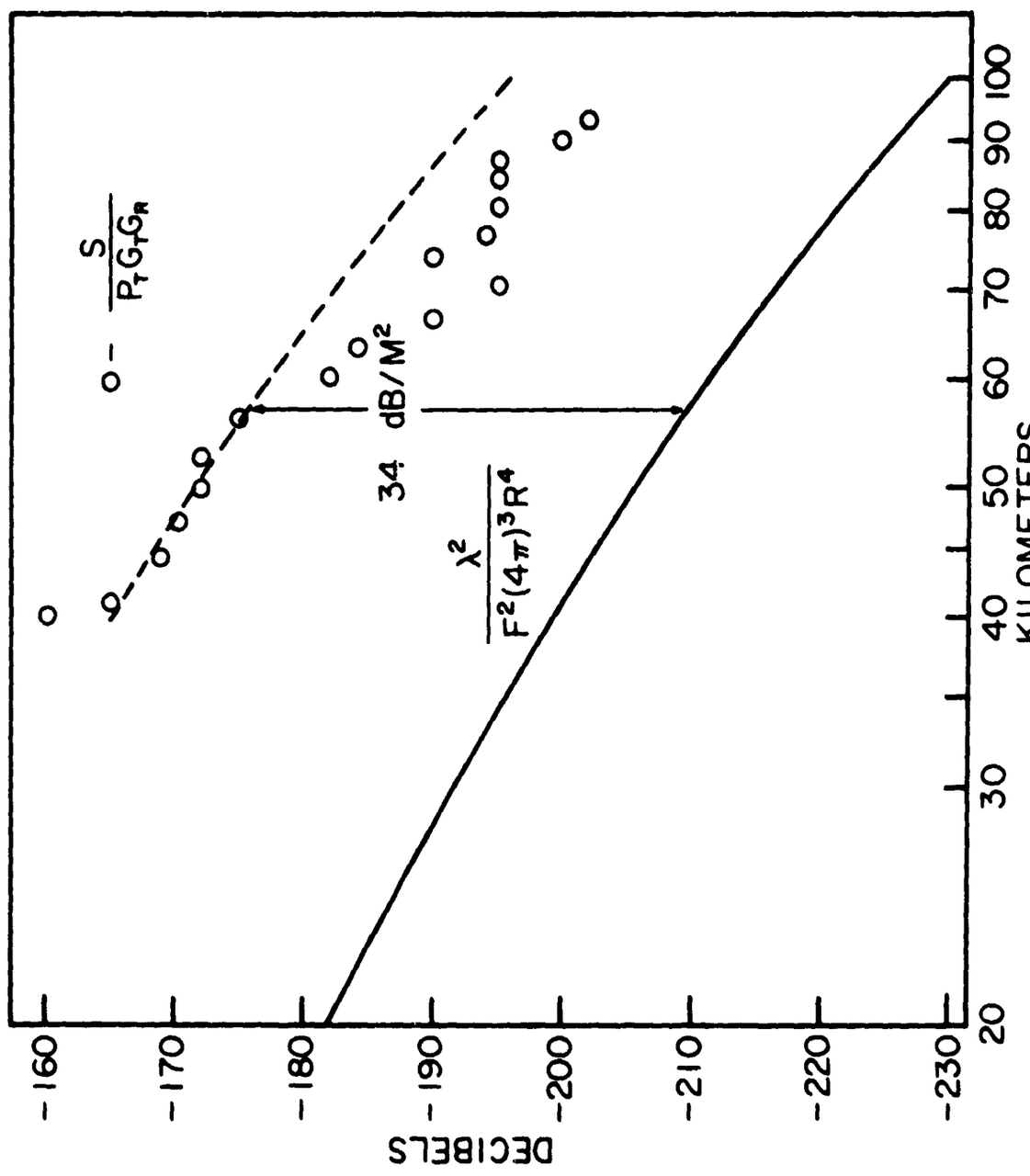

(S) Figure 7. Normalized Signal Levels from USS Lloyd Thomas (U)

(S)

(U)

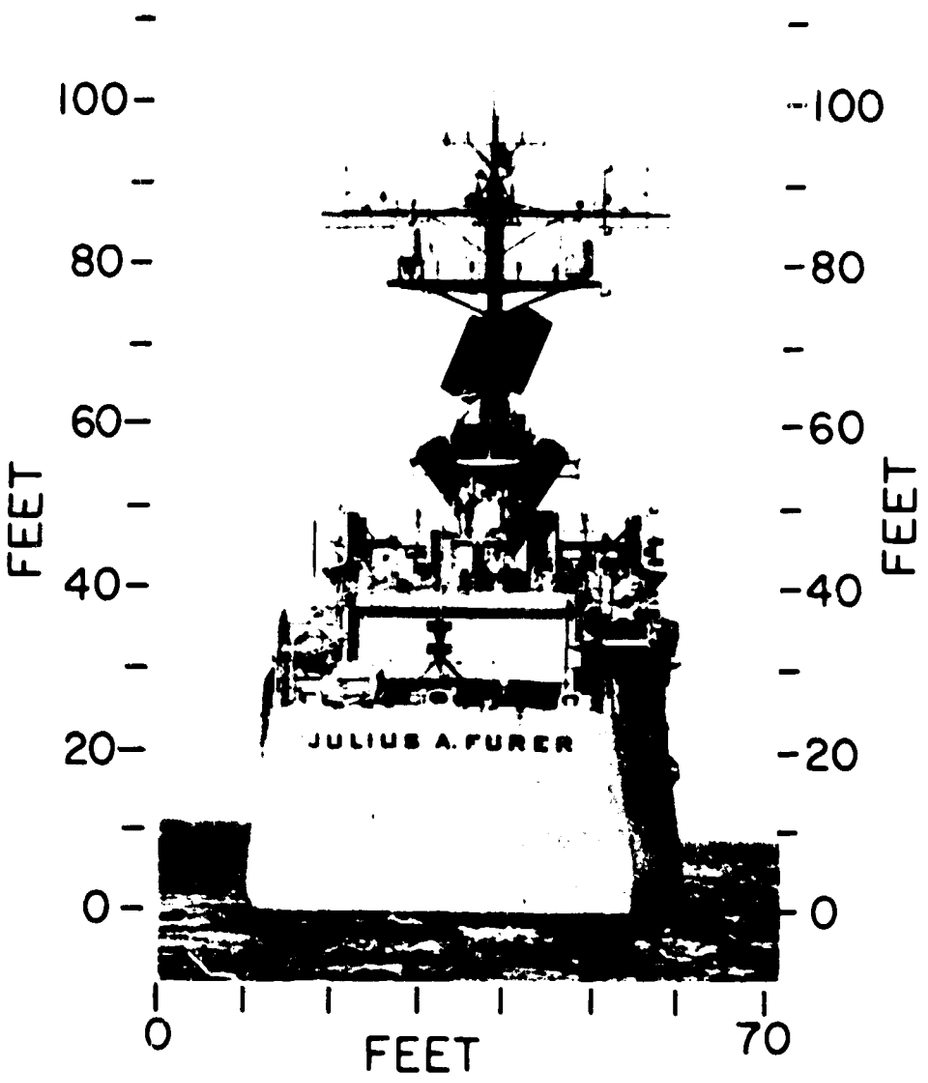

(U) Figure 8. USS Julius A. Furer, DEG-6 (U)

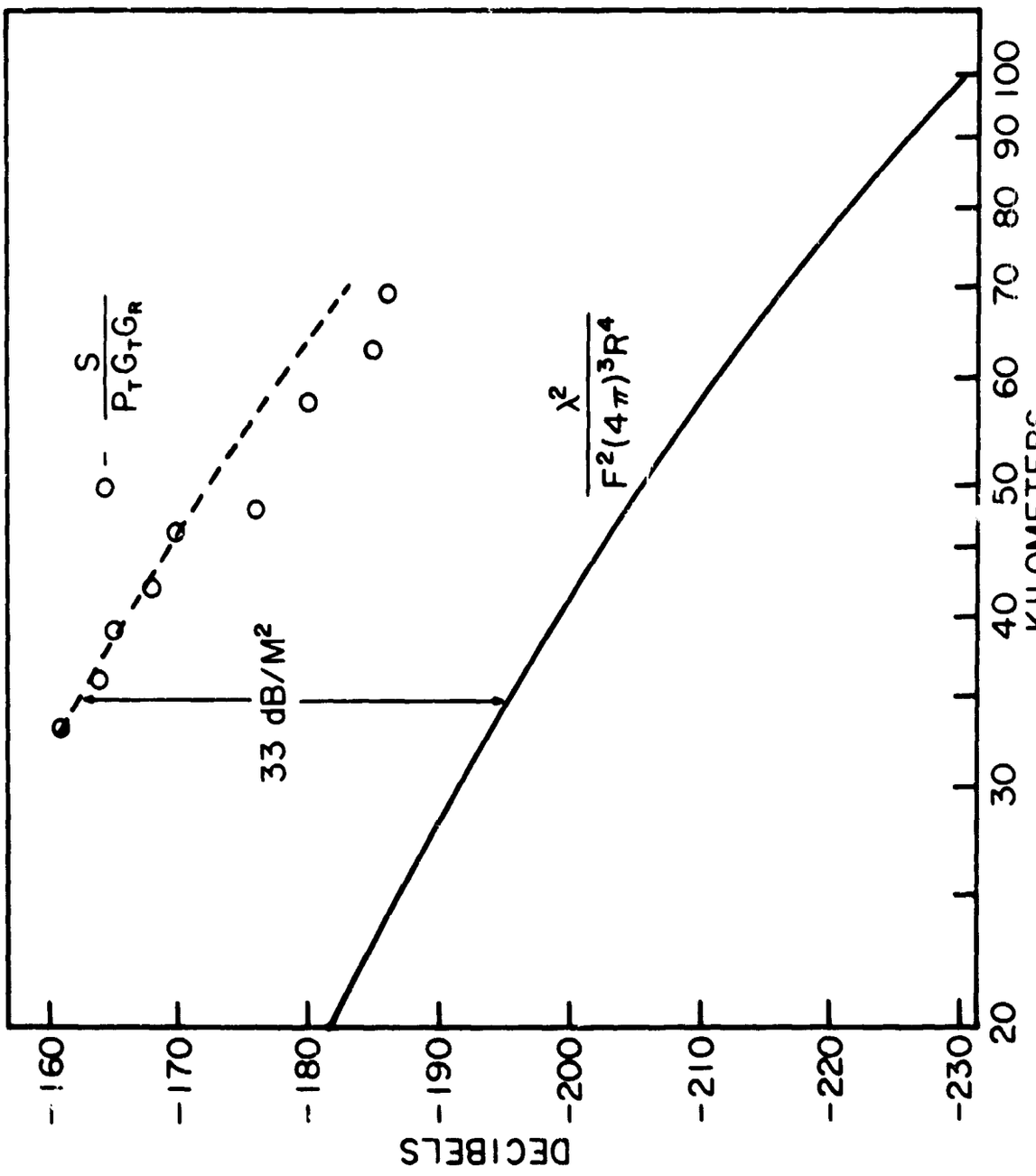

(S) Figure 9. Normalized Signal Levels from USS Julius A. Furer (U)

(S)

HF BACK SCATTER FROM A SHIP'S WAKE (U)

D. D. Crombie

Institute for Telecommunication Sciences
ESSA Research Labs. Boulder, Colorado 80302

I INTRODUCTION (U)

(U) In 1968 the writer suggested at a Defense Science Board (DSB) meeting that the highly periodic structure of a ship's wake might have a large resonant scattering cross-section. It was also suggested that at some aspects, at least the Doppler shift of signals resonantly scattered from the wake would be different from that of the signals resonantly scattered from the sea. As a result Dr. H. Kurss has investigated how the Doppler shift from a wake depends on the ship's velocity, on the direction of incidence, and how its value at resonance compares with the Doppler shift of the sea clutter. He has also investigated how the scattering cross section depends on the same factors. This note will summarize his results.

II DOPPLER SHIFT (U)

(S) The Doppler shift of the signal back scattered from the sea is given by

$$(\Delta f_r)_s = \pm (2^{1/2}\ 3^{1/4}/4\pi)\,(g/v\,|\cos(\theta \pm \theta_c)|^{1/2})$$

while the Doppler shift of the signal scattered from the wake at resonance is given by

$$(\Delta f_r)_w = (3^{1/2}/4\pi)\,(g/v)\,(\cos\theta/|\cos(\theta \pm \theta_c)|)$$

Thus the ratio is given by

$$(\Delta f_r)_w/(\Delta f_r)_s = \pm a\cos\theta/|\cos(\theta \pm \theta_c)|^{1/2}$$

where $a = 3^{1/4}/2^{1/2} = 0.9306$, θ is the angle between the direction of the transmitter, as seen from the ship, and the direction of the ship's motion, and v is the ship velocity while g is the acceleration of gravity. The angle θ_c is the inclination of the cusp lines of the wake to the direction of travel, and has a value $\theta_c = 19^{\circ}\ 28'$.

(S) Equation 1 is plotted in Figure 1, and shows that except when θ is in the region of 20 to 40° there is a significant difference in the two Doppler shifts. This difference should enable a wake echo to be separated from the sea clutter in a properly designed monostatic system.

III SCATTERING CROSS SECTION (U)

(S) Dr. Kurss has also developed formulae giving the scattering cross section of the wake. An approximate version, which assumes that the width of the cusp line is $\pi/\sqrt{2}k_w$, is

$$\sigma = \text{const}\,(K/k)^2\, N^{4/3} f(\theta)$$

where the const = 24.1, and

$$K/k = 1.845\, n^{1/3} \zeta_n$$

where ζ_n is the elevation of the nth crest along the cusp line. N is the number of crests along the illuminated portion of the cusp line. The factor $f(\theta)$ contains the angular dependence and is given by

$$f(\theta) = \left| \frac{\sin(\theta \pm \theta_t)}{\cos(\theta \pm \theta_c)} \right|$$

where θ, θ_c and θ_t are shown in Figure 1. The variation of $f(\theta)$ with θ is shown in Figure 2. It is evident that the cross section is zero when $\theta = \theta_t$, but otherwise shows no rapid dependence on θ.

(S) At a ship velocity of 20 knots, the frequency (fr) of resonance with cuspidal components of the wake, along the direction of the ship's velocity, is ~2.0MHz, the wake wavelength (λ_ω) is ~75m. If the wake amplitude is 0.75m (1/100 of the wavelength) one wavelength behind the ship, K/k = 1.37. If the illuminated length of the wake is 10km, N = 10,000/75 = 133 and $N^{4/3} \simeq 700$. From Figure 1, $f(\theta) \simeq 0.74$. Thus the scattering cross section for one component of the wake is ~23,500m^2, at resonance.

(S) Yim and Tulin indicate that the surface wake of a submarine 30 ft. in diameter, 327 ft. long, at a depth of 82 ft., and having a velocity of 20 knots will have an amplitude of 0.27 meters at 5 wavelengths behind the submarine. Thus,

$$K/k = 1.845\,(5)^{1/3} \times .27 = 1.1.$$

The other parameters being the same, the cross section of one arm of the wake is~9100m^2 at resonance.

(S)

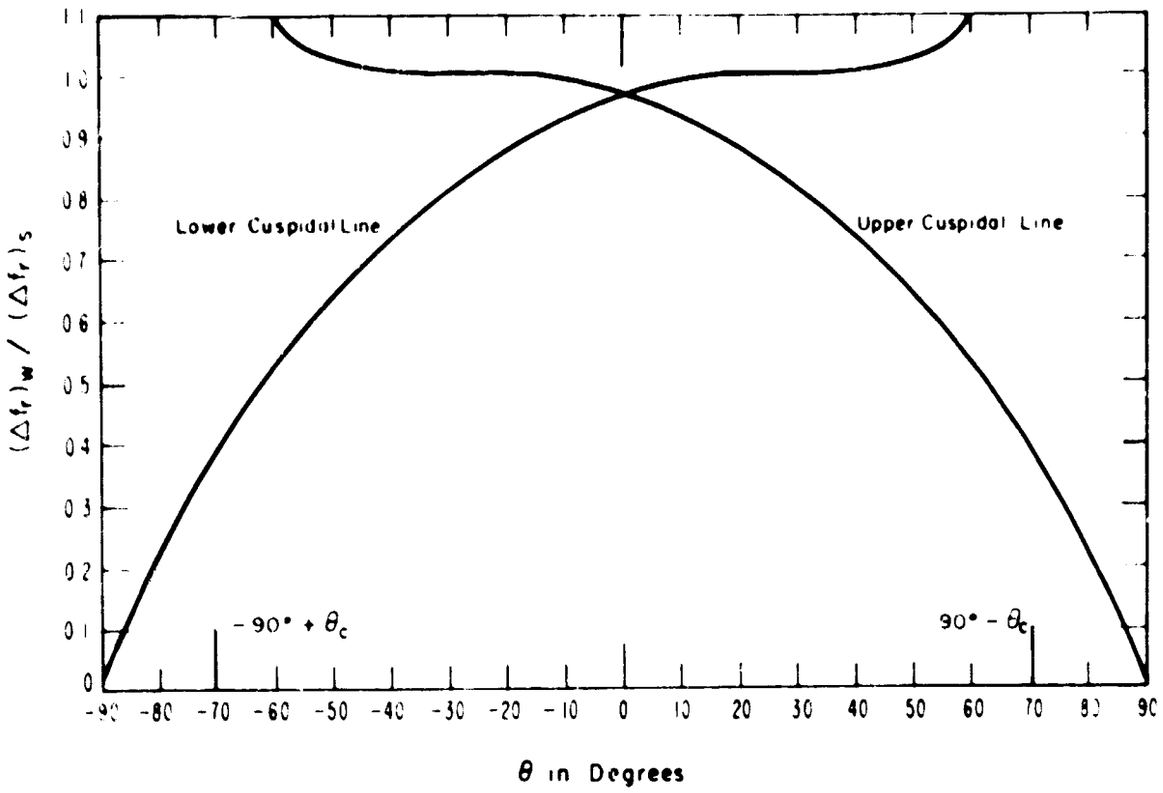

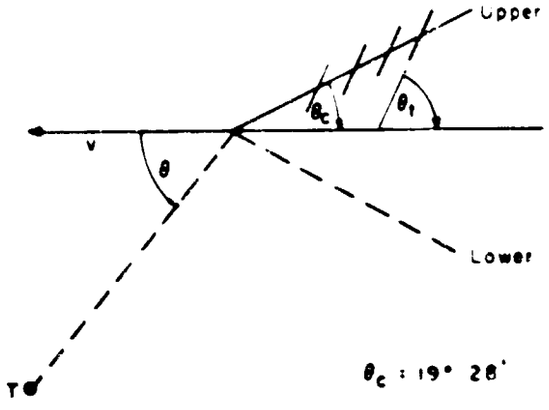

(S) Figure 1. Angular Dependence of the Ratio of Doppler Shifts from a Wake and the Sea at Resonance (U)

(S)

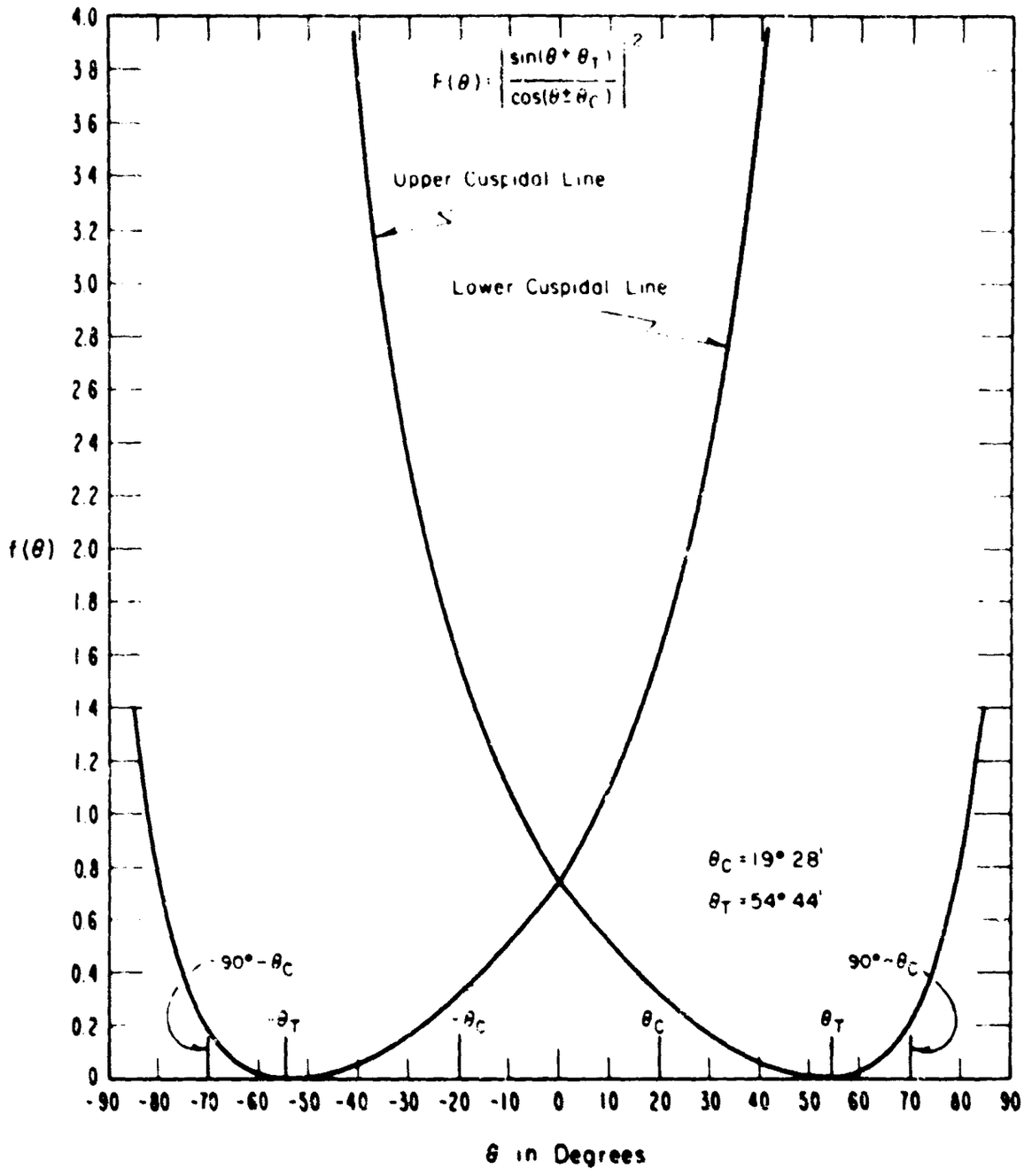

(S) Figure 2. Angular Dependence of the Wake Cross-section at Resonance (U)

IV NOTES ON DETECTION OF SUBMARINE AND SHIP WAKES (U)

(S) Current calculations indicate that the radar cross-section of a wake can be very large ($\sim 10^4 m^2$) at resonance.

(S) The frequency of the radar depends quite critically (< 1%) on the ship's velocity and heading. Thus the radar must step with very small changes, in frequency.

(S) The Doppler shift of the wake differs significantly from the Doppler shift of the sea, over quite a wide range of azimuth angles. However, the differences are such that Doppler resolution of 1/100 Hz or so are required. This implies observation tunes of a few minutes. The use of a bistatic radar is also contra-indicated.

(S) Submarines produce surface wakes of significant amplitude if they are shallow enough and fast enough. Current calculations suggest that the wakes might be detected for depths of up to 200 ft and for speeds greater than 20 kts (lower speeds require smaller depths).

(S) At such speeds radar frequencies as low as 1 MHz are required. At these frequencies the obtainable radar range is quite large compared with those obtainable at higher frequencies because of the small ground wave attenuation.

(S) Provided the wake Doppler can be separated from the clutter Doppler, a radar for detecting wakes will be noise limited. Thus the minimum wake amplitude which is observable will depend only on ambient noise levels and transmitter power.

(S) I visualize that a radar for detection of wakes would consist of a pulsed monostatic system with 360° illumination. Pulse rates should be as high as possible consistent with avoidance of skywave clutter. Each pulse will be transmitted at a different (by < 1%) frequency from the previous one. The complete frequency scan will be completed within half the period of the Doppler shifts expected. Successive signals at the same frequency will be added coherently.

(S) After signals from one or both "arms" of the wake are detected their bearing can be determined by various methods. It is presumed that the received signals will be processed as indicated above in several range gates.

THIS PAGE INTENTIONALLY LEFT BLANK

FLEET AIR DEFENSE (U)

PRECEDING PAGE BLANK - NOT FILMED

FLEET AIR DEFENSE REQUIREMENTS (U)

Paul T. Stine

Radar Division, Naval Research Laboratory
Washington, D.C. 20390

I INTRODUCTION (U)

(S) Our Navy's problem in terms of fleet air defense (FAD) requirements is posed by the fact that fleet units must operate in a hostile environment under constant surveillance by trawlers, submarines, "neutral" shipping vessels, aircraft, certain types of land-based sensors, and possibly satellites, each making use of sensing techniques available as a result of a rapidly advancing technology. In order to operate effectively, our fleet units need improved surveillance data providing detection, identification, and location or track of a threat while sufficient time remains for defensive reaction. This surveillance capability needs to be available under all weather conditions, effective under EMCON operating conditions, highly reliable, and capable of providing data of sufficient accuracy and timeliness as to be useful to shipboard defensive systems. In addition, the surveillance system must not obviate an appropriate offensive/defensive balance within fleet units.

II DOCUMENTED REQUIREMENTS (U)

(S) Officially, the Navy's requirements for fleet air defense are covered by General Operational Requirement (GOR) 17 titled "Surface Anti-Air Warfare" which essentially says that all ships must be able to defend themselves against short-range missiles, and large tactical units must be able to counter threats from all sources including space vehicles. Advanced Development Objective (ADO) 17-23X, "Shipboard Surface Wave Radar" deals more specifically with the probable threat and possible requirements for shipboard surface-wave radar as a means of over-the-horizon (OTH) detection of the threat.

III NATURE OF THE THREAT (U)

(S) The threat as defined by ADO 17-23X, summarized in Figures 1 and 2, is a low-flying (40 ft altitude) target capable of at least 100-nmi range and having a radar cross section (RCS) of one

(S)
square meter in the high frequency (HF) band. This RCS seems to be reasonable as substantiated by model measurements shown in Figure 3. Along with low-flying attack aircraft and such air-launched missiles as the SS-C-2 (SAMLET), the patrol boat-launched SS-N-2 (STYX) missile and the frigate or submarine-launched SS-N-3 (SHADDOCK) missile are commonly accepted as being representative of today's threats. The actual range capabilities of the SS-N-2, SS-C-2, and SS-N-3 are 22, 45, and 250 nmi respectively. It is reasonable to expect that the threats of the near future will be capable of flying farther, lower, and faster than the above mentioned missiles.

IV THE REAL NEED (U)

(S) In summary, the Navy's real need seems to be a surveillance system having the following basic characteristics and performance:

- All-weather operating capability.
- Effectiveness under EMCON conditions.
- Large-area coverage (approximately a 300-nmi radius from fleet unit).
- Mobility to cover operating area of interest.
- Compatibility with ships defensive and offensive weapons systems.
- High reliability.
- Ability to detect, identify, and track small (RCS $\approx 1M^2$), low flying (H $\approx$ 10 ft) targets.
- Azimuthal accuracy of $\pm 5^{\circ}$ or better (as seen from the fleet unit).
- Range accuracy of $\pm$ 5 nmi or better (as seen from the fleet unit).
- Velocity accuracy of $\pm$ 5 knots or better (relative to fleet unit).

(C)

ADO 17-23X: SHIPBOARD SURFACE WAVE RADAR

BRIEF

"To accomplish the development work necessary to prove the military usefulness, technical feasibility, and financial acceptability of a Shipboard Surface Wave Radar."

ULTIMATE OBJECTIVES

a. "To provide early detection of low-flying air targets at a range of 100 miles or more."

b. "To provide azimuth angle and time that the threatening air target will enter the normal defensive radar envelope."

c. "When the objective is achieved, a decision whether or not to continue into Engineering Development will be made by CNO."

(C) Figure 1. ADO 17-23X, Brief and Objectives (U)

SECRET

(this page confidential)

(S)

ADO 17-23X: SHIPBOARD SURFACE WAVE RADAR

AMPLIFYING DATA SUMMARY

a. Performance Desired

- Detection of low-flying 1-m^2 target at 100-nmi range
- Range resolution of ± 1 nmi
- Azimuth accuracy of ± 5°
- Velocity resolution of ± 10 knots
- Five frequency bands within HF band
- Rapid shifting between frequency bands

b. Constraints

- Lightweight and compact
- Suitable for installation in a DD or larger ship
- Compatible with current shipboard power limitations
- No harmful interference to HF communications systems
- No physical harm to personnel in exposed locations

(S) Figure 2. ADO 17-23X, Summary of Amplifying Data (U)

SECRET

(S)

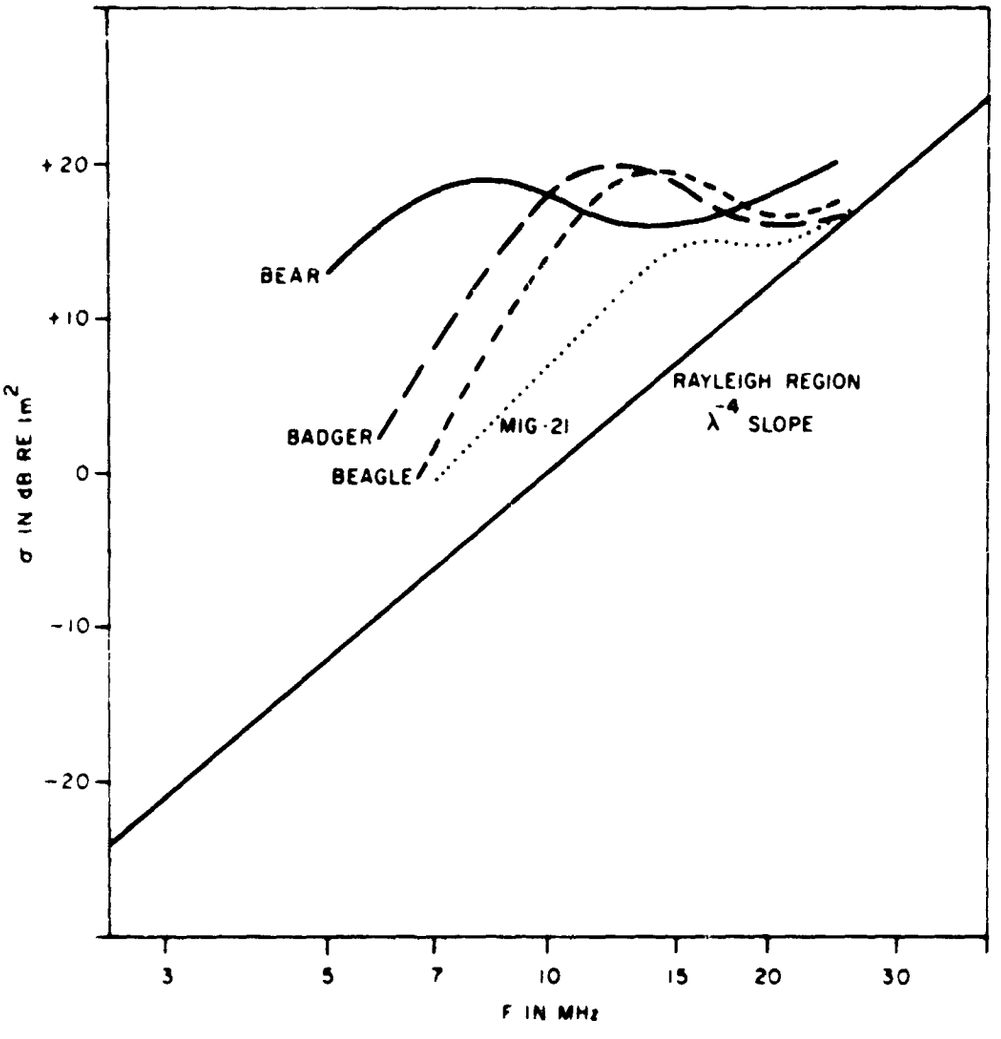

(S) Figure 3. Nose-on (± 30°) Vertically Polarized Radar Cross Sections vs Frequency (U)

V POSSIBLE OTH SOLUTIONS (U)

(S) A list of possible solutions to the Navy's large-area surveillance problem includes AEW radar, helicopter-borne radar, passive ECM, satellite surveillance, skywave radar, surface-wave radar, and microwave radar propagating in the evaporative duct. Needless to say, each has its advantages and limitations. Both AEW radar and helicopter radar methods of looking over the horizon suffer from weather and logistics problems. Passive ECM is useless against a non-radiating threat. Satellite surveillance faces severe logistics, weather, and accuracy problems. Skywave radar has range and azimuthal accuracy limitations along with problems of propagation path availability as illustrated in Figure 4. Monostatic surface-wave radars, due to high surface-wave attenuation, would require powerful transmitters and large antennas as illustrated in Figures 5 through 7, would be limited by practical considerations to detection ranges of about 50 to 100 nmi and would not be usable under EMCON conditions. Microwave radar propagation in the evaporative duct would also violate EMCON conditions and is probably limited to ranges of 50 to 100 nmi. In addition, much remains to be learned about the time, space, and thickness variabilities of evaporative ducts.

(S) One other possible solution is a hybrid system in which one or more optimally designed mobile skywave radars each operate monostatically to provide large-area surveillance ($\simeq$ 500-nmi radars) around a fleet unit, the surveillance data being transmitted to the fleet unit by regular communication links. Inasmuch as the skywave radars are illuminating the area of interest, fleet units can be equipped to make bistatic detection and location of threats coming within a range of about 50 to 100 nmi as shown in Figures 8 and 9. In this approach, the range accuracy of the bistatic data is quite dependent upon strategic positioning of the skywave illuminators relative to the fleet unit as shown in Figure 10. Although the bistatic range accuracy of such a system leaves something to be desired, it would appear to have all of the desired characteristics listed under Section IV with a high probability of solving the total problem.

VI CONCLUSIONS (U)

(S) It is concluded that the hybrid skywave/surface-wave system suggested above and summarized in Figure 11 offers a practical solution to the Navy's problem of OTH surveillance, and it is recommended that steps be taken toward implementation of such a system.

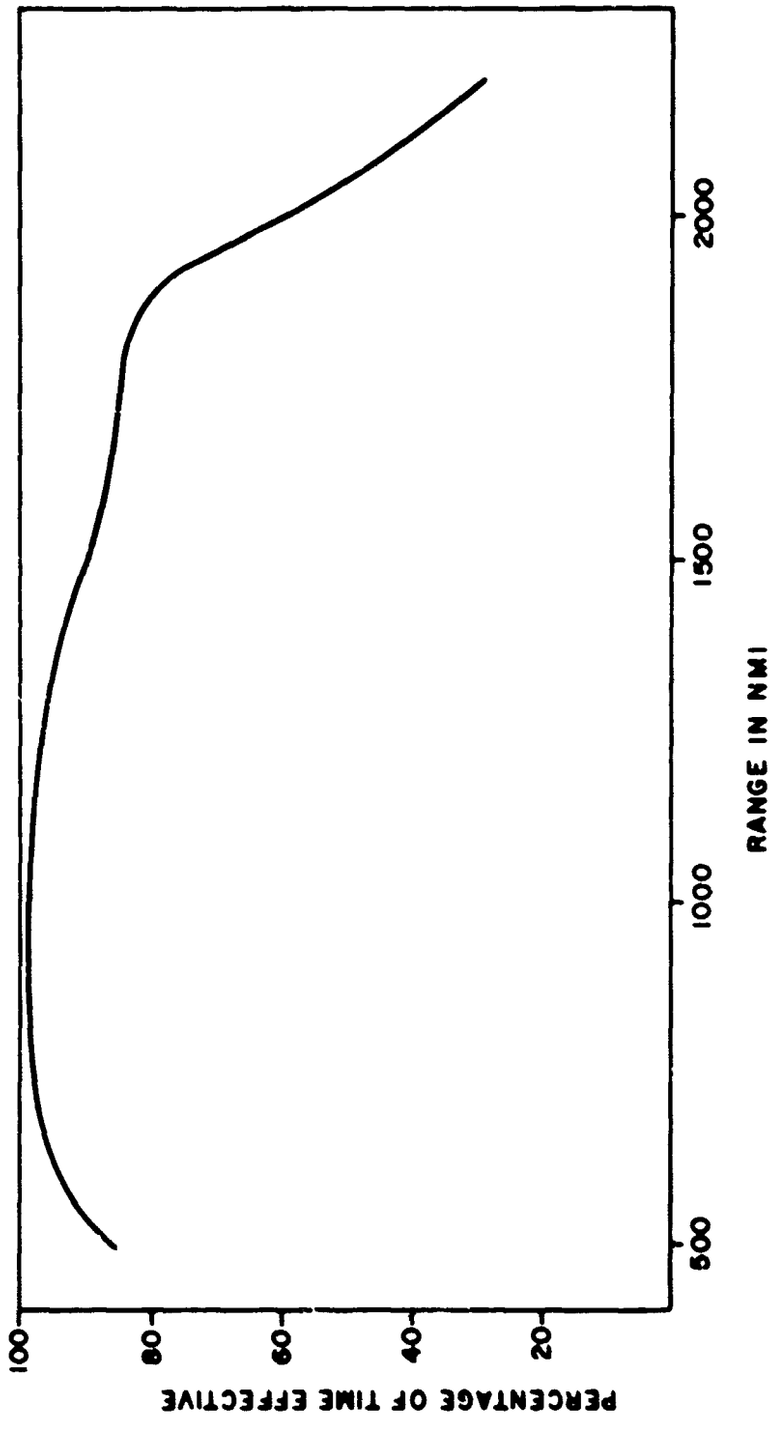

(U) Figure 4. Percentage of Time Radar is Effective as a Function of Range (U)

(U)

(S)

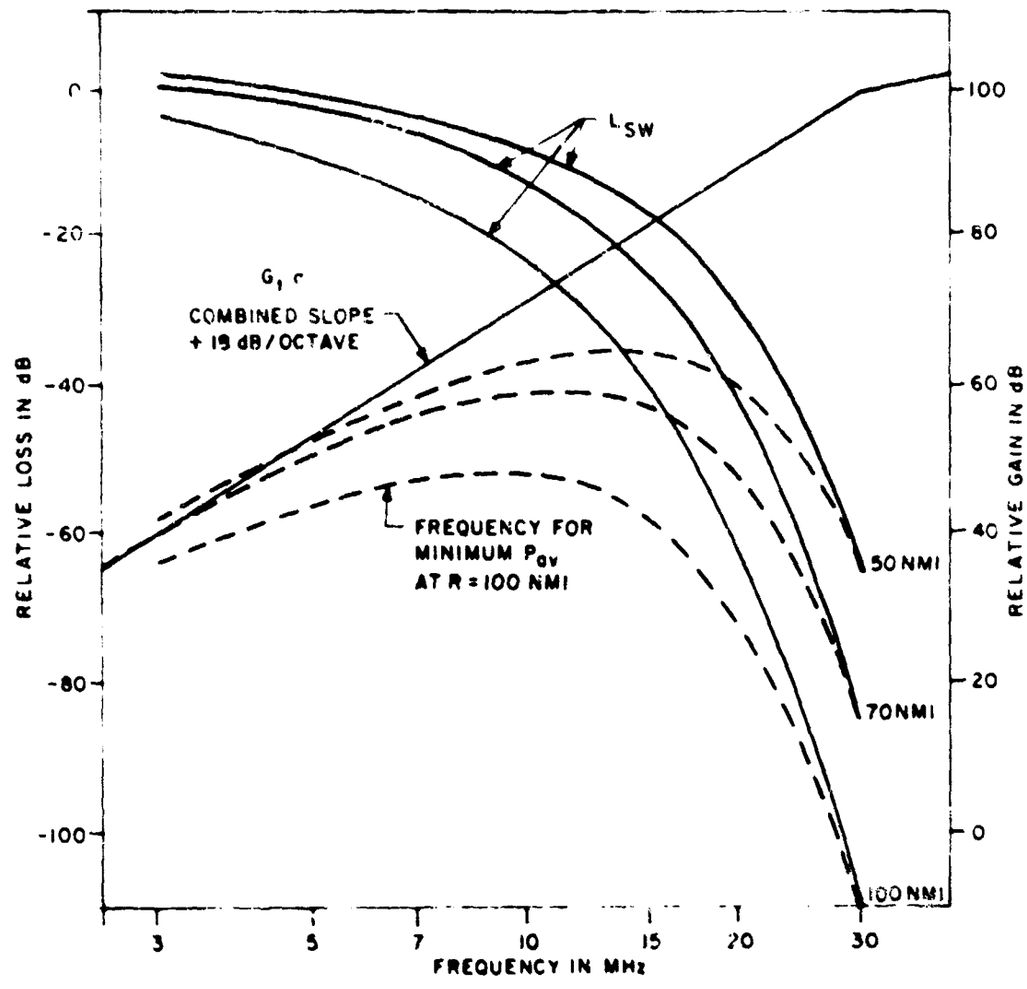

(S) **Figure 5. Determination of SSWR Optimum Frequency for Minimum Transmitter Power Requirement (constant antenna aperture assumed with small target in Rayleigh region below 30 MHz) (U)**

(S)

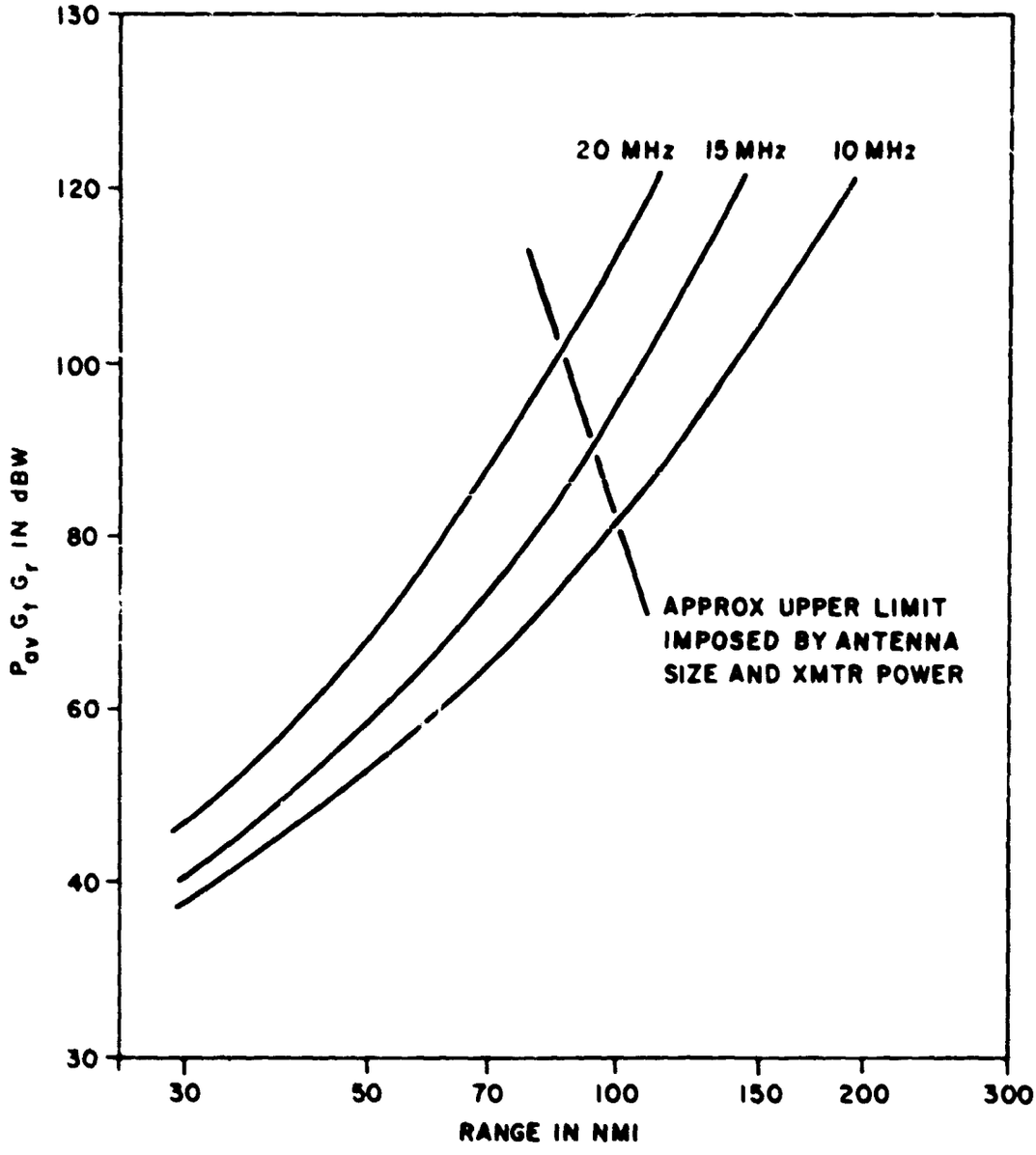

(S) Figure 6. Product of Transmitter Power, Transmitter Antenna Gain, and Receiver Antenna Gain for SSWR (Monostatic)Case (U)

(S)

CHARACTERISTIC	HIGH PERFORMANCE MONOSTATIC SYSTEM	INTERMEDIATE MONOSTATIC SYSTEM	MINIMUM SIZE MONOSTATIC SYSTEM	BISTATIC SYSTEM
Ship Size Req'd.	Mod Light Carrier	Frigate	Destroyer	Destroyer
Probable Shipboard Antenna	Large Dipole Array	Rotatable Log Periodic Array	Rotatable Log Periodic Array	Crossed Spaced Loop
Avg. Transmitter Power	100 kW	30 kW	10 kW	200 kW (Remote)
Primary Power Req'd	300-500	120-200 kW	60-100 kW	10-20 kW
"Below Deck" Weight	15 Tons	10 Tons	7.5 Tons	5 Tons
"Below Deck" Space Req'd	1000 ft.^{2}	700 ft^2	550 ft^2	350 ft^2
Range Capability (On 1-M^2 Low Flying Target)	100 nmi	80 nmi	60 nmi	60 nmi
Range Accuracy	±1 nmi	±1 nmi	±1 nmi	Depends on Geometry
Azimuth Accuracy	±3°	±10°	±15°	±5°

(S) Figure 7. Estimated Characteristics of Shipboard Surface Wave Radar Systems (U)

SECRET

(S)

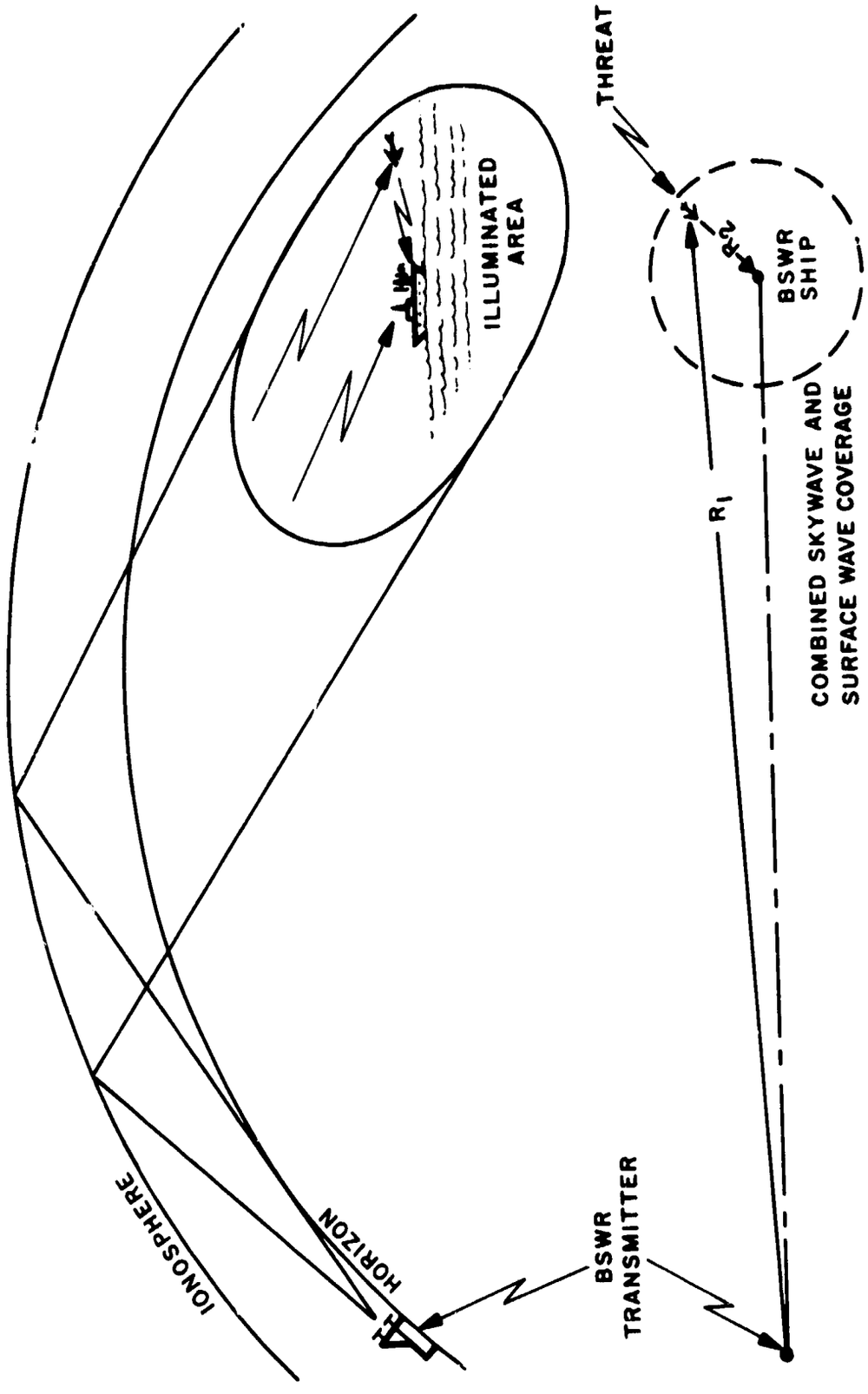

(S) Figure 8. Bistatic Surface Wave Radar Concept and Geometry (U)

(S)

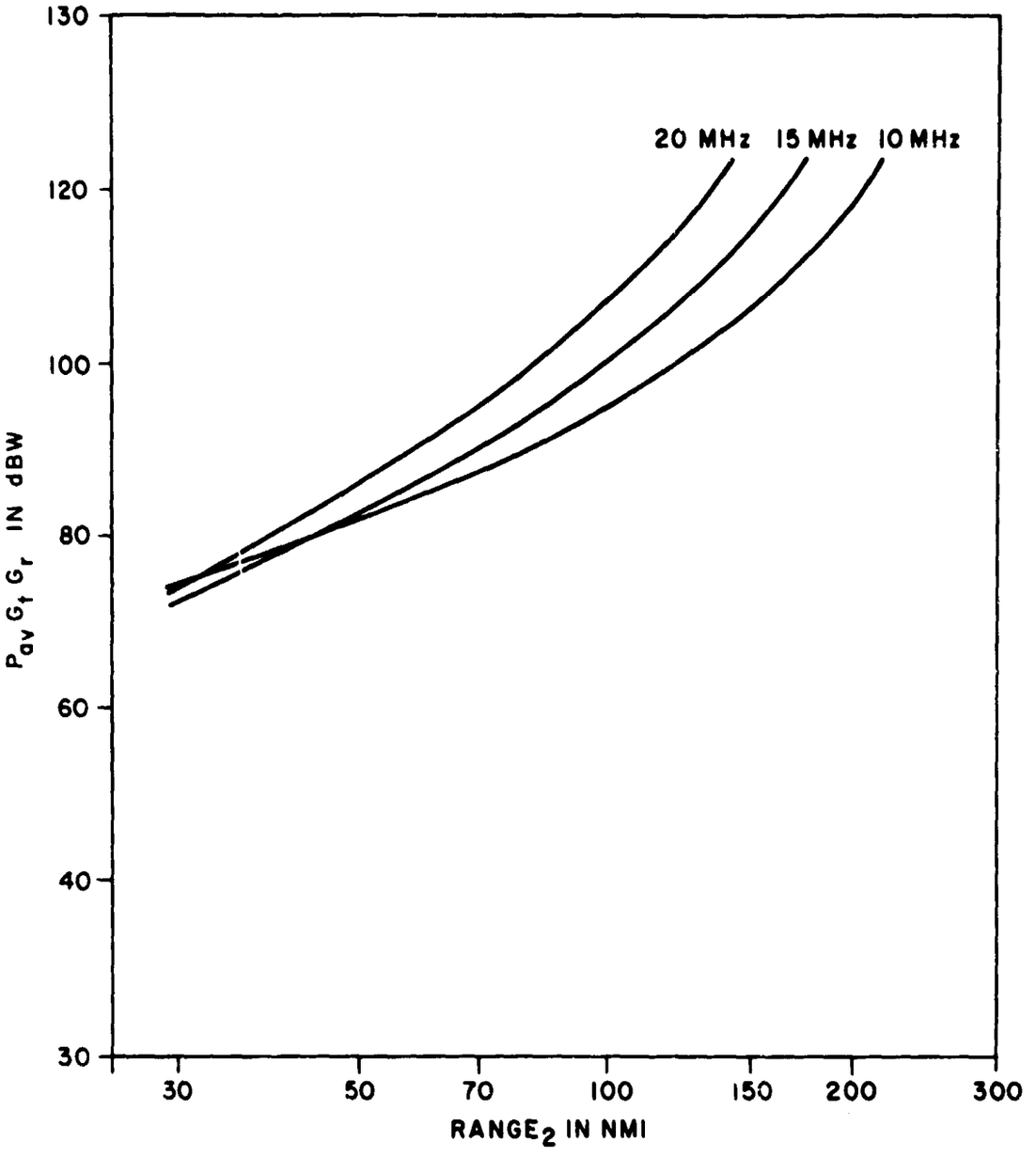

(S) Figure 9. Product of Transmitter Power, Transmitter Antenna Gain, and Receiver Antenna Gain vs Range from Ship to Target for BSWR Case (U)

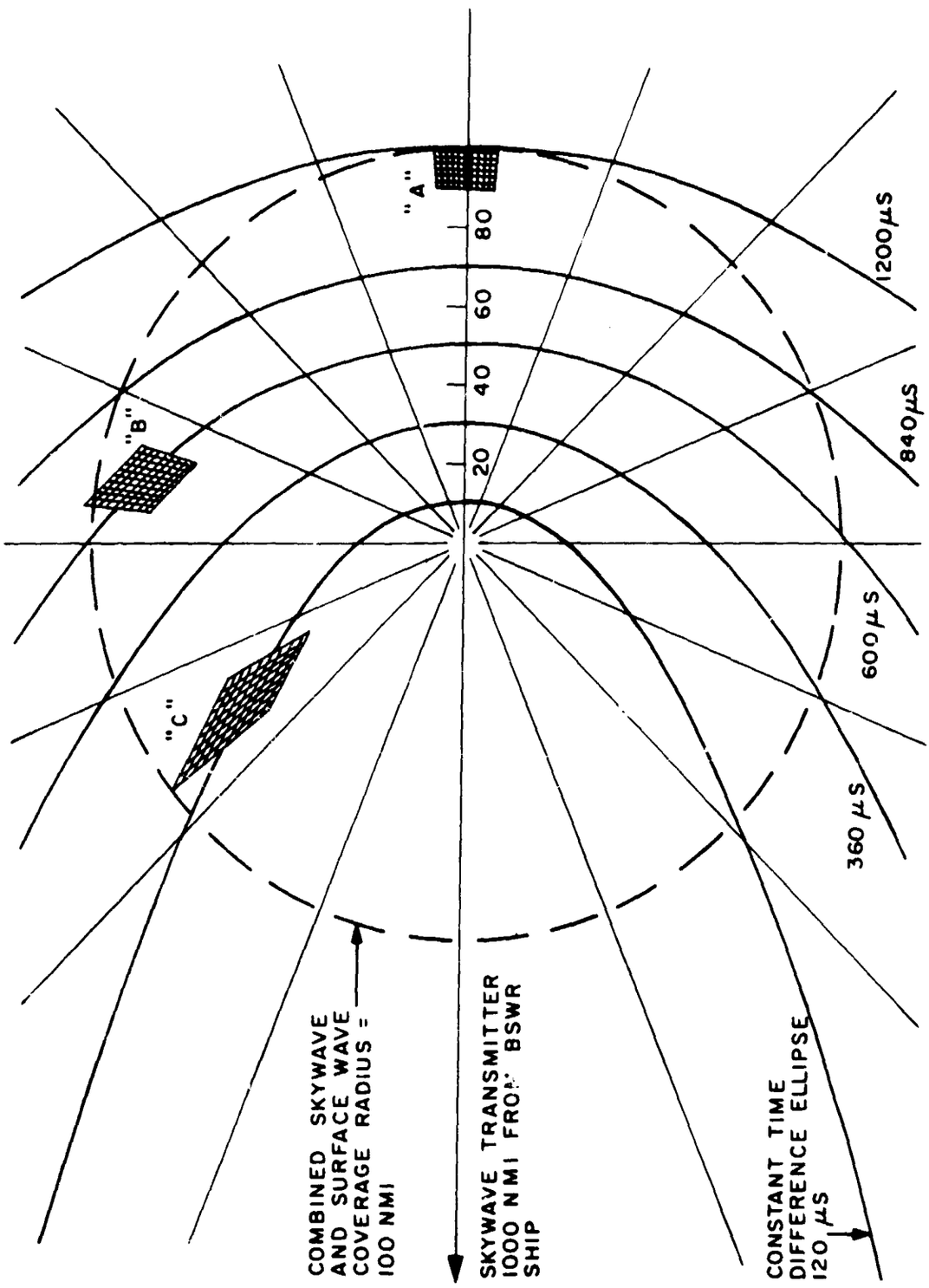

(S) Figure 10. Illustration of Geometric Limitations of BSWR Range Accuracy (U)

(S)

(S)

PROPOSED METHOD OF OTH THREAT DETECTION

1. Use a remotely located OTH skywave radar to detect and locate a threat and possibly to communicate this "early warning" to the ship or task force under attack.

2. Equip one or more ships in a task force with a bistatic surface wave radar capability such that they can make use of the illumination of the threat by the skywave radar.

3. Equip one or more ships in a task force with a monostatic surface wave radar capability to provide improved data on OTH targets which have been identified as threats.

SECRET

(S) Figure 11. Hybrid System for OTH Surveillance (U)

FLEET AIR DEFENSE REQUIREMENTS FOR EARLY WARNING (U)

Richard J. Hunt

The Johns Hopkins University
Applied Physics Laboratory
8621 Georgia Avenue
Silver Spring, Maryland 20910

I INTRODUCTION (U)

(C) This paper discusses gross requirements for detection and alerting of a Naval Task Force against the primary anti-ship cruise missile threat. A system which adequately meets this threat will almost certainly satisfy requirements of lesser threats. An example of a coordinated missile attack which might be expected against a Task Force in the open ocean is discussed to highlight the salient features of the various types of weapons available to the enemy. To provide adequate AAW defense against such an attack, the AAW force commander requires warning of an impending attack with enough time so that he may use his defensive AAW weapons in the best way. The actions that need to be taken to prepare the defense, together with factors affecting decisions, are outlined. Gross requirements for threat recognition, time and bearing are given. Because of the need to communicate early warning information, a functional description of an intership communication system based on NTDS is provided (Figure 1).

(U) The ensuing discussion follows each of the charts in the presentation.

II COORDINATED MISSILE ATTACK (FIGURE 2) (U)

(C) The Soviet Navy has been growing considerably during the last 10 years with the introduction of many new types of ships, missiles and aircraft. The anti-ship missile threat has now reached a level of quality, diversity, force size and geographical deployment that establishes it as a major constraint on U S fleet operations. The threat, although developing in detail, is established in general pattern and cannot be expected to change radically any more than the U S could easily diverge from the attack Carrier Task Force concept.

(U) A well coordinated missile attack in open seas might be expected as shown in Figure 2.

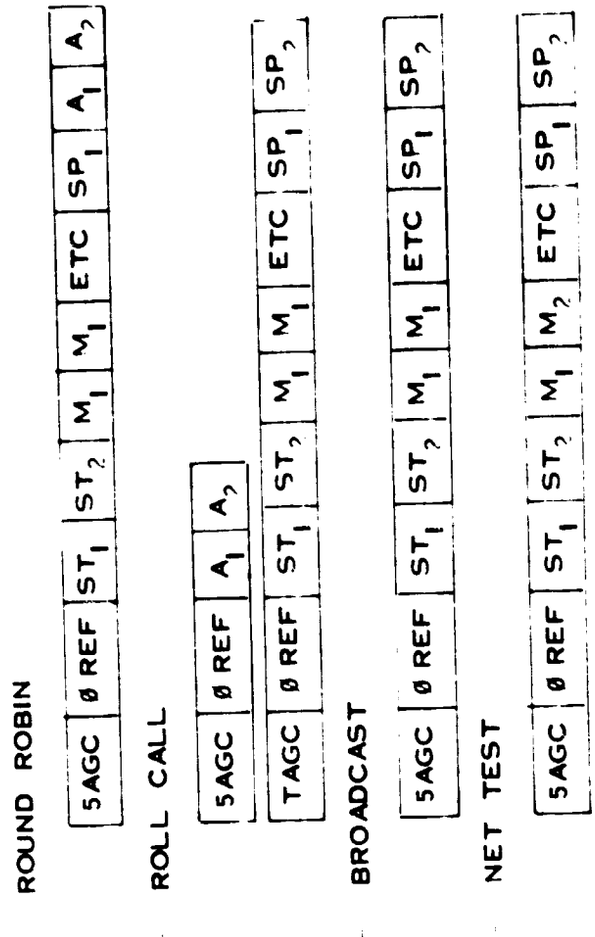

(U) Figure 1. NTDS Modes of Net Operation (U)

(U)

(C) This group is capable of launching 45 to 55 missiles at the USN force within a period of about 5 to 10 minutes. About 40 to 45 missiles will be successfully flying objects and will enter the air space about the USN force. Approximately 25-35 should be operable seeking missiles. It should be noted that 40 to 45 missiles are engageable targets since the defenses cannot know which seekers are operable. The defenses are thus faced with about 5 to 11 targets per minute if the attack is well coordinated. These targets may be approaching the defense over about as large as 120° angular sector.

(C) It should be noted that roughly half the missiles came from submarines, meaning the surfaced launch platforms are essentially undetectable until 2 to 3 minutes before launch.

(C) The enemy can be expected to support such an attack with high levels of stand-off barrage jamming. In addition, air traffic density will be high and can be expected as a normal part of the environment. Traffic density will be variable depending primarily on distance to shore. Typically, on the order of 50-100 friendly air tracks can be expected for operations close in to shore and 20-50 friendly tracks for open ocean situations.

III FUNCTION OF EARLY WARNING (FIGURE 3) (U)

(C) The primary purpose of early warning is to provide timely information to the AAW force commander so as to ensure that the actions necessary for preparing weapon systems to best cope with an attack have been taken. The actions that are taken will depend on the information available to the commander and the level of confidence he has in the validity of the information.

(C) The most critical factor in a good defensive posture is bringing system manning levels to GQ. Commanders are reluctant to take this action unless timely and positive threat recognition can be provided. Recent fleet exercises have demonstrated that detection of targets with modified condition 3 watches is the single most limiting factor in defensive capability against simulated high density raids.

(C) To bypass the many normal sequential steps in the processing of targets, SAM and EW systems are being built today (some elementary systems have already been installed) with so-called 'Threat Responsive Modes' of operation. Basically, this system concept depends on adequate recognition or identification of the threat. Some thoughts on providing positive threat recognition are shown on the next chart. If the fleet has chosen to use EMCON as a deceptive measure and positive threat recognition can be obtained, doctrine should be established to remove radiation silence.

(C) Some of the actions which will enhance detection and target processing are to employ limited azimuth search by the operators of radar consoles, to use fire control radars in automatic sector search and to bring the force PIM to a direction which will unmask radars and launchers. These actions depend on an adequate knowledge of attack bearing.

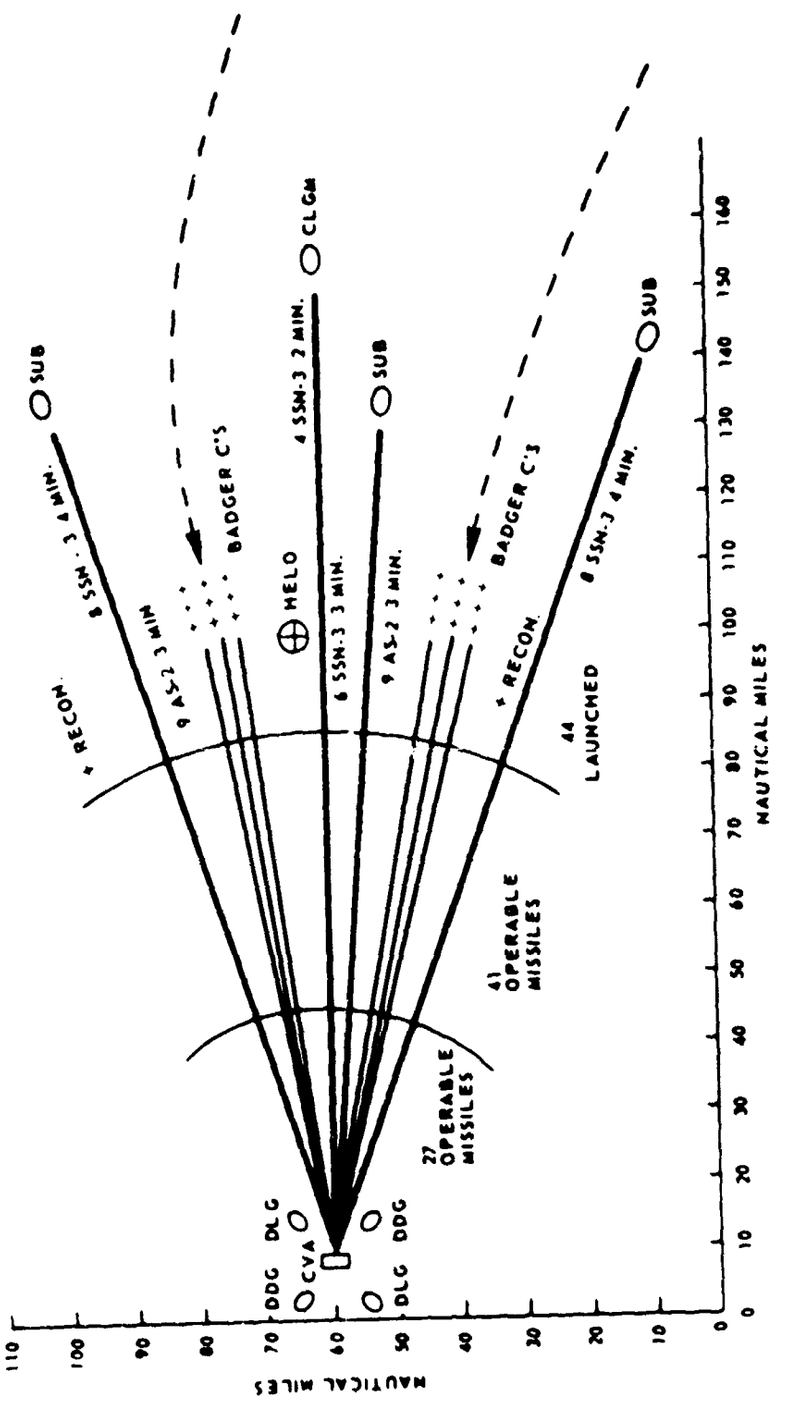

(C) Figure 2. Well Coordinated Missile Attack (U)

(C)

(C)

- PROVIDE INFORMATION WHICH WILL ASSIST THE AAW FORCE COMMANDER IN BRINGING SHIPS EQUIPMENTS & SYSTEMS TO BEAR IN THE BEST WAY

FACTORS AFFECTING DECISIONS	ACTION ITEMS
POSITIVE THREAT RECOGNITION & TIME AVAILABLE	GQ MANNING LEVELS
POSITIVE THREAT RECOGNITION	EMPLOY THREAT RESPONSIVE MODES REMOVE EMCON STATUS
ATTACK BEARING	CONCENTRATED AZIMUTH SEARCH USE OF FCR SECTOR SEARCH PATTERNS UNMASKING EQUIPMENT
ATTACK BEARING & TIME AVAILABLE	INTERCEPTOR & ASW AIRCRAFT DEPLOYMENT DISPOSITION OF SURFACE ELEMENTS

CONFIDENTIAL

CONFIDENTIAL

(C) Figure 3. Function of Early Warning (U)

(C) The use of interceptors, both CAP and DLI, depends on sufficient time to bring these systems to bear against a known attack bearing. Interceptors can play a primary role in destroying launch vehicles prior to missile launch, destroying jamming aircraft and assisting in the identification process. Timely knowledge of an attack bearing can help the force commander in redeployment of surface elements in a way to best defend the high-value target. Redeployment may be particularly appropriate if ships have been disposed in missile traps or are on ASW missions and the threat information clearly establishes that the attack is vectored to the high-value target.

IV THREAT RECOGNITION (Figure 4) (U)

(C) Since the key element in taking actions for a good defensive posture depends on positive threat recognition, it is useful to examine characteristics of the threat appropriate to the system under consideration which may be germane to identification. The most striking characteristics of the missile threat, independent of radiation signatures, are the Doppler separation from the launch vehicle and the kinematic profile of the target. The airlaunched missiles current today are discernible by a Doppler of about 50 knots which probably will not be smaller than this in the future. Subs will surface prior to launch for a few minutes and are subject to detection before missiles are fired so that the Doppler from surfaced vessels is a threat indication. Obtaining velocity vector to within 10° will give the force commander an indication of the success or failure of missile traps and dictate the need for ship redeployment.

V GROSS REQUIREMENTS TO ALERT FORCE TO IMMINENT ATTACK (Figure 5) (U)

(C) Time and bearing requirements for the several defensive systems are shown on this chart. Time requirements translate into range based on current missile speeds of about M1.0 and possibly M2.0 in the future. The limiting factor in time is the delay associated with bringing ships to GQ. Ten minutes implies a range from the task force of the order of 100-200 nmi which corresponds roughly to possible missile launch range and is therefore compatible with the requirements for positive threat recognition. Time requirements for poor ship disposition, however, are not satisfactory for the force commander to alter deceptive deployment tactics.

(C) Bearing requirements for search radars are based on limited experience in fleet exercises which show that operators do not detect targets from simultaneous bearings separated more than 90°. Fire control radar bearing accuracies should be within the automatic sector search patterns of these radars which vary from 15° to 20°.

(C)

- SOME CHARACTERISTICS OF THREAT
  - SEPARATION OF ATTACKING MISSILE FROM LAUNCH CRAFT
    - AIRPLANE (DISCERNIBLE BY ~ 50 KNOT DOPPLER RESOLUTION WITH A 50 NM RANGE RESOLUTION
    - SURFACED SUBMARINE
    - SURFACE VESSELS
  - TARGET PROFILE
    - SPEED
    - ALTITUDE
    - VELOCITY VECTOR ($<10^{\circ}$)
- CAPITALIZE ON ABOVE CRITERIA TO KEEP PROBABILITY OF FALSE ALARM LOW

CONFIDENTIAL

CONFIDENTIAL

(C) Figure 4. Threat Recognition (U)

CONFIDENTIAL

SAM GUN & EW SYSTEMS

TIME	TRANSIT	~5-10 MIN	WITH GOOD SHIP DISPOSITION
		~1/2 HR	WITH POOR SHIP DISPOSITION
	ON-STATION	~1-5 MIN	WITH GOOD SHIP DISPOSITION
		~1/2 HR	WITH POOR SHIP DISPOSITION
BEARING	FOR SEARCH RADAR		~ 60°
	FOR FCR	WITHIN REASONABLE FCR SECTOR SEARCH	-15°-20°

INTERCEPTOR SYSTEMS

TIME	CAP	~3 MIN FROM 100 NM CAP STATION	
	DLI	~15 MIN	
BEARING		WITHIN AI RADAR SCAN	~20°

CONFIDENTIAL

(C) Figure 5. Gross Requirements to Alert Force to Imminent Attack (U)

(C) For interceptors, a CAP station at about 100 nmi requires sufficient time to achieve intercept of the launch craft prior to missile launch. Greater detection ranges will permit the interceptors to act in the role of threat identification and could well provide the information in time for force redeployment for effective surface action. Bearing accuracies for interceptors should be within the AI radar scan.

VI POSSIBLE COMMUNICATION CONTROL (Figure 6) (U)

(C) With regard to intership communication of detection information, the critical question is: Is the force using EMCON? If there is high confidence in threat identification, then independent of EMCON status, doctrine should be to use the normal communication channels. If routine detections occur in the system without positive threat indications, then if the force is not in EMCON, normal communications should be used. On the other hand, if the force is in EMCON, intership communications should not be used but the control ship should have the computer capacity in algorithms essential for computation of inferences on threat hostility.

VII INFORMATION FLOW TO PROVIDE INPUTS TO THE ID PROCESS (U)

(C) Systems of the future will use more sophisticated computer computational schemes to correlate observations and intelligence and planning information. A number of actions must be integrated to improve the ID process. Each combat unit which must engage contacts or assist in identification must perform the subprocesses of identification as shown in Figure 7.

(C) The initial ingredients in the process are the plans, codes and information available concerning friendly forces. These provide part of the inputs to the correlation process of the ID function. The observations made on contacts provide the other inputs. Out of this then comes the degree of correlation between the data on hand and the observations which is then applied to an inductive or inference-making device to derive an estimate of the degree of hostility of the contact.

(C) This identification process must supply the degree of hostility information to the threat evaluation function to ensure that there is an efficient processing of targets, i.e., that weapons can be assigned to hostile targets in a timely manner. Identification should also carry through to the weapon commitment stage so as to provide a final estimate of contact hostility when a weapon is committed.

CONFIDENTIAL

- IF HIGH CONFIDENCE OF THREAT DISCLOSURE, THEN USE NORMAL COMMUNICATIONS
- IF ROUTINE DETECTIONS WITH NO POSITIVE THREAT INDICATIONS THEN
  - FOR FORCE NOT IN EMCON USE NORMAL COMMUNICATIONS
  - FOR FORCE IN EMCON NO INTERSHIP COMMUNICATIONS BUT CONTROL SHIP SHOULD HAVE COMPUTER CAPACITY & APPROPRIATE ALGORITHMS FOR COMPUTATION OF INFERENCE ON HOSTILITY

CONFIDENTIAL

(C) Figure 6. Possible Communication Control (U)

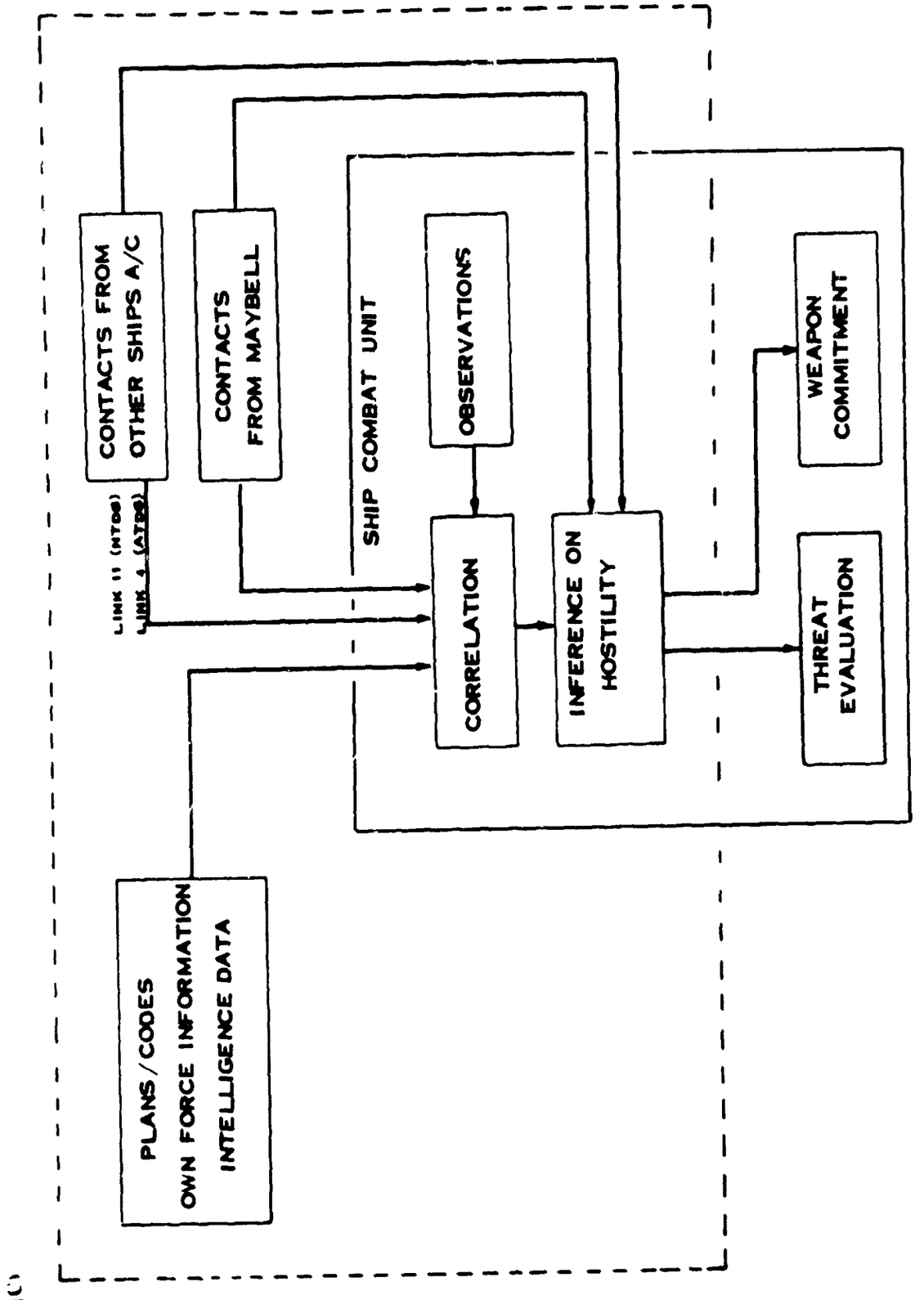

(C) Figure 7. Information Flow to Provide Inputs to Identification Process (U)

PRECEDING PAGE BLANK - NOT FILMED

FAD HISTORY (U)

J. M. Headrick

Naval Research Laboratory
Washington, D. C.

(S) The missile threat to ships was the inspiration for considering bistatic HF radar. The method was to use remote sky-wave illumination of low-altitudes targets near a ship and to detect the target-scattered energy by a ground-wave path to a ship-mounted receiving radar station. Some sample calculations were made in 1967 that suggested feasibility. Figure 1 gives expected monostatic sky-wave radar performance for a set of assumed radar and target parameters. The ionospheric model was per ITSA-1. Figure 2 gives expected monostatic ground-wave radar performance for three operating frequencies spread over a greater frequency range than the set required in Figure 1. In Figure 3 bistatic performance is given for the required frequency extremes. These computations indicate the bistatic method has possibilities; the analysis is treated in more detail in an appendix of the MSDS Group Secret Report "Missile-Threat Ship Defense Study" (U) of 8 May 1968.

(S) A series of experimental tests have been made using ESSA transmissions for illumination and the MADRE facility on Chesapeake Bay for reception. Figure 4 is an early example that shows resonant wave echoes received by ground wave. Figure 5 is a later example with higher power. In addition, some tests have been conducted using the ESSA-received signal as a reference.

(U) The ARPA FAD experiments were planned to completely demonstrate the basic feasibility of low-altitude bistatic detection and to expose both the capabilities and required system design features.

(S) It is felt that the ARPA FAD tests have demonstrated the basic bistatic feasibility of detection of the low flyer. Giving a "quiet" fleet unit such a detection capability may have several applications. However, the skywave illuminator should also be used as a monostatic radar, and it can complement the bistatic system, give greater range detection and fill blind azimuths. In some cases it may be desirable to have the fleet unit operate ground-wave monostatic after the first missile detections.

(U)

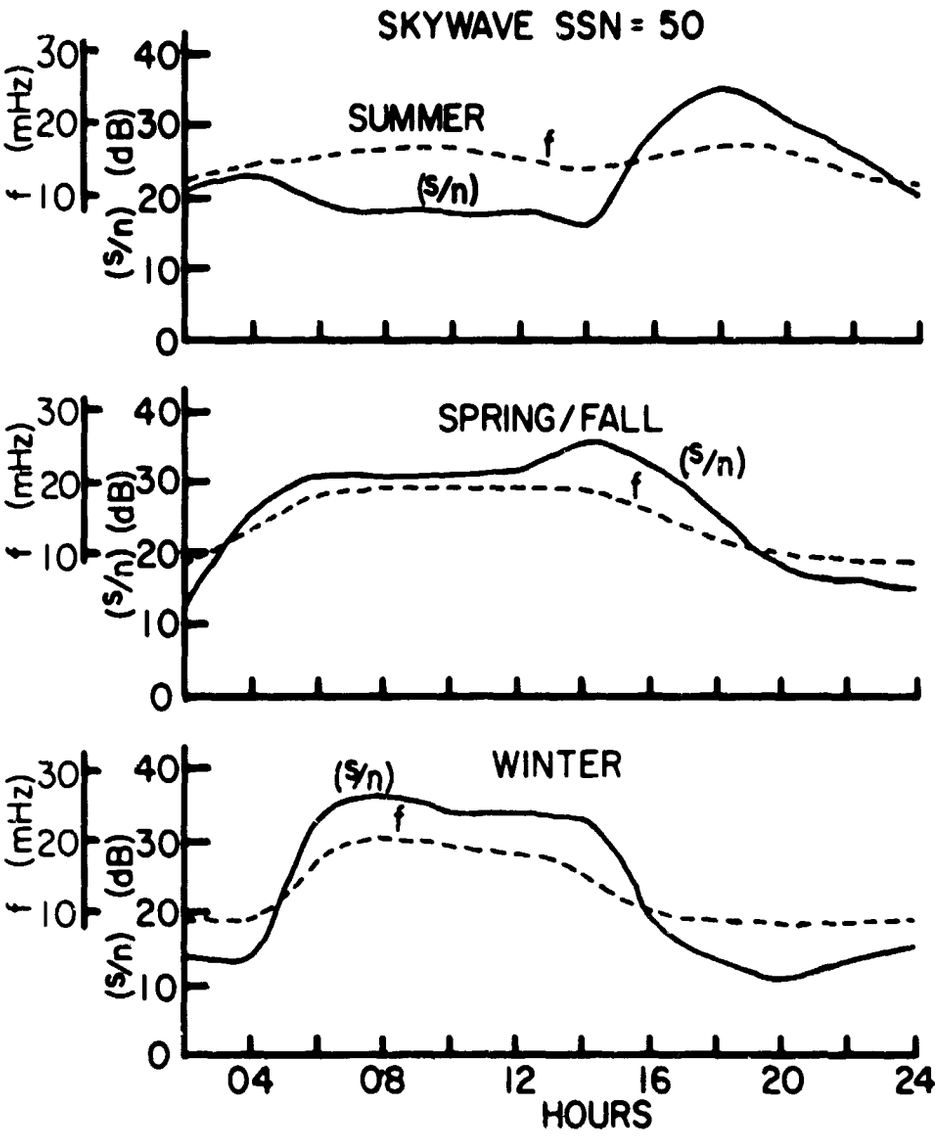

(U) Figure 1. Monostatic Radar Performance Prediction for 1000-nmi Range. σ = 40 Log (f/5), P = 53, T = 10, G = 24 + 5 Log (f/10), N = 148-12.6 ln (f/3) (U)

UNCLASSIFIED

UNCLASSIFIED

(U)

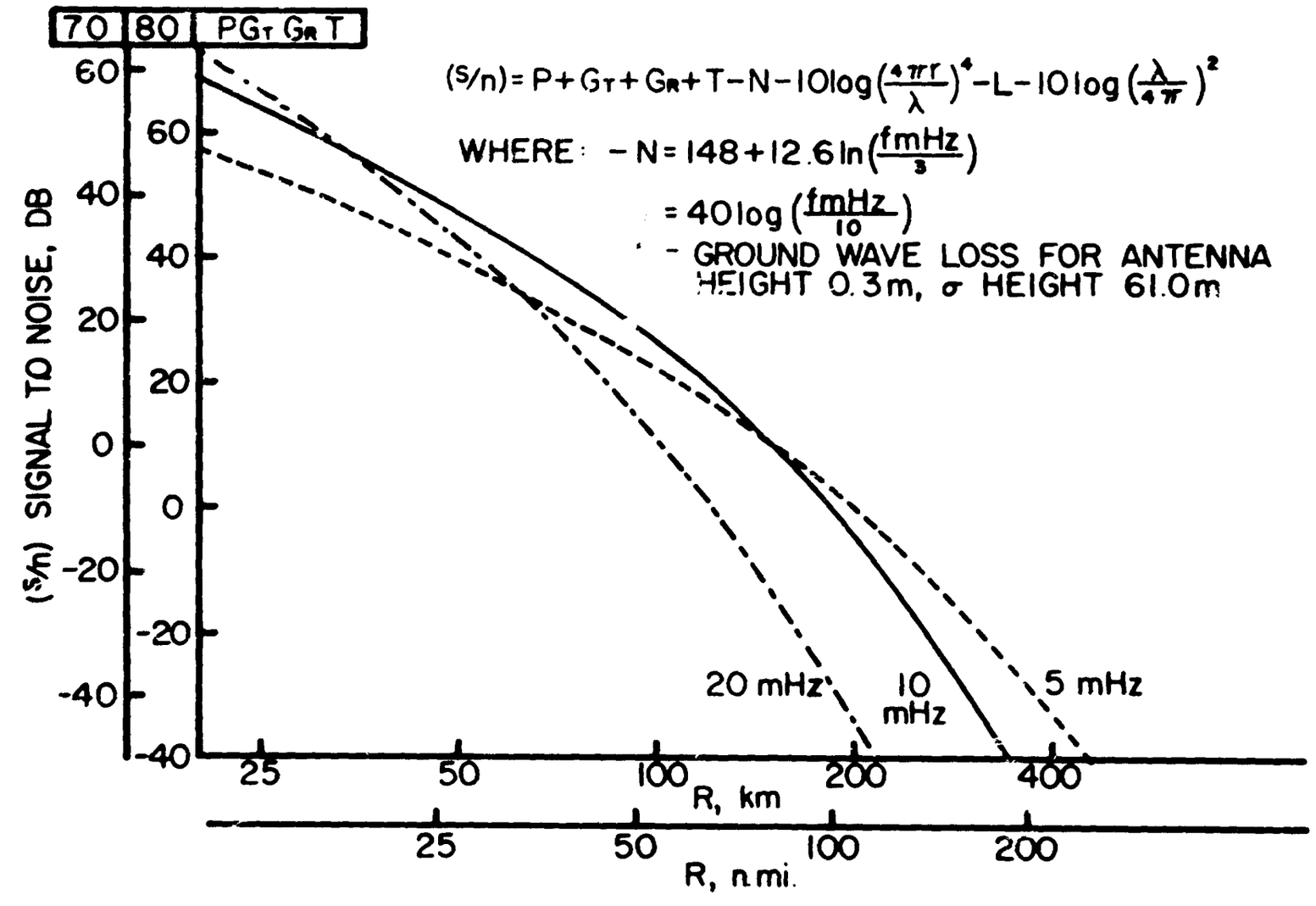

(U) Figure 2. Monostatic Surface Wave Radar (U)

(U)

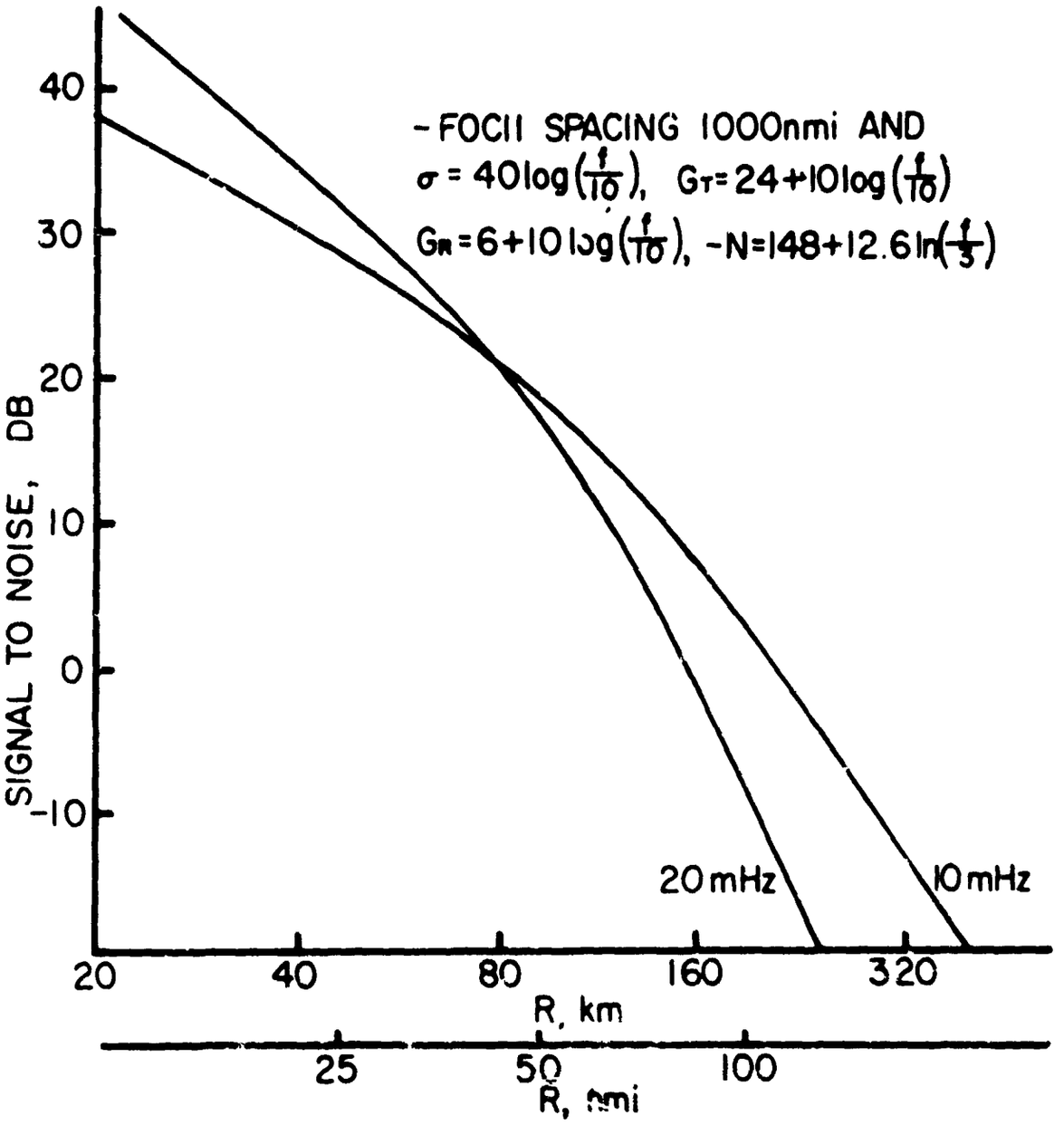

(U) Figure 3. Bistatic Performance Example (U)

(U)

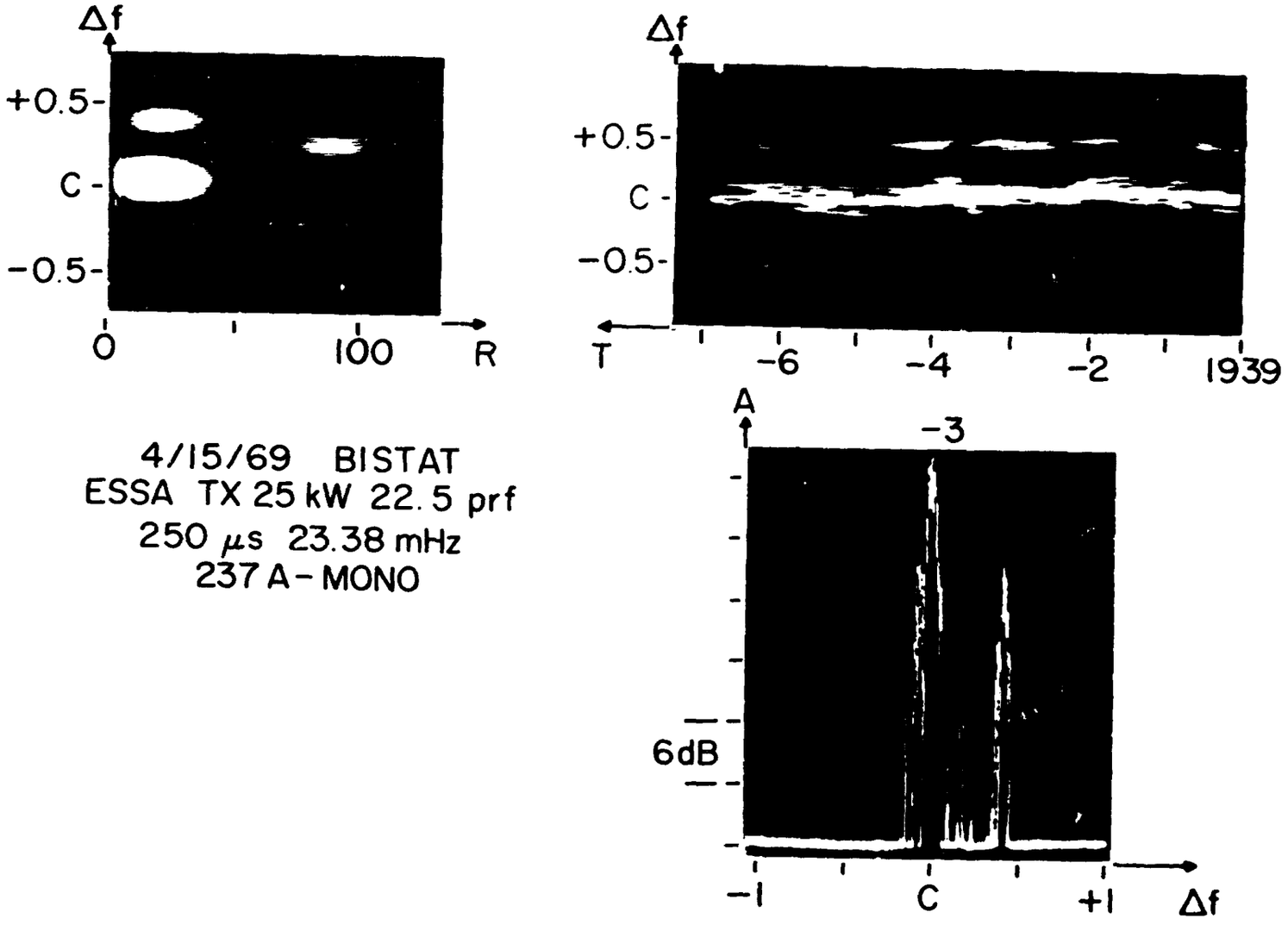

(U) Figure 4 Bistatic ESSA, T x 25 kW, 22.5 prf, 250 μs, 23.38 MHz, 237A-Mono, 4/15/69 (U)

UNCLASSIFIED

(U)

UNCLASSIFIED

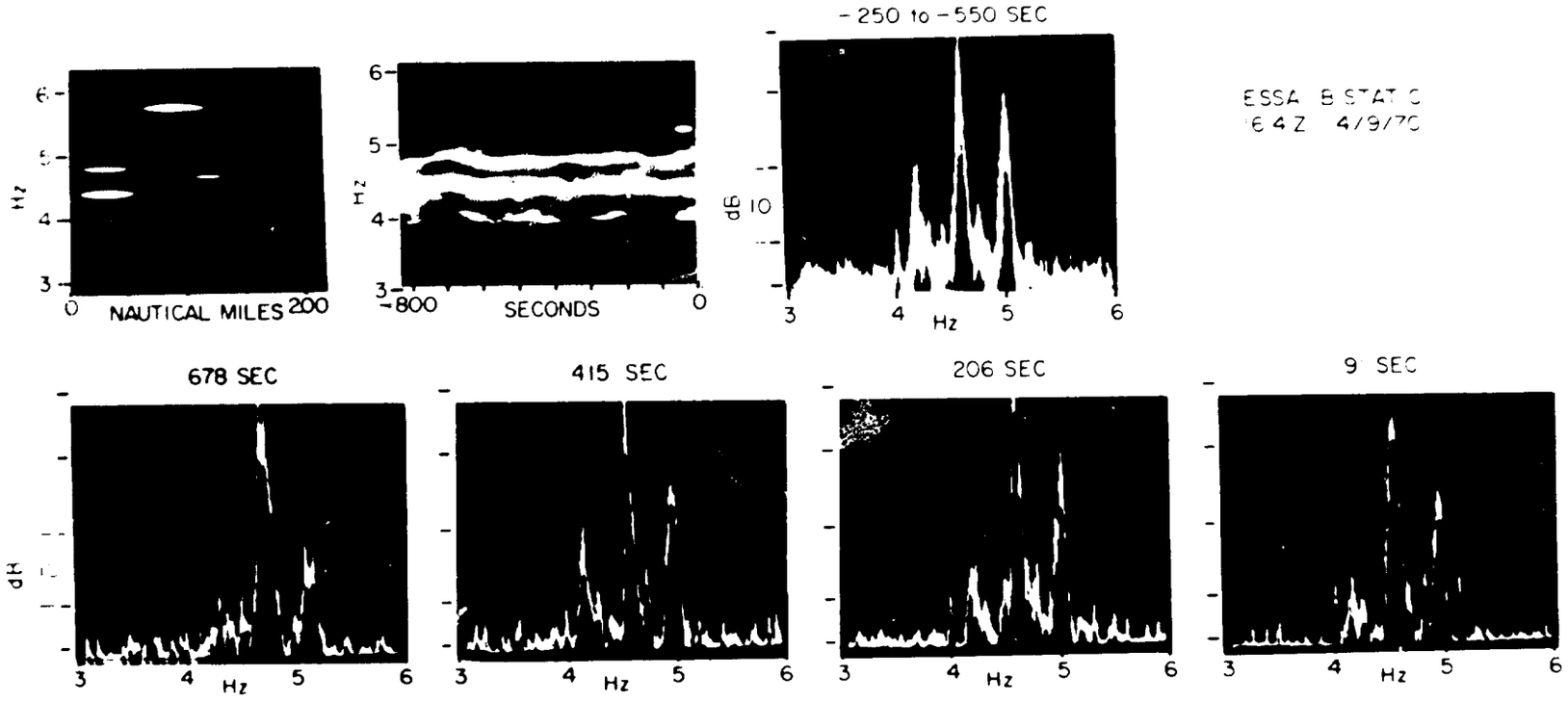

UNCLASSIFIED

(U) Figure 5. ESSA Bistatic 1614Z, 4/9/70 (U)

NRL DATA ANALYSIS (U)

J. M. Hudnall

Naval Research Laboratory
Washington, D. C.

(U) It was planned that NRL 1) illuminate for part of the Fleet Air Defense (FAD) tests, 2) develop computer programs for signal analysis using I and Q plus monopulse channels including methods of display, and 3) after-the-fact examine and analyze the data using both the MADRE signal processor and a computer plus the developed programs. The contribution would be a capability for fine-frequency and long-storage-time analysis plus a variety of displays.

(U) To accomplish task (3) NRL required that the data be recorded on 7-track tape in an IBM-compatible format. Due to a long series of events, not one reel of tape meeting the requirements exists. Thus only Tasks 1 and 2 have been done plus considerable unexpected work in trying to achieve Task 3. Since the FAD source of a clutter versus frequency description was to be NRL's, some fragments of data will be shown here that do give pertinent examples.

(U) Figures 1 through 6 are the examples. In general the signal exhibited two or three amplitude peaks as a function of frequency. It is hoped that weather and sea-state conditions can be compared with the energy distribution.

(U) In Figure 1, doppler (Hz) time delay (pseudo range) is shown at 16:52:50Z, on 10 February 1970. The analysis bandwidth is 2/14 Hz.

(S) In Figure 2, a doppler time history is given for an 0.25-ms range gate starting on the time delay of the second earliest strobe of Figure 1. A short aircraft track is evident. The bandwidth is 4/14 Hz.

(U) Figure 3A was made with an 0.25-ms range gate starting at the earliest strobe of Figure 1. Figure 3B was started on the second strobe.

(U) Figure 4A and B show amplitude versus Doppler displays made for the last two strobes of Figure 1. The resolution bandwidth is 1/28th.

(U) Figure 5A and B show displays similar to those of Figure 3, but made for operation on 16.16 MHz.

(U) Figure 6 shows computer-generated spectra for 27 February 1970.

(U)

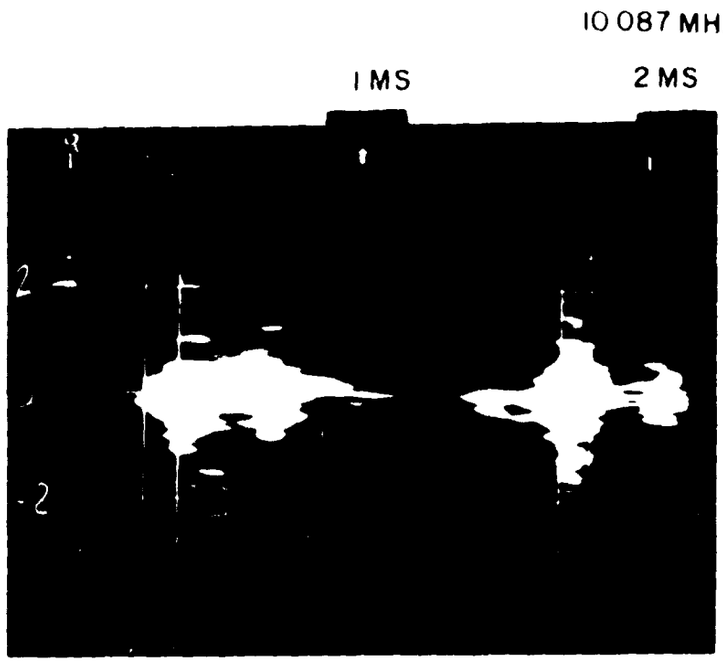

(U) Figure 1. Doppler Time-Delay Space, 10 February 1970 (U)

(S)

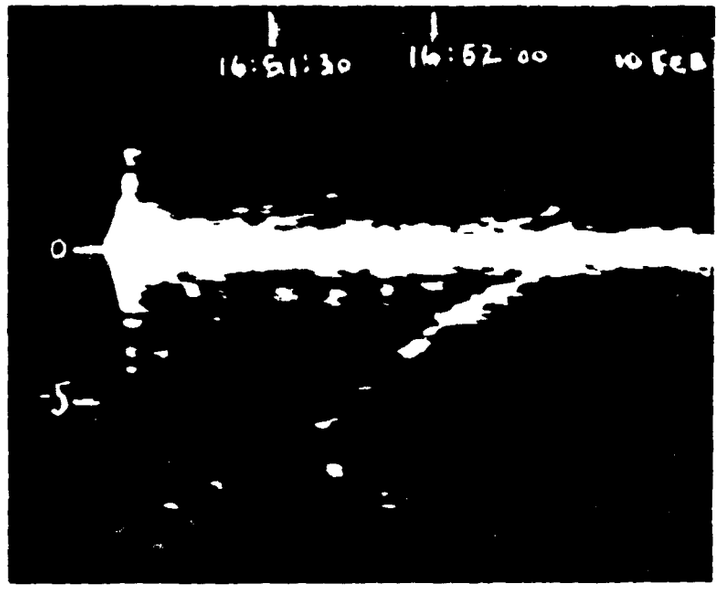

(S) Figure 2. Doppler Time History for an 0.25-ms Range Gate (U)

10.087 MHz

(U)

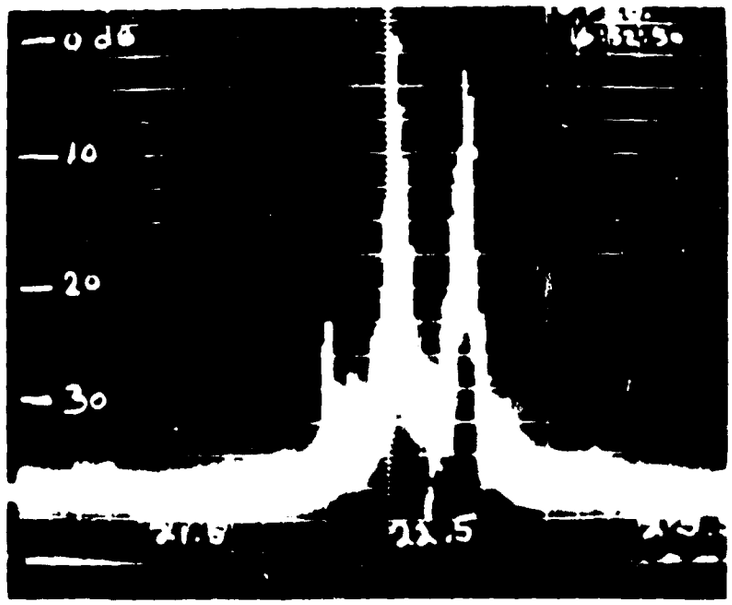

A.

BANDWIDTH 1/28 Hz

(U)

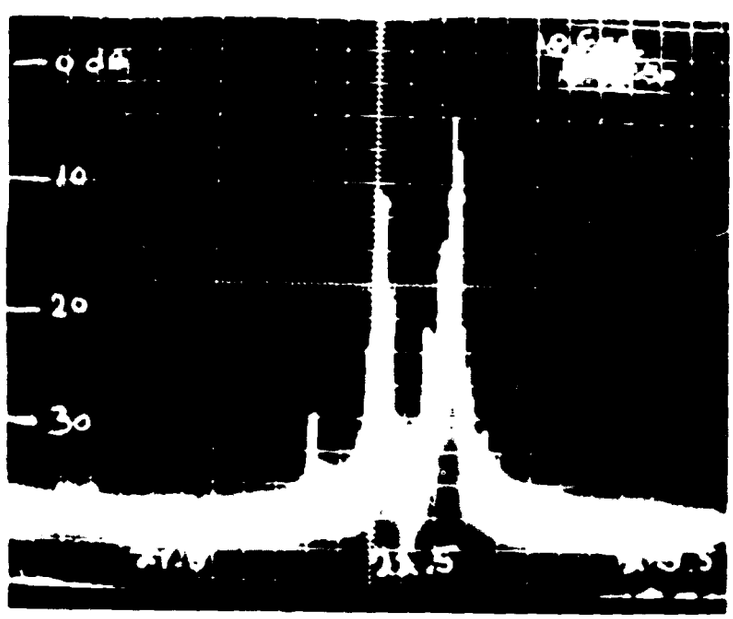

B.

(U) Figure 3. Amplitude vs Doppler Analyses, 10.087 MHz (U)

10.087 MHz

(U)

A.

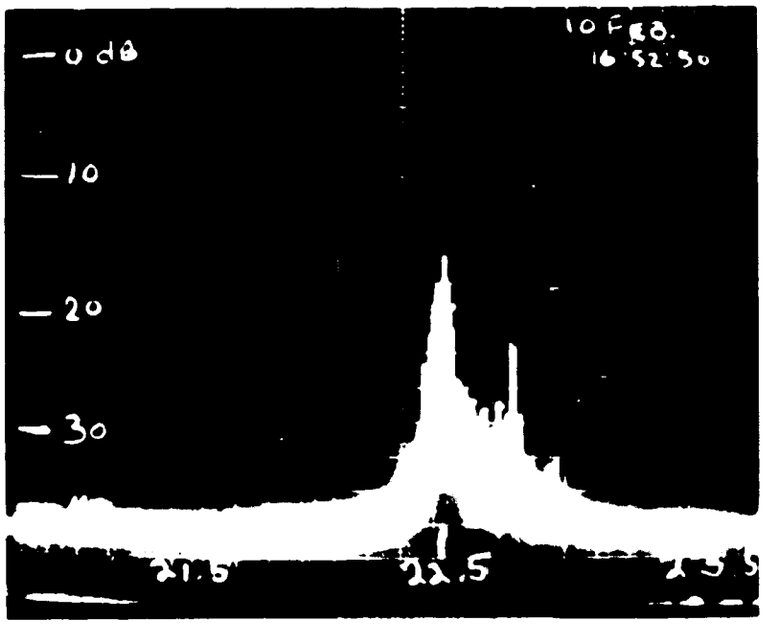

(U)

B.

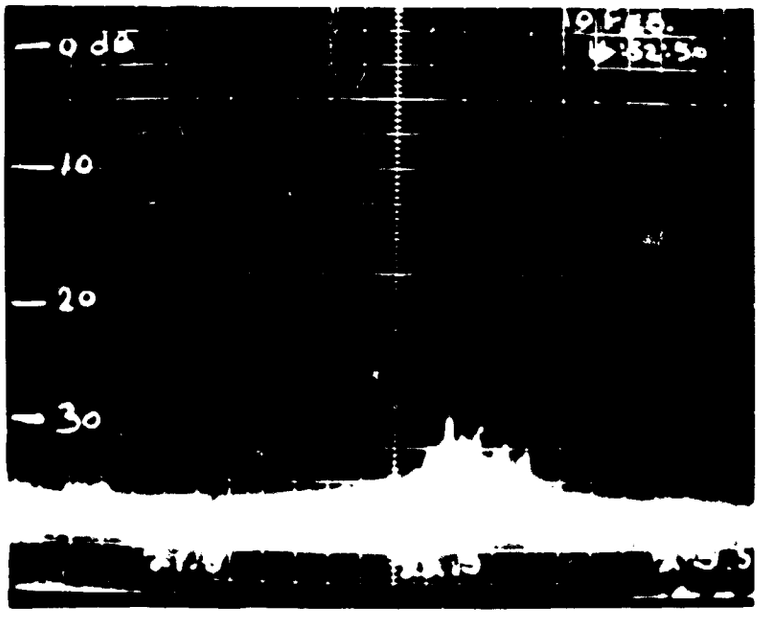

(U) Figure 4. Amplitude vs Doppler Displays (U)

(U)

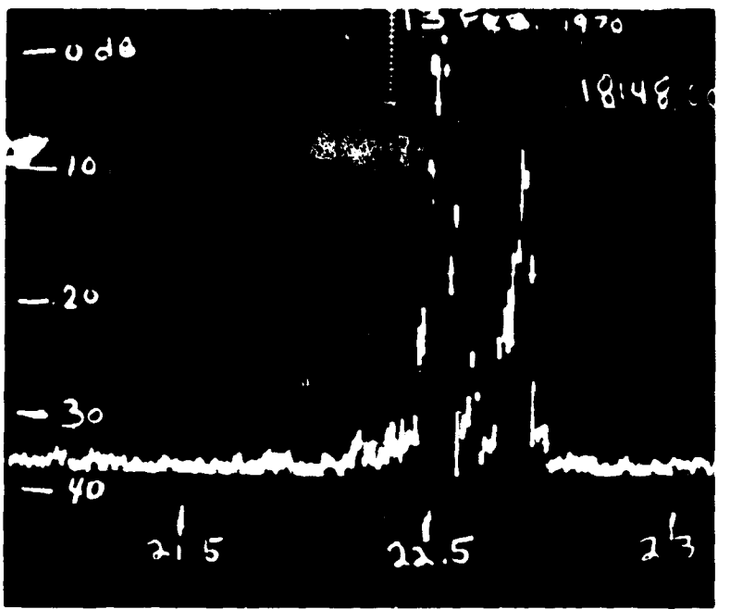

A

(U)

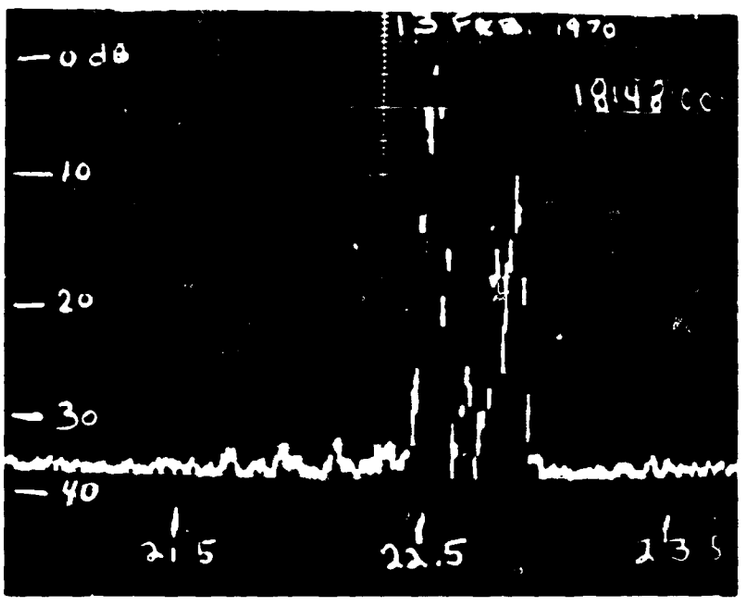

B.

(U) Figure 5 — Amplitude vs Doppler Analyses, 16 to 16 MHz (U)

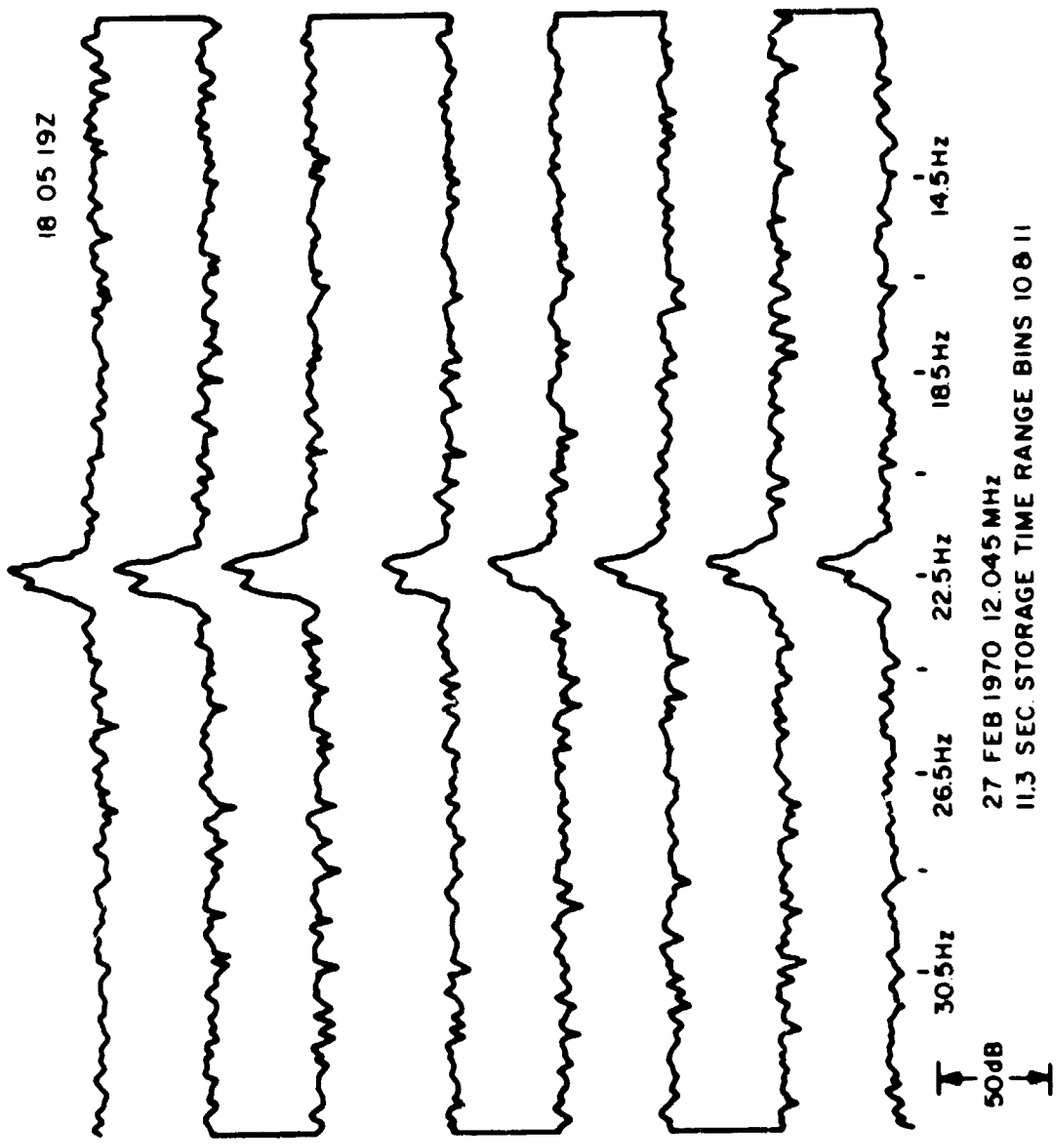

(U) Figure 6. Computer-Generated Spectra, 27 February 1970 (U)

(U)

FAD EXPERIMENT OF FEBRUARY, 1970 (U)

Thomas D. Scott

ITT Electro-Physics Laboratories, Inc.
3355 52nd Avenue
Hyattsville, Maryland 20781

I INTRODUCTION (U)

(S) The Fleet Air Defense Experiment which was conducted in January and February of 1970 used a skywave HF radar signal from the ARPA-ONR CHAPEL BELL facility at WHITEHOUSE, Virginia, to illuminate the area around a receiving field site at Cape Kennedy, Florida. The receiving site recorded both the incident skywave field strength from WHITEHOUSE and bistatic radar reflections from a Navy P3B aircraft, flying on prescribed flight paths between 20 and 120 km offshore from Cape Kennedy. A large portion of these paths were over the radar horizon from the receiving site because the airplane was at a very low altitude.

II EQUIPMENT (U)

(S) The skywave illumination was provided by a 500 kW (Peak) power transmitter with an antenna with approximately 9 dB gain at the angles and frequencies used. The bistatic echoes were received on a 17 dB gain antenna at Cape Kennedy. The transmission format was a binary phase coded 1.55-ms pulse which was compressed to a length of 50 μs. Pulse doppler and monopulse processing at the receiving site provided range, doppler frequency (velocity), and azimuth tracking of the target. Modulated antennas, installed on two buoys, which were anchored 25 and 50 km offshore served as control targets and provided frequency, range, and azimuth calibrations. Communications via HF radio were maintained at all times between the transmitter, receiver, and the aircraft.

III RESULTS (U)

(S) Successful detection of the target aircraft was made out to a range of 100 km from the receiving site even with the non-optimized system used for this experiment.

(S) An example of the tracking results is given in Figure 1 which shows a typical zig-zag flight path in the upper left corner. In the upper right corner is an azimuth versus time plot calculated on the basis of LORAN data collected on board the aircraft along with the azimuth versus time record made at Cape Kennedy. This record illustrates the azimuthal tracking capability of the equipment. The graph and data on the bottom of Figure 1 show the computed and observed doppler frequency history of the aircraft echo as it executes its zig-zag path.

(S) In addition to the pragmatic results on aircraft detection and tracking, data were gathered to permit the determination of path loss, noise, and bistatic target cross sections. The bistatic cross section of the P3B aircraft was found to be between 5 m^2 and 100 m^2 and was a function of angle. The noise figures for a 20-kHz system were generally about 7 dB larger than those predicted by CCIR for a narrow band system in the daytime and about 10 dB larger at night. The path losses on the skywave path agreed quite well with predictions.

IV CONCLUSIONS (U)

(S) The main purpose of the experiment was to test the feasibility of a hybrid (skywave-surface wave) system for passive detection of low flying aircraft at ranges beyond conventional ship radar coverage limits. The experiment proved the feasibility of this fleet air defense concept and provided data on some of the problems and limitations of such a system.

(S)

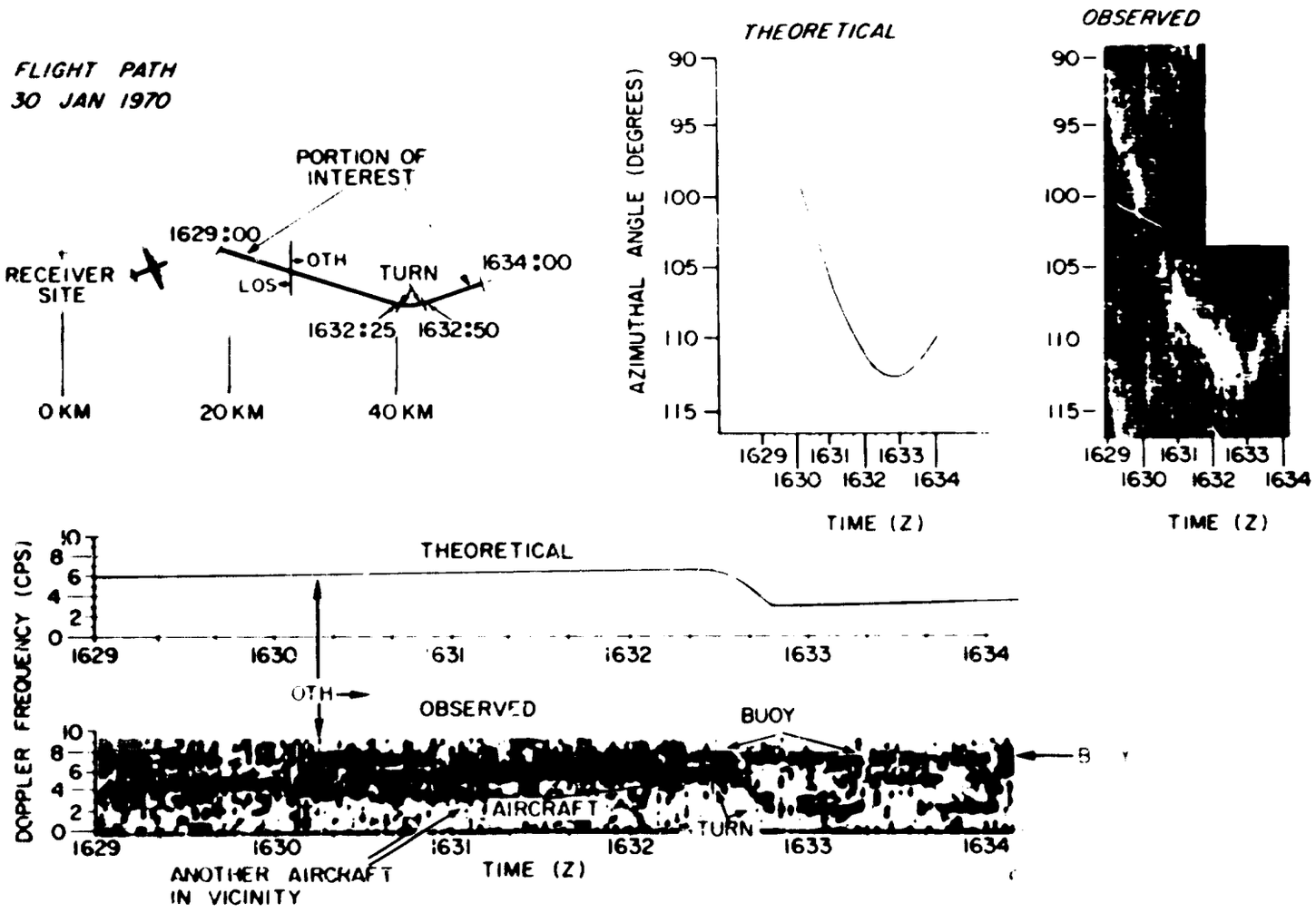

(S) Figure 1. Passive Detection of Over-the-Horizon Aircraft during the Fleet Air Defense Tests (S)

PRECEDING PAGE BLANK - NOT FILMED

FAD RADAR SYSTEM STUDY (U)

Wesley N. Mollard

ITT Electro-Physics Laboratories, Inc.
3355 52nd Avenue
Hyattsville, Maryland 20781

I INTRODUCTION (U)

(S) In a paper titled "FAD Experiment of February, 1970 (U)" presented at this workshop, Thomas D. Scott gave some results of the Fleet Air Defense (FAD) experiments which were carried out in January and February of this year. Those results clearly demonstrated the feasibility of the hybrid skywave/surface wave radar concept.

(S) Following this demonstration of feasibility, ARPA has directed this contractor to undertake a preliminary system study directed toward a potential tactical system employing such a hybrid-mode radar for fleet air defense. It was clear at the outset that such a radar system would provide the fleet with the critical function of maintaining an early warning surveillance capability while still preserving complete electromagnetic-radiation silence. This joint capability would protect the fleet against a surprise attack, and at the same time deny an enemy the use of fleet-generated radiation for the purposes of fleet location or weapons guidance.

(S) The overall objectives of this study are to investigate the application of the hybrid-mode radar to the problem of fleet air defense, and to determine the future actions necessary to permit the development of an operational system. The first step in reaching these objectives is to inter-relate the nature of the potential threats with the characteristics of the defensive systems available to the fleet in order to ascertain the performance criteria which must be met by the hybrid-mode radar. From these performance criteria, it is then possible to generate meaningful engineering specifications for such a radar. The above analysis will then help to identify those areas which still require research, development, test, and evaluation (RDTE) efforts, indicating the areas which constitute the state-of-the-art, those which require further study, and, especially, the principal areas of risk.

(S) This current study draws upon past study efforts to the greatest extent possible. In particular, considerable use is being made of certain of the results from a previous ITT-EPL study of a CONUS OHB (Over-The-Horizon Backscatter) system conducted for the USAF. The CONUS study is especially useful

(S)
insofar as certain threats and OHB performance criteria are concerned. Although the present study and this past study differ with respect to the mode of radar operation and the overall problem, they nevertheless have important areas of commonality, such as frequency regime, range of doppler frequency offsets, target types, etc. In addition, maximum use will be made of other completed studies in particular areas, such as threat models and defensive systems. By drawing on this extensive background of existing information, it will be possible, even in a modest study effort, to ensure coverage of the problem to a depth that establishes meaningful bounds on the important parameters entering into the problem.

(S) Figure 1 shows a general outline of the FAD system study as it is being carried out by ITT-EPL. The flow chart in Figure 2 illustrates more clearly the inter-relationships among the various parts of the study effort. The major elements making up the flow chart are summarized in the following paragraphs.

II KEY STUDY AREAS (U)

A. Threat Considerations (U)

(S) The various threat models which are officially postulated to be in enemy inventories in the 1970 - 1980 era are being investigated. The threat models include both specific weapon characteristics and attack scenarios. The individual weapons extend from aircraft attacking with short-range weapons, aircraft employing long-range, air-to-surface missiles, and surface-to-surface missiles launched by surface vessels or submarines. The variety of scenarios will extend from small-scale sneak attacks through large-scale engagements. These threat models are being integrated to establish threat-model, performance envelopes which define such parameters as altitude-versus-range, range-versus-time-to-target, density of attackers, etc.

B. Defensive System Considerations (U)

(S) The defensive systems available for fleet use in the 1970 - 1980 era include sensors and active defense weapons. Among the sensors are shipboard radars for acquisition, tracking, and fire control, and airborne radars and other possible sensors (such as LWIR). The active defensive weapons include air-to-air missiles carried by carrier-launched aircraft, surface-to-air missiles, and anti-aircraft artillery. The various capabilities of these respective elements of the defensive systems are being organized into performance envelopes which indicate the accuracy and timeliness required from an early warning system so that effective use can be made of the defensive systems. An additional aspect of the consideration of the defensive systems is the important feature of the "hand-off" from the early warning system to the shipboard terminal defense system. This and other specific interaction between the FAD system and the other fleet defensive systems lead to a set of "interface requirements" which must be met to ensure effective cooperation among the various defensive systems.

(S)

SECRET

I. INTRODUCTION
- STATEMENT OF PROBLEM AND ROLE OF FAD

II. OVERALL SYSTEM CONCEPTS

III. THREAT CONSIDERATION
- MISSILE TARGETS
- AIRCRAFT TARGETS

} HF SIGNATURES

IV. SHIPS RADAR DEFENSES

V. INTERFACE OF FAD RADAR WITH SHIPS RADARS

VI. FAD RADAR REQUIREMENTS

VII. CONCLUSIONS-RECOMMENDATIONS

SECRET

(S) Figure 1. Topical Outline of FAD Radar System Study (U)

(S)

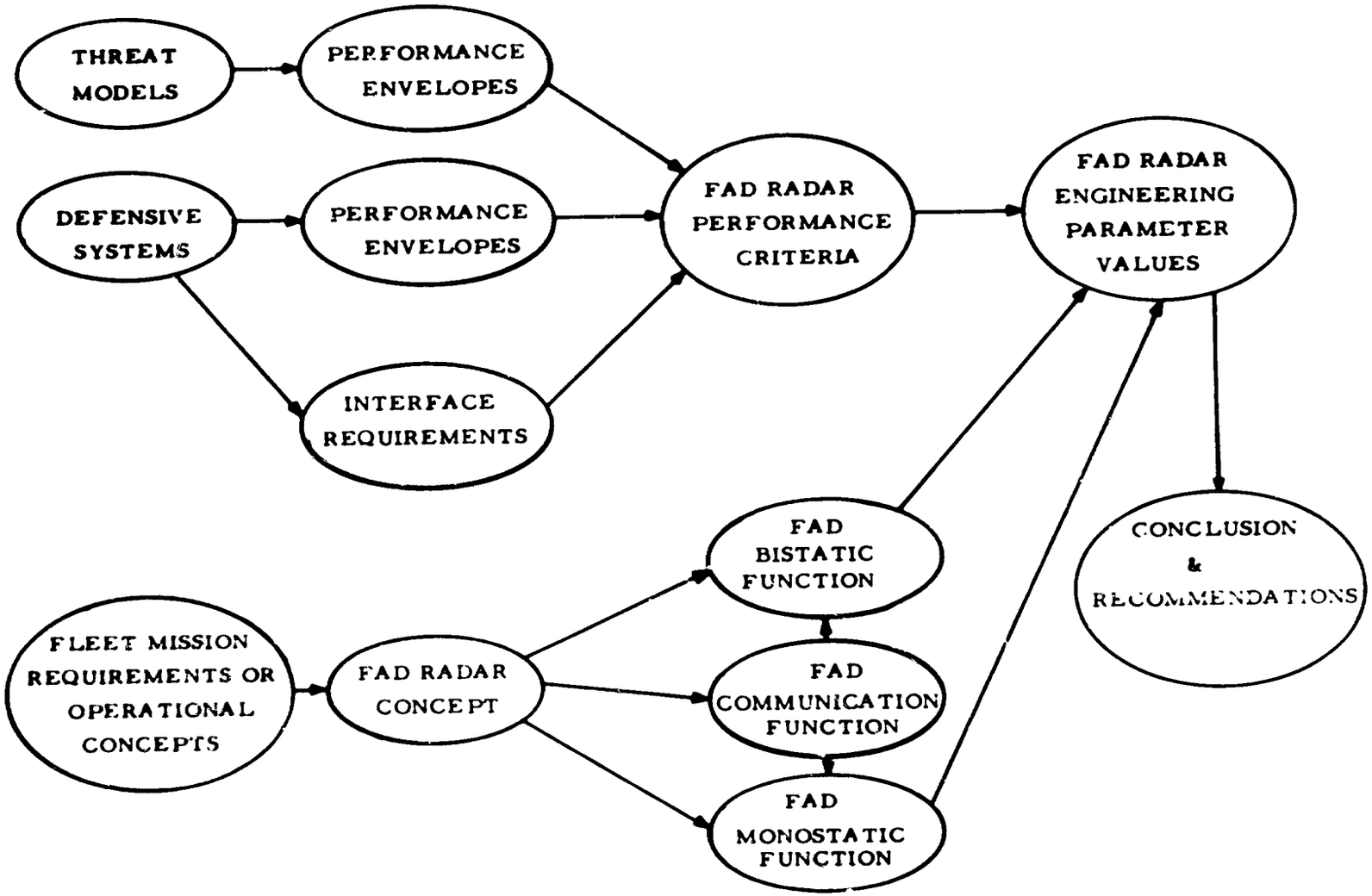

(S) Figure 2. FAD Radar System Study Flow Chart (U)

C. FAD Radar Performance Criteria (U)

(S) The performance envelopes of the threat models and the defensive systems and the interface requirements will then be used to establish definitive performance criteria for the FAD system so that it can play an effective role in fleet defense.

D. Fleet Mission (U)

(S) Clearly, the use of a naval fleet is not limited to a single, easily categorized, type of operation. It is therefore necessary to consider a variety of fleet operational concepts in order to determine the possible manners in which the FAD concept can be applied in the various circumstances. Among the aspects requiring consideration if the question of whether the FAD system should be simply added to ships regularly in service, or whether it should be deployed on special-purpose dedicated vessels, or some alternative between these extremes. Another important consideration is the extent to which the FAD system might be employed in a special-purpose communication system simultaneously with its radar use.

E. FAD Radar Function (U)

(S) The nature of the skywave illumination in the present FAD concept is such that it is clear that the illuminator can also act as a monostatic radar. The addition of this function could provide early-warning information at greater ranges than could be hoped for in the bistatic configuration, without, however, offering the self-contained capabilities provided by the bistatic radar. It is important in the study to define the optimum roles for each of the two possible modes of operation.

F. FAD Radar Engineering Parameter Values (U)

(S) The net output of the FAD performance criteria and the fleet mission requirements will then be a definitive presentation of the necessary engineering specifications of a FAD system which can provide effective early warning to the fleet in event of attack threats originating beyond the range of other ship sensors, a range which may be set physically because of the radar horizon, or operationally by conditions of electromagnetic control.

III CONCLUSIONS AND RECOMMENDATIONS (U)

(S) The output of the study will be a report in which the FAD engineering specifications are defined, and in which recommendations are made for action in areas requiring additional RDTE.

PRECEDING PAGE BLANK - NOT FILMED

SHIP DETECTIONS (U)

J. L. Ahearn

Naval Research Laboratory
Washington, D. C.

(S) The first positive HF radar ship detection by NRL was made on 29 June 1968. The detection was by skywave at 15.595 MHz, 22.5 prf, 072 T ± 7° with an approximate $\cos^2$ shaped pulse about 700 μs long. Figure 1 is a set of pictures illustrating these observations. The ship can be seen at - 0.8 Hz. It was later identified as the Grotedyk, length 534 ft, beam 67 ft and with a KKMMFM superstructure. The ship was observed for 5 hours from 10 AM to 3 PM local time. The maximums of received signal gave a radar area of about 1500 m^2.

(S) A second example of ship detection is given in Figure 2. Operating parameters were 15.595 MHz, 22.5 prf, 084 T ± 7°. This target was the Forrestal, length 1034 ft, beam 250 ft. Maximums in signal strength yielded a radar area of about 13,000 m^2. The target is at - 1.5 Hz and the clutter amplitude (given in relative dB) versus frequency characteristic is an example of how well behaved it can be. Note that a 10:1 reduction in pulse width would make the ship detectable at any speed except that of the resonant waves.

(U) Figure 3 is a ground-wave amplitude versus frequency plot made at 30-nmi range, and this is shown to exhibit frequency resolving capability without ionospheric effects. In this example a 50-second time sample was used.

(U) Another example of doppler resolving capability is given in Figure 4. This gives doppler versus range for a 50-μs pulse length and only 10 seconds dwell time.

(S) It is felt that by adapting to (or taking out) undesired ionospheric effects there are genuine possibilities for ship traffic plotting by HF radar.

(S)

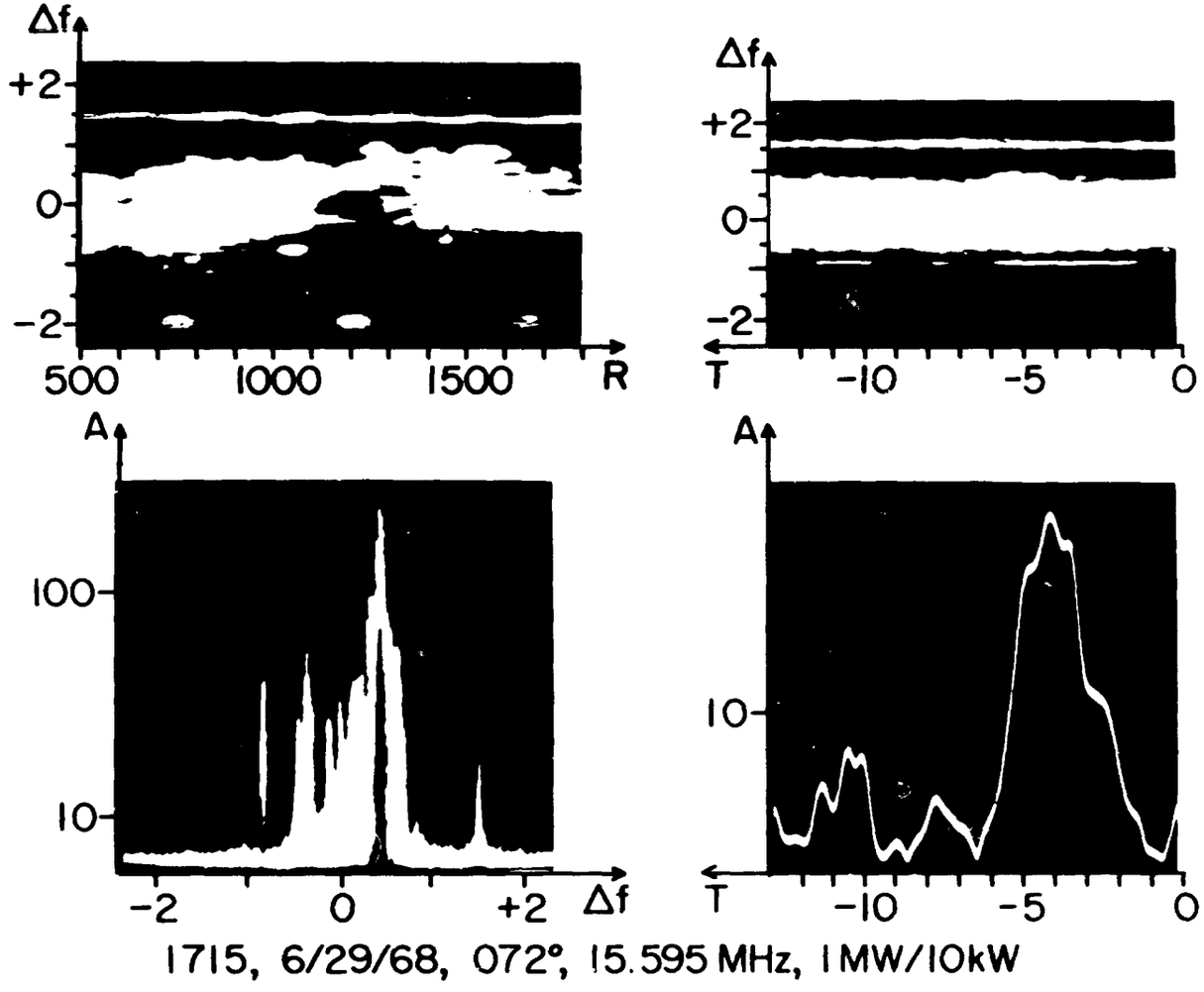

(S) Figure 1. 6/29/68, 1715, 070°, 15.595 MHz, 1 MW/10 kW (U)

(S)

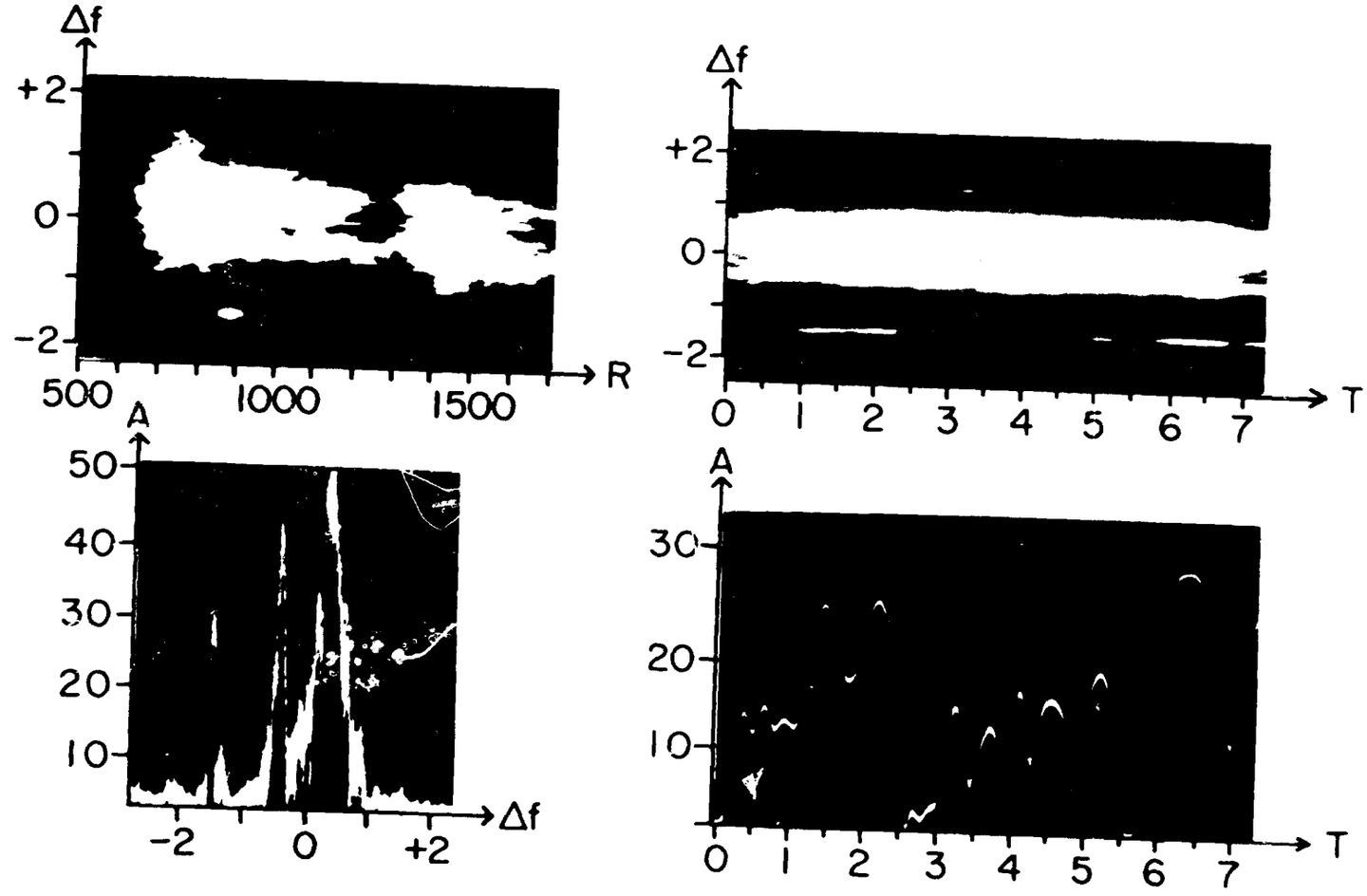

(S) Figure 2. 7/23/68, 1843, 084° 15.595 MHz, 2.3 MW/10 kW (U)

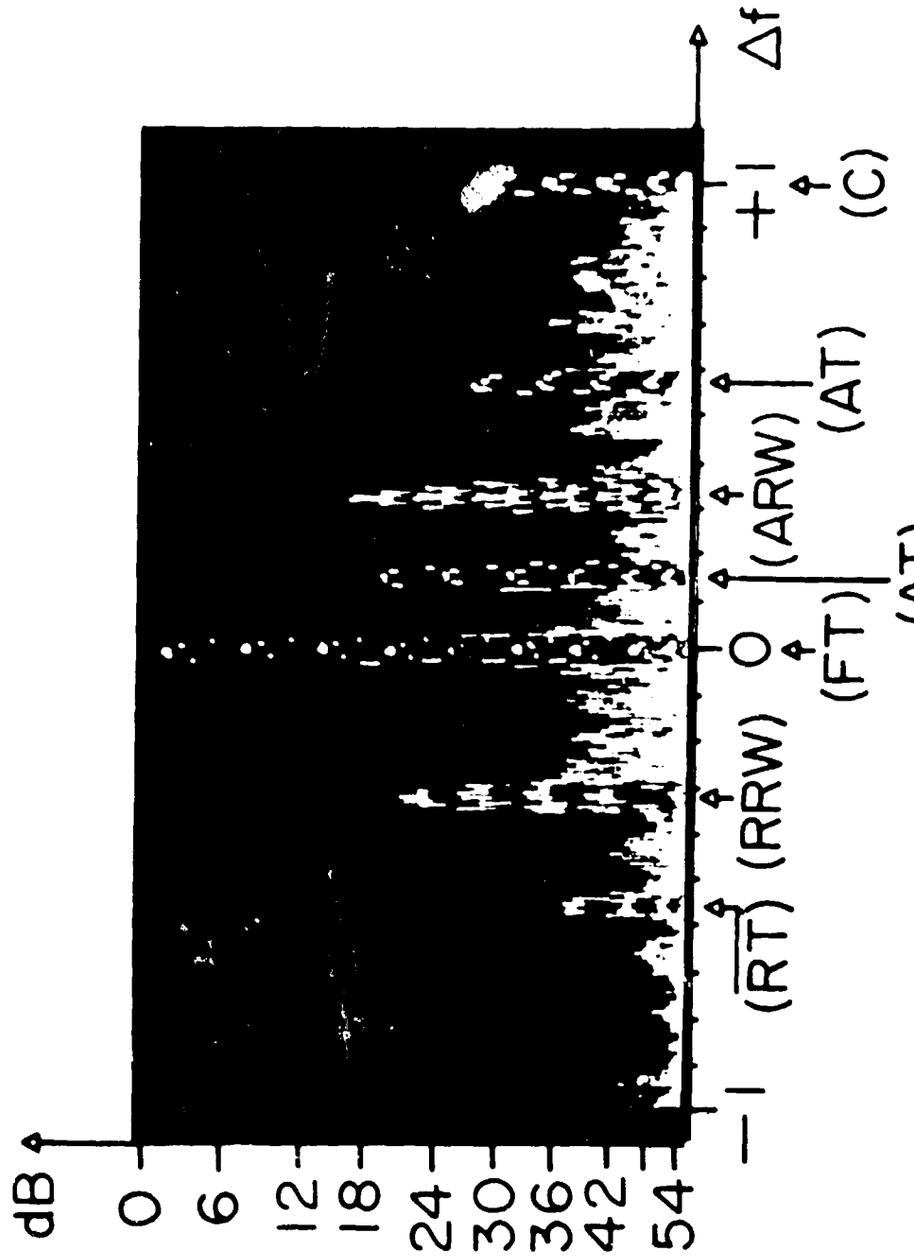

(U) Figure 3. 8/12/69, 03:03:33 GMT (U)

(U)

142

(S)

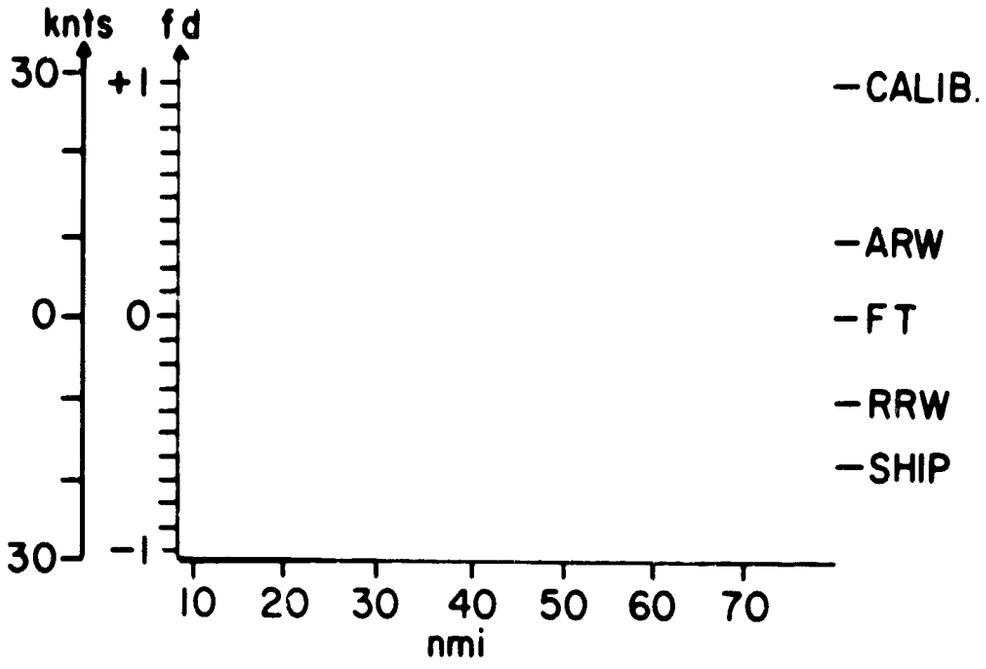

(S) Figure 4. Ground Wave Doppler Resolving Capability (S)

PRECEDING PAGE BLANK - NOT FILMED

HIGH RESOLUTION SEA BACKSCATTER (U)

J. R. Barnum

Radioscience Laboratory
Stanford, California 94305

I INTRODUCTION (U)

(S) Stanford University's part in Project MAY BELL has been to study the feasibility of detecting ships OTH by means of sweep-frequency-CW radar while receiving on a very wide aperture antenna array. It has become necessary to know the HF radar cross-sections of typical ships at sea, and to measure the properties of sea clutter using sky-wave propagation. A partially-controlled experiment was also run, in which the detection of a 500-foot cargo ship was attempted. The purpose here is to summarize these topics, and to specify what further work is necessary.

II SHIP CROSS SECTIONS AT HF (S)

(S) Under a subcontract from Stanford, Technology for Communications International (TCI), measured the backscatter from ship models at the Naval Electronics Labs (NEL).

(S) A total of 99 radar cross-section (σ) patterns for a DE-1030 destroyer and a Forrestal Carrier were obtained at frequencies between 3 and 22 MHz, for elevation angles between 3.5 and 20 degrees. Bistatic and surface wave measurements were also performed at 3 and 7 MHz. The data were obtained using 1/48-scale models at 48 times the HF value. The correspondence to the realistic (full-size) cases at HF should be close.

(S) For vertical polarization, the cross-sections are 10^3 to 10^5 m^2 for the destroyer, and 10^4 to 10^6 m^2 for the carrier. Horizontally-polarized cross sections are down 3 to 19 dB for the destroyer (depending on ship orientation), and 0 dB for the carrier, at a 20-degree elevation angle. The "surface wave" cross-sections are of the same magnitude as the above, and when the radar becomes bistatic, the scatter is only 0 to 5 dB lower in amplitude.

(U) The number of nulls in all the patterns increase with frequency, but at a faster rate for the ship. Bistatic patterns contain fewer nulls.

(U) The accuracy in measurement of max σ is usually ± 3 dB For 20 to 30 percent of the patterns, a slight to moderate error in pattern null structure occurs; however, enough data was taken so that further measurements of this type are unnecessary.

III SKY-WAVE PROPAGATED SEA CLUTTER (U)

(U) The radar cross-section of a sea patch was measured in the Gulf of Mexico using a portable repeater operated on board a cargo ship. Using high azimuthal resolution (½-degree beamwidth) and small equivalent pulses (4-10 μ s) the sea cross-section was reduced to 10^4 m^2. The sea's cross-section per unit area was then calculated to lie between 10^{-3} and 10^{-2}.

(U) Fixed frequency experiments have been performed to ascertain the effect of controlled transmitter polarization on backscatter amplitude as a function of range in the Pacific Ocean. The results show that it is possible to reduce the clutter by about at least 10 dB by switching the transmitter between vertically and horizontally polarized antennas, while receiving on the 2.5-km Los Banos array. The effect is not observed when using a 4-degree beamwidth antenna, which was explained using swept azimuth data and computer-raytracing backscatter synthesis to show that polarization rotation is very sensitive to azimuth changes.

(S) It is now concluded that such a control over sea clutter magnitude should aid in ship detection. The sea reflects the characteristic (ordinary and extraordinary) waves to the receiver such that time delay of all received modes are constrained to be equal. By contrast, a ship represents a discrete target and reflects these modes while keeping the ground range constant. Because of this difference, one could simultaneously null out the sea clutter while maximizing the ship's return. It is therefore clear that some control over the radar's polarization will help detect ships at sea, i.e., when the sounder's antenna is large enough, and when the ionosphere permits the polarization phenomena to occur.

IV OTH SHIP DETECTION (S)

(S) On the basis of the results described in Parts I and II (above), it is probable that a ship could be detected on a total power basis using the ARPA-ONR Wide-Aperture Research Facility (WARF). This follows from the measurement of a 10^4 m^2 total sea cross section, which is less than σ's for broadside ships. The control of the sounder's polarization may facilitate this detection.

(S) Detection-oriented experiments have shown that oil platforms (or groups of them) were seen in the Gulf of Mexico. When a 10^5 m^2 -cross-section repeater was operated on a 500-foot cargo ship between New Orleans and Houston, the repeater's echo was visible 90 percent of the time. Echoes from the ship's position (other than the delayed repeater echo) were also seen occasionally, but these may have been from platforms.

(S) The experimental results demonstrate that ¼-to ½-degree azimuthal, and 4-to 10- μs time delay resolutions are obtainable using the WARF system, as predicted. Targets with cross-section comparable to those for broadside ships have been detected on a total power basis using the system. It has not yet been proved, however, that a ship was detected.

V FUTURE WORK (U)

(S)

- Measure more sea clutter magnitudes and polarization dependence at HF
- Study ways to use polarization control in OTH ship detection
- Run several well-controlled ship detection experiments
- Investigate use of repeaters as permanently-stationed reference targets at sea
- Develop Doppler-filtering for sea backscatter data processing on the SFCW waveform

PRECEDING PAGE BLANK - NOT FILMED

BUOY TACTICAL EARLY WARNING (S)

PRECEDING PAGE BLANK - NOT FILMED

BTEW CONCEPTS (U)

Allen M. Peterson

Stanford Research Institute
Menlo Park, California

(S) Surface-wave beyond-the-horizon radar dates back to work undertaken before 1950 in the United Kingdom.[1] Shortly thereafter a program was started by Raytheon[2] and continued by MIT Lincoln[3] Laboratory until 1957. The final report by Lincoln Laboratory clearly demonstrated the feasibility of beyond-the-horizon detection even in the 1950-1960 time frame.

(S) A renewed interest in Surface-wave radars was initiated in the 1968 IDA JASON Summer Study[4] during a review of OHD radar techniques. This study occurred in La Jolla, California and the possibility of using anchored, buoy-mounted transmitters of relatively low power levels ($\simeq$ 100 watts) arose in discussions with personnel from Scripps Institution of Oceanography. Low power appeared possible since buoys could be distributed along a "fence-line" or in an array so that the distance from the transmitter to the target (aircraft or missile) could be kept small and the large surface wave losses could be limited to the path from target to a land-based receiving installation.

(S) Following the 1968 JASON Study ARPA initiated a research program to investigate the possibilities of the surface wave systems including the buoy-based transmitters. A number of "catamaran" buoys were procured from Scripps and instrumented by APL. Detection experiments were implemented by Raytheon for the BTEW technique.

(S) In addition, surface wave propagation measurements were implemented to study the relationship of losses to "sea state" conditions. This appeared essential based on theoretical studies carried out by Barrick[5] who found that, under rough sea conditions, 10 dB or more signal losses would occur in the desireable frequency range near 10 MHz. Losses of this amount, which appear to have been confirmed, certainly make the system application more difficult.

(S) Sea clutter caused by resonant or "Bragg" scattering from sea waves was also raised as a source of concern in system applications. Studies now appear to show that the Bragg-scattered signals are sufficiently confined in frequency extent that they will not seriously limit system performance for aircraft or missile detection because of the larger Doppler shifts associated with these targets.

(S) One potentially desireable feature of surface wave techniques is their immunity to nuclear propagation blackout. In fact, sufficiently widespread nuclear blackout could cause a reduction in background noise level and ionospherically propagated interference.

(S) It appears probable that enough has been learned during the BTEW experimental program to permit meaningful system studies in the near future. Certainly it should be possible to define required future experiments based on the research which is being reviewed today.

REFERENCES

1. F. D. Boardman, J. W. F. Canning, and G. Ord, "Initial Trials of the Orange Poodle" (U), Report No. 2156, Telecommunications Research Establishment, Malvern, Worco, England, July 1953, SECRET

2. Raytheon Manufacturing Company, "Research and Investigation for Ground Wave Radar" (U), Quarterly Report No. 3, Contract AF19(122)-286, Jan 1 - Mar 31, 1951, SECRET

3. C. A. Stutt, "On the Feasibility of Ground Wave Radar" (U), Technical Report No. 145, Lincoln Laboratory, MIT, Lexington, Mass, June 12, 1957, CONFIDENTIAL

4. A. M. Peterson, "Surface-Wave Radar" (U), IDA JASON Research Paper P-485, Contract DAHC15-67-C-0011, March 1969, SECRET

5. D. E. Barrick, "Theory of Ground-Wave Propagation Across A Rough Sea at Dekameter Wavelengths" (U), Research Report, Battelle Memorial Institute, Columbus, Ohio, January 1970, UNCLASSIFIED

BTEW-1 FEASIBILITY TESTS (U)

Bruce B. Whitehead

Raytheon Company
Equipment Division
OHD Advanced Development Department
Spencer Laboratory
Burlington, Massachusetts

I INTRODUCTION (U)

(S) The BTEW-1 Feasibility tests were carried out during the period January-March 1970 in the vicinity of the Raytheon transmitter site on Carter Cay in the Bahamas. A total of eight flight tests were made; one was chosen for detailed analysis. This paper describes that analysis and draws conclusions that may be used in a system design using the BTEW-1 concept.

II NOMINAL SYSTEM AND TEST PARAMETERS (U)

(C) For the selected test the system parameters are summarized in Figure 1. The aircraft flight plan is shown in Figure 2. The aircraft made successive passes from CC to G3 and returned at altitudes ranging from 250 feet to 14,000 feet. All passes were made at speeds of approximately 250 knots.

III OBSERVED AND PREDICTED DOPPLER (U)

(S) Figure 3 shows the observed and predicted Doppler for the CC-G3 flight at 6000 feet. This and all the Doppler predictions were based on the measured true ground speed of the aircraft. All computed Dopplers are for a ground wave propagation path from the transmitter to the target. Two possible propagation paths have been taken into account for the target to receiver path. These two return paths result in two predicted dopplers. In Figure 3 only the ground wave prediction is shown and it can be seen that the observed Doppler clearly corresponds to this mode. In Figure 4, a composite predicted Doppler is illustrated. The Doppler track with the largest frequency excursion is the ground wave mode whereas the

NOMINAL SYSTEM AND TEST PARAMETERS

RECEIVER SITE	– –	CAPE KENNEDY
TRANSMITTER SITE	– –	CARTER CAY
AIRCRAFT	– –	NAVY P3V (LOCKHEED PROP-JET ELECTRA)
ANTENNAS	– –	RX ANT 16 ELEMENT BSA TX ANT λ/4 MONOPOLE $G_T G_r$ = 16 db
ALTITUDES	– –	250′ ⟶ 14,000′ LINE OF SIGHT –– 17,000′
FREQUENCY	– –	10.167 MHZ
TRANSMITTED POWER	– –	2.25 KW

(S) Figure 1. Nominal System and Test Parameters (U)

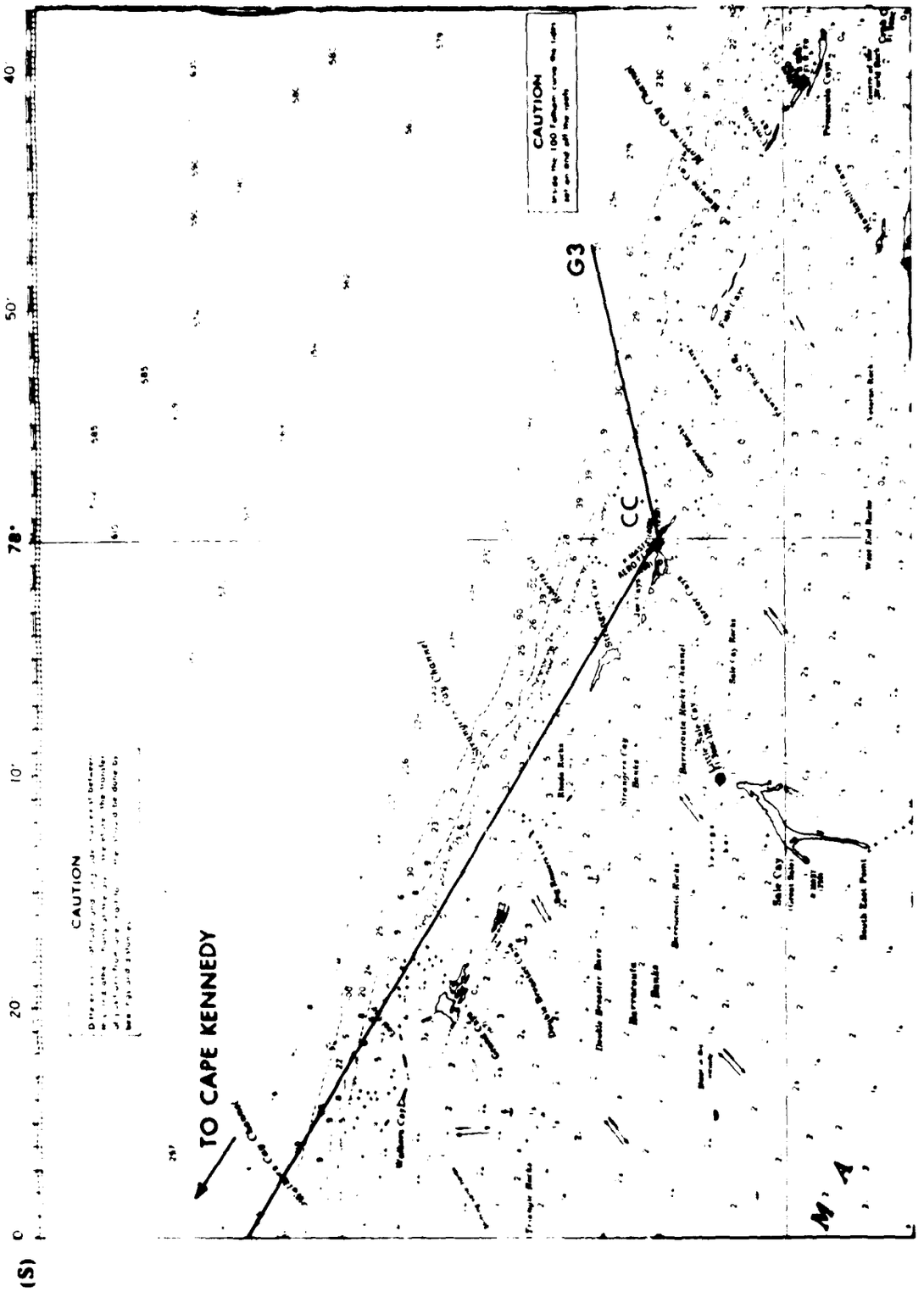

(S) Figure 2. Map of CC-G3 Flight Path (U)

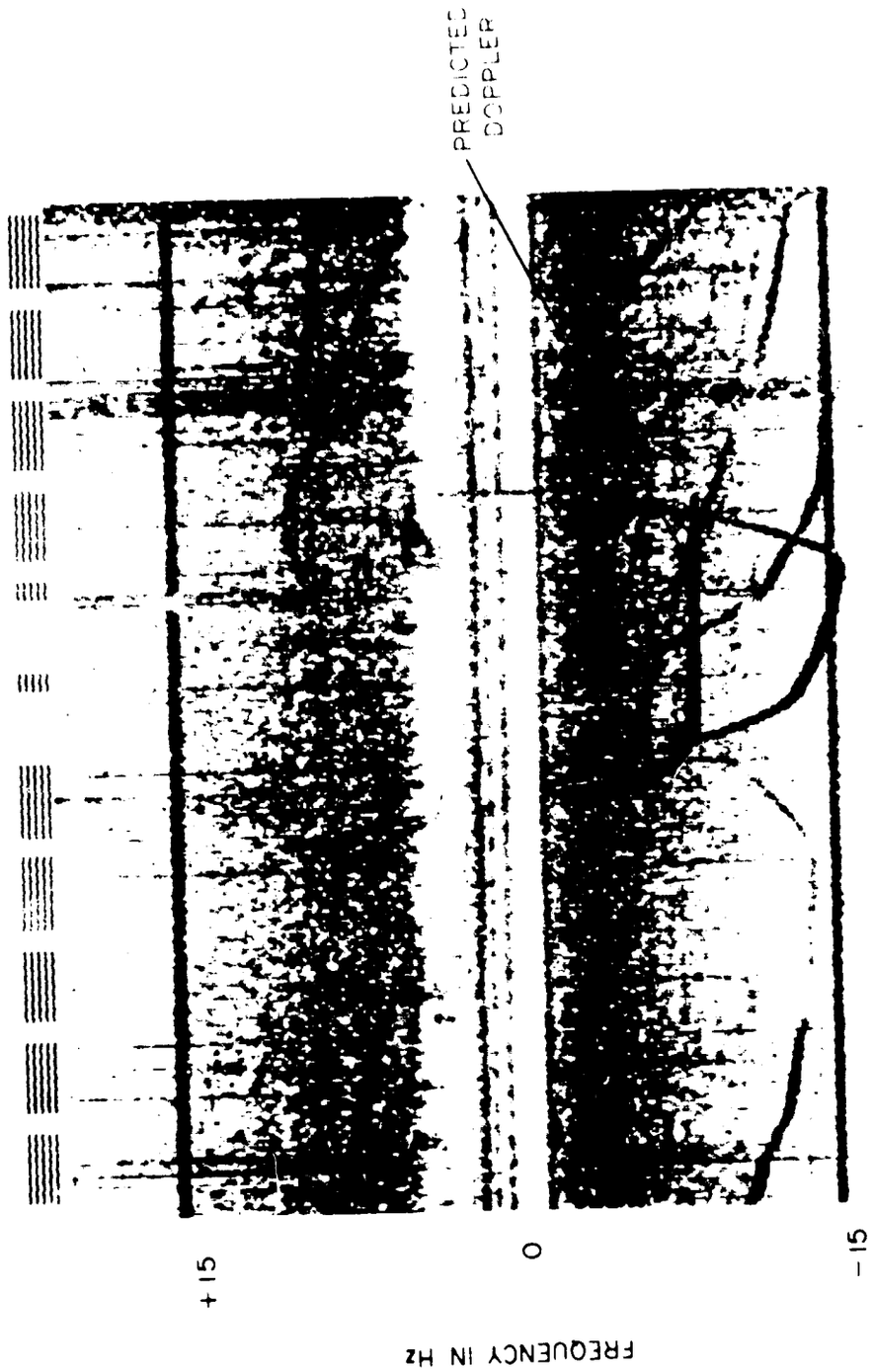

(S) Figure 3. Observed Facsimile Target Signal Path, CC-63 Altitude 6000 Ft (U)

(S)

inner Doppler track has been calculated using a single hop F layer (300-km) return mode. It can be seen that the largest observed Doppler track is clearly due to the ground wave mode. However, a small track corresponding exactly to the sky wave return is also clearly visible.

(S) Figure 5 illustrates the simultaneous detection of a controlled aircraft on 10 MHz and 15 MHz. This detection was made when there were few other aircraft in the area and hence the absence of other doppler tracks. With the addition of a ranging capability similar results could be achieved for the previous illustration.

(C) Of further interest is the presence of sky wave on the 10 MHz track whereas 15 MHz shows no sky wave detection at all.

(S) The observed presence of both modes reaffirms the fact that a purely ground wave mode of detection is being realized.

IV OBSERVED AND PREDICTED TARGET SCATTERED RECEIVED POWER (U)

(C) Predicted target scattered received power was computed using the following parameters:

a. Path loss attenuation as given by Dr. D. Barrick for Sea State 0.

b. System parameters as shown in Figure 1.

c. A reference target cross-section of 200 square meters.

(S) Figure 6 shows the predicted and observed received power for the pass from CC-G3 at 6000 feet (the scale on the left has been referenced to the input of a calibrated receiver and hence does not reflect the actual received power at the antenna). It can be observed that there is an approximate 10 dB discrepancy between the predicted received power for a 200-m^2 target and the observed signal power for the P3V aircraft.

(U) Since it is expected that the cross-section of an aircraft changes with its aspect, it is instructive to eliminate this variable by plotting it against the observed difference in received power from a prediction using a constant cross-section (e.g. 200-m^2).

(U) This has been done in Figures 7 and 8. The abscissa shows the difference in the observed received power below that which would be predicted for a 200-m^2 target. The ordinate is the angle of illumination in degrees below an azimuthal plane parallel to the surface of the earth.

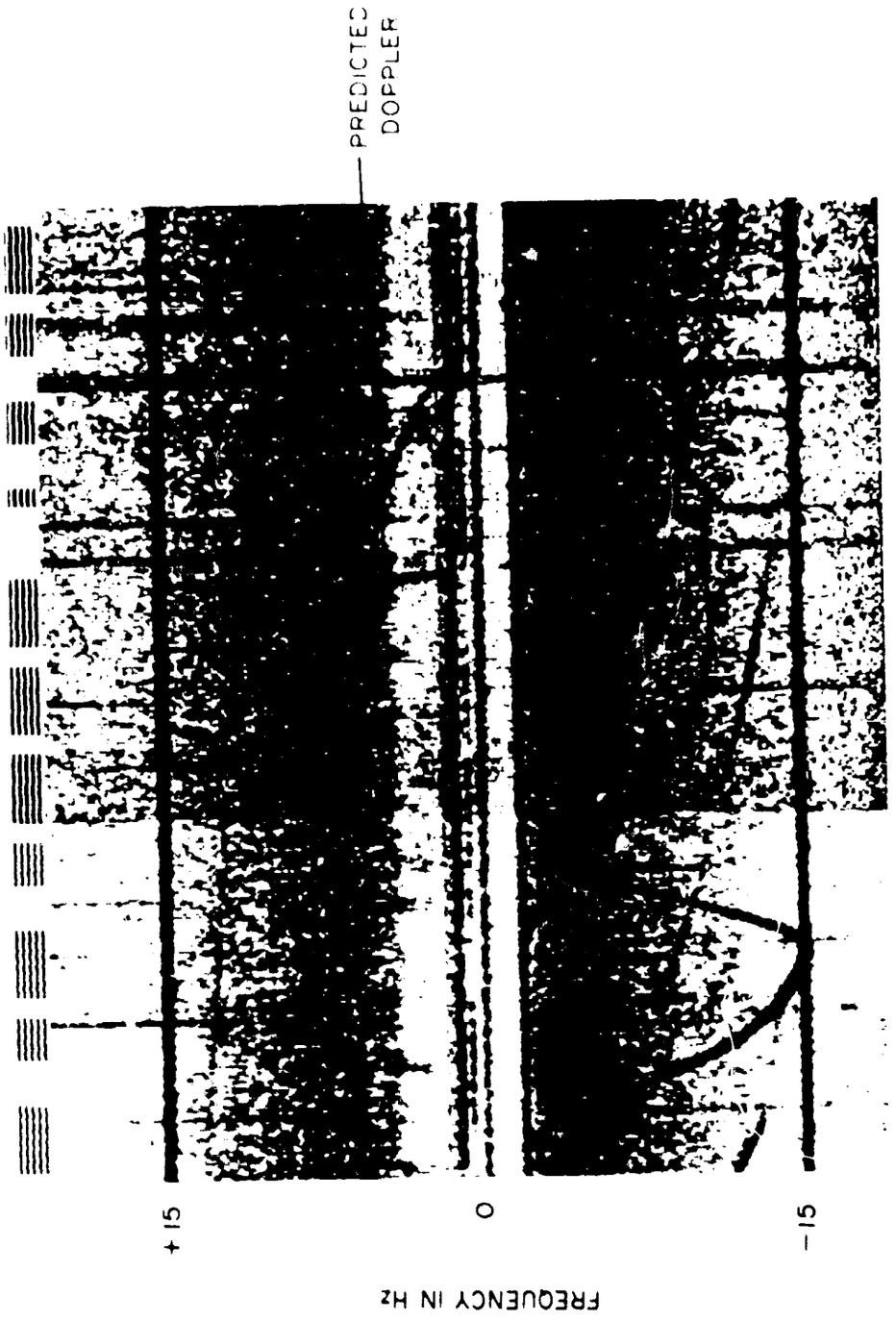

(S) Figure 4. Observed Facsimile Target Signal Path G3-CC, Altitude 250 Ft (U)

(S)

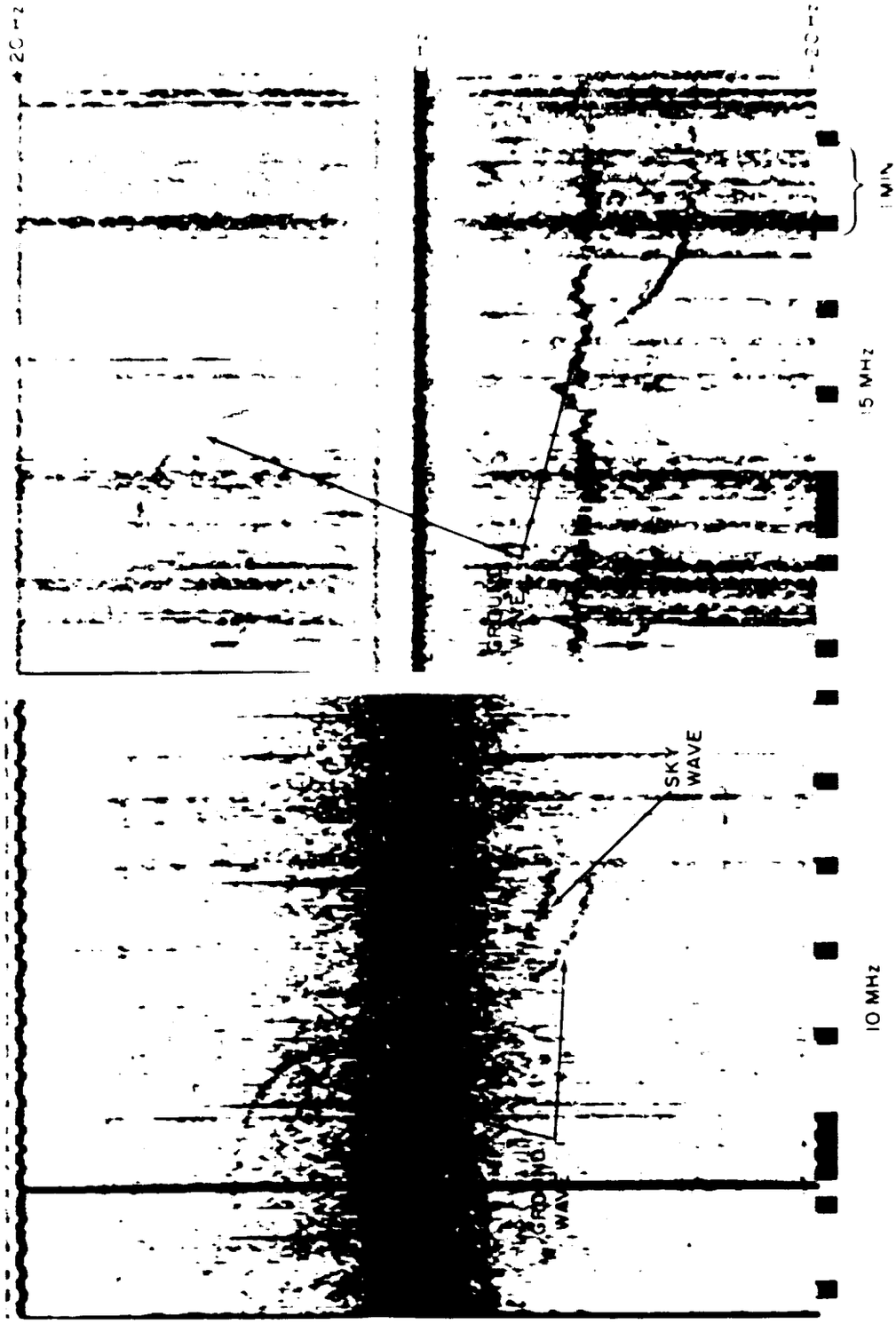

(S) Figure 5. Simultaneous Aircraft Detections at 10 MHz and 15 MHz (C)

(S)

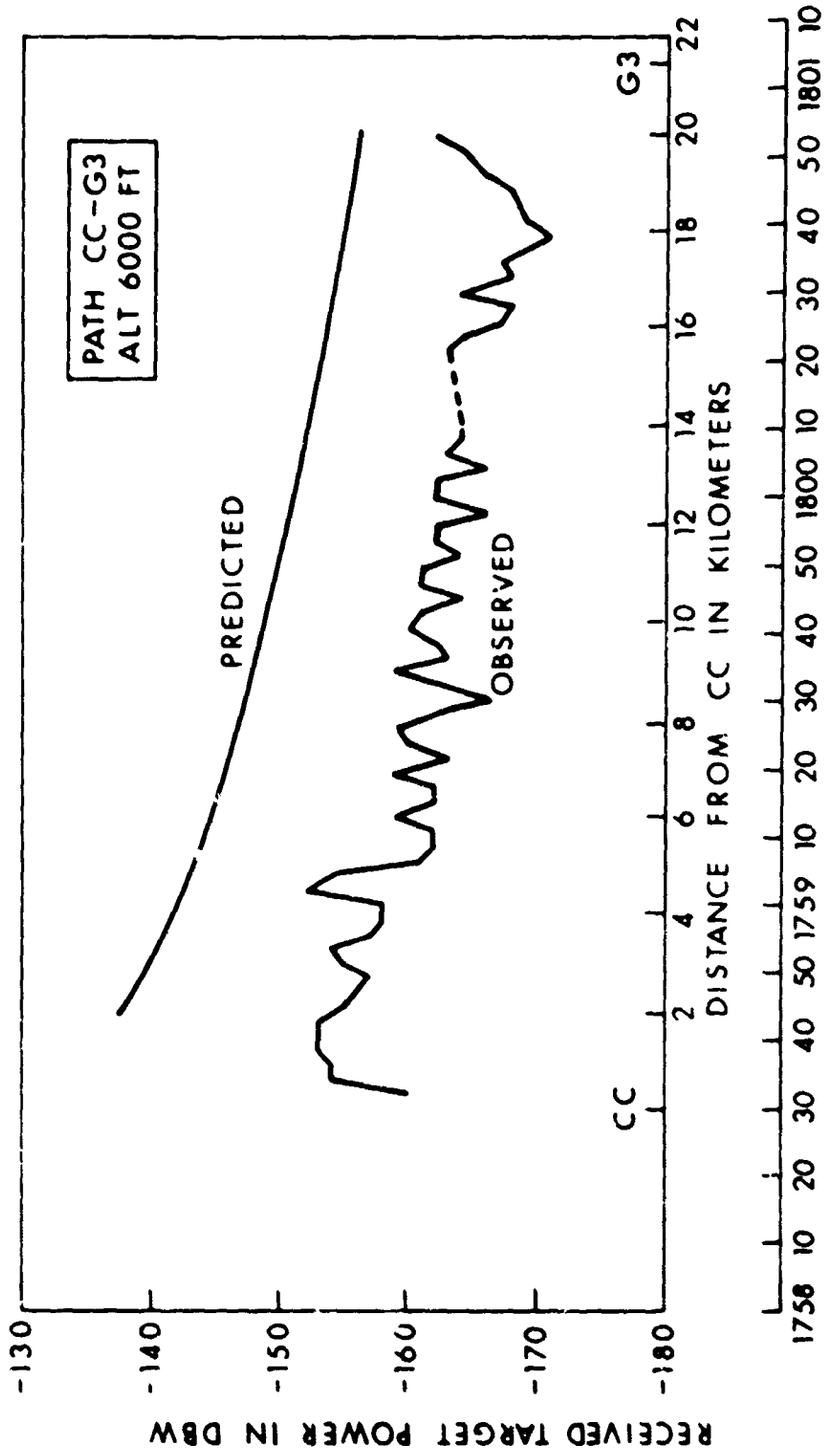

(S) Figure 6. Target Received Power Predicted vs Observed (U)

(S)

(S) These plots can be looked at as correlograms. Assuming all other parameters to be constant, all observed points at a given angle should yield the same received power. As can be clearly seen, a least squares fit of all observed points would yield a line about which the deviation would be only about 1-2 dB. This is well within experimental error.

(S) Figure 9 shows the least square plot for each of Figures 7 and 8. The abscissa has been changed to reflect observed cross-section in square meters. Two additional points have been shown on this graph. They are monostatic cross-sections obtained from a laboratory model study by ITT-EPL. They are shown here to illustrate the compatibility of the two independent observations.

V CONCLUSIONS (U)

(S) It has been shown the the BTEW-I concept is phenomenologically feasible. The results of the flight tests indicate a strong correlation between observed and predicted values of received power and Doppler excursion. This implies then that a system design using the above techniques should yield results commensurate with predictions.

(U)

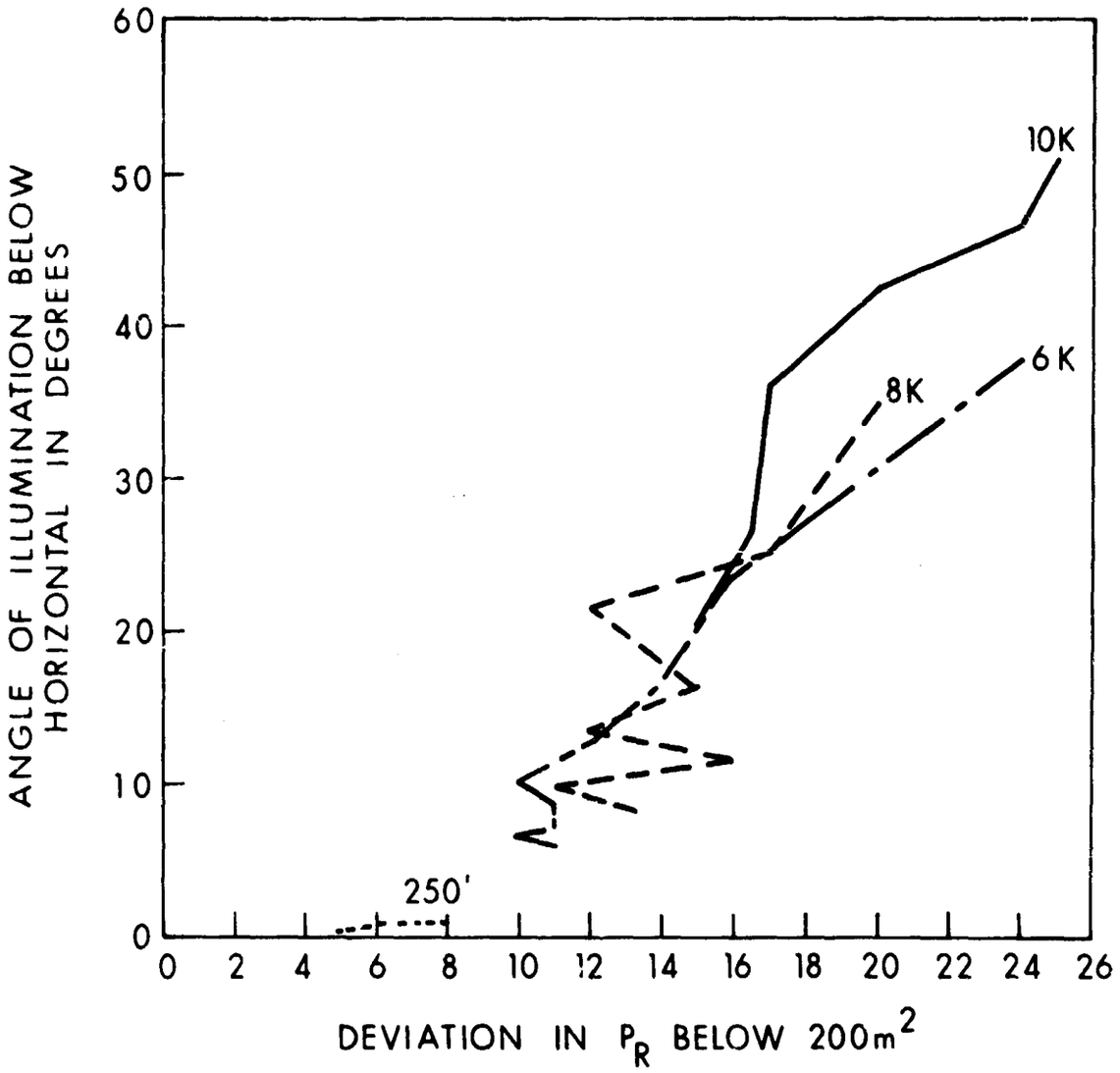

(U) Figure 8. G3-CC Data Summary Correlogram (U)

(U)

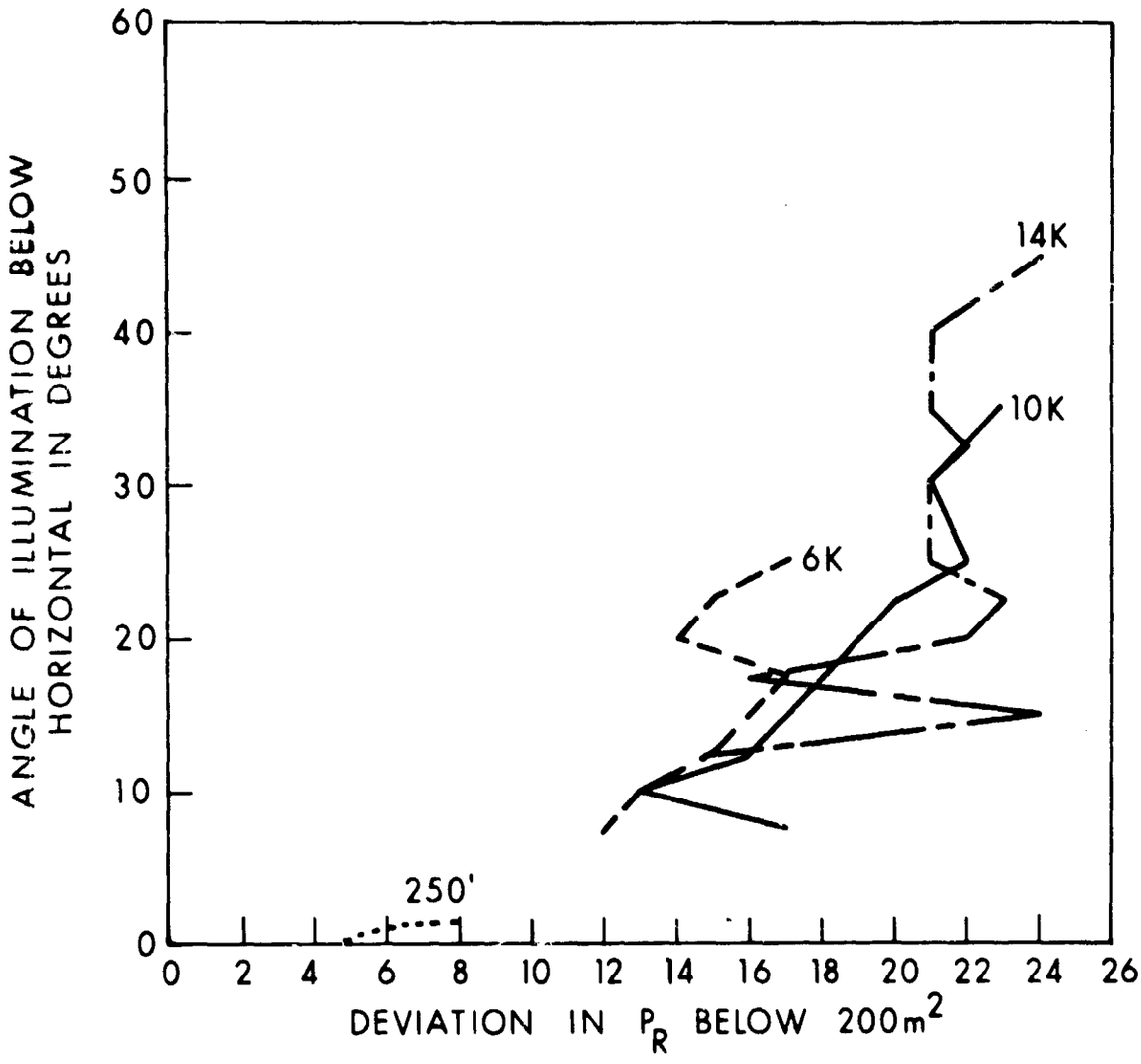

(U) Figure 7. CC-G3 Data Summary Correlogram (U)

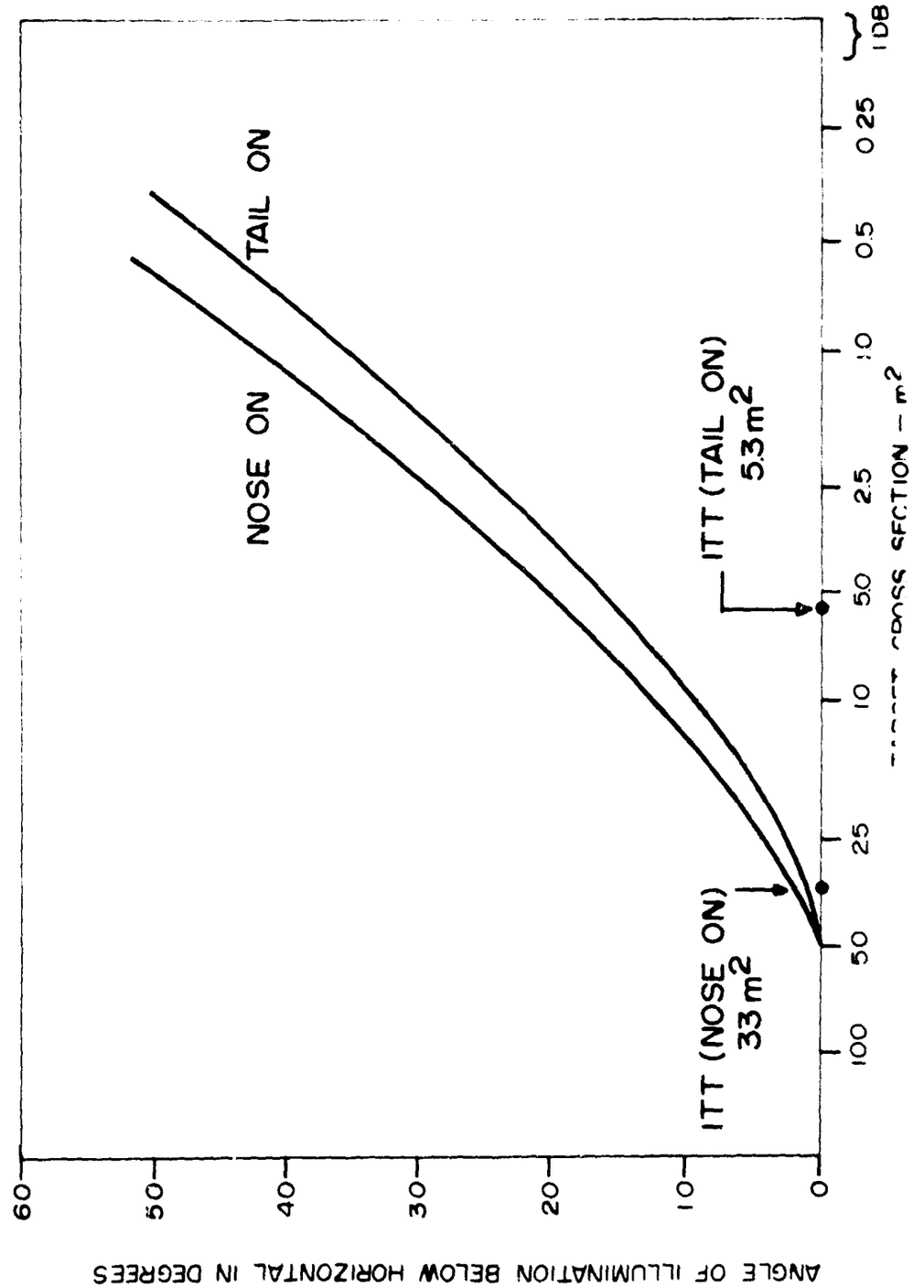

(S) Figure 9. Smoothed Target Cross Section vs Angle of Illumination (U)

(S)

SLBM OBSERVATIONS (U)

Henry M. Baker

Raytheon Company
Equipment Division
OHD Advanced Development Department
Spencer Laboratory
Burlington, Massachusetts

(S) In addition to the detection of aircraft, as discussed in other MAY BELL workshop papers, the BTEW system can be used for the detection of submarine-launched ballistic and cruise missiles (SLBM, SLCM). During the data take in Florida, the opportunity to collect data during one SLBM launch occured. This event, ETR Test 2989, was a Poseidon missile. It was launched from the USS Observation Island on 24 March 1970 at a range of 55 km from the receiver site. During this launch, two CW frequencies were being transmitted (5.152, 10.167 MHz) from Carter Cay, BWI. The frequencies were monitored at the Cape Kennedy receiving site using the vertically polarized quater-wave-length monopole antennas.

(S) The facsimile display of the spectral content of the 5.152 MHz signal is shown in Figure 1. There are three distinct portions of the missile-induced signature. These are the hard echo (T+40 to T+100 sec), wide-band noise-like burst (110-170 sec) and an ionospheric echo effect (180-480 sec). The hard echo is the skin track of the missile; the wide-band noise-like burst is a staging echo; and the ionospheric perturbation is standard.

(S) The ±15 Hz sidebands observed in the data were present during many days of the data recording. They occured on each frequency being observed and at first were thought to be associated with the ITT passive modulator buoys. ITT personnel indicated, however, that their equipment was not producing the side-bands at these frequencies. A complete test was made on the Raytheon equipment and the results indicated the sidebands were not produced in the receiving equipment. Therefore, the source of these sidebands remains an unknown.

(S) A predicted Doppler frequency shift for this test was obtained using the missile post flight data. As can be seen in Figure 2, the observed skin track did agree closely with these predictions.

(S) Figure 3 shows that the same type of data was observed on the 10.167 MHz frequency. Again three portions of the signature are present, with a more pronounced hard echo. The predicted doppler

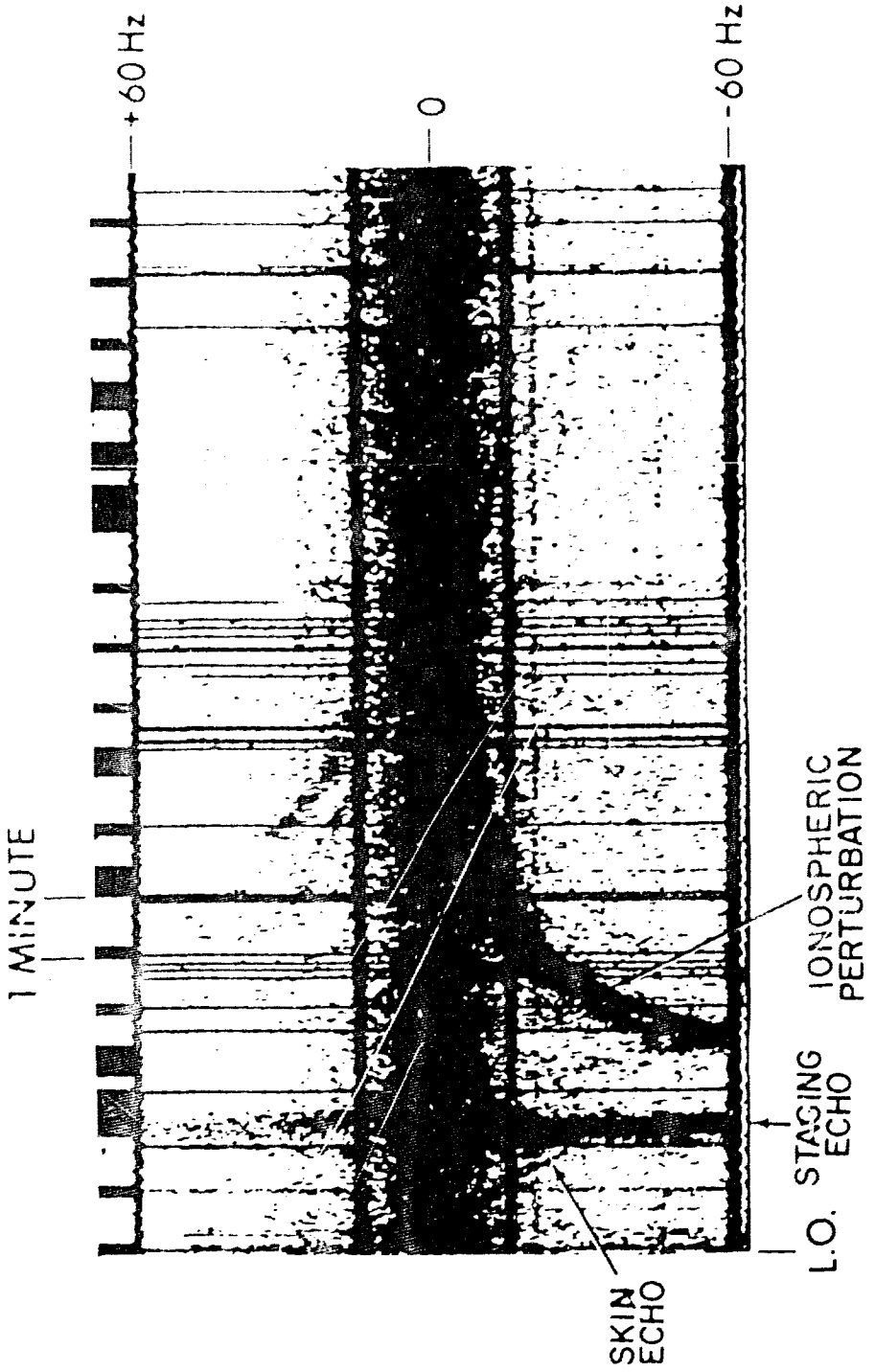

(S) Figure 1. Spectral Data Observed on 5.152 MHz (U)

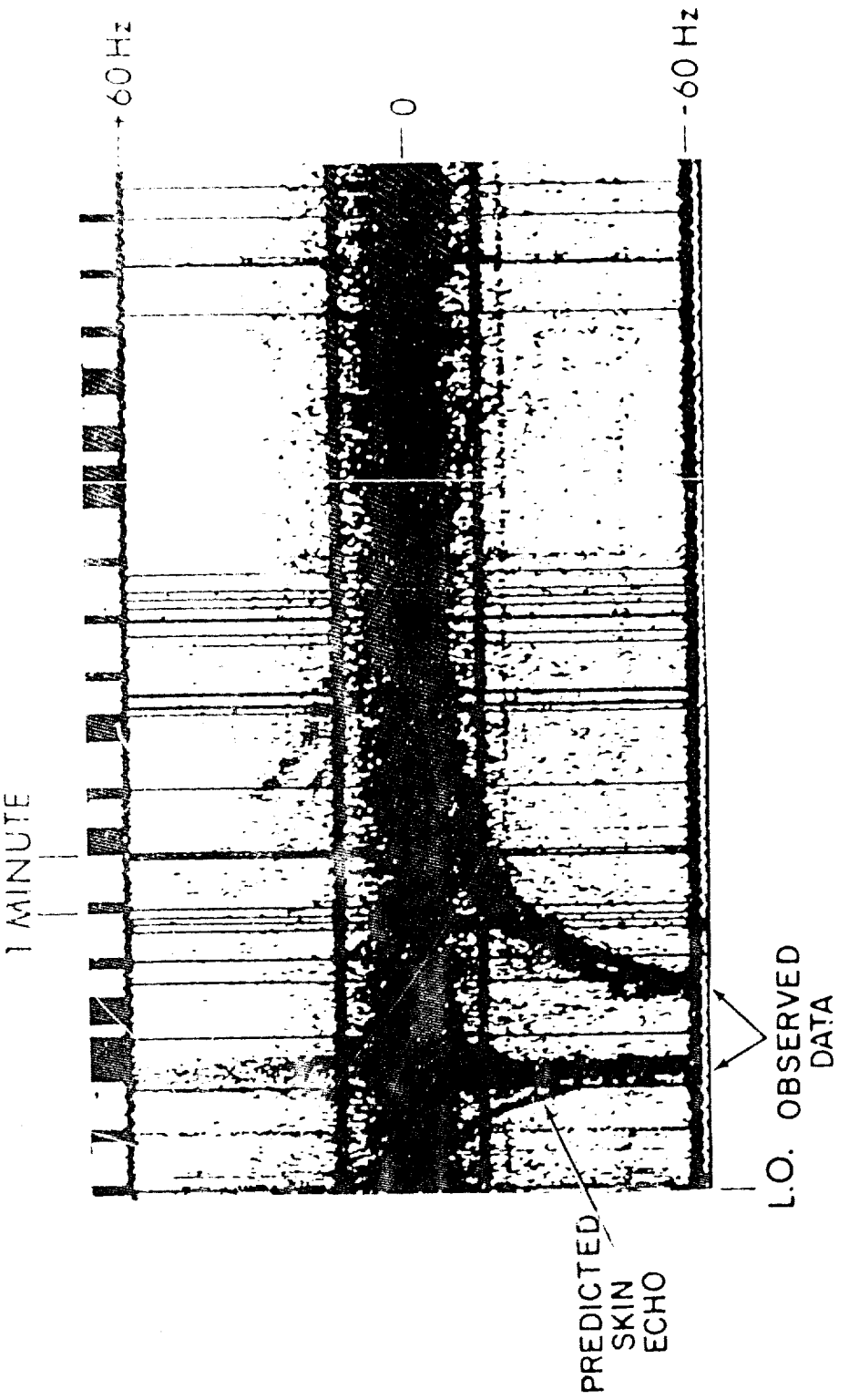

(S) Figure 2. Spectral Data Predicted on 5.152 MHz (U)

(S)
shift again shows good correlation with the received hard echo, Figure 4. Notice that the received carrier masks the initial 40 seconds of the predicted signature.

(S) The geometry associated with the event is shown in Figure 5. The tick marks on the trajectory show the altitude of the vehicle and the time of flight. Note the region 40 to 100 seconds where the hard echo was observable. At the signature onset (T + 40 seconds) the missile had travelled a horizontal distance of only 5.5 km. By the time of signature drop-out at 100 seconds, a total range of 87 km had been traversed.

(S) The altitude and velocity plots versus time for the vehicle are shown in Figure 6. Tick marks on these curves indicate the onset and the portion of the hard echo seen in the data.

(S) The lower plot of Figure 7 shows the comparison of a computed and the observed signature received power on the two frequencies. The computed received power is based on a $1m^2$ target cross-section and was normalized to the existing system parameters. The 5 MHz computed and the actual power received curves agree closely. This indicates that the observed cross-section on the 5-MHz frequency was on the order of $1m^2$. The upper plot of Figure 7 shows the measured cross section on the 10-MHz frequency versus time. At signature onset, the cross-section was $57m^2$ and as the missile's altitude increased the cross-section decreased. It is assumed that this decrease in cross-section is due to the mismatch between the polarization of the vertical transmitting and receiving antennas and the missile orientation which becomes more horizontal as the vehicle moves downrange. This polarization mismatch was also observed by SRI and has been reported.[1]

CONCLUSIONS (U)

(S) A BTEW system is capable of detecting SLBM missiles at a very low altitude.

(S) Because the carrier masks the very low doppler frequencies, the altitude of earliest detection is dependent on the geometry involved. A means of reducing the carrier spread without a loss of system sensitivity or a means of cancelling the carrier would allow a Doppler signature of less than ± 2 Hz to be observed and permit the missile to be detected at a lower altitude.

(S) The three observable portions of the missile related signature are created by independent effects; therefore, the probability of at least one of the three portions of the signature being detected is very high and if more than one portion of the signature is observed a missile launch warning can be issued with a very high confidence.

(S) With a deployed multi-station BTEW system where the hard echo is observed on three or more independent paths, missile trajectory information can be derived in real-time from analysis of the Doppler records for the observing paths.

REFERENCE

1. G.N. Oetzel, "SLBM Radar Cross Section at HF (U)," Stanford Research Institute, February 1970, SECRET.

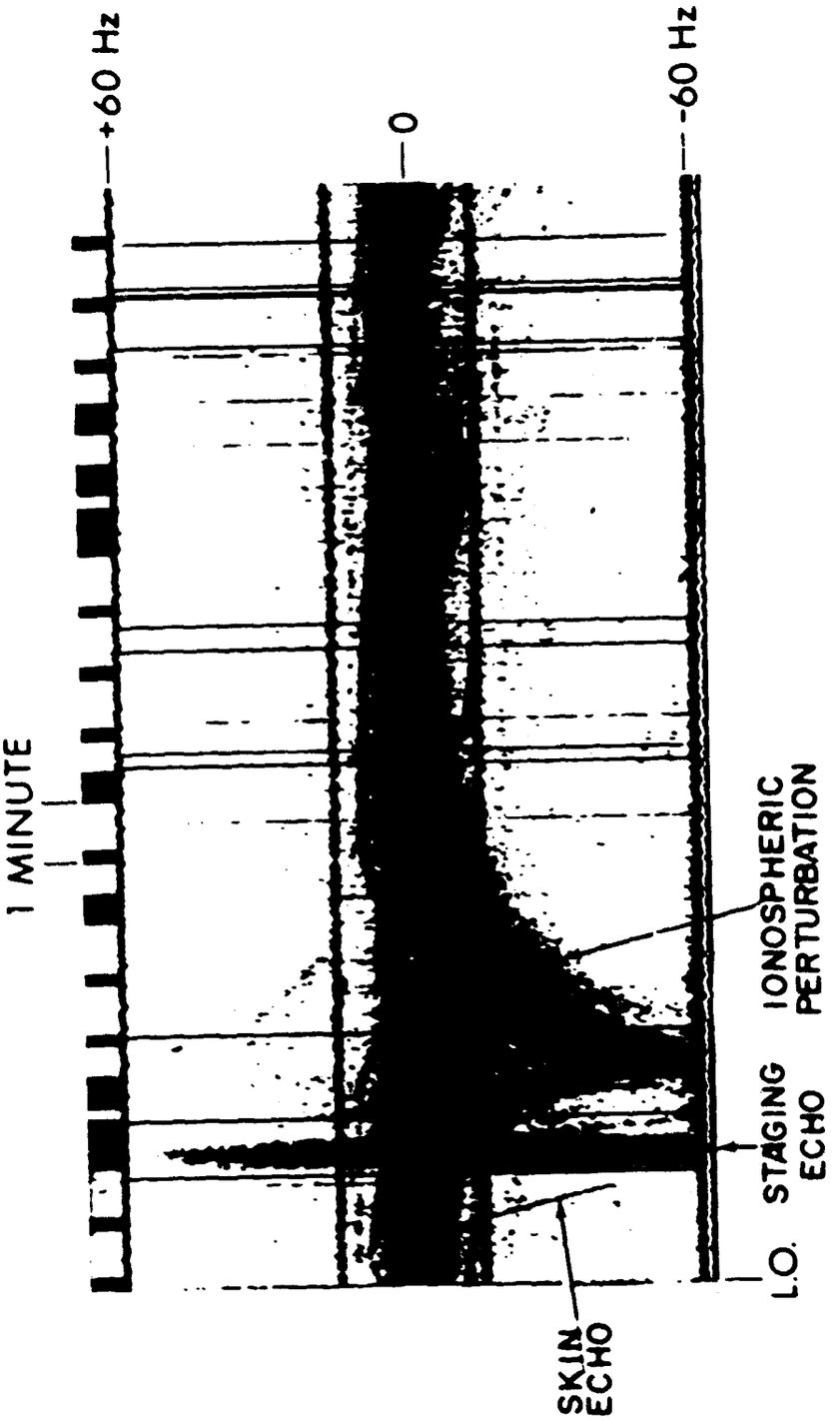

(S) Figure 3. Spectral Data Observed at 10.167 MHz (U)

(S)

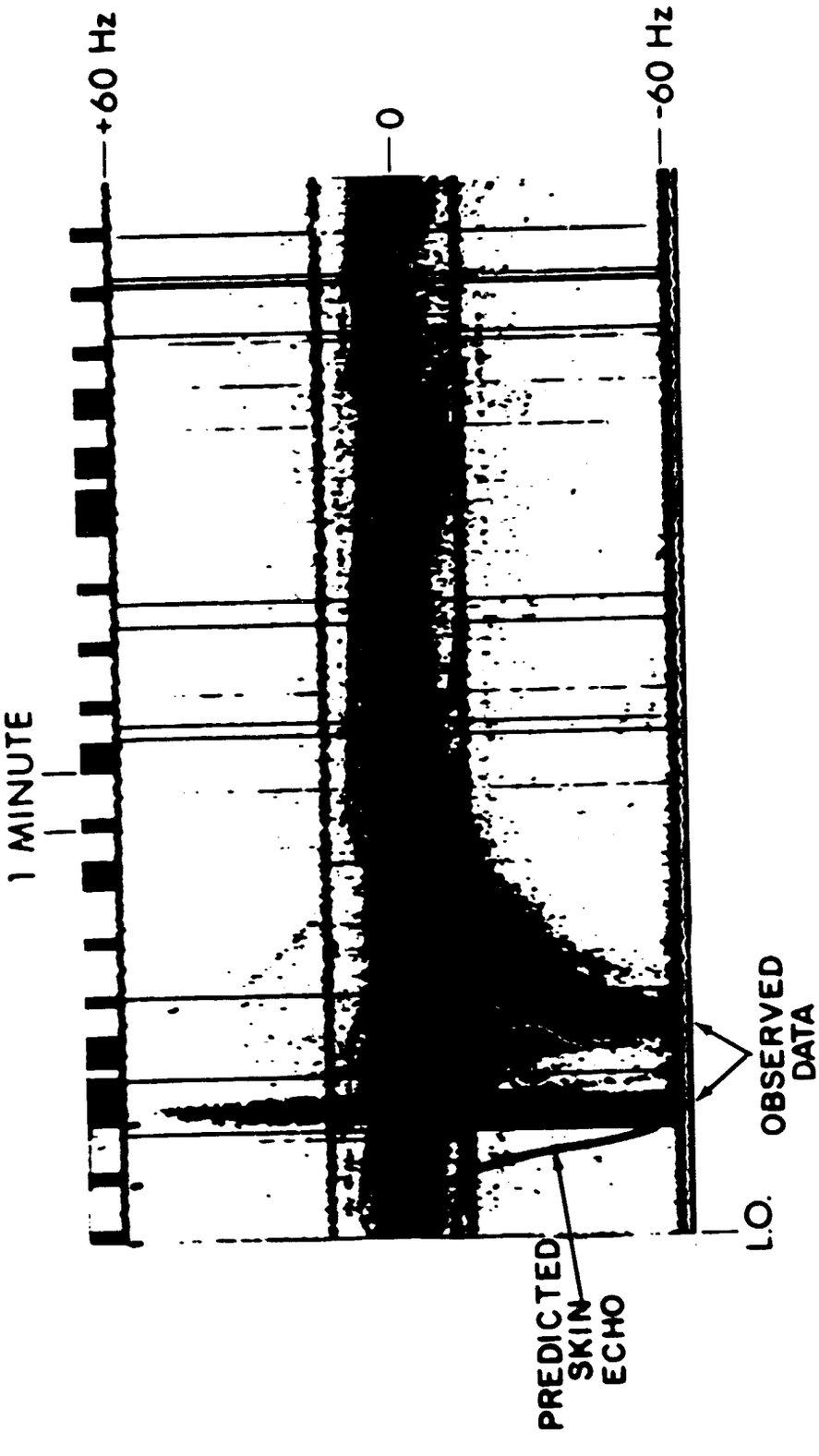

(S) Figure 4. Spectral Data Predicted on 10.167 MHz (U)

(S)

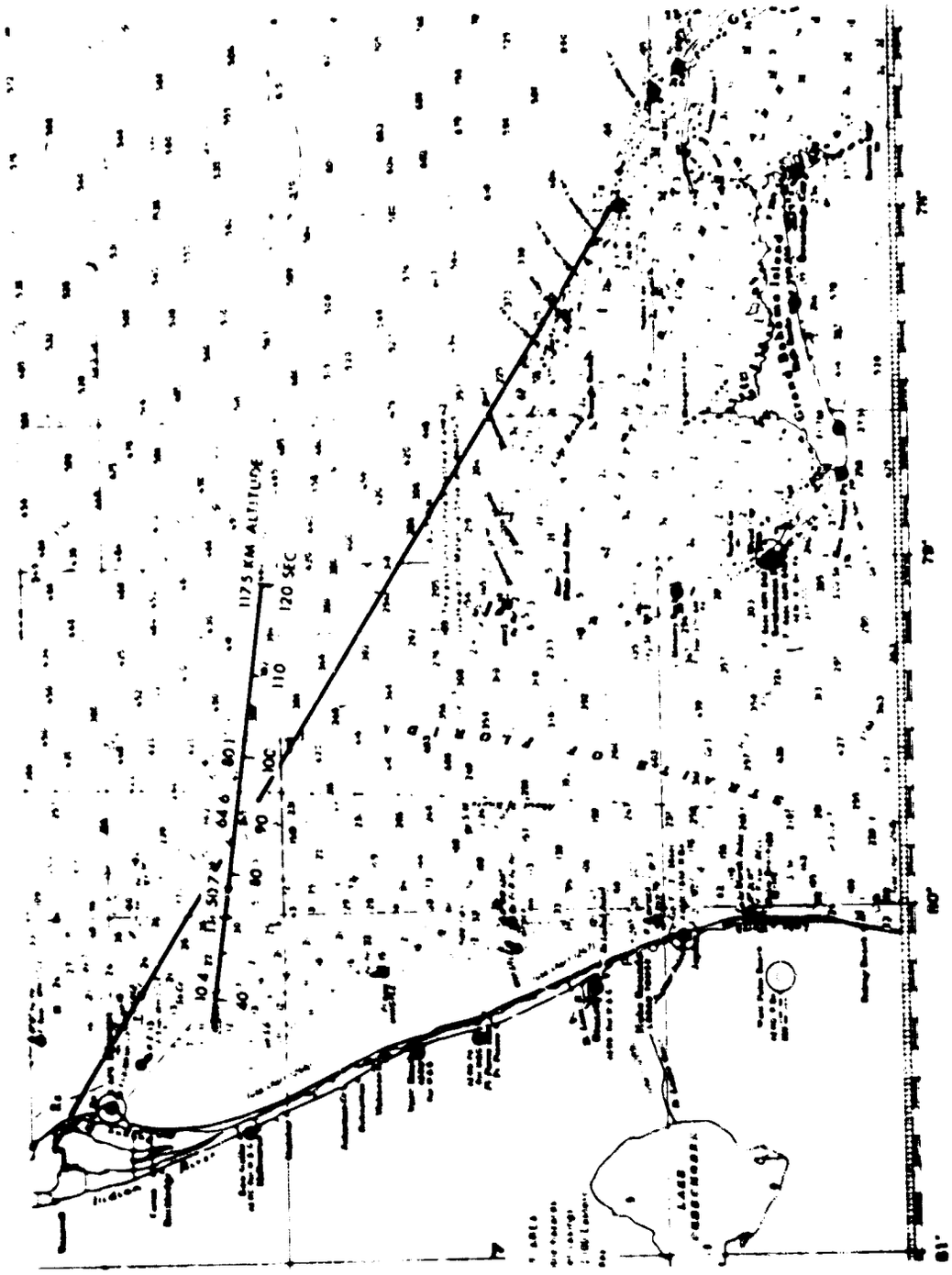

(S) Figure 5. Geometry of ETR Test 2989 (U)

(S)

(S)

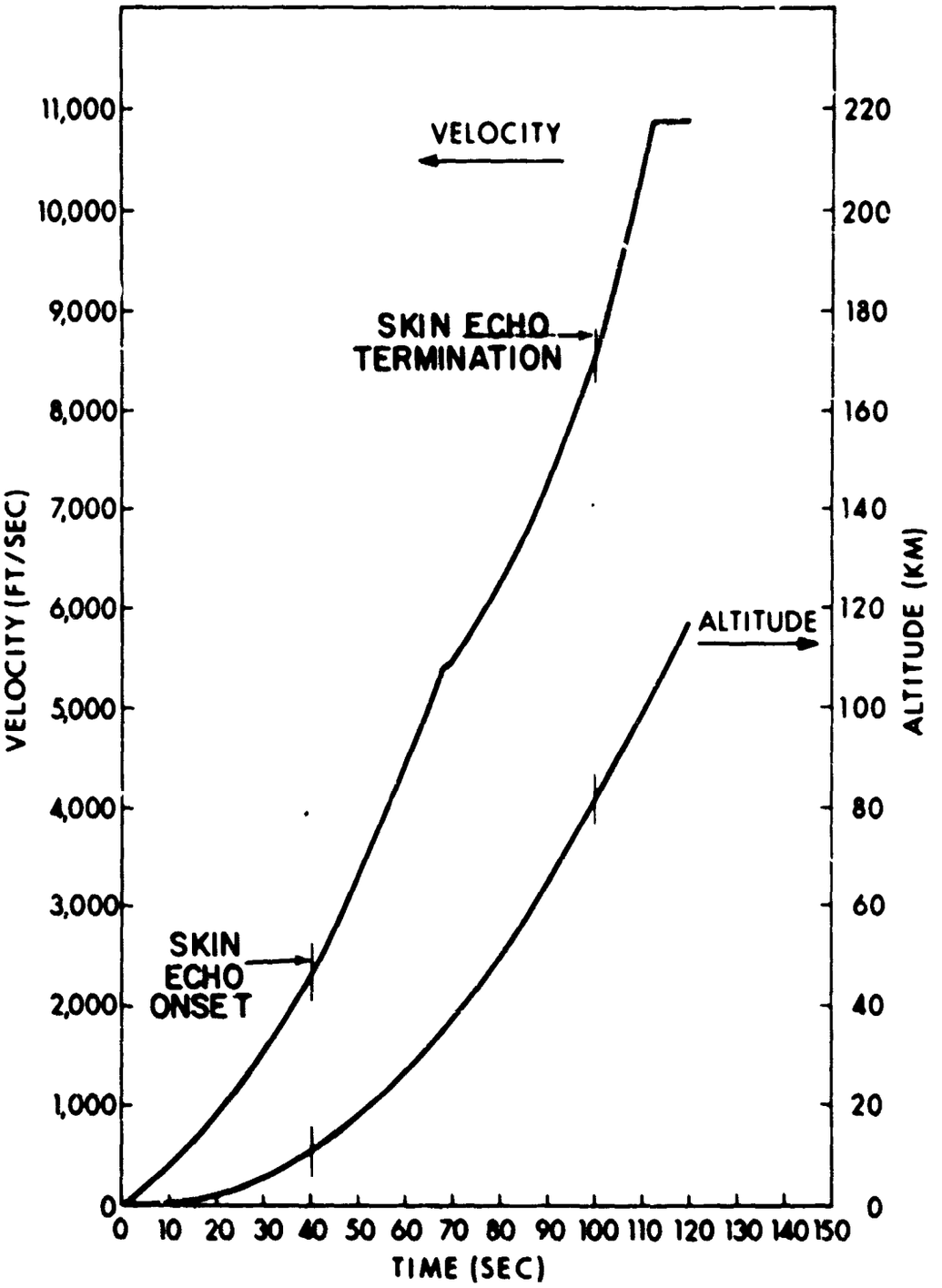

(S) Figure 6. Missile Altitude and Velocity vs Time (U)

(U)

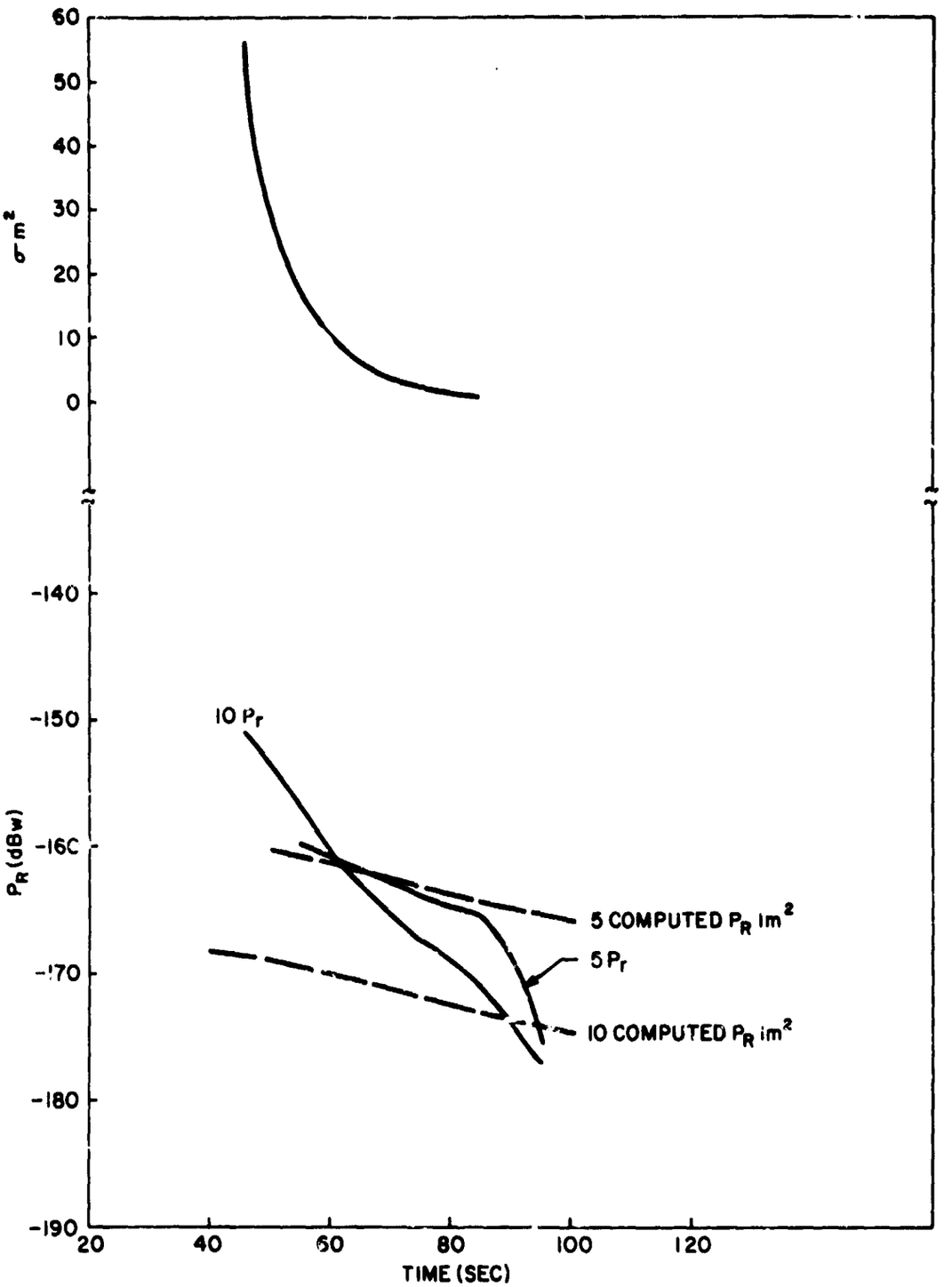

(S) Figure 7. Cross-section (U)

PROJECT AQUARIUS (BTEW-2) (U)

K. D. Snow

Sylvania Electronic Systems - West
Mountain View, California 94040

I INTRODUCTION (U)

(S) Project Aqua... is a part of the ARPA-sponsored ocean surveillance program under Project MAY BELL. The primary goals of the project as shown in Figure 1 are to experimentally demonstrate the feasibility of detecting submarine launched ballistic missiles and low flying aircraft, and to compare the experimentally observed detection ranges. The results of the experimental work completed to date indicate that target aircraft can be detected at the theoretically predicted range and that the concept is feasible providing there is sufficient radiated power from the transmitter.

II EXPERIMENTAL NETWORK (U)

(S) The experimental setup consists of using a bistatic HF continuous wave radar consisting of a low power ocean-based bouy transmitter and high sensitivity receivers located on the coast. A detection is made by observing the doppler-shifted signal that is scattered from a moving target such as an airplane or an SLBM. The target is illuminated by line-of-sight or groundwave energy from a transmitter. The scattered doppler-shifted return is received by ionospheric skywave as illustrated in Figure 2.

(S) The experimental system geometry is shown in Figure 3 with the bouy transmitter located approximately 120 kilometers off the Cape Kennedy coast. A high power set of transmitters is located at Carter Cay in the Bahaman Islands and the high sensitivity receiving system at Vint Hill Farms Station in Virginia.

(C)

PROJECT AQUARIUS

GOALS

- PARTICIPATE IN MAYBELL PROGRAM -- BTEW-2
- DETERMINE BTEW-2 FEASIBILITY
- DETECT LOW FLYING AIRCRAFT USING BOUY-GROUND WAVE-SKYWAVE CONCEPT
- DESIGN A DETAILED BTEW-2 EXPERIMENT

RESULTS

- DETECTED TEST AIRCRAFT AT PREDICTED RANGE
- BTEW-2 FEASIBLE WITH SUFFICIENT TRANSMITTER POWER OR ANTENNA GAIN

SECRET

(this page confidential)

(C) Figure 1. Project Aquarius Goals and Results (U)

(S)

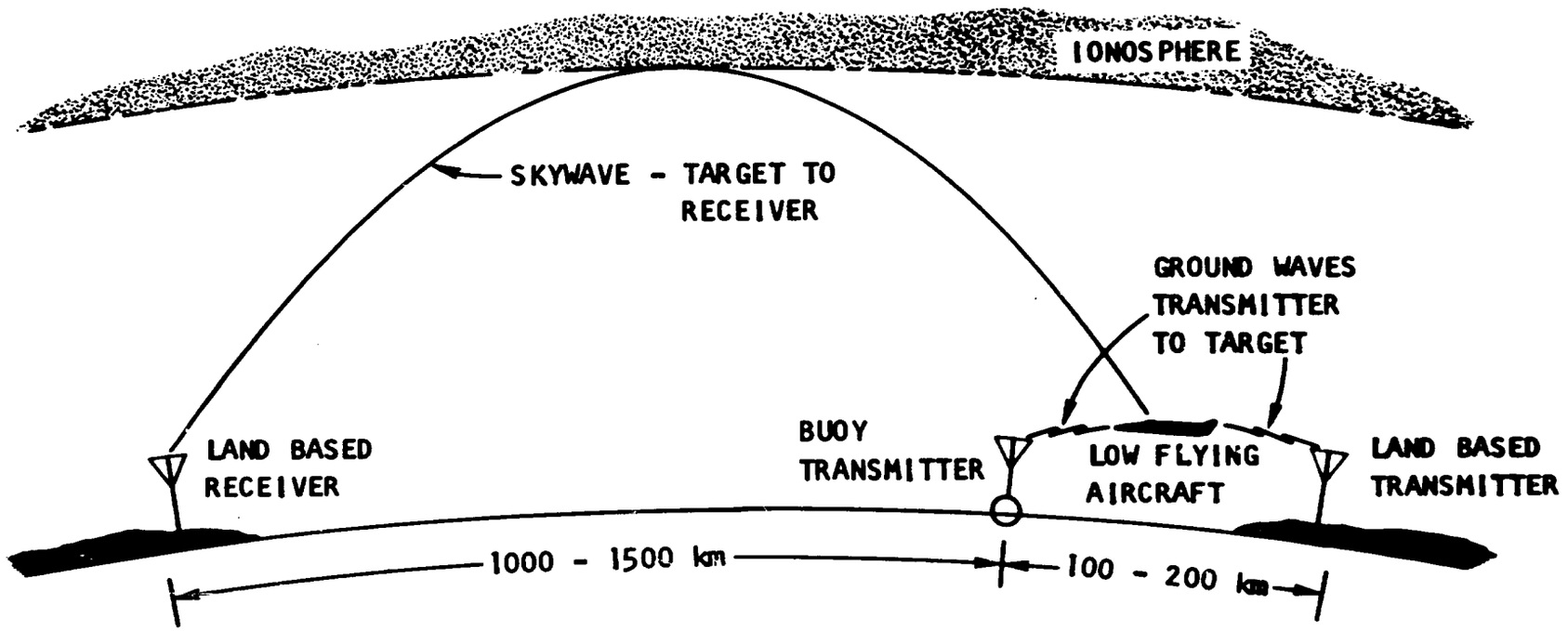

SECRET

SECRET

(S) Figure 2. Project Aquarius, Basic System Concept (U)

(U)

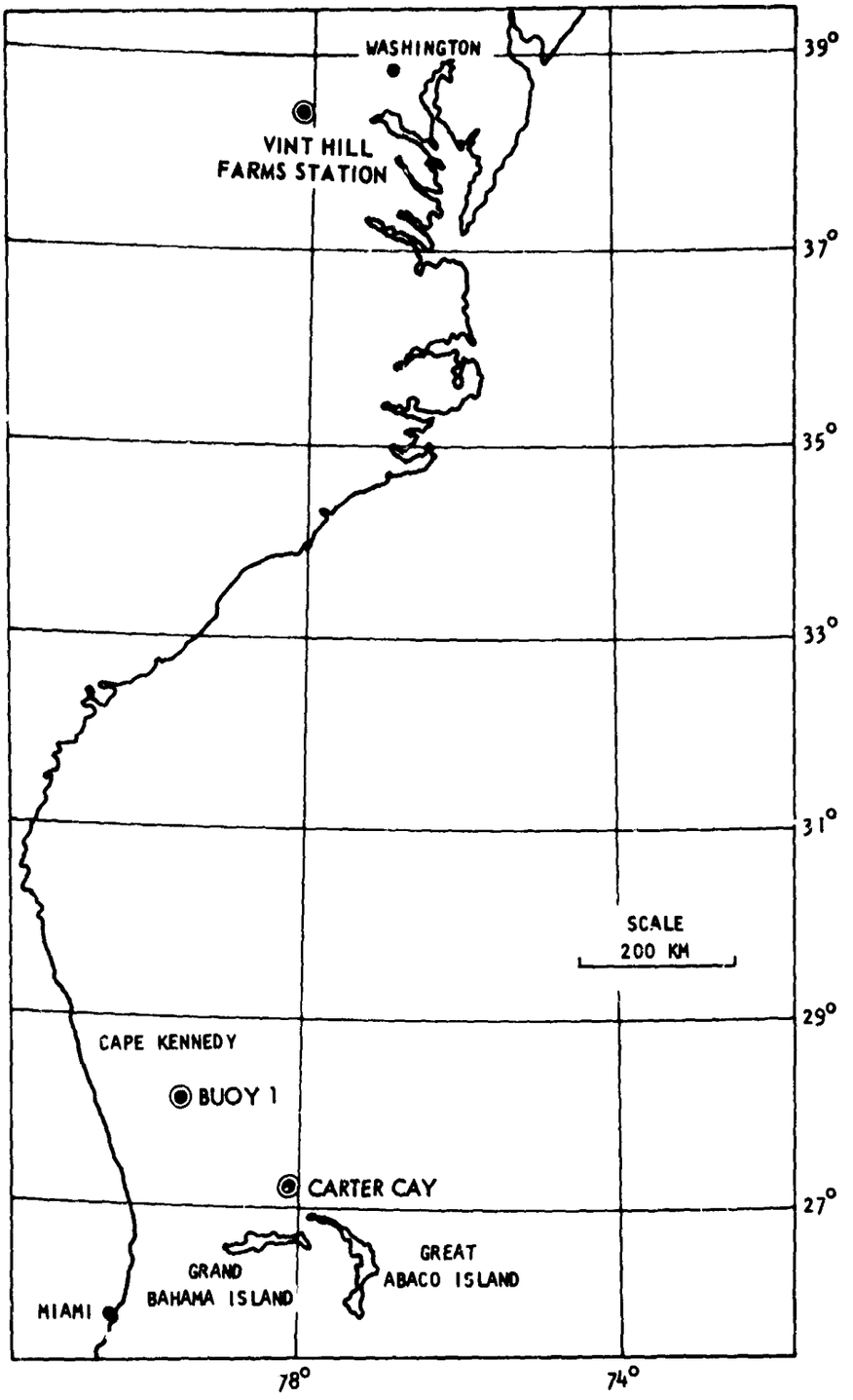

(U) Figure 3. Network Geometry (U)

III RECEIVING SITE (U)

(U) The block diagrams of the two receiving systems are shown in Figures 4 and 5. Figure 5 shows a 12-channel receiving system, including a DF set connected to an LDAA steerable antenna. The twelve analog receiving channels use R-390A receivers and drive a real-time analog spectral display and a twelve-channel analog tape recorder. The other receiving system is a van-mounted high dynamic range digital processing system containing synthesizer controlled receivers, digital spectrum analysis and both an analog and digital PCM recording capability.

IV AIRCRAFT TESTS (U)

(S) Figure 6 lists the operations of aircraft flights and hearability tests through 10 February 1970. On 27 January during the controlled tests, the P3B controlled aircraft was detected at two different times on two different frequencies. The flight path and the detection regions for this 27 January flight are shown in Figure 7. The data collected in real-time is shown in Figure 8. The data at the top of the figure shows the detected doppler signature lasting for a period of approximately 30 seconds for the 10.167 MHz frequency. The detection is at a range of approximately 9 kilometers from Carter Cay and exists during the time when the plane banks following a turn over checkpoint C5. The lower half of the figure shows the second detection on the 15.595 MHz frequency, again lasting for approximately 16 kilometers from Carter Cay. The same characteristic signature exists and is also present at the time when the plane is banking during a turn over checkpoint D4. Both of these signatures seem to be at times when there is specular reflection from the transmitter at Carter Cay to the receiver at Vint Hill Farms Station. Figure 9 is an expanded view of the flight path and includes the detection regions for these two detections. By assuming turns are completed by first flying over the checkpoint and then making a maximum turn rate for the next checkpoint, the doppler shifts predicted from this type of flight plan match very closely to the actual observed data as shown in Figure 8.

V SUMMARY (U)

(S) To summarize, the goals of the project have essentially been met; that of demonstrating the feasibility of the bouy tactical early warning system. However to make this system useful for detections at any range beyond a few kilometers, the effective radiated power from the transmitter will have to exceed the 2000 watts used for the Carter Cay detections of the controlled aircraft flights.

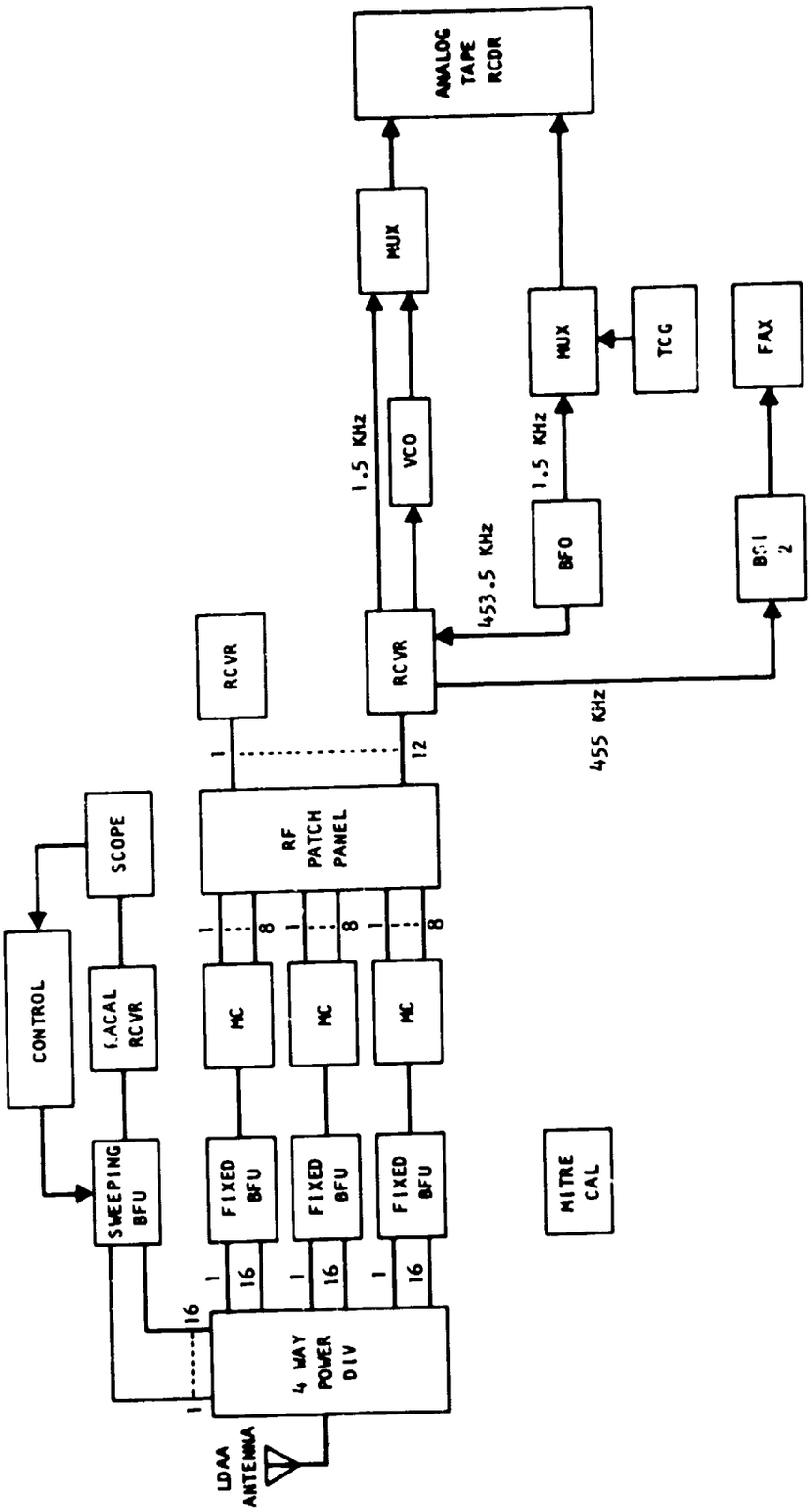

(U) Figure 4. Analog System Block Diagram (U)

(U)

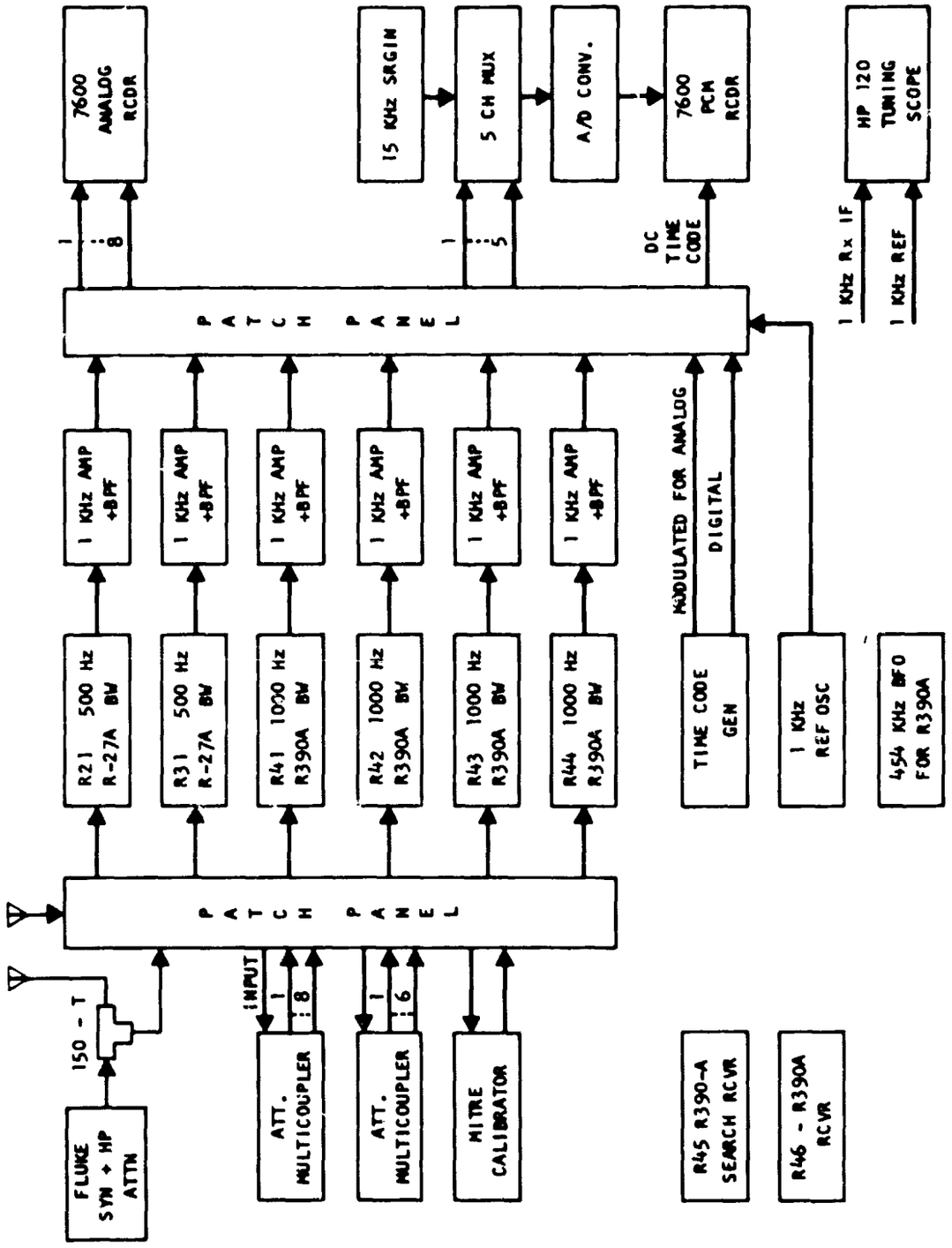

(U) Figure 5. System Block Diagram (U)

(U)

(U)

UNCLASSIFIED

DATE	TYPE	FREQUENCIES (MHz)	MEASUREMENT OR DETECTION TIMES (GMT)
18 DEC 69	AC	5.8	1750-1755 2000-2005
	AC	9.259	ND
	AC	10.167	ND
27 JAN 70	AC	15.595	1656
27 JAN 70	AC	10.167	1712
5 FEB 70	HB	20.250	1500
	HB	10.167	1500
	HB	10.167	2100
	HB	20.250	2100
10 FEB 70	HB	9.259	1430
	HB	5.8	1430

AC = AIRCRAFT ND = NOT DETECTED HB = HEARABILITY

(U) Figure 6. Summary of Operations (U)

UNCLASSIFIED

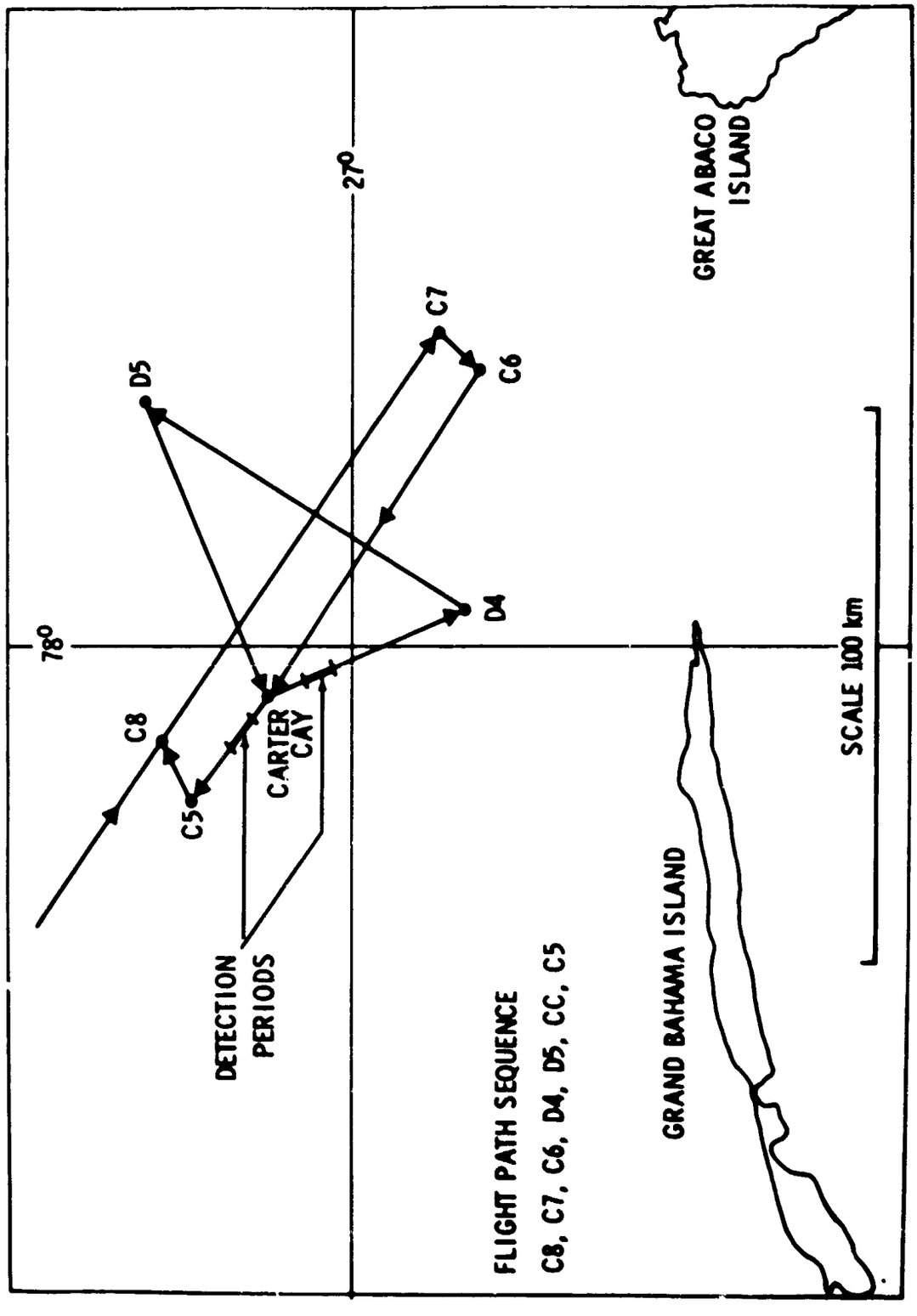

(U)

(U) Figure 7. Controlled Aircraft Flight, 27 January 1970 (U)

(S)

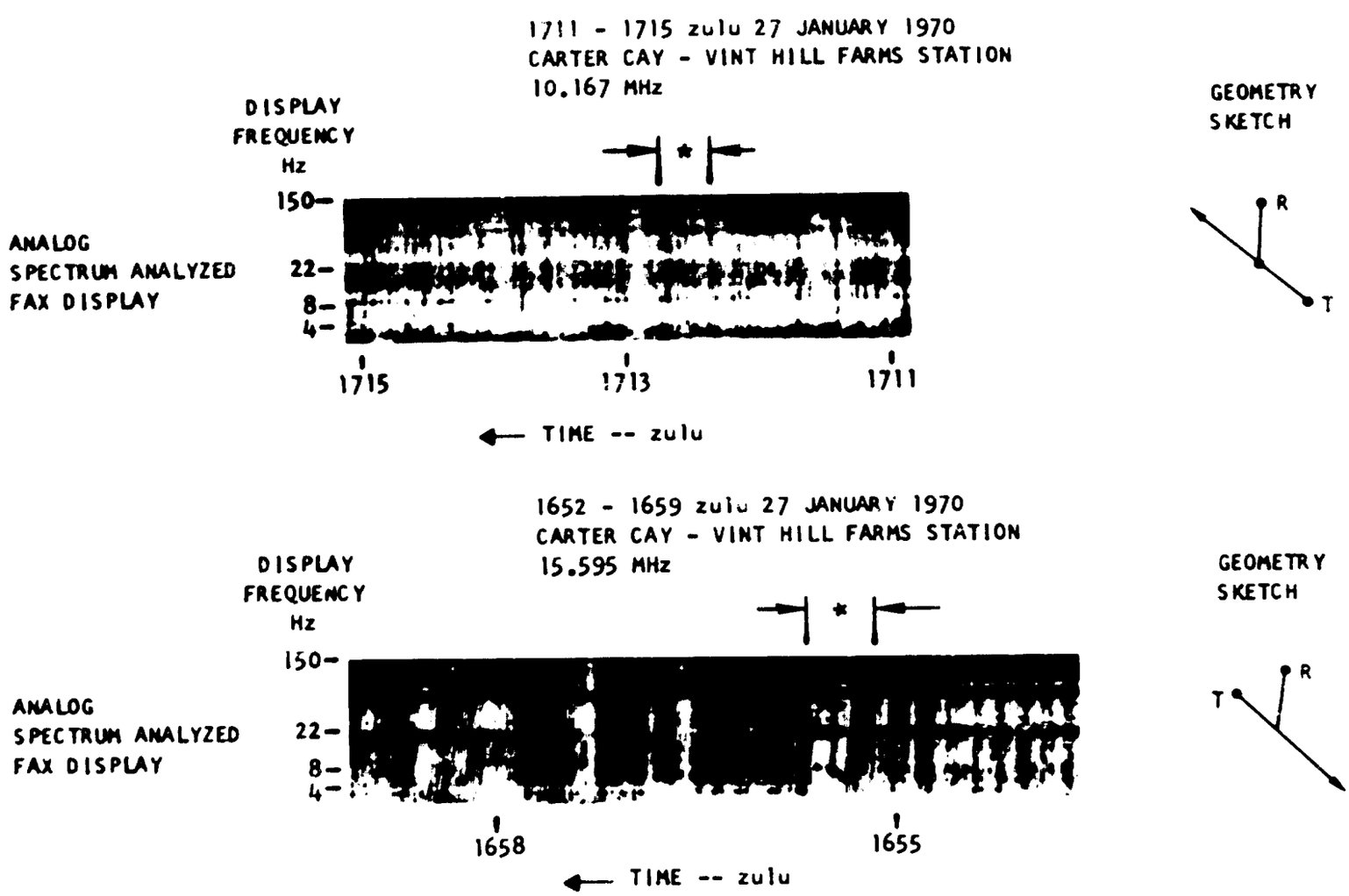

(S) Figure 8. Aircraft Detections (U)

(S)

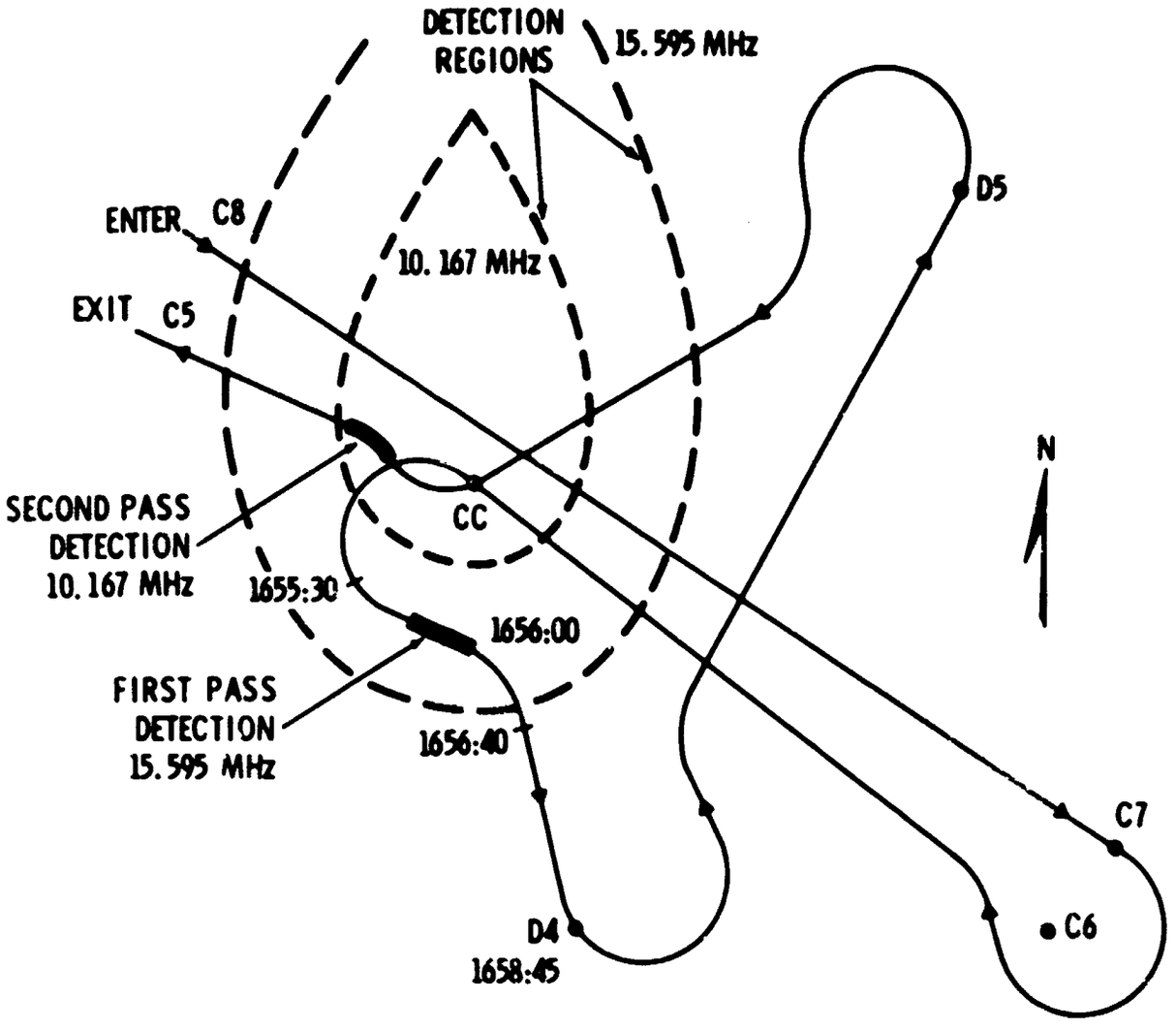

FREQ •	10.167 MHz	15.595 MHz
σ •	100 m^2	100 M^2
NOISE •	-137 dbw	-145 dbw
GAIN •	17 db	25 db
POWER •	2 kw	2 kw

(S) Figure 9. Predicted and Observed Detection Regions (S)

BUOY CONSIDERATIONS (U)

Daniel M. Brown

Scripps Institution of Oceanography
La Jolla, California

I INTRODUCTION (U)

(U) The buoy must be designed as part of a system. Considerations of this system are –

How much antenna motion can be tolerated?

How much power will be needed to run it?

What is the expected service life?

What security problems must be considered?

What provisions should be provided for servicing at sea?

What unusual sea conditions exist that might dictate a buoy different from a "standard" buoy? – And with what impact on cost?

II MOTION (U)

(U) Antenna people must consider the real needs for antenna motion, as this has the greatest affect on choice of buoy concepts. Small surface-following floats, such as the Bumblebee, can respond to as little as a 2-second period roll. The mast and buoy can overcome this period by its mass so that hulls will not respond to high frequency waves. When waves are taller, the hull merely follows the sea surface slope at whatever natural frequencies exist. Larger surface-following floats have greater payload and can overcome most choppy sea-state conditions.

(U) Non-surface-following floats such as a spar buoy will hold most motion to a minimum up to the point of resonance where it begins to oscillate up and down.

(U) A spar buoy must be quite large (80 feet or more) to keep the mast out of the water in most sea

(U)
states. Size is not bad if it is consistent with all other requirements.

III POWER (U)

(U) Motion generators develop power in proportion to their size, but the motion may not always be available, or an unusual lack of motion (wind or wave) may exceed expectations and exhaust the battery reserve. Stored energy has weight and dictates a buoy displacement proportional to the service life. Diesel or propane 4-cycle generators radiate considerable noise through the water which can be used to locate the buoy. Nuclear power presents a political problem if a buoy breaks loose and comes ashore. If they are not too far offshore shore-based power could be run out to a line of buoys through undersea cables, and up to the buoy.

IV SERVICE LIFE (U)

(U) The buoy should be designed for servicing on-station at sea, or for replacement in the event of failure of some sort, or for routine maintainance. In addition to servicing, buoy design needs to reflect shipboard handling and deployment considerations.

(U) Any of the proven materials used for a ship or boat can also be used for a buoy to compliment the antenna needs, e.g., steel, plywood, fiberglass, ferrocement.

(U) Mooring lines of nylon rope, jacketed with polyethylene in areas of fishbite or wear, can be used for long periods of time – 18 months to 2 years.

V SECURITY (U)

(U) People will visit a buoy if they find it. Should it have an "open hatch alarm" that radios to a shore base? Should it be self scuttling in event of theft, or breaking loose, or by radio command? If it does not have all the navigational lights, horns, bells etc., what about maritime liability in the event of a collision? Should the buoy be designed for no service access after a hatch is welded shut? Also, it must have a "silent" power source so that it can't be located by hydrophones.

VI SERVICE AT SEA (U)

(U) Consideration of method of service is vital in design. If it is to be boarded at sea it must be provided with the necessary hatches and handrails to board in moderate sea. If it is designed for

(U)
replacement, then quick-disconnect systems or exchangeable mooring attachments must be provided as well as shipboard lifting or retrieval gear.

VII IMPACT OF UNUSUAL SEA CONDITIONS ON COST (U)

(U) A "standard" design can be used in most ocean areas, but in some areas such as the Gulf Stream, or areas of excessive icing, special designs may be necessary to survive these conditions, which would increase costs to more than that of a "standard" buoy.

PRECEDING PAGE BLANK - NOT FILMED

MAY BELL PLATFORM PROBLEMS (U)

Dr. Frank Bader

The Johns Hopkins University
Applied Physics Laboratory
8621 Georgia Avenue
Silver Spring, Maryland 20910

I SUMMARY (U)

(S) SCRIPPS Oceanographic Institution "Bumblebee" type oceanographic buoys were used as ocean platforms for radio transmitters during BTEW studies. Although used for a purpose and at locations other than those for which designed, the buoys functioned in a satisfactory though perhaps non-optimum manner. This discussion presents our interpretation of the BTEW buoy requirements together with a discussion of problems encountered in use of buoy-mounted radio equipment.

II REQUIREMENTS (U)

(U) In summary the buoy requirements are ruggedness to withstand storms, stability as an antenna platform and load carrying capability to accommodate the radio transmitters, power supplies and other payload. Cost should be moderate with a relatively long life (years) in use. The buoy should provide suitably protected spaces for electronics and a mounting base for a monopole antenna of 20 to 30 feet in height. The "payload" includes 14 lead-acid storage batteries weighing about 1000 pounds and about 50 pounds each of electronics and telemetering sensors, with a large part of the latter weights being related to watertight containers.

III OPERATIONS (U)

(U) Of the four SCRIPPS "Bumblebee" buoys furnished to the Applied Physics Laboratory by ARPA, three of these were equipped with transmitters and the fourth was turned over to ITT-Electro Physics Laboratory for emplacement of a broadband antenna and passive modulator. Two buoys, one equipped by APL and the other equipped by ITT, were emplaced first on the Chesapeake Bay and subsequently off Cape Kennedy, Florida for over-the-horizon tests.

(U) The Chesapeake Bay tests were a "shakedown" of electronic equipment and not a test of buoy seaworthiness. The Cape Kennedy moorings are shown in Figure 1 with the APL buoy at a 120 kilometer (65 mile) range within the outer fringe of the Gulf Stream and the ITT-equipped unit at 50 kilometers (27 ½ nmi) in the inner margin of the Gulf Stream. Water depths were around 2400 feet and 250 feet respectively. The Gulf Stream speed was around 2 knots at these locations imposing 100 to 200 pounds drag on the moorings. The mooring problems are very similar to Naval paravane towline problems which have been studied extensively by the Naval Ship Systems Command, David Taylor Model Basin and, for example, discussed in their report number 533 of October 1944 by Messrs. L. Landweber and M. H. Protter. In summary, the horizontal stream forces upon the buoys due to currents and wind drag may produce horizontal pulls upon the mooring of 100 to 200 pounds, these coupled with stream forces on mooring lines produce mooring line tensions of between 700 and 2000 pounds force depending on mooring line length (often called scope); with lesser values of line tension occurring for longer lengths of mooring line. At the bottom of the mooring line, one must provide a sufficient "dead weight" to overcome the vertical component of the mooring line tension plus a suitable anchor to imbed into the ocean bottom to resist horizontal stream forces upon the buoy.

(U) Figure 2 shows the arrangement used to moor the APL equipped Bumblebee buoy. This was used satisfactorily three times. The first mooring was for only a week in December 1969 with the buoy being taken up intentionally because tests were to be recessed for Christmas. The succeeding mooring made on January 20, 1970 held for a month until the buoy had to be taken up for repairs to the antenna and electronics. A swedged cable joint, shown in Figure 3, was found to be on the verge of failure due to the use of an aluminum-magnesium sleeve used through error in place of Nicopress sleeves recommended by SCRIPPS (and used on every other joint). The buoy was refitted and remoored 17 March and held its moorings through mid April without failure until test termination. Mooring components were recovered and found to be intact and undamaged except for the scraping during take-up.

(U) During emplacements, several storms were observed at Cape Kennedy with waves up to 12 feet high, the buoys survived although the antenna upon the APL-equipped buoy was damaged, apparently through excessive roll which caused the tips of the antenna "top hat" to roll into the water and be broken off by wave force. Buoy environmental data telemetry indicated that even for relatively calm seas the buoy would generally be rolling plus or minus 10 degrees. The buoy arrangement is shown in Figure 4.

IV CONCLUSION (U)

(S) The Bumblebee buoys were satisfactory for the purposes of the BTEW surface wave radio propagation measurements. More stable platforms would be desirable for a tactical buoy-mounted over-the-horizon radar transmitter. Ideally, the buoy hull should maintain an attitude tangent to the local water

(U)

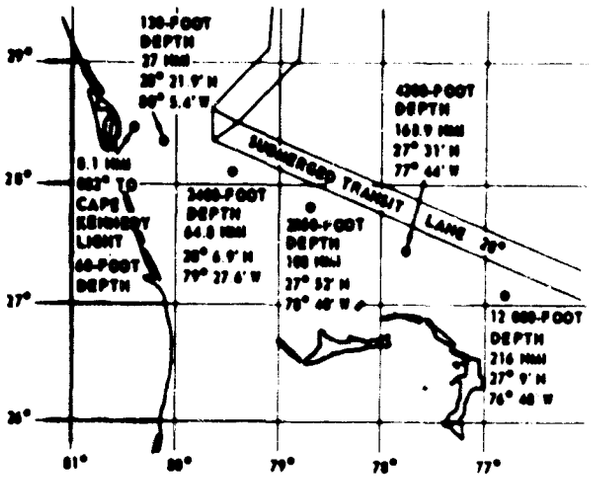

(U) Figure 1. MAY BELL Buoy Locations, Revised 1 December 1969 (U)

(U)

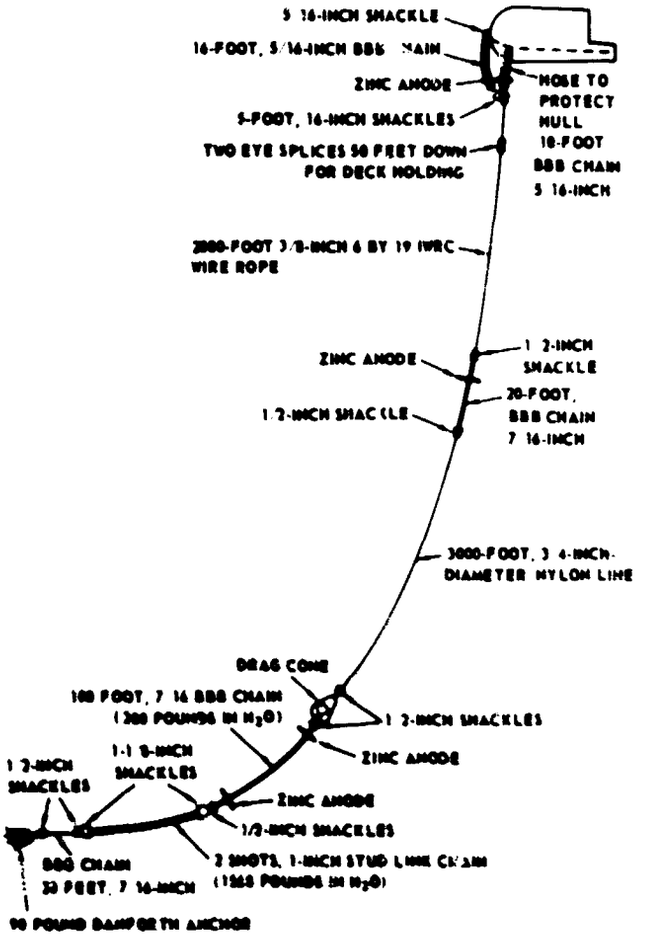

(U) Figure 2. Anchoring System for MAY BELL Buoy Located 70° 39' West by 28° 12' North at a Depth of ~ 2400 ft (U)

(U)

(U) Figure 3. Corrosion Failure of Swedge Joint (U)

(U)

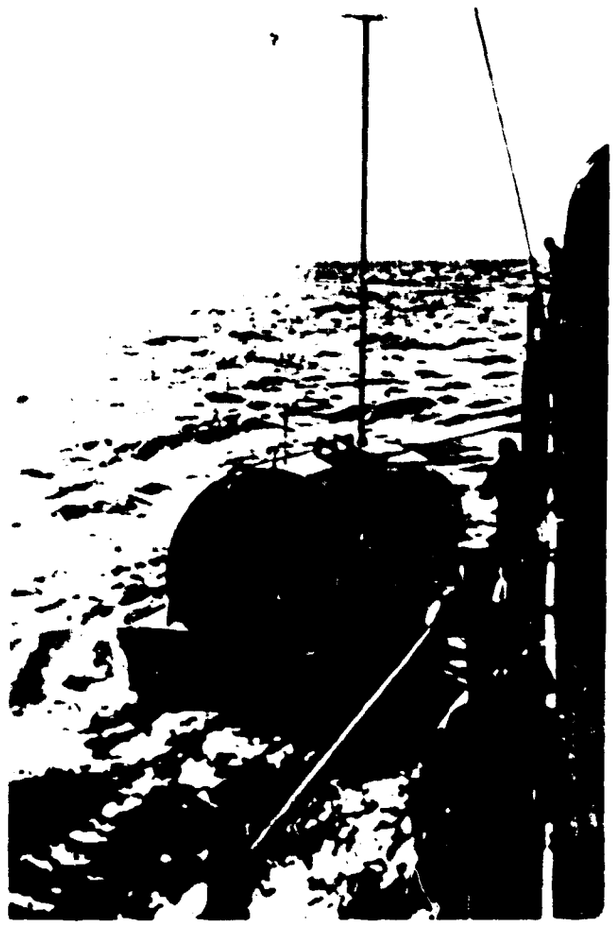

(U) Figure 4. MAY BELL Buoy Arrangement (U)

(S)

surface at a constant height so that the transmitter antenna properties were not altered through change in elevation or tilt with respect to the local water surface. The ONR-Convair "Monster" buoy is apparently of this configuration but buoy cost and size are several orders of magnitude larger than that for the Bumblebee buoys. If large (1 kW or larger) transmitters are to be employed, such large buoys may be needed to carry electrical power supplies and fuel for continuous operation over a period of months.

PRECEDING PAGE BLANK - NOT FILMED

BTEW SYSTEMS ANALYSIS: CLUTTER (U)

Donald E. Barrick

Battelle Memorial Institute
505 King Avenue
Columbus, Ohio 43201

I INTRODUCTION (U)

(S) Last spring a brief study was undertaken to calculate expected target-to-clutter ratios for a CW BTEW configuration. An aircraft was selected to fly near the deck on an approaching course. The object was to find how much lower the total received target signal would be from the total received clutter signal, and also from the direct signal transmitted by the buoy. While spectral processing can certainly be used to detect target signals 40-50 dB below the clutter and carrier due to the different dopplers involved, ultimate limits on such clutter suppression technique are set by the dynamic range of the system. Thus the purpose of the present study is to indicate the required dynamic range; as well as the clutter improvement ratio needed for CW detection and tracking of aircraft targets in a high-clutter environment.

II APPROACH (U)

(U) The example to be considered is not meant to prove a point; it may not even be representative of the final geometry selected for a BTEW system. It is merely chosen to obtain a feel for the order of magnitude and dependence of the target-to-clutter and target-to-direct signal ratios on the range and path.

(S) For the hypothetical system examined, an omnidirectional buoy transmitter is located 300 km from the shore-based receiving antenna. The latter is assumed to be a steerable array of half-wave dipoles 750 feet long with a beamwidth of about 10°. A gaussian pattern is employed for convenience. The frequency assumed for the example is 7MHz. The gain of the transmitting antenna is 1.64; the gain of the receiving antenna is $36 \exp \left\{-.693 \left[(\theta - \theta_0)/5^\circ \right]^2 \right\}$. θ_0 is the direction in which the receiver beam is pointing with respect to the transmitter-receiver baseline. A simple CW signal is employed so that no direct range resolution is possible.

(U) In calculating the received signals, the basic transmission loss is used to describe propagation. This quantity was discussed in a paper titled "Theory of Attenuation and Clutter (U)" presented by this author at another session of this workshop. Curves of loss across the sea were presented in that report. For this problem, Sea State 2 is assumed in entering the loss curves.

(S) As applied to the aircraft, the radar range equation can be rewritten in terms of L_T and L_R, the basic transmission losses from transmitter-to-target and target-to-receiver, as follows:

$$L_o = -10 \text{ Log}_{10} \frac{P_R}{P_T} = L_T + L_R - G_T - G_R - 10 \text{ Log}_{10} \left(\frac{4\pi\sigma}{\lambda^2} \right),$$

where

P_R = Received power
P_T = Transmitted power
L_o = Overall transmission loss
G_T and G_R = The free-space antenna gains
σ = The radar cross section of the aircraft. The latter is taken to be 40 m^2 throughout the problem.

(S) The above equation is expressed in decibels. Figure 1 shows a possible radar-target geometry in which the aircraft is approaching on a course 20 ° from the baseline. Its range from the receiver is 370 km. The receiving antenna beam is pointed directly at the aircraft. For this single configuration, the overall loss, L_o, is 201 dB; actually, L_o is computed versus range for the aircraft approaching on two courses, 20° from the baseline and on the baseline. The receiving antenna is pointed at the target in both cases.

(C) To compute the received clutter signal, the same procedure is applied to a target which in this case is a patch of sea of area $R_R \Delta R_R \Delta\theta$, as shown in Figure 2. Here, the sea has an average bistatic scattering cross section per unit area, σ^o,, of -30 dB; this number is somewhat lower than its fully developed value of -23 dB, so as not to be overly pessimistic. A numerical integration must be performed, summing the powers received from all patches. Figure 2 shows how the overall transmission loss is computed for a particular patch, the i, j-th patch. The receiver beam is pointed 20° off the baseline. Figure 3 shows the weights of all such patches in their contributions to the total received clutter. The total loss for all of the clutter, computed by summing the absolute power received from each patch, is 143.5 dB. This clutter calculation is also performed for the receiver beam pointed along the baseline as well, in which case the overall clutter loss is 125.8 dB.

(C) Finally, the power in the direct signal from the transmitter to the receiver is computed. The latter is done for beam positions 20° and 0° from the baseline. The loss corresponding to these two cases is 142.4 dB and 94 dB.

(S) These numbers are then used to compute the target signal-to-clutter ratio for the aircraft approaching on the two paths as a function of range. The results are shown in Figures 4 and 5. In Figure 5, the notch at 300 km occurs when the aircraft passes directly over the buoy, in which case the target signal becomes very large. Hence the signal-to-clutter ratio drops at this point.

(C) Figures 6 and 7 show the target-signal to direct-signal ratios for the same two approach courses.

III CONCLUSIONS (U)

(S) Several conclusions can be drawn from these curves. For one thing, the target must be close to the buoy fence before the two ratios drop below about -60 dB. This latter number might be taken as a state-of-the-art dynamic range for a radar receiver and processor, although by no means the ultimate possible.

(S) Another conclusion is that the worst approach path is the one along the baseline. There, the strong direct signal would tend to swamp the weak aircraft signal, except possibly when the aircraft passes over the transmitter. Over most of the path, the target echo will be 80 dB or more below the direct signal. Of course, the better ratio for the 20° path is only possible here because the beam of the receiving antenna is pointed away from the buoy, and hence the direct signal is weaker. A non-directional receiving antenna would result in a bad ratio for both aircraft courses.

(S) The above ratios become better for the buoy fence closer to the shore and also for the aircraft target at a higher altitude. Studies similar to that done here are to be undertaken for fences at different locations and also for more realistic antenna patterns and target cross sections. Phase-coded signals, which permit exclusion of signals from all except the desired range cell, will certainly offer improvement over a CW system, and are to be included in further studies.

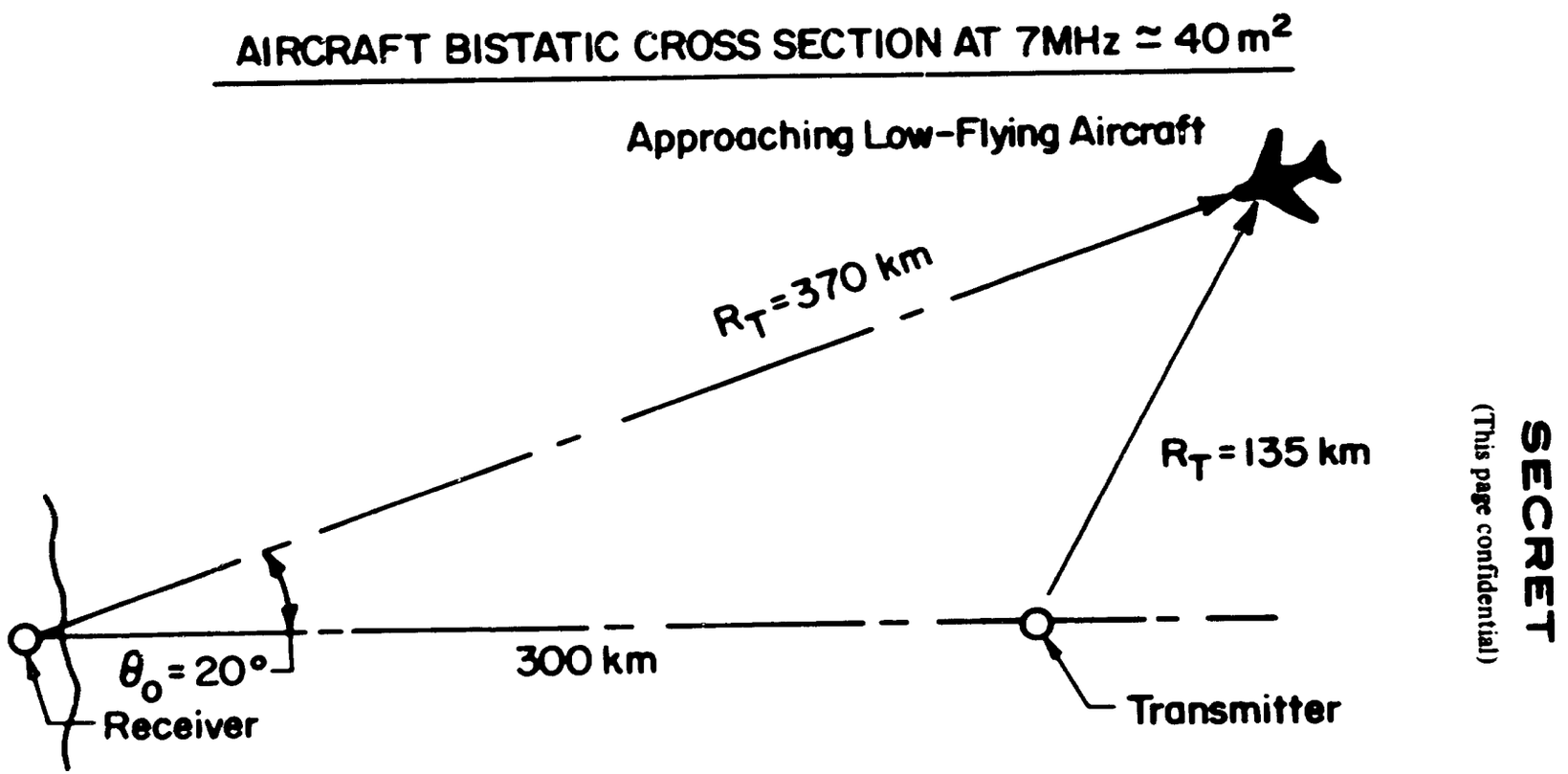

(C) Figure 1. Sample Calculation of Overall Transmission Loss for Signal Reflected from Aircraft Target at 370 km Range. (U)

UNCLASSIFIED

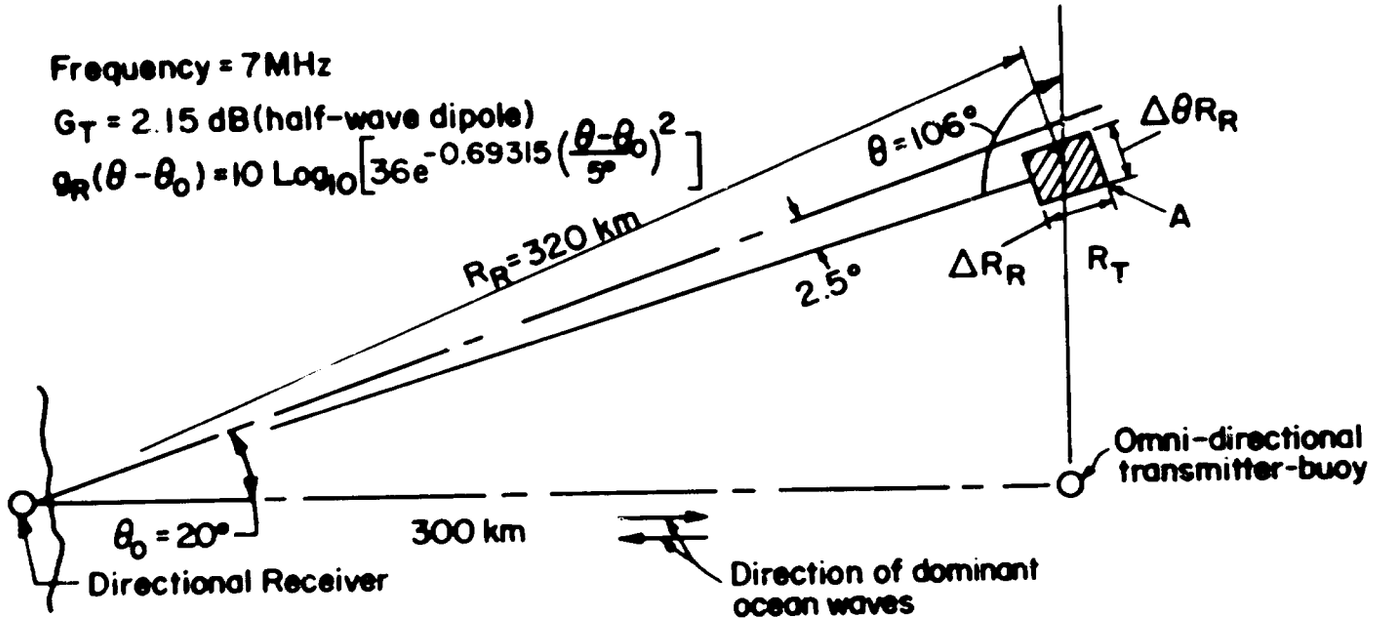

$\sigma_c^0 = -30.4$ dB (Sea State 2)

$A = R_R \Delta R_R \Delta\theta \simeq 280\ km^2$ (ΔR = 20 km, $\Delta\theta$ = 2.5°)

$g_R(\theta-\theta_0)$ = gain function for directional receiving antenna, an array of half-wave dipoles of length 750 feet, it has a 10° beamwidth. A gaussium pattern is used for convenience.

For Sea State 2 (10 knot wind)

L_{oij} = 157.7 dB for patch shown (i, j th patch)

(U) Figure 2. Example of Calculation of Received Clutter Power (Expressed as Overall Transmission Loss) from One Patch of Sea. Receiver Beam is Pointed 20° from the Baseline. (U)

UNCLASSIFIED

(U)

UNCLASSIFIED

UNCLASSIFIED

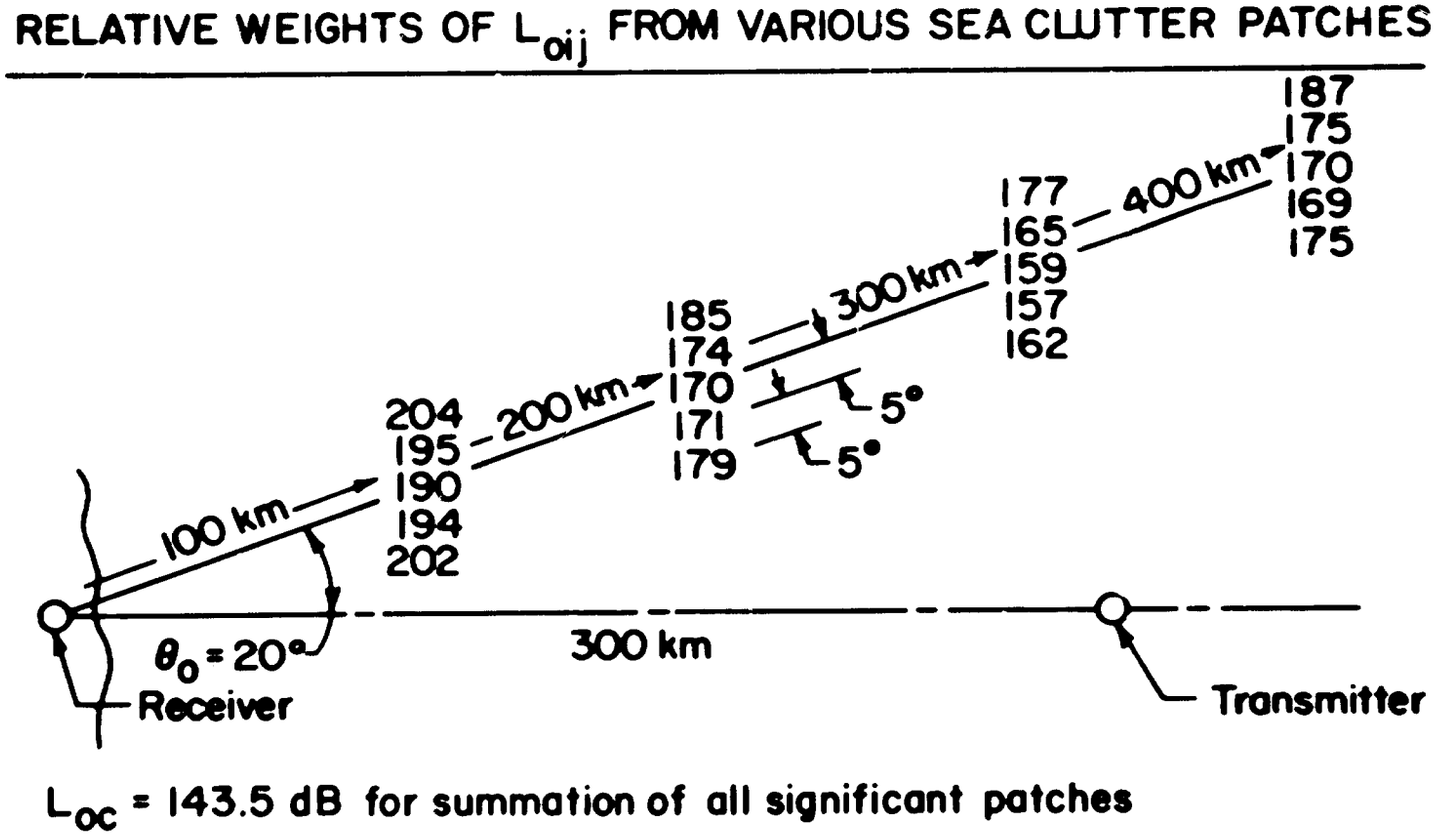

(U) Figure 3. Relative Weights of Overall Losses for Various Patches of Clutter. A High Number (in dB) Indicates Weaker Received Signal. (U)

(C)

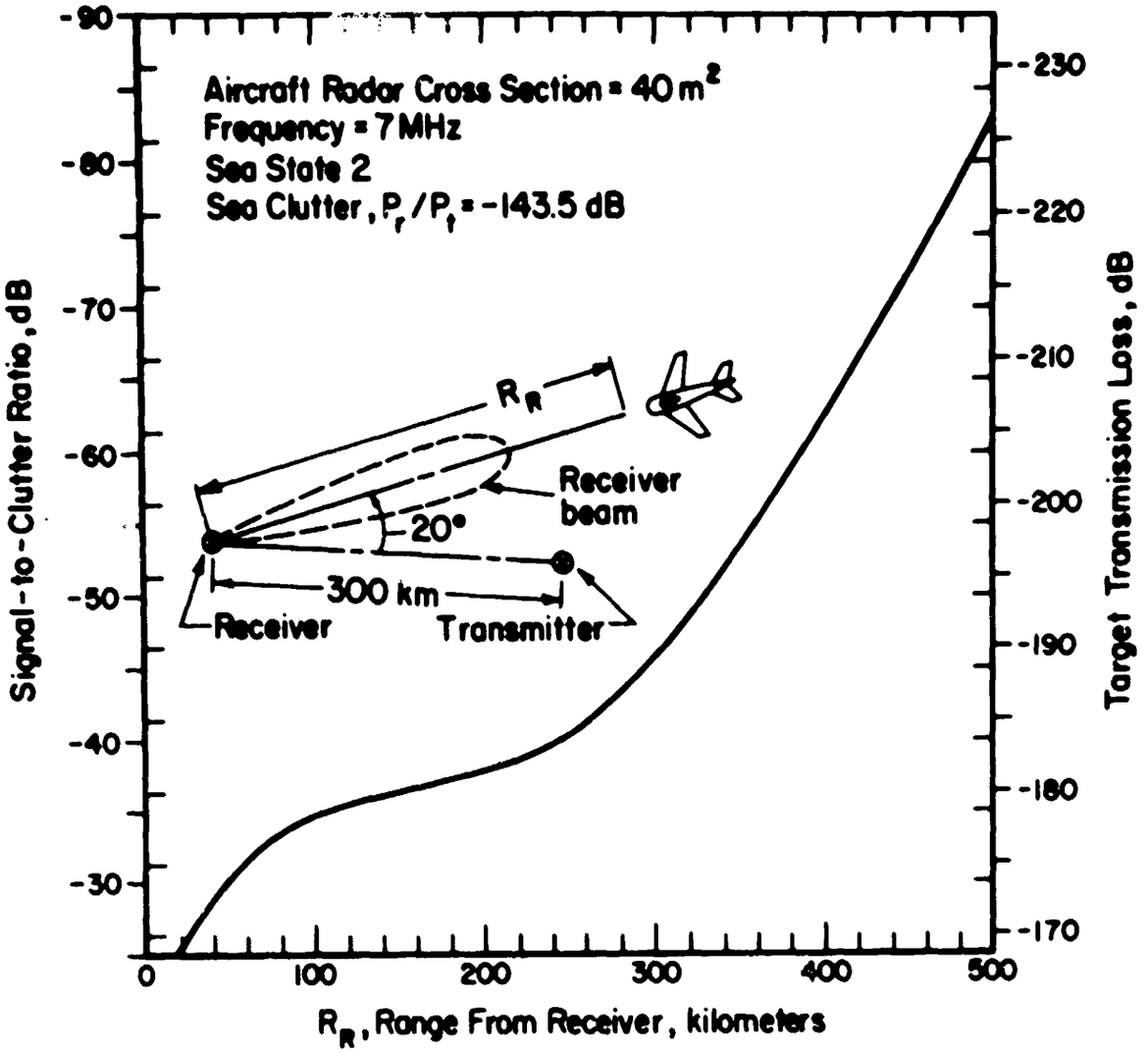

(C) Figure 4. Target Signal-to-Clutter Ratio vs Range for Aircraft and Antenna Beam on 20° Line from Baseline. (U)

(C)

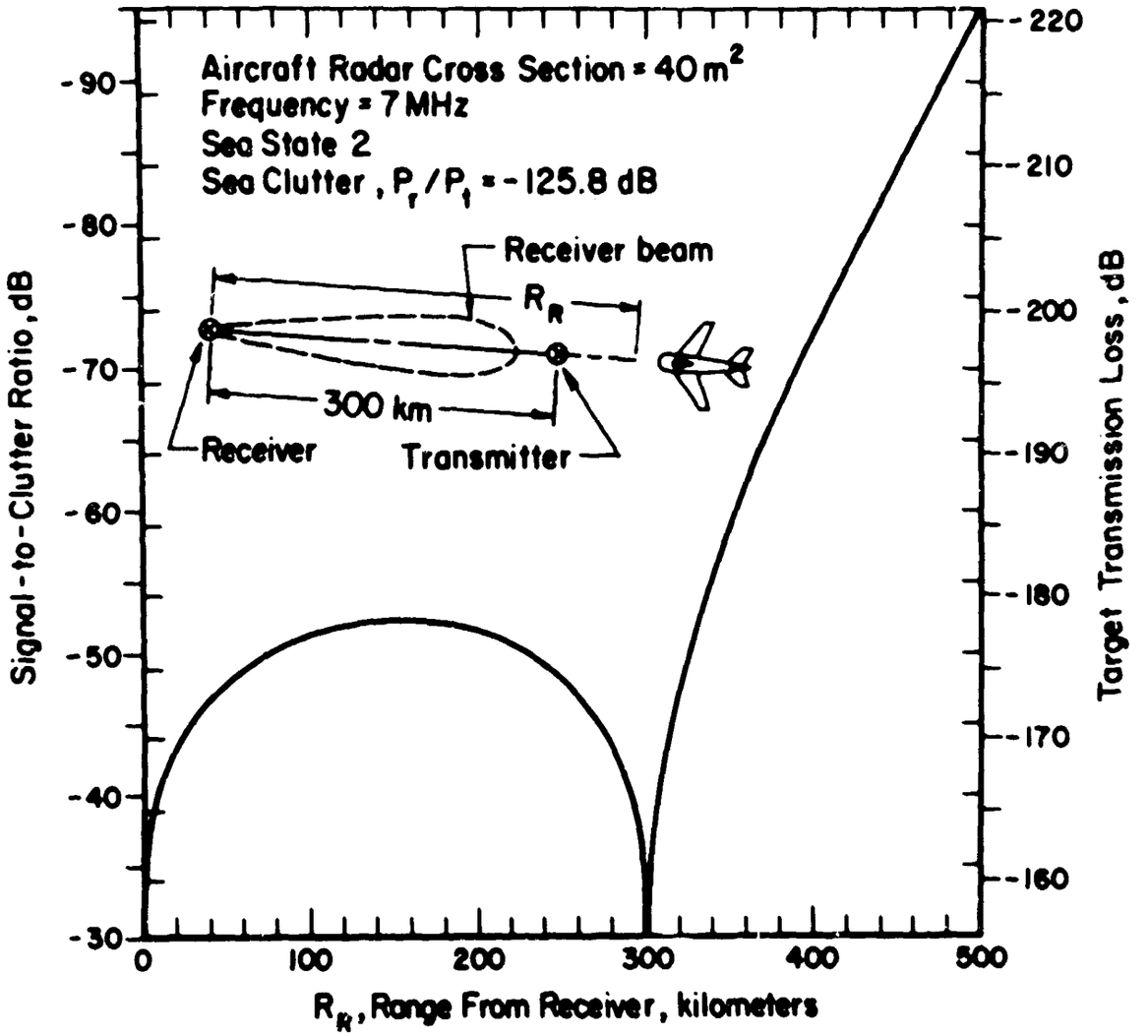

(C) Figure 5. Target Signal-to-Clutter Ratio vs Range for Aircraft and Antenna Beam along the Baseline. (U)

(C)

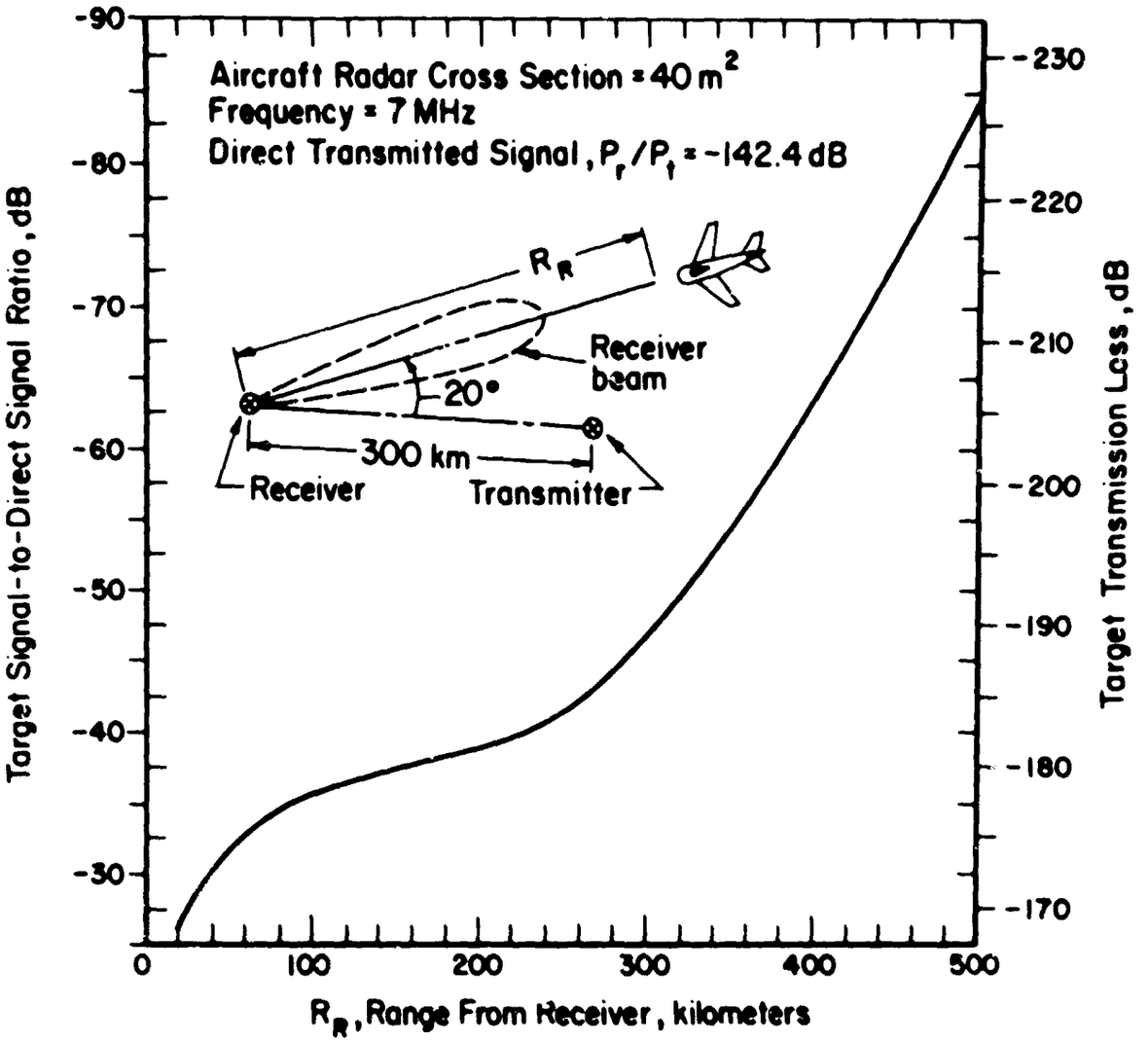

(C) Figure 6. Target Signal-to-Direct Signal Ratio vs Range for Aircraft and Antenna Beam on 20° Line fromBaseline. (U)

(C)

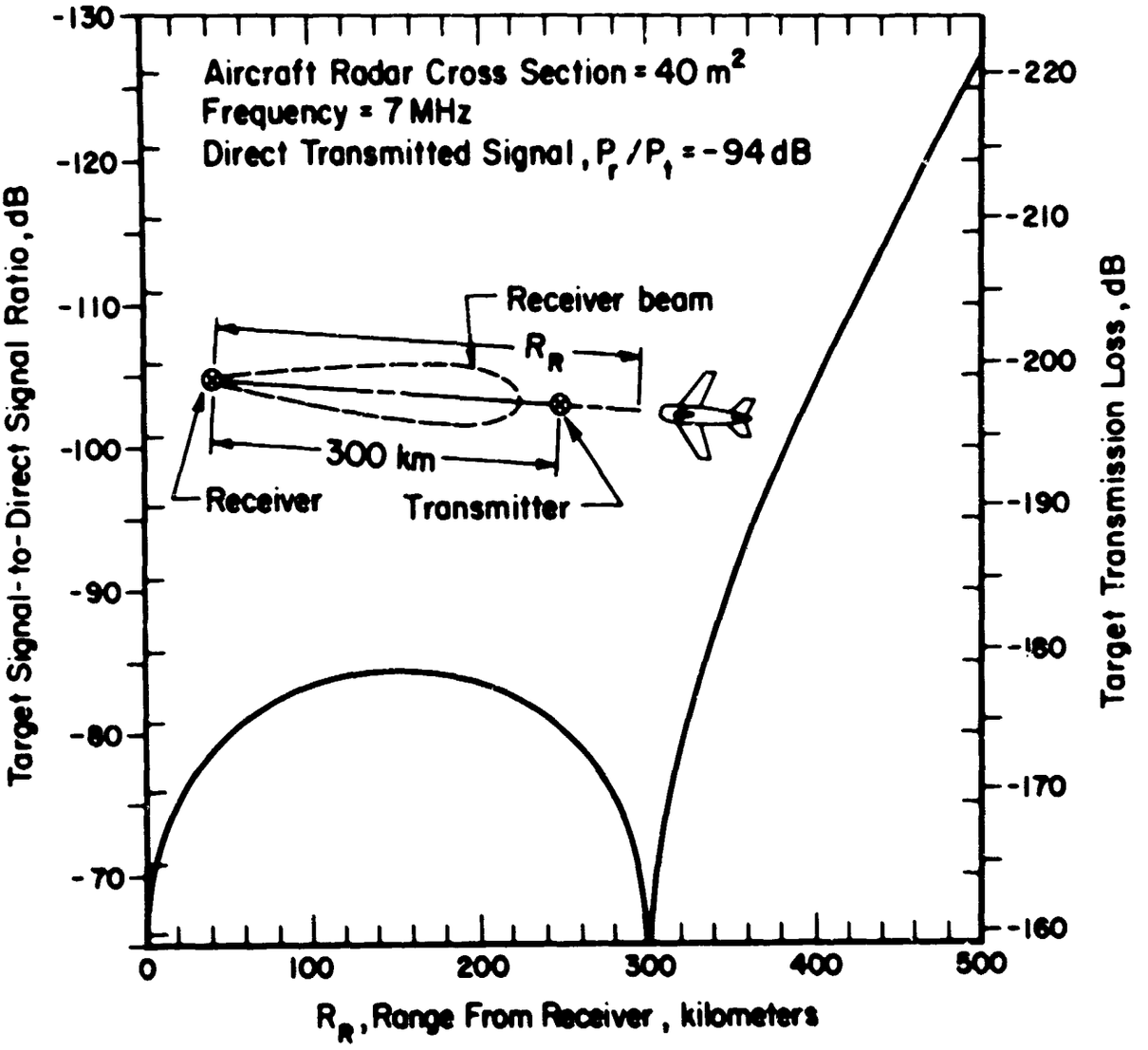

(C) Figure 7. Target Signal-to-Direct Signal Ratio vs Range for Aircraft and Antenna Beam Along the Baseline. (U)

THE BUOY TACTICAL EARLY WARNING SYSTEM CONCEPT, BTEW-I (S)

L. Edwards

Raytheon Company
Equipment Division
OHD Advanced Development Department
Spencer Laboratory
Burlington, Massachusetts

(S) The BTEW concept originally evolved from the thought that OTH surveillance might be achieved, even during times of nuclear blackout, by using a system based upon ground wave propagation. Such a system would, in fact, enjoy increased range and sensitivity at time of nuclear blackout because lesser amounts of noise would reach the receiver via ionospheric paths.

(S) Monostatic Ground Wave Radar systems had been considered in the past; however, it was well known that such systems achieve long range coverage only at the cost of very high power. To overcome this disadvantage it was suggested that a buoy terminal in a bistatic mode might permit long range detection while power and system gain factors were kept to levels more attractive from a cost viewpoint.

(C) Lacking a specifically defined performance requirement it was decided to take the approach of attempting to define the capabilities, or potential capabilities, of the concept as a function of system gain.

(S) In general it is desired to determine the practical usefulness of the concept as applied to the entire coastal defense problem, as well as to the defense of specific strategic areas such as the Florida straits or the Northeast industrial complex.

(S) The propagation and feasibility tests that were conducted off the Florida coast demonstrated that standard radar calculation techniques, coupled with Barrick's loss model, could be used to describe coverage areas. Actually to calculate coverage areas, it is necessary to define the deployment concept being examined, the various system parameters and the threat or expected target. Four different deployment concepts were examined:

- The monostatic radar case
- A shore transmitter and buoy receiver
- A buoy transmitter and shore receiver
- Buoy-to-buoy pairs

(S)
The expected threat encompasses targets from the SLCM size to larger bombers and SLBM's. At a typical ground wave operating frequency of 10 MHz the cross sections of these targets range from about 1 m^2 for the SLCM, about 100 m^2 for the attack bombers, and about 10^4 m^2 for an SLBM when it reaches the lower ionosphere. The system parameters chosen for each of the deployment concepts examined are shown in Figure 1.

(S) The coverage by the monostatic system is shown in Figure 2. The map area shown covers the eastern seaboard from Boston and the Massachusetts Cape area down to the Washington-Baltimore-Chesapeake Bay area. The system is shown located on the lower end of Long Island. The inner concentric circles represent the range out to 125 km where detection could be achieved by simply pulse modulating the 200 kW transmitter with a 100-μs pulse. The outer sector represents the area that could be covered out to 250 km using a 1-ms (long) pulse with a 10:1 pulse compression code that allowed range resolution of about 15 km. With 8-degree azimuthal resolution provided by the antennas this would allow target location to within about a 15 km square at a range of about 200 km.

(S) The additional coverage that would be afforded by adding a buoy receiver to the complex is illustrated in Figure 3. This variation provides coverage out to 300-350 km from the shore station.

(S) The coverage provided by the Bistatic II Buoy Transmitter - Shore Receiver system is described in Figure 1 and shown in Figure 4. Three shore receiver stations and seven buoys provide a radar fence at 200-225 km range from the Massachusetts Cape area down the coast to the Washington Area.
(S) The Bistatic III buoy-pair concept provides limited aircraft coverage. The buoys can be spaced at about 100-km intervals; but by using either ground wave or satellite telemetry modes back to shore, they could provide warning at greater off-shore distances plus offering much greater surveillance of SLBM's. A possible East coast buoy fence system is illustrated in Figure 5.
(S) Figure 6 has been prepared to illustrate the magnitude of a system designed to provide surveillance for the entire Eastern coast of the United States. Ten shore stations operating both monostatically and bistatically with about 30 off-shore buoy receivers would provide continuous coverage from Nova Scotia down around the tip of Florida out to a range of about 350 km.

(S) The basic feasibility of the BTEW-1 concept has been successfully demonstrated. A system of modest size, and therefore presumably modest cost, can provide off-shore detection coverage out to ranges of 300 to 400 kms. SLBM coverage can be obtained to significantly greater ranges.

(S)

MONOSTATIC SYSTEM PARAMETERS	BISTATIC I BUOY RECEIVER – SHORE TRANSMITTER
G_T = 22 dB G_R = 22 dB F = 10 MHz σ = 100 m^2 P_T = 100 kW (200 kW PEP) 3 dB efficiency loss Noise = -154 dBW/1-Hz band P_R = Noise + 9 dB = -145 dBW SEA STATE 3	G_T = 22.5 dB G_R = 1 dB (2 dB - 1 dB) F = 10 MHz σ = 100 m^2 P_T = 100 kW 3 db efficiency loss Noise = -154 dBW/1-Hz band P_R = Noise + 9 dB = -145 dBW SEA STATE 3
BISTATIC II BUOY TRANSMITTER – SHORE RECEIVER	BISTATIC III BUOY TRANSMITTER – BUOY RECEIVER
G_T = 1 dB G_R = 22 dB F = 10 MHz σ = 100 m^2 P_T = 1 kW 3 dB efficiency loss Noise = -154 dB/1-Hz band P_R = Noise + 9 dB SEA STATE 3	G_T = 1 dB G_R = 1 dB F = 10 MHz σ = 100 m^2 P_T = 1 kW Noise = -154 dBW/Hz band P_R = Noise + 14 dB SEA STATE 3

(S) Figure 1. System Parameter Tabulation (U)

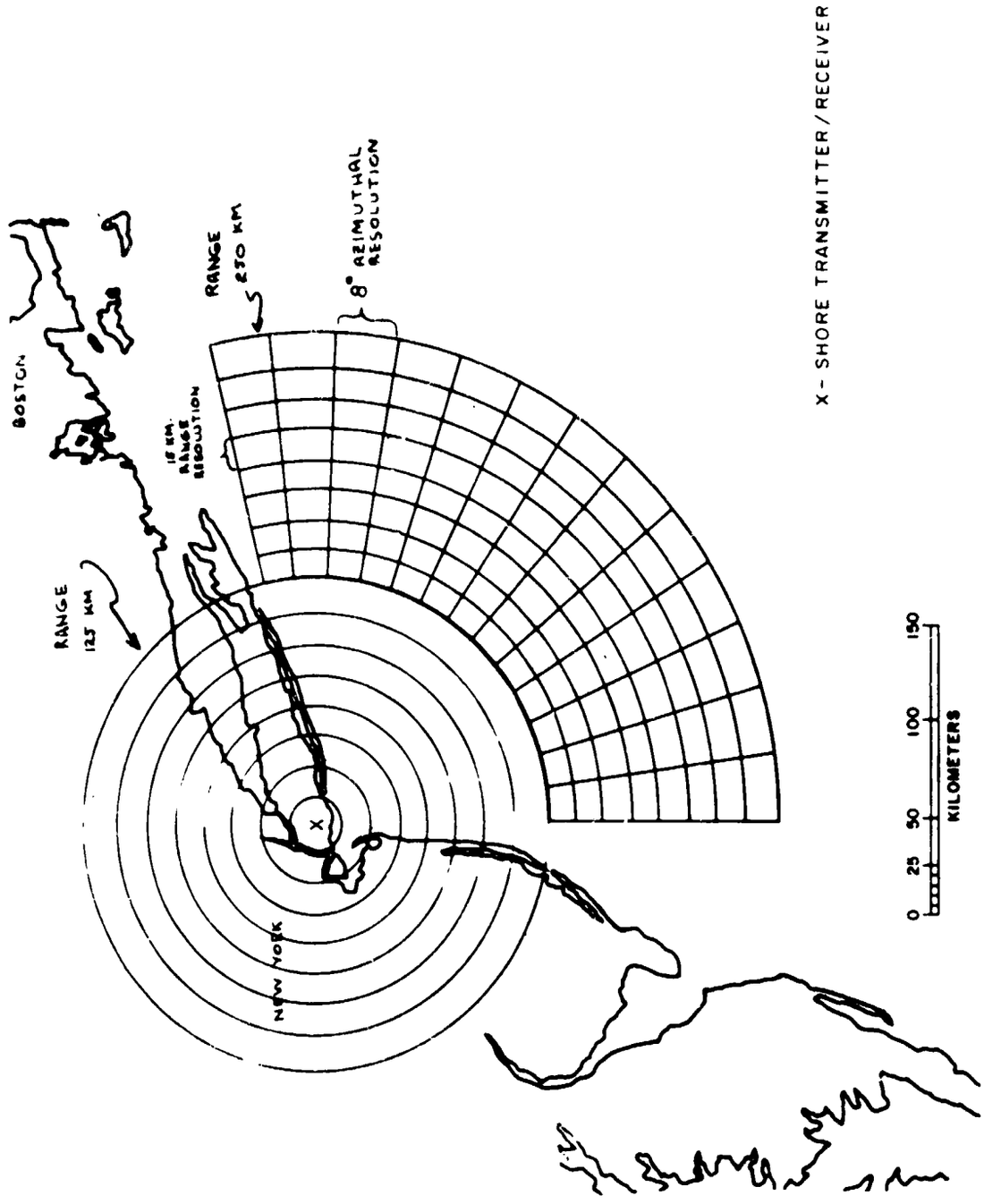

(S) Figure 2. Monostatic System Coverage (U)

(S)

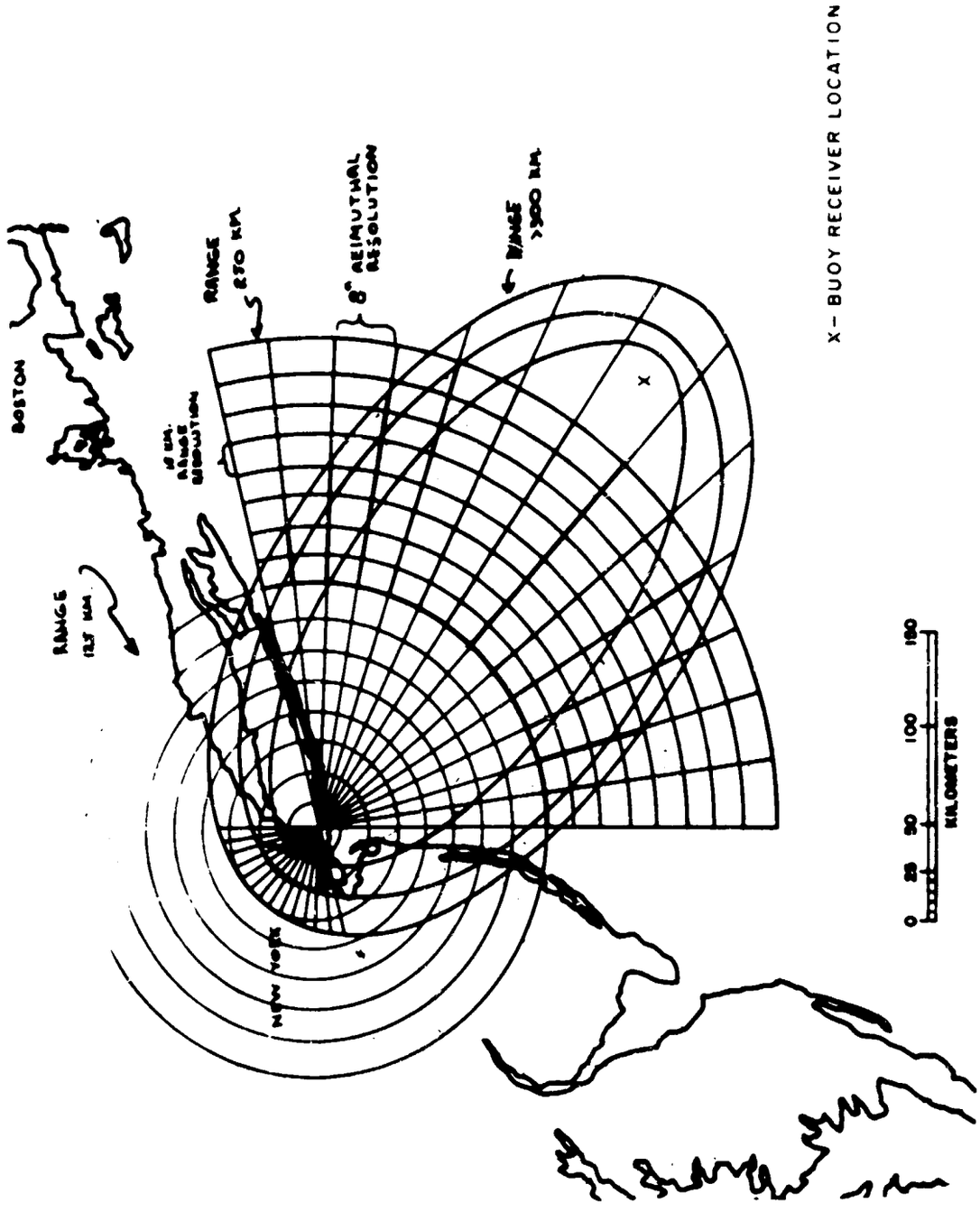

(S) Figure 3. Extending Coverage by Adding a Buoy Receiver (C)

(S)

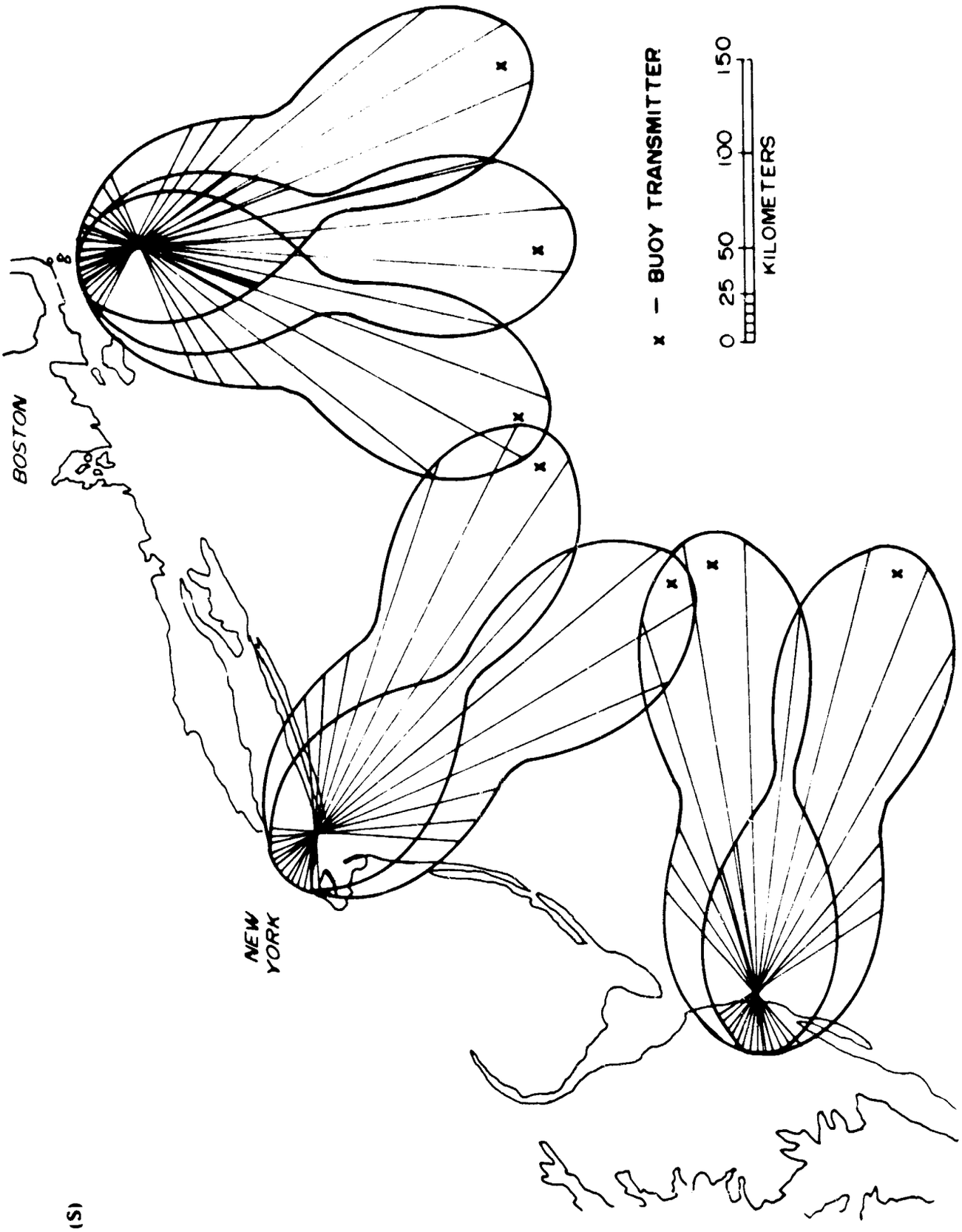

(S) Figure 4. Coverage Using 3 Receiver Stations and 7 Buoy Transmitters (S)

(S)

(S)

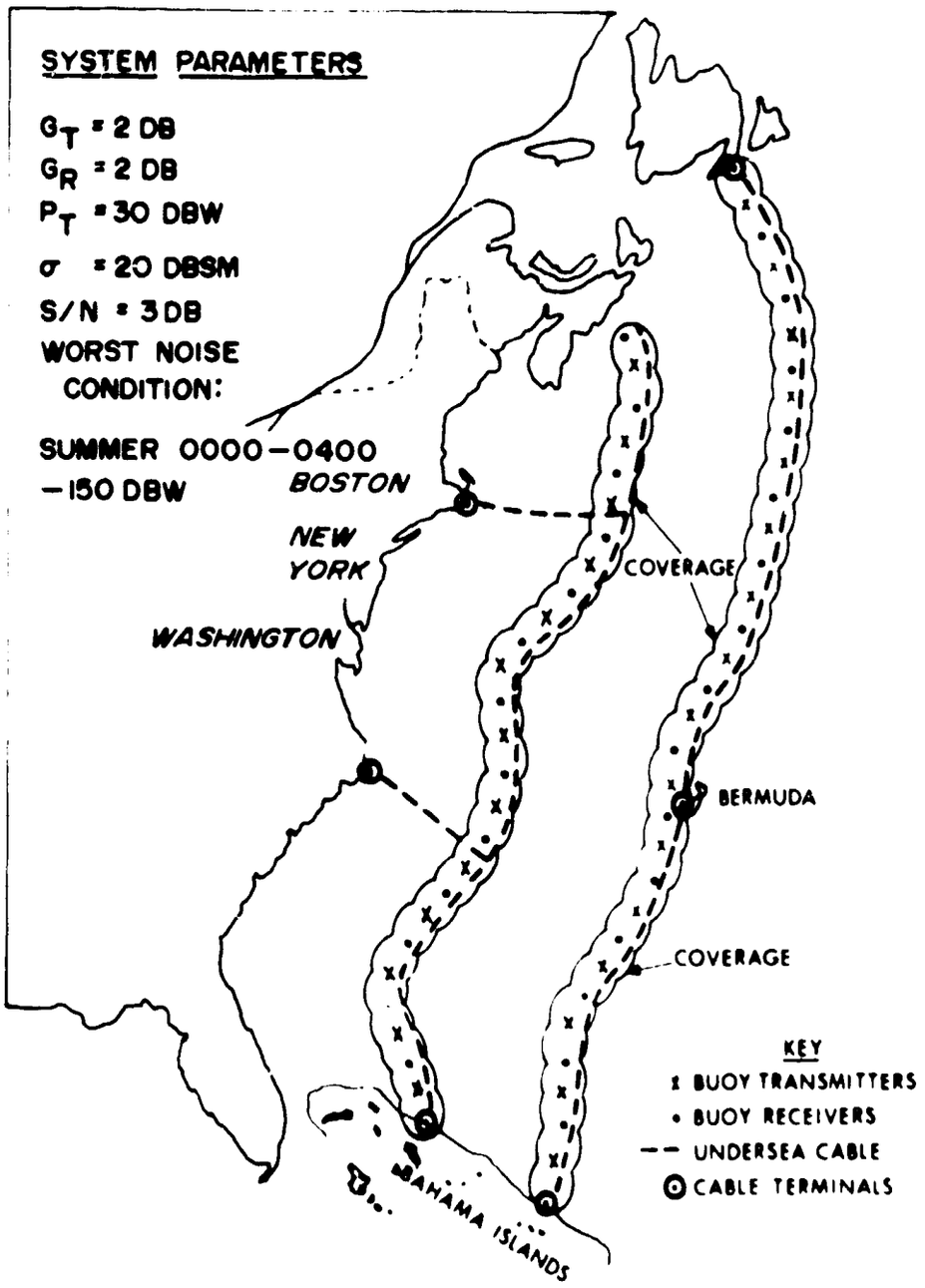

(S) Figure 5. Coverage Map of Fence Radar Using Buoy Pairs (U)

(S)

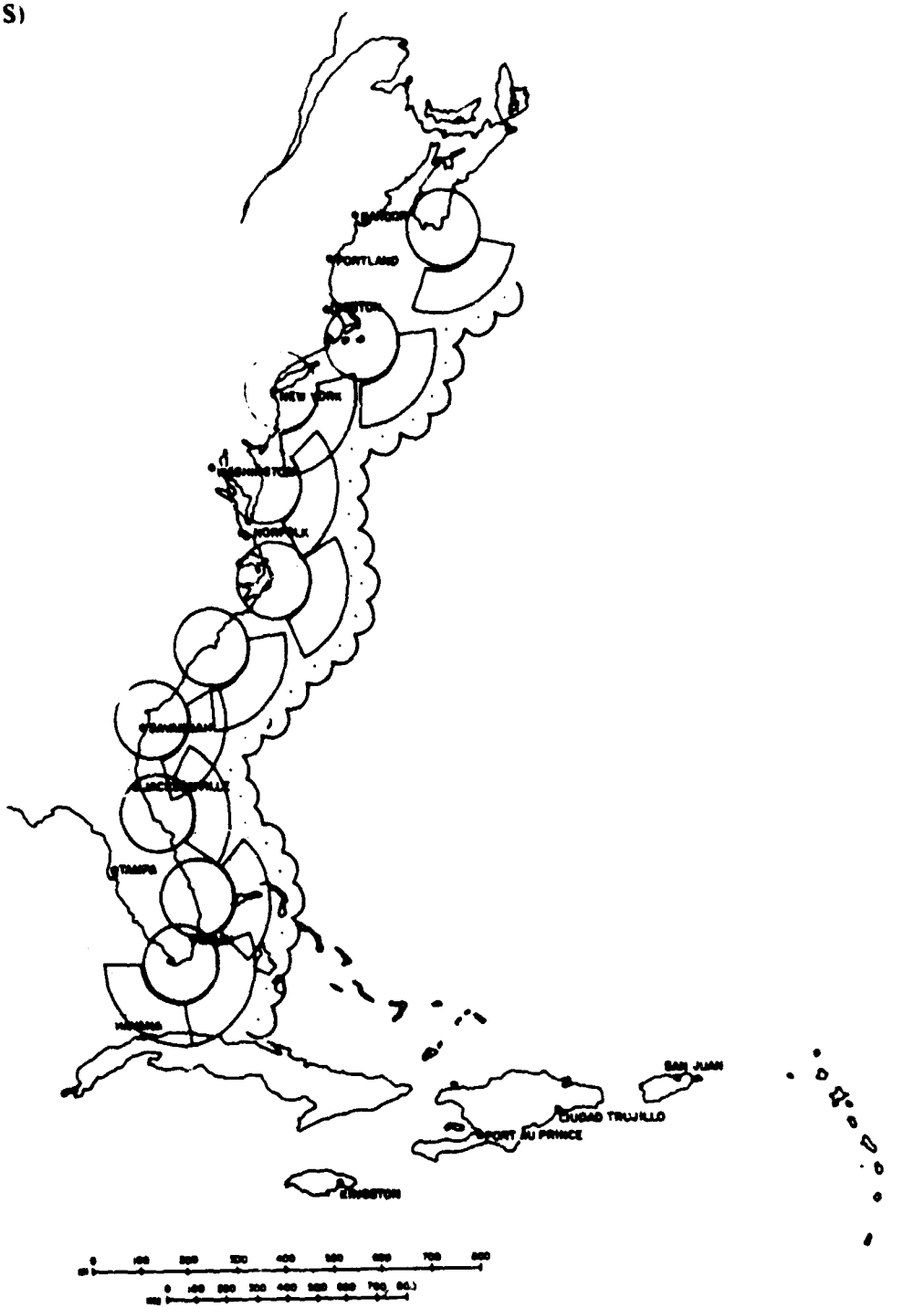

(S) Figure 6. East Coast Coverage Using 10 Monostatic Shore Stations and About 30 Buoy Receivers (S)

COMPARISON OF SEVERAL BTEW SYSTEM CONFIGURATIONS (U)

J. W. Follin, Jr.

Applied Physics Laboratory
The Johns Hopkins University
8621 Georgia Avenue
Silver Spring, Maryland 20910

(C) A relative comparison of different system configurations can be made without detailed target and ambient noise conditions by comparison of illuminating power at the target for several geometries. For example, Figure 1 shows the power delivered to a buoy from a shore radar with an aperture of 1 kilometer and an average power of 1 megawatt as a function of range to the target. Also shown are the powers delivered to a target from a buoy radiating one kilowatt isotropically. By comparing these cases for which the power on target is identical, it is possible to determine the buoy spacing for which the signal-to-noise at the land-based receiver is the same for both systems. It must be realized that the target aspect, and hence its radar cross section, may differ; and the Doppler shift expected, especially for SLBMs, will also differ.

(C) The second set of curves in Figure 2 shows a comparison in which the system is run backward, transmitting from land and receiving on the buoy. This system has an advantage of 30 dB in average power while all of the antenna gains are comparable. In addition, it is probable that the ambient noise in the vicinity of the buoy is less than that in the vicinity of the land-based radar, perhaps by 10 dB. This shows that, for system ranges of 500 kilometers from shore, a buoy spacing of 400 kilometers gives comparable performance directly between adjoining buoys, and improved performance closer to the individual buoy locations.

(C) For the skywave case we oversimplified the ionospheric path to the line-of-sight minus 10 dB, and the illumination density, as shown in Figure 3. Figure 4 shows the comparison of monostatic versus bistatic. It is apparent that rather high buoy densities are required to compete with the monostatic radar skywave case.

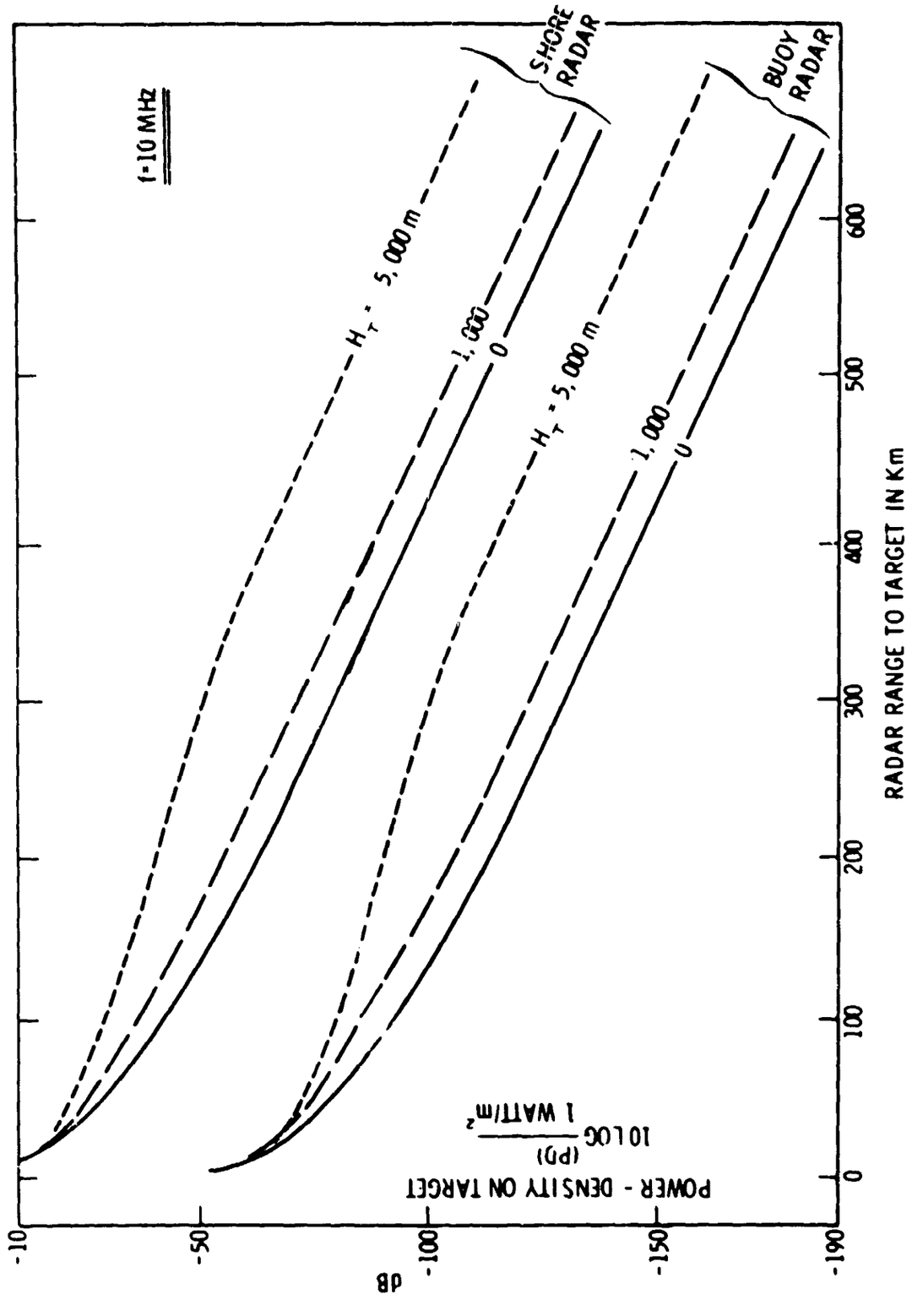

(C) Figure 1. Power Densities on Target for Ground Wave Transmission of Shore Radar (U)

(C)

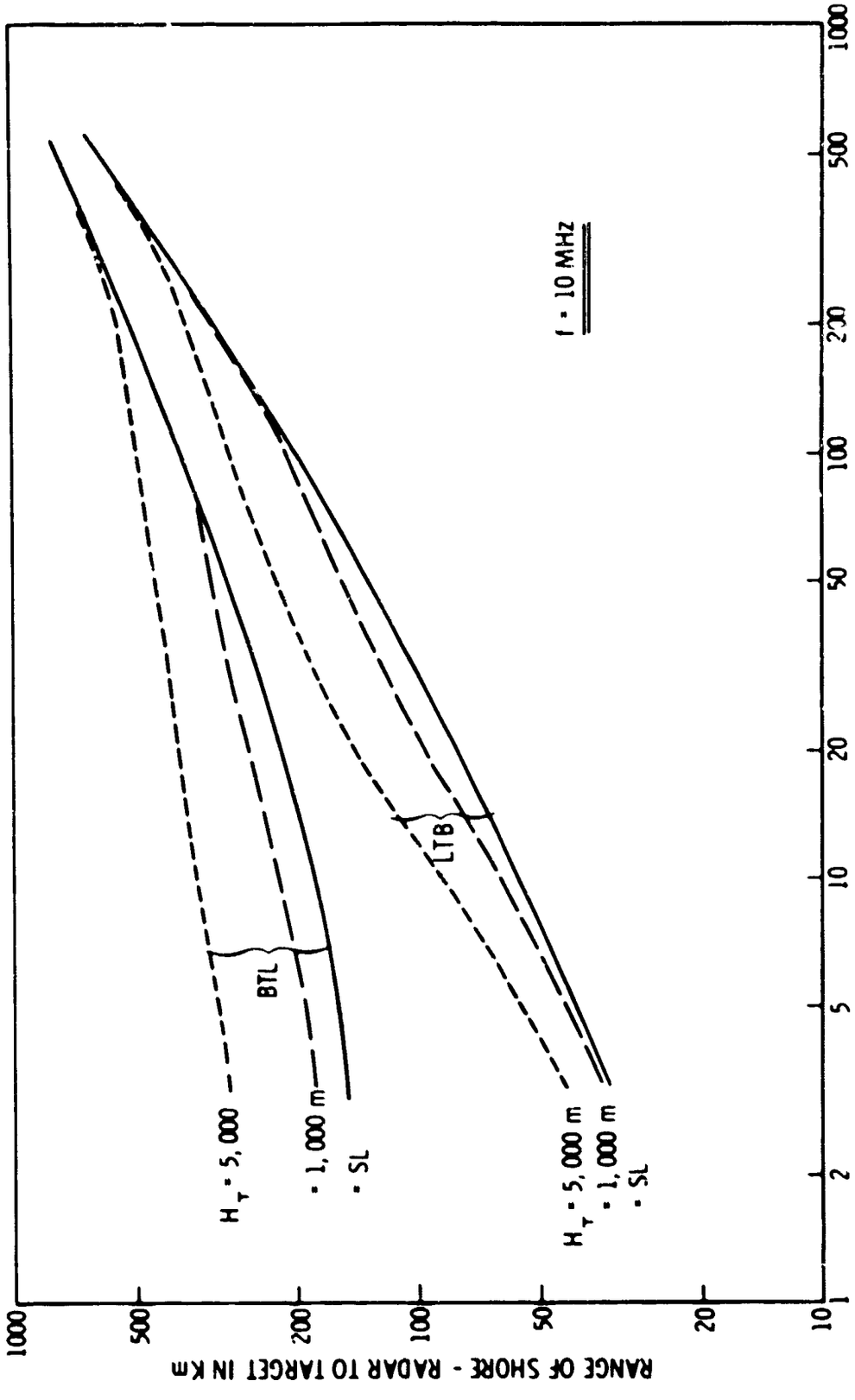

(C) Figure 2. Comparison of Various Systems for Ground Wave Transmission of Shore Radar (U)

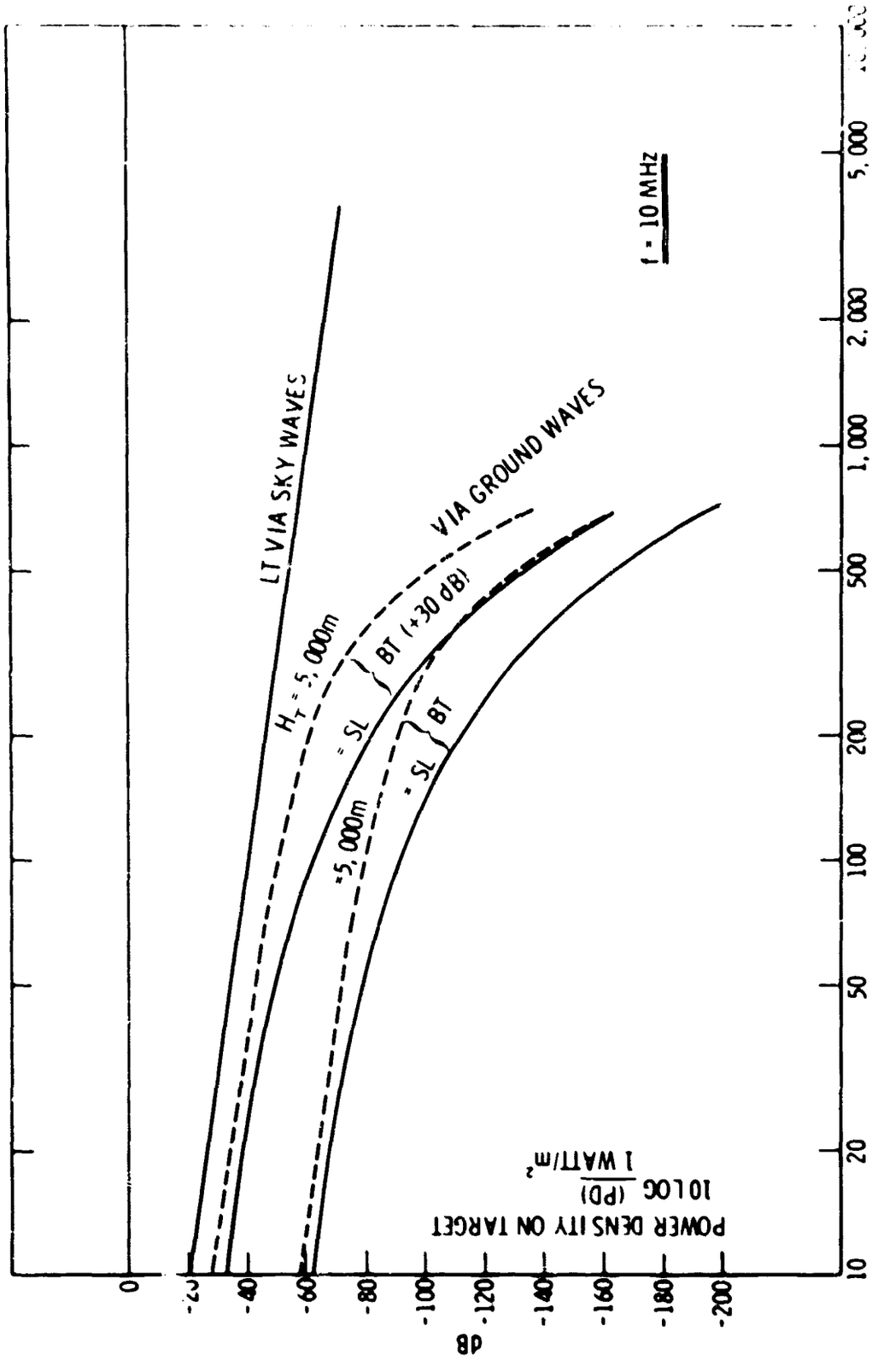

(C) Figure 3. Comparison of Power Densities on Target (U)

(C)

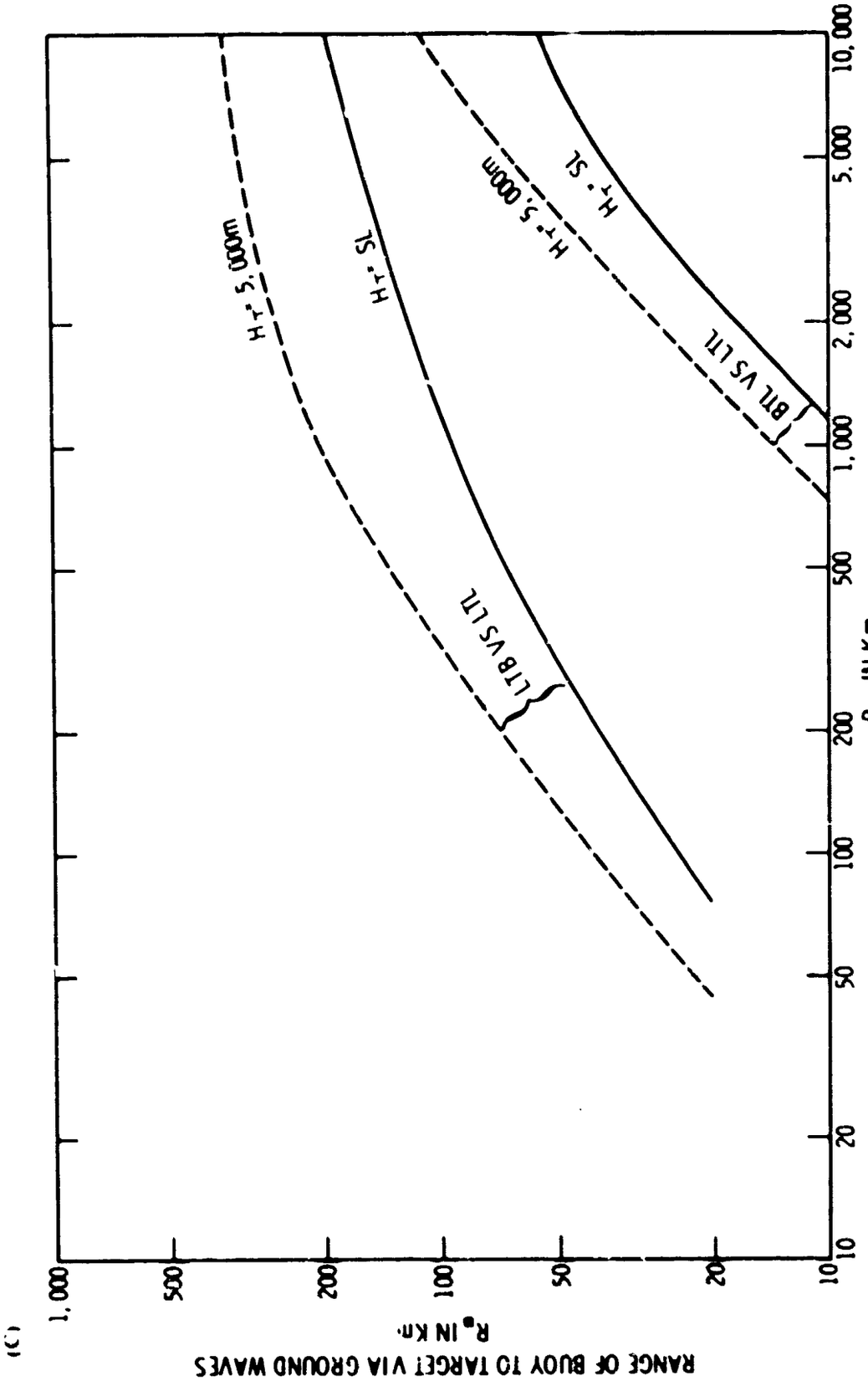

(C) Figure 4. Comparison of Various Systems at 10 MHz on the Basis of Equal S/N (U)

(C) These comparisons between systems only suggest which one is preferable, not whether it can in fact cut the mustard, and more detailed calculations such as those presented by the preceding speakers are needed to determine system effectiveness. However, before final conclusions can be drawn it seems a safe conclusion to draw that BTEW surface wave systems are useful, but for the skywave case much more analysis is required, especially with a disturbed ionosphere.

SECTION 3

PANEL REPORTS (U)

PANEL REPORTS (U)

I CONCLUSION (U)

A. Path Loss (from Carter Cay) (U)

(U) Average absolute received path loss compares well with predicted average loss (Sea States 0-1), to 1-2 dB.

(U) Total spread on received path loss at 5 and 10 MHz compares well with predicted variations with sea state by Barrick; i.e., about 3 dB at 5 MHz and about 9 dB at 10 MHz. At 15 and 20 MHz, the data points are too few to permit any conclusions.

(U) Day-to-day correlation between measured path loss and predictions based on hindcast wind and wave data is generally poor, except for two or three days when there were significant changes in sea state. However, day-to-day correlation of the three sources of hindcast data is also poor. Hence, in the absence of actual ocean spectrum measurements, day-to-day correlation of measurements with predictions is not expected to be a meaningful test of sea state dependence.

(U) Correlation between 5, 10, 15 and 20 MHz path loss measurements on a day-to-day basis should provide some test of dependence on sea state. If more data points can be obtained at 5, 15 and 20 MHz, such correlations will be meaningful.

(U) Day-to-day variations in path loss due to equipment systematic errors are believed to be less than 2 dB (Dr. L. Wetzel provided rough calculations to document this conclusion).

(U) Conductivity variations of the sea water (based on analysis) had no important role in received signal loss variations.

(U) Possible effects of ducting are completely unknown. No way is known of assessing this factor from existing measurements, nor are any predictions or even estimates available (to anyone's knowledge) on the seriousness of ducting over the sea at HF.

(U) There is some evidence of possible direct signal spectral broadening due to the moving sea surface, especially at the higher frequencies. However, limited high sea state occurences and possible contamination by sky-wave make any final conclusions about spectral broadening impossible.

B. Sea Clutter (from the Buoy and Carter Cay) (U)

(U) Comparisons of clutter measurements with wave heights and directions are meaningful primarily for the buoy measurements; too much of the area in the various range gates around Carter Cay consists of land, shoals, or shallow water, especially the significant backscatter region behind the transmitter. Hence, correlations are to be based primarily on buoy data.

(U) Buoy measurements were restricted to only the 5-MHz data for about 10 days in March. Some possibility exists for examining clutter spectra at 10 MHz from the December measurements.

(U) Clutter spectra permit detailed analysis only in the 1½-Hertz mode, i.e., spread out so that the resonant Bragg scatter ocean waves whose Dopplers lie within one Hertz of the curves can be observed.

(U) On the basis of existing measurements, the predicted mechanism is well confirmed from the "clutter occupancy" of the spectrum. The "pedestals" predicted for bistatic geometries are present, and their width and position varies exactly as predicted throughout the different range gates, phase code rates, and frequencies.

(U) Correlation of 5-MHz spectra with expected spectra based upon ocean wave height and direction hindcast data for several days shows excellent agreement and again confirms the predicted mechanism.

(U) Total scatter cross section, σ^0, as deduced from measurements on several days with moderate seas, agrees reasonably well with predictions and with measurements of Crombie, Headrick and others. There remain differences of definition of σ^0, but these will be resolved so that more of these independent comparisons can be made directly.

(U) Little can be deduced from the measurements about the region between the carrier and the clutter pedestals during higher sea states. While some records for higher sea states show this region well filled in compared to similar records for calm seas, too few such comparisons are available. No present first-order theory offers estimates for this region either.

(U) Measurements at 5 MHz show higher clutter levels than would have been deduced from the "cutoff" of the wind-wave models. Often the latter models on the days in question would have predicted no scatter because of the absence of resonant ocean waves. Thus the measurements show that the standard windwave models are not reliable in the lower regions because of the presence of some longer ocean waves, or swell.

(S) Agreement between theory, the Raytheon measurements, and the measurements of others is so good that the theoretical models can be used reliably for system design purposes at HF. This is especially true in aircraft or SLBM defense where high Doppler shifts are expected. Use of the models for low-velocity target systems (such as ship detection) must be tempered somewhat by uncertainties in clutter level around the first-order spectral pedestals of the model.

C. Sea-State Observations (U)

(U) There were three significant regions of sea involved in the Carter Cay – Cape Kennedy propagation path: 1), shallow water near the Florida coast (about 30 km); 2) the moving currents of the Gulf Stream; and 3), the shoal waters near the Bahamas (about 55 km). Distinctly different ocean-wave conditions were consistently observed from the surveying aircraft in these three regions.

(U) Wind speed and direction has been plotted on a daily basis at both Cape Kennedy and Grand Bahama Island. Wave hindcast data showing waveheight and direction for the general region of the Atlantic has also been plotted on a daily basis.

(U) The possible sources of information about the state of the sea mentioned above correlated poorly on a day-to-day basis.

(U) Aerial photographs of the sea wave were made for 18 days. The goal of these flights was the direct construction of isotropic water-wave spectra using the Stilwell coherent optics technique. Due to the use of the wrong type of film, such spectra cannot be computed from any of the photographs.

(U) The above photographs can and will be used to deduce rough information about ocean-wave directionality.

(U) Laser profilometer measurements were also recorded along the propagation path during the 18 flights. Because of uncertainties involving aircraft motion contaminating the height data, no usable ocean wave spectra have yet been available.

(U) Aircraft motions were recorded during the eighteen flights as an accelerometer output. NRL personnel have stated that this accelerometer output will be analyzed and the knowledge of the resulting aircraft motion spectrum will be used to obtain the true ocean-wave spectrum. They have promised that these spectra will be processed within one month.

(U) Hindcast data show that over the three-month measurement period, the seas were relatively calm with a Sea State 6 being reported only once. Average conditions appeared to be Sea State 1 to Sea State 3.

(U) Accelerometer and inclinometer data telemetered from the buoy is of insufficient quantity and reliability to allow the inference of sea state conditions.

II RECOMMENDATIONS (U)

A. Additional Measurements (U)

(U) The Committee on Theory and Measurements recommends additional path loss measurements. The suggestion was initiated by Dr. Allen Peterson and discussed in some detail by the committee. The reasons that additional path loss measurements were felt necessary are listed below.

- (U) Path loss measurements at 5, 15 and 20 MHz at present appear too few and sporadic to permit conclusions or even trends to be established.

- (U) Overlapping days, i.e., days on which path loss at more than one frequency was obtained, are very few. Overlap on the days with high sea states or high weather conditions (i.e., conducive to possible ducting) does not exist. Without many such overlapping days, effects of the environment cannot be studied or related to measurements.

- (U) Spectral widening of the direct signal by the moving sea during high sea states appears to be a possibility from one or two records, but again too little data is available during high seas to permit any conclusions about this important phenomenon.

- (U) Much of the time the ground-wave signal was contaminated by sky-wave. It was only near the end of the three-month period that phase-coded emissions at 5 and 10 MHz permitted positive separation of ground-wave from sky-wave.

- (U) The weather in the area from January through March does not normally undergo great changes. Temperature and seas appear to vary less about a mean than during warmer summer months and hurricane seasons.

- (U) Nearly one-third of the path crosses shoals, while much of the remainder crosses the Gulf Stream. Hence, most of the path consists of water whose surface is not typical of deep-water ocean.

(U) The suggested investigation would consist of and emphasize the following parts:

- (U) A long path over deep water would be selected, preferably with end points on land so as to reduce expense of the measurements. The path should be 300 to 400 km long. A possible path considered and recommended stretches between

(U)
Cape Cod and northern Maine, near the Bay of Fundy; over 90 percent of this path is over water more than 500 feet deep. Reported seas in this area are quite high and often influenced by Northeasterly storms blowing nearly parallel to the propagation path.

- (C) Phase-coded, highly stable signals at 5, 10, 15 and 20 MHz should be employed. The phase-code is necessary to ensure separation of the ground-wave from the sky-wave.

- (U) Path-loss measurements should be made twice daily over a period of five months. The measurement period chosen should include both summer and winter weather.

- (U) Field-strength probes should be used daily to calibrate the main transmit and receive antennas. The field structure from the main antenna out along the beach and into the water should also be probed, at least once during the period.

- (U) The main antennas should be kept simple, i.e., vertical quarter-wave monopoles.

- (C) Path-loss signals for the ground-wave should be measured in Range Gate 0, i.e., the range gate corresponding to the arrival time of the direct signal. Spectral processing should be available so as to allow better than 0.01-Hertz resolution. This will permit a study of direct signal broadening due to sea wave motion and (possibly) atmospheric turbulence.

- (U) Range Gates 1, 2, 3, 4, etc. should also be spectrally examined (occasionally) to permit study of sea clutter and sky-wave signals.

- (C) One wave spar should be used to measure and telemeter the isotropic ocean wave spectrum somewhere near the path midpoint.

- (U) Pulsed sea backscatter measurements should be made near the receiver site, in the manner reported by Crombie in his papers presented in these proceedings. These measurements appear to allow fairly accurate and inexpensive calculation of the isotropic ocean waveheight spectrum.

- (U) Hindcast wind and wave data should be collected. Also, quantitative meterological data versus altitude and position should be gathered where possible to permit calculation and study of the refractivity.

- (U) Signal strength versus range should be measured at least once during the experiment. This could be done with a transmitter on a small boat or from various other shore points.

- (U) Horizontal polarization near the receiving antenna should be measured several times, especially during high seas. This will indicate the presence of any de-polarization from steeply sloping ocean waves.

B. Additional Processing of Existing Data (U)

(U) NRL should be asked to complete analysis of wave data from their profilometer records for the 18 flights. This ocean-wave data should be plotted beside the path loss measurements for the same days.

(U) Raytheon should, where possible, process and plot more points of path loss on 5, 15 and 20 MHz.

(U) The total number of reliable path-loss points on each frequency should be calculated.

(U) The mean and variance of the path loss signals on each frequency should be calculated.

(U) Mean and variance of expected (or predicted) path loss should be calculated for each frequency based on the hindcast waveheight data on the days of observations.

(U) Averages of several clutter spectral records in the 1½-Hertz mode should be made, especially for days such as March 23 and March 26 when clutter is clearly in evidence. These averages should be made over a duration for several independent samples (an independent sample in the 1½-Hertz mode is 162 seconds long).

SECTION 4

TASK ABSTRACTS (U)

TASK ABSTRACTS (U)

THEORETICAL STUDIES; CALCULATIONS SURFACE WAVE (U)

Organization (U)

(U) Battelle Memorial Institute

Specific Objective (U)

(U) Determination of surface wave attenuation and clutter as a function of sea state, range, frequency and aspect angle.

System Concept-Relation and Importance (U)

(U) Important to all concepts where surface wave propagation is involved in predicting the clutter amplitude and doppler of the sea and the range performance.

THEORETICAL STUDY-ATTENUATION OVER IRREGULAR INHOMOGENOUS TERRAIN (U)

Organization (U)

(U) ESSA

Specific Objective (U)

(U) Development and application of theoretical techniques for determining the surface wave attenuation over surfaces having different dielectric constants and conductivities.

System Concept-Relation and Importance (U)

(U) Applicable in predicting system performance where surface wave is used and land sea interfaces occur. Typical examples involve an antenna located on land and using surface wave for transmission or reception; or where energy used in surface wave mode must traverse an island. This is important in determining system losses that reduce range or cause shadow zones (e.g., islands).

BISTATIC SEA ATTENUATION AND CLUTTER MEASUREMENTS (U)

Organization (U)

(U) Raytheon

Specific Objectives (U)

(U) Substantiated the theoretical calculations of attenuation and clutter of surface wave propagation as a function of sea state, frequency, distance, and aspect angle.

System Concept-Relation and Importance (U)

(S) Applicable in predicting the performance of all systems where ocean surface wave is used in propagating to and/or from target.

MONOSTATIC SEA CLUTTER MEASUREMENTS (U)

Organization (U)

(U) FSSA

Specific Objective (U)

(C) Determine and correlate with sea state the monostatic clutter spectrum as a function of range (0-150 km) and frequency.

System Concept-Relation and Importance (U)

(C) Important in predicting range performance and clutter rejection requirements of a land based or ship based monostatic radar.

SLBM CROSS-SECTION (U)

Organization (U)

(U) Stanford Research Institute

Specific Objective (U)

(S) Compile and summarize the available data on the theoretical calculation and measurements of SLBM cross-sections.

System Concept-Relation and Importance (U)

(S) Required for the design and performance prediction of HF radar systems against SLBM's.

SHIP CROSS-SECTION MODEL MEASUREMENTS (U)

Organization (U)

(U) Stanford University

Objective (U)

(S) Calculate theoretically and measure experimentally cross-sections of two representative scale model ships as a function of frequency, aspect angle and polarization at HF.

System Concept-Relation and Importance (U)

(C) Required to determine ship detection system performance calculations.

SHIP CROSS-SECTION MEASUREMENTS (U)

Organization (U)

(U) Naval Research Laboratory

Objective (U)

(C) Measure cross-sections of actual ships at specific aspect angles and frequencies with the MADRE radar.

System Concept-Relation and Importance (U)

(C) Demonstrates that ships can be detected using pulse Doppler Radar. Provides check points at specific frequency and aspects to correlate with model measurements. Provides input for system performance calculations.

WAKE STUDY (U)

Organization (U)

(U) ESSA

Specific Objective (U)

(S) Determine theoretically the size, aspect, frequency, and spectral characteristics of ship and submarine wakes applicable to HF radar.

System Concept-Relation and Importance (U)

(S) Ship wakes may be of sufficient size and spectral characteristics so as to enhance the nominal ships cross-section and increase the capability to detect and track ships.

(S) Under certain high speeds and shallow depths of travel submarines may produce wakes that are detectable with HF radar.

FLEET AIR DEFENSE (FAD) TEST NO. 1A (U)

Organization (U)

(U) ITT-Electro Physics Laboratory/Naval Research Laboratory

Objective (U)

(S) To conduct an initial demonstration of the feasibility of detecting and tracking aircraft with the Fleet Air Defense (FAD) concept using distant sky-wave illumination from a ground-based transmitter and receiving the target reflected energy via a surface wave to a land-based receiver. Compare the concept using two different signal formats.

System Concept-Relation and Importance (U)

(S) An important initial demonstration to ensure there are no major problems in the basic concept prior to proceeding with a shipborne receiver installation. Ensures that dynamic range, target cross-polarization cross-section and clutter can be handled by known technology. The concept is important in providing a silent fleet surveillance capability.

MONOSTATIC DOPPLER SEA CLUTTER MEASUREMENTS (U)

Organization (U)

(U) Naval Research Laboratory

Specific Objective (C)

(S) Determine the Doppler characteristics of sea clutter using the MADRE radar.

System Concept-Relation and Importance (U)

(S) Provides typical Doppler sea clutter records for the design of pulse Doppler ocean surface surveillance radars. Measurements are limited in frequency range (10-26 MHz) and at a specific fixed frequency at any one time.

MONOSTATIC HIGH RESOLUTION SEA CLUTTER MEASUREMENTS (U)

Organization (U)

(U) Stanford University

Specific Objective (U)

(S) Determine the amplitude and polarization characteristics of sea scatter in azimuth and FM/CW high resolution techniques.

System Concept-Relation and Importance (U)

(S) It may be possible to detect ships on the surface of the ocean on a power basis. That is if resolution cell size is reduced in range and azimuth until its cross section due to sea clutter is less than that of the ship.

SHIP AHOY NO. 1A (U)

Organization (U)

(U) Stanford University

Objective (U)

(S) Investigate the feasibility of detecting ships using an FM/CW technique on a power-only basis by reducing the size of the range azimuth cell.

System Concept-Relation and Importance (U)

(S) The Doppler radar technique will not detect ships with low radial velocities or that are stationary. This concept will permit detection of ships under such circumstances.

BUOY TACTICAL EARLY WARNING (BTEW) TEST NO. 1 (S)

Organization (U)

(U) Raytheon

Objective (U)

(S) Conduct an initial demonstration of detecting aircraft and missiles using the BTEW concept, transmitter on a buoy with a land-based receiver in real-time at short ranges using surface wave propagation.

System Concept-Relation and Importance (U)

(S) The use of the BTEW concept can provide coverage beyond microwave radar coverage and in the skip zone of OHD backscatter skywave radar coverage for CONUS defense and special tactical applications. The technique is not dependent on the ionosphere and can operate after a nuclear detonation. In fact after a nuclear detonation, galactic and other user noise will decrease and coverage of this concept will be increased.

BUOY TACTICAL EARLY WARNING (BTEW) TEST NO. 2 (S)

Organization (U)

(U) Sylvania

Objective (U)

(S) Conduct an initial demonstration of the detection of aircraft using the BTEW concept, transmitter on a buoy with a land-based receiver in real-time at long ranges using surface wave propagation from transmitter to aircraft and sky-wave from aircraft to receiver.

System Concept-Relation and Importance (U)

(S) The use of the BTEW long range concept should extend the range of SLBM and aircraft coverage beyond the range of OHD sky-wave backscatter radar.

SUPPLEMENTARY

INFORMATION

ADVANCED RESEARCH PROJECTS AGENCY
3701 NORTH FAIRFAX DRIVE
ARLINGTON VA 22203-1714

ERRATA AD - 514939 ERRATA

August 19, 1996

MEMORANDUM FOR DEFENSE TECHNICAL INFORMATION CENTER

SUBJECT: Declassification of Reports

The following documents have been declassified and released under a Freedom of Information request and are therefore in the public domain and may be marked with the "A" statement:

AD 513725, Project Aquarius Special Report EDL M 1380
AD 509068, Project Aquarius Annual Report EDL G 915
AD 507423, Project Aquarius Quarterly Report EDL G 900
AD 514939L, MAYBELL Technical Workshop
AD 515288L, Project Aquarius Final Report EDL E 184

Matt T. Donlon
Director
Security and Intelligence Office

cc:
F.A. Koether
(96-45)

(5)